

Development and Optimization of Peptide-Based, Tumor-Associated Macrophage (TAM)-Targeting Therapeutics

Chayanon Ngambenjawong

A dissertation
submitted in partial fulfillment of the
requirements for the degree of

Doctor of Philosophy

University of Washington

2017

Reading Committee:

Suzie H. Pun, Ph.D., Chair

Patrick S. Stayton, Ph.D.

Cole A. DeForest, Ph.D.

Program Authorized to Offer Degree:

Bioengineering

©Copyright 2017

Chayanon Ngambenjawong

University of Washington

Abstract

Development and Optimization of Peptide-Based,
Tumor-Associated Macrophage (TAM)-Targeting Therapeutics

Chayanon Ngambenjwong

Chair of the Supervisory Committee
Professor Suzie H. Pun, Ph.D.
Department of Bioengineering

Cancer is one of the leading causes of death and is a subject of intense research worldwide. Within the past few decades, cancer immunotherapy has emerged as an important arm of cancer therapies following the prominent success of immune checkpoint blockade therapies and chimeric antigen receptor (CAR)-T cell therapies. While the first wave of cancer immunotherapy focuses on an adaptive immunity (T cells), a fruitful opportunity exists to modulate an innate immunity for anti-cancer therapies. Tumor-associated macrophages (TAMs) are one of the most studied innate immune populations due to their abundance in tumor microenvironment. In most tumors, the majority of TAMs expresses M2-like phenotypes and supports pro-tumoral functions, whereas the minority expresses M1-like phenotypes with anti-tumoral functions. Several investigational pre-clinical strategies to modulate TAMs, either depleting them or stimulating their tumoricidal functions, are delivering promising results with high translational potential. Chapter 1 provides a review on the current update in TAM-targeted therapeutics. To potentiate the reported TAM-modulating agents, several TAM-targeted drug delivery systems are being developed by us and others. This thesis focuses on optimization of the active targeting ligand (M2pep) previously shown to bind to M2 macrophages and M2-like TAMs. Chapter 2

explores synthesis and evaluation of targeting avidity of divalent and tetravalent M2pep, as well as the effect of ratiometric display of M2pep versus therapeutic cargo in regard to therapeutic selectivity. Chapter 3 and 4 report affinity and serum stability optimization of M2pep via amino acid sequence modifications and peptide macrocyclization. Rationalizing further M2pep optimization based on the context of acidic tumor microenvironment, Chapter 5 demonstrates the development of low pH-responsive M2pep. Chapter 6 further elaborates the development of multivalent M2pep utilizing a biocompatible polymer to confer both enhanced avidity and serum stability. Finally, chapter 7 concludes the major findings and provides recommendations for future optimization in regard to human translation.

TABLE OF CONTENTS

Chapter 1. Progress in tumor-associated macrophage (TAM)-targeted therapeutics	1
1.1 Introduction	2
1.1.1 Mononuclear phagocyte system.....	2
1.1.2 Macrophage polarization	3
1.2 Macrophages in tumorigenesis	4
1.2.1 Macrophage polarization in tumor development	4
1.2.2 Clinical implication of TAMs	6
1.3 Pharmacological modulation of macrophages/TAMs.....	6
1.3.1 Bisphosphonate	6
1.3.2 Inhibition of growth factor signaling	8
1.3.2.1 CSF-1R inhibition.....	8
1.3.2.2 RON inhibition.....	9
1.3.3 Modulation of macrophage phagocytic activity	13
1.3.3.1 Antibody-dependent cellular phagocytosis (ADCP)	13
1.3.3.2 Inhibition of CD47-SIRP α signaling	14
1.3.4 Inhibition of inflammatory monocyte/macrophage recruitment.....	14
1.3.4.1 Inhibition of CCR2-CCL2 signaling.....	14
1.3.4.2 Inhibition of CXCR4-CXCL12 signaling.....	15
1.3.5 Immunostimulation by anti-CD40 agonistic antibody.....	15
1.3.6 Inhibition of angiogenic signaling	16
1.3.7 Metabolic modulation of macrophages/TAMs	17
1.3.7.1 mTOR inhibition.....	17
1.3.7.2 Modulation of PPAR γ -Gpr132-lactate signaling.....	17
1.3.7.3 Inhibition of metabolism of amino acids and lipids.....	18
1.3.7.4 Modulation of essential elements and vitamins	18
1.3.8 Modulation of macrophage scavenger receptors	19
1.3.9 Chemotherapy drugs	20
1.3.10 Activation of Toll-like receptors (TLRs).....	21
1.4 Targeted drug delivery systems to macrophages/TAMs.....	21
1.4.1 Passive targeting to macrophages/TAMs.....	22
1.4.2 Active targeting to macrophages/TAMs	23
1.5 Macrophages as a therapeutic depot.....	25
1.6 Perspectives on TAM-targeted therapeutics.....	27

1.7 Acknowledgments	28
1.8 References	28
1.9 Supplementary information	48
Chapter 2. Synthesis and evaluation of multivalent M2pep peptides for targeting alternatively activated M2 macrophages	54
2.1 Introduction	55
2.2 Materials and methods	57
2.2.1 Materials	57
2.2.2 Multivalent peptide synthesis	57
2.2.2.1 Peptide synthesis	57
2.2.2.2 Synthesis of [Mal] ₂ -Biotin and [Mal] ₂ -Cys(Trt) divalent linkers	58
2.2.2.3 Synthesis of [Mal] ₄ -Biotin tetravalent linker	59
2.2.2.4 Synthesis of [M2pep] ₂ -Biotin and [M2pep] ₄ -Biotin	59
2.2.2.5 Synthesis of [M2pep] ₂ -Cys(Trt) and deprotection of Trt protecting group	59
2.2.2.6 Synthesis of [M2pep] ₂ -[KLA] and [M2pep] ₂ -[KLA] ₂	60
2.2.3 Generation of bone marrow-derived macrophages	60
2.2.4 Binding study	60
2.2.5 <i>In vitro</i> cytotoxicity study	61
2.2.6 <i>Ex vivo</i> cytotoxicity study	61
2.3 Results and discussion	62
2.3.1 Multivalent targeting ligands	62
2.3.1.1 Synthesis of multivalent M2pep	62
2.3.1.2 Binding and cytotoxicity studies of multivalent M2pep with primary cultured macrophage	63
2.3.2 Multivalent pro-apoptotic KLA cargo	66
2.3.2.1 Synthesis of multivalent KLA constructs	66
2.3.2.2 Cytotoxicity study of multivalent M2pepKLA	67
2.3.3 <i>Ex vivo</i> evaluation of multivalent constructs with TAMs	69
2.4 Conclusions	72
2.5 Acknowledgments	72
2.6 References	72
2.7 Supplementary information	77

Chapter 3. Serum stability and affinity optimization of M2 macrophage-targeting peptide (M2pep)	85
3.1 Introduction	86
3.2 Materials and Methods	87
3.2.1 Materials	87
3.2.2 Peptide synthesis	88
3.2.2.1 Biotinylated peptides	88
3.2.2.2 Sulfo-Cy5-labeled peptides.....	89
3.2.3 Serum stability study.....	89
3.2.4 Bone marrow harvest	89
3.2.5 Binding study	90
3.2.6 <i>In vivo</i> biodistribution study in CT-26 and 4T1 tumor models	90
3.2.7 Statistical analysis	91
3.3 Results and Discussion.....	92
3.3.1 The effect of N-terminal acetylation on serum stability and binding activity of M2pepBiotin	93
3.3.2 The effect of D-amino acid substitutions on serum stability and binding activity of AcM2pepBiotin	94
3.3.3 The effect of L-amino acid substitutions on serum stability and binding activity of AcM2pepBiotin	96
3.3.4 The effect of cyclization on serum stability and binding activity of M2pepBiotin	98
3.3.5 The effect of Y12y on serum stability and binding activity of AcM2pep(RY)Biotin	100
3.3.6 Binding of M2pep analogs post serum incubation	101
3.3.7 Biodistribution of M2pep analogs in CT-26 and 4T1 tumor models.....	102
3.4 Conclusions	103
3.5 Acknowledgments	104
3.6 References	104
3.7 Supplementary information.....	107
Chapter 4. Engineering an affinity-enhanced peptide through optimization of cyclization chemistry	111
4.1 Introduction	112
4.2 Results and Discussion.....	114
4.2.1 Peptide synthesis	114

4.2.2 <i>In vitro</i> binding study.....	115
4.2.3 Circular Dichroism (CD) measurement.....	120
4.2.4 <i>In vitro</i> serum stability study	121
4.3 Conclusions	124
4.4 Materials and Methods	124
4.4.1 Materials	124
4.4.2 Synthesis of biotinylated M2pep analogs	125
4.4.2.1 General peptide synthesis strategy.....	125
4.4.2.2 Disulfide-cyclized M2pep(RY)Biotin	126
4.4.2.3 Amide-cyclized M2pep(RY)Biotin	126
4.4.2.4 Triazole-cyclized M2pep(RY)Biotin.....	126
4.4.2.5 DFBP-cyclized M2pep(RY)Biotin	127
4.4.2.6 DFS-cyclized M2pep(RY)Biotin.....	127
4.4.3 Bone marrow harvest and macrophage culture.....	127
4.4.4 <i>In vitro</i> binding study.....	128
4.4.5 CD measurement.....	128
4.4.6 <i>In vitro</i> serum stability study	128
4.5 Acknowledgments	129
4.6 References	129
4.7 Supplementary information.....	133
Chapter 5. Reversibly-switchable pH-dependent peptide ligand binding via 3,5-diiodotyrosine substitutions	139
5.1 Introduction	140
5.2 Results and Discussion.....	142
5.2.1 Peptide synthesis.....	142
5.2.2 pH-dependent binding activity of M2pep and AcM2pep(RY) at pH 6 and 7.4	143
5.2.3 The effect of K9H substitution on pH-dependent binding activity.....	144
5.2.4 3,5-diiodotyrosine substitutions impart pH-dependent binding to M2pep	146
5.2.5 Acetylated Y-Î peptide exhibits improved serum stability compared to AcM2pep(RY)Biotin.....	147
5.2.6 Demonstration of reversible, pH-dependent modulation of peptide binding affinity	150
5.3 Conclusions	151
5.4 Materials and Methods	152
5.4.1 Materials	152

5.4.2 Peptide synthesis	152
5.4.3 Bone marrow harvest and culture of primary macrophages	153
5.4.4 <i>In vitro</i> binding study.....	153
5.4.5 Serum stability study.....	154
5.5 Acknowledgments	154
5.6 References	154
Chapter 6. Multivalent polymers displaying M2 macrophage-targeting peptides improve target binding avidity and serum stability.....	158
6.1 Introduction	159
6.2 Experimental section	160
6.2.1 Materials	160
6.2.2 Synthesis of peptides.....	161
6.2.3 Synthesis of peptide-grafted polymer	162
6.2.3.1 Synthesis of Biotin-functionalized RAFT chain transfer agent (Biotin-CTA).....	162
6.2.3.2 Synthesis of Biotin-poly(HPMA- <i>st</i> -APMA)	162
6.2.3.3 Functionalization of Biotin-poly(HPMA- <i>st</i> -APMA).....	163
6.2.3.3.1 Maleimide functionalization (Biotin-poly(HPMA- <i>st</i> -(Mal-APMA))).....	163
6.2.3.3.2 Azide functionalization (Biotin-poly(HPMA- <i>st</i> -(Azi-APMA))).....	163
6.2.3.4 Peptide grafting.....	164
6.2.3.4.1 Grafting via thiol-maleimide conjugation.....	164
6.2.3.4.2 Grafting via copper(I)-catalyzed alkyne-azide cycloaddition (CuAAC) conjugation.....	164
6.2.3.5 Determination of peptide valency on peptide-grafted polymers.....	164
6.2.4 Bone marrow harvest and culture of primary macrophages	165
6.2.5 <i>In vitro</i> binding study.....	165
6.2.6 <i>In vitro</i> binding study post serum incubation	166
6.3 Results and Discussion.....	166
6.3.1 Design and synthesis of peptide-grafted polymers	166
6.3.2 <i>In vitro</i> binding study.....	168
6.3.3 <i>In vitro</i> binding study post serum incubation	170
6.4 Conclusions	171
6.5 Acknowledgments.....	172

6.6 References	172
6.7 Supplementary information.....	174
Chapter 7. Summary of major findings and recommendations for future directions	175
7.1 Major findings	176
7.2 Future directions.....	177
7.2.1 Investigation on strategies to modulate M2-TAMs utilizing different immunodulating agents delivered via the developed M2pep-based M2-TAM-targeted delivery platform	177
7.2.2 Towards human translation.....	178
7.2.2.1 Preliminary binding studies of M2pep analogs on human macrophages	178
7.2.2.2 Proposed strategies to improve affinity/selectivity of M2pep towards human M2 macrophages/TAMs	180
7.2.2.2.1 Extended library screening	180
7.2.2.2.2 Tumor microenvironment-responsive M2pep for human TAM-targeting	181
7.2.2.2.3 Selectivity enhancement via heterobivalent display of multiple targeting peptides	181
7.2.2.2.4 Optimization of polymeric backbone for display of M2pep....	182
7.3 References	182

LIST OF FIGURES

Chapter 1. Progress in tumor-associated macrophage (TAM)-targeted therapeutics

- 1.1 Normal physiological macrophage functions that can promote (M2) or reduce tumor growth (M1) 5
- 1.2 Strategies to promote passive and active targeting of macrophages/TAMs 23

Chapter 2. Synthesis and evaluation of multivalent M2pep peptides for targeting alternatively activated M2 macrophages

- 2.1 *In vitro* binding of multivalent M2pepBiotin 64
- 2.2 Cytotoxicity curves of multivalent M2pepBiotin 66
- 2.3 Cytotoxicity curves of multivalent M2pepKLA 69
- 2.4 *Ex vivo* cytotoxicity evaluation of multivalent M2pep 71
- S2.1 Flow cytometry gating strategy for *ex vivo* cytotoxicity evaluation 80
- S2.2 Internalization of multivalent M2pep 81
- S2.3 Cytotoxicity of M2pepKKKC and its scrambled version 82
- S2.4 Cytotoxicity of the control linkers 83
- S2.5 Apoptosis assay on multivalent M2pep-treated M2 macrophages 84

Chapter 3. Serum stability and affinity optimization of M2 macrophage-targeting peptide (M2pep)

- 3.1 Serum stability and binding studies of M2pepBiotin and AcM2pepBiotin 94
- 3.2 Serum stability and binding studies of W10w 95
- 3.3 Serum stability and binding studies of W10P, W10Y, and K9R 97
- 3.4 Serum stability and binding studies of cyclic M2pep(RY)Biotin 99
- 3.5 Serum stability and binding studies of Y12y 100
- 3.6 Binding study of M2pep analogs post serum incubation 101
- 3.7 *In vivo* biodistribution study of M2pep analogs 103
- S3.1 Serum stability and binding studies of AcM2pep(RY)Biotin 107
- S3.2 Serum stability study of W10(P,D,T,R,H) 108
- S3.3 Binding curves of M2pepBiotin and cyclic M2pep(RY)Biotin 109
- S3.4 Flow cytometry gating strategy for analysis of intratumoral biodistribution of M2pep analogs 110

Chapter 4. Engineering an affinity-enhanced peptide through optimization of cyclization chemistry

- 4.1 Schematics of M2pep and cyclic M2pep(RY) analogs 114
- 4.2 Binding curves of M2pep analogs on M2 and M1 macrophages 116
- 4.3 Binding curves of DFBP-cyclized M2pepBiotin 117

4.4 Binding study of DFBP control peptide and binding study of DFBP-cyclized M2pep(RY)Biotin in PBS and PBSA	118
4.5 Binding curves of FF and F(F5)F(F5)-cyclized M2pep(RY)Biotin.....	120
4.6 CD spectra of M2pep analogs	121
4.7 Serum stability of cyclic M2pep(RY) analogs	123
S4.1 On-resin synthesis of cyclic M2pep(RY) analogs	134
S4.2 Confirmation of successful synthesis of Triazole-cyclized M2pep(RY)Biotin.....	135
S4.3 Unsuccessful attempt on on-resin synthesis of DFS-cyclized M2pep(RY) analogs	136
S4.4 Cell viability of DFBP-, FF-, and F(F5)F(F5)-cyclized M2pep(RY)Biotin.....	137
S4.5 Stability of DFS-cyclized M2pep(RY)Biotin	138
Chapter 5. Reversibly-switchable pH-dependent peptide ligand binding via 3,5-diiodotyrosine substitutions	
5.1 Engineering of tumor microenvironment (low pH)-responsive targeting peptides	142
5.2 Binding study of M2pepBiotin and AcM2pep(RY)Biotin at pH 7.4 and 6	144
5.3 Binding study of M2pep(H9)Biotin at pH 7.4 and 6.....	145
5.4 Binding study of diiodotyrosine-substituted M2pep(R9) analogs at pH 7.4 and 6.....	147
5.5 Binding and serum stability study of Ac-Y-Î-Î	149
5.6 Post-binding peptide elution study on M2 macrophages	151
Chapter 6. Multivalent polymers displaying M2 macrophage-targeting peptides improve target binding avidity and serum stability	
6.1 Binding study of M2pep peptides and peptide-grafted polymers	169
6.2 Binding study of M2pep peptides and peptide-grafted polymers post serum incubation	171
Chapter 7. Summary of major findings and recommendations for future directions	
7.1 Binding study of M2pep peptides and peptide-grafted polymers on human macrophages	179
7.2 Binding study of M2pep peptide-grafted polymers on human macrophages	180

LIST OF TABLES

Table

1.1 FDA-approved drugs whose mechanisms of action may involve modulation of macrophages/TAMs	5
1.2 Selected compilation of drugs in clinical trials whose mechanisms of action may involve modulation of macrophages/TAMs.....	11
S1.1 Extended compilation of drugs in clinical trials whose mechanisms of action may involve modulation of macrophages/TAMs	48
S2.1 Molecular weights of synthesized peptides	77
3.1 Amino acid sequences and molecular weights of M2pep analogs	92
4.1 Protected amino acids used for cyclization.....	126
S4.1 Molecular weights of synthesized peptides	133
5.1 Amino acid sequences and molecular weights of M2 macrophage-targeting peptides	143
6.1 Amino acid sequences and molecular weights of the synthesized peptides	162
6.2 A panel of peptide-grafted polymers and calculated peptide valency	168
S6.1 Dilution schematic for binding study post serum incubation	174
7.1 A panel of peptides and peptide-grafted polymers and calculated peptide valency	178
7.2 A panel of peptide-grafted polymers and calculated peptide valency	179

LIST OF SCHEMES**Scheme**

2.1 Multivalent M2pep analogs and their linkers.....	63
2.2 Multivalent M2pepKLA analogs and their linkers	67
S2.1 Synthesis of [M2pep] ₂ -Biotin and [M2pep] ₄ -Biotin.....	78
S2.2 Synthesis of [M2pep] ₂ -[KLA] and [M2pep] ₂ -[KLA] ₂	79
6.1 Synthesis schematic of Biotin-CTA and peptide-grafted polymers	167

ACKNOWLEDGMENTS

Completing a PhD study is a challenging task physically and mentally, the process of which would not have been achievable without supports from various people in life. Hence, I would like to acknowledge these important people who have made the completion of my PhD study possible.

First, I would like to acknowledge my adviser, Dr. Suzie Pun, for her tremendous supports throughout and beyond my PhD journey. Thank you for putting your best interest in my and other students' learning in all aspects ranging from science to life. Thank you for always listening to my problems and obstacles in research and engaging in a two-way communication on ideas and thoughts to bring out the best solutions to the problems that we try to solve. Your sincere understanding and sympathy on the several down days in research as well as your thoughtful suggestions eased out the tense. I truly appreciate your interest in well-being of me and other students inside and outside the lab. Thank you for leading by example how a great mentor one can be and should be.

Next, I would like to thank my PhD committee members; Dr. Cole DeForest, Dr. Patrick Stayton, and Dr. André Lieber, for your thoughtful feedbacks during exams and meetings, for your willingness to let me have access to your lab instruments, and for your help in preparing me for the next step post-PhD completion.

There are several past and present Pun lab members whom I would like to acknowledge:

Julio, my one and only undergraduate mentee during my PhD: Thank you for staying with me these past 3 years and contributing with endless help on different research projects. Thank you for letting me be your mentor which enables me to have another perspective from the mentor's point of view and experience joy and appreciation as you become more and more independent in scientific thinking and performing different experiments over time.

Maryelise, my biology mentor when I joined the Pun lab: Thank you for teaching me in all aspects of macrophages, TAMs, tumor immunology & immunotherapy, and everything biologically! Thank you for showing how persistent one should be in tackling difficult research projects.

Joan, my chemistry mentor when I joined the Pun lab: Thank you for teaching me to try to understand and rationalize each step of chemical synthesis, establishing a firm fundamental needed to tackle chemistry-oriented research, and instilling the invaluable sense of always rinsing flasks twice to maximize the yield!

Dave: My PhD research would not be possible without your help and training on peptide synthesis optimization as well as passive learning from random chemistry conversation and active learning from fixing and maintaining various instruments in lab. Thanks also for being a great hangout companion outside the lab!

Heather: Thank you for bringing creativity in research to the lab and showing how one could be very productive despite working on lengthy biological experiments. Thank you for your help in various experiments as well as for sharing insightfulness on macrophage biology.

Julie: Thank you for your leadership in maintaining order in the lab at the start of my PhD study.

Leslie: Thank you for having the best way to say hi to me in the lab as well as inviting me to dinners at various events. Also, thanks for your tips and help as I prepare for post-graduation job hunting.

Kevin: Thank you for asking me, “how’s your weekend?” every week at the start of my PhD in the lab even though you always got the same short answer (“Good.”) with no elaboration. But finally, I speak more and more and maybe too much sometimes. Thanks for asking me to hang out at various times and taking care of me in various events.

Christine, my cumulatively the longest officemate since the early days in the cubicle: Thank you for your constant curiosity for knowledge and information which unintentionally makes you our office honorary human search engine that feeds us more information on virtually any topics we talked in the office. Thanks also for being a great hangout companion outside the lab!

The dynamic trio (so-called by Maryelise) – thank you for the early days of bringing freshful energy to the lab and now for being very reliable seniors in helping to keep the lab in order:

Bob, faithful hangout buddy, and the one who also introduced the wonder of decafluorobiphenyl (DFBP) to me, which turned out to be one of my favorite molecules in my graduate study and ignited my interest in bioconjugate chemistry.

Gary, one of the hardest working people I know, who also has a great determination (and passion for solving kidney diseases). I’m sure you will be a great professor you aspire to be.

Brynn: Thank you for maintaining the lab flow cytometer which is a bread and butter instrument in the lab. Thank you, together with Gary, for being open to embracing new technologies (NGS and aptamer display) for the lab which greatly expand the lab research capability in various dimension.

David: Thanks for sharing passion on “beautiful” bioconjugation chemistries and for sending me interesting papers on these.

Albert: Officemate in the last few quarters of my PhD. You work hard in the lab so I’m sure you’ll do well!

The “next generation” dynamic quartet: Meilyn, Emmeline, Alex, and Ian – thank you for bringing the next wave of freshfulness to the lab and strengthening the “Pun lab, fun lab” philosophy.

Nataly: Thank you for helping to maintain lab in order and thank you for being the powerhouse in tackling the important receptor identification works in the lab.

Drew: Thank you for deciding to try DFBP for peptide cyclization; I'm looking for an ally to further explore (and possibly appreciate) the wonder of DFBP! Also, thanks for your thorough thoughts and suggestion during planning of animal experiments.

Hua, Paul, Yilong, and Tianyu: The Chemistry subgroup post-docs who expose me to various interesting ideas and strategies in synthetic chemistry during group meetings.

In addition, I would also like to thank friends in Seattle who made my experience here a memorable one as well as friends back home who maintain long-lasting friendship and come out to join me for dinner during my visits back home.

Finally, I would like to thank my parents for all their endless supports through years and for always prioritizing my and my siblings' education. Thanks to my brother and sister for taking care of our parents as I'm away from home.

DEDICATION

To my mom and dad

my brother and sister

Chapter 1

PROGRESS IN TUMOR-ASSOCIATED MACROPHAGE (TAM)-TARGETED THERAPEUTICS

Chayanon Ngambenjawong, Heather H. Gustafson, Suzie H. Pun

Abstract

As an essential innate immune population for maintaining body homeostasis and warding off foreign pathogens, macrophages display high plasticity and perform diverse supportive functions specialized to different tissue compartments. Consequently, aberrance in macrophage functions contributes substantially to progression of several diseases including cancer, fibrosis, and diabetes. In the context of cancer, tumor-associated macrophages (TAMs) in tumor microenvironment (TME) typically promote cancer cell proliferation, immunosuppression, and angiogenesis in support of tumor growth and metastasis. Oftentimes, the abundance of TAMs in tumor is correlated with poor disease prognosis. Hence, significant attention has been drawn towards development of cancer immunotherapies targeting these TAMs; either depleting them from tumor, blocking their pro-tumoral functions, or restoring their immunostimulatory/tumoricidal properties. This review aims to introduce readers to various aspects in development and evaluation of TAM-targeted therapeutics in pre-clinical and clinical stages.¹

¹ Reprinted with permission from Ngambenjawong et al. (2017) Adv Drug Deliv Rev. Copyright© 2017 Elsevier

1.1 Introduction

Macrophages, key cells in the innate immune system, are the main component of the mononuclear phagocyte system (MPS) [1], which also include bone marrow progenitors and blood monocytes. Recent studies have revealed that the different components of the MPS system are derived in various stages of embryotic development and are not all from the same progenitor lineage [2,3]. Macrophage functions are as diverse as their lineages and play important roles in normal homeostasis and disease development [4,5]. This is especially true in acute and chronic inflammatory disease states such as wounds, malignancy, and autoimmune disorders. There is increasing evidence that macrophages play a central role in both normal and diseased tissue remodeling including angiogenesis, basement membrane breakdown, leukocyte infiltration, and immune suppression [4]. As such, the macrophage has emerged as a central drug target in a variety of disease states, including the tumor microenvironment (TME). This review focuses on drug strategies in malignancies that affect macrophage, while the reader is referred to excellent recent reviews for more information on other aspects of macrophage biology, including macrophage physiological function [5], the role of the macrophage in tumorigenesis [6], and the clinical applicability and translation [7] of macrophage drug targets.

The review first provides an introduction to macrophage and the role of macrophage populations in tumor development. Cancer therapy strategies involving macrophages in the following three areas are then presented: 1) identifying drug targets for modulation of TAM activities, 2) engineering carriers that promote, in increasing order of cell specificity, effective delivery of drug cargos to systemic macrophages, tumor-localized TAMs, or subtype-specific pro-tumoral M2-TAMs, and 3) utilizing the tumor-homing property of macrophages for cell-based therapies.

1.1.1 Mononuclear phagocyte system

First described in the starfish by Ilya Ilyich Mechnikov in 1882, phagocytes are an evolutionarily conserved subset of leukocytes that maintain organismal homeostasis in all multicellular species, [8]. This cell type, especially within mammalian species, is distributed throughout the body and present within each tissue to perform specific functions [3]. Microglia, the tissue-resident macrophages within the brain, facilitate neurological synapse pruning for memory maintenance [9] and serve as an immunological defense in an immune privileged

environment [10]. Kupffer cells in the liver clear foreign, pathogenic, and waste materials from circulation [11]. Splenic red pulp macrophages are responsible for the recycling process of red blood cells [11–13]. Specific macrophage subsets in protective barriers, such as the Langerhans cells in the skin [14] and the alveolar macrophages within the lung [15], are responsible for both clearing pathogenic material and raising local inflammatory responses. Intraglomerular mesangial cells in the kidneys regulate blood flow [16]. The monocytes in blood circulation provide a reservoir of macrophages for mounting immune and inflammatory responses [17]. Further, the monocytes are derived from the bone marrow where hematopoietic progenitors generate monocytes and also osteoclastic cells which maintain bone function. Finally, there is mounting evidence to suggest that Hofbauer cells, the macrophages of the placenta, maintain signaling crosstalk from mother to baby during embryogenesis [18,19]. It is clear that MPS cells are part of a complex system that maintains the health and function of tissue and organs and therefore hold key roles in homeostasis and disease development. The complexities of different macrophage functions within different tissues are covered in several recent reviews [20–22].

1.1.2 Macrophage polarization

Macrophages are a plastic cell type capable of reacting to microenvironmental cues [23]. During pathogenesis, this cell type is among the first responders, recognizing pathogen-associated patterns (PAMPs) like lipopolysaccharide (LPS) [24]. LPS engages the Toll-like receptor 4 (TLR-4) on the surface of macrophages to activate transcription factors (e.g. interferon regulatory factors (IRFs) and nuclear factor kappaB (NF- κ B)) to mount an inflammatory response [24,25]. These pro-inflammatory polarized macrophages (M(LPS)), release a variety cytokines, including IL-1 β , IL-6, and TNF- α , facilitating the local recruitment of more macrophages and leukocyte infiltrate to fight against pathogenic insult [26]. In contrast, in wounding microenvironments, extensive release of inflammatory cytokines is potentially detrimental to overall tissue repair. Instead, macrophages respond to cytokines IL-4 and IL-13 released by damaged cells resulting in activation of the STAT6 transcription factor through the Janus kinase – signal transducers and activators of transcription (JAK-STAT) pathway, effectively turning on signature anti-inflammatory genes like arginase (Arg1) and resistin-like molecule α [26–28]. These gene regulatory pathways facilitate the recruitment of more immunoregulatory macrophages (M(IL-4)), release of immunoregulatory cytokines, and

induction of processes like angiogenesis and basement membrane remodeling [29,30]. Based on pro-inflammatory and anti-inflammatory functions of macrophages under different stimuli, a broad classification has been proposed to generalize macrophages as classically activated M1 (pro-inflammatory, activated by LPS or interferon gamma (IFN γ)) or alternatively activated M2 (anti-inflammatory, activated by IL-4, IL-13, or IL-10) phenotypes [31]. Interestingly, these pro-inflammatory and anti-inflammatory pathways can converge with one another [32,33]. Oftentimes, wound sites are also susceptible to pathogen insult, so a balance between macrophage types is necessary for wound resolution. As such, both macrophage types exist within these environments, including macrophages that perform both functions and macrophages that are completely off the M1 and M2 spectrum [32,33]. Clearly, macrophage functions within a specific environment or in a specific disease or homeostatic state are complex. Nonetheless, macrophage activation within these environments and the key roles of macrophage in the development of resolution of complications or disease initiation are well-recognized. As such, macrophages are an important potential therapeutic target [26,34].

1.2 Macrophages in tumorigenesis

1.2.1 Macrophage polarization in tumor development

Macrophages are a large component of the leukocyte infiltrate into the TME. Over the last several decades, tumor-associated macrophages (TAMs) have been a subject of intense study for their impact on leukocytes, cytokines, and inflammatory mediators that either block or propagate tumor progression. Interestingly, the macrophage has been identified as a driver for inflammation, not only in cancer but in other disease states. Indeed, chronic inflammation that arises from diseases such as inflammatory bowel disease, silicosis, and asbestosis, pre-dispose these sites to cancer development. Readers are directed to Elinav et al.'s excellent review on this topic [35].

Interestingly, macrophages seem to have divided loyalties, on one hand promoting tumor resolution (M1/M(LPS)) and on the other propagating tumorigenesis (M2/M(IL-4)) (Figure 1.1). Studies done almost a half century ago have shown that M1 macrophages have the capacity to kill and remove tumor cells, in line with the primary physiological function of M1 macrophages to remove foreign materials [36]. The M1 cells initiate cytokine production within the TME and facilitate tumor cell destruction through recruitment of pro-immunostimulating leukocytes and

phagocytosis of tumor cells. However, studies within that same research period show that M2 macrophages have a central role in tumor propagation [37]. The M2 cells drive tumor development in both primary and metastatic sites through their contributions in basement membrane breakdown and deposition, angiogenesis, recruitment of leukocytes, and overall immune suppression [37–39]. It is important to note that, like normal homeostasis, macrophages within TME are not limited to M1/M(LPS) or M2/M(IL-4) states; they may reside in-between or off this spectrum. Removal of all macrophage populations regardless of polarization state has emerged as a potential therapeutic option, as there is a significant reduction in both primary and metastatic tumorigenesis [40]. However, as illustrated later within this review, the strategy has had a limited clinical impact, unless delivered in combination with other immunological agents, due to limitations in drug delivery and macrophage targeting [41]. On the other hand, the macrophage, regardless of polarization state retains the capacity for plasticity, including the ability to switch between phenotypes as a function of microenvironmental cues. Thus, altering the macrophage phenotype within TME from immune-suppressive to immune-promoting is currently being explored for therapeutic applications [41].

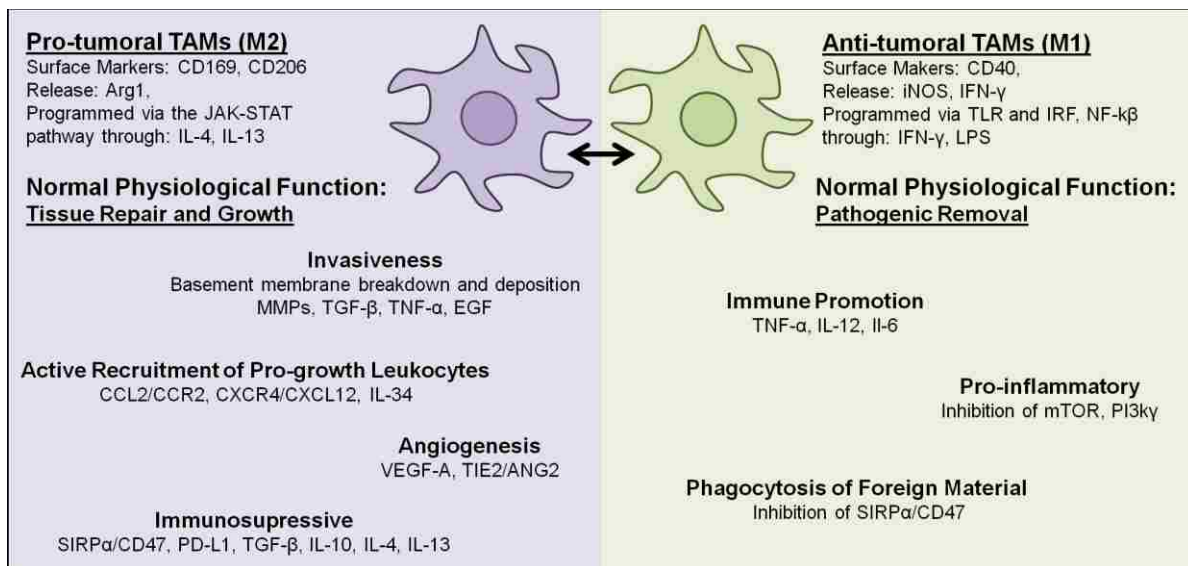


Figure 1.1 Normal physiological macrophage functions that can promote (M2) or reduce tumor growth (M1).

1.2.2 Clinical implication of TAMs

Clinically, the presence of macrophages within primary tumors have been shown to be correlated with poorer prognosis in almost all tumors [7,42], with the exception of colon cancers [43]. Interestingly in recent years, clinicians have expanded these studies to investigate both M1 and M2 phenotypes within these microenvironments. Increasing levels M1 macrophages within these sites indicate better prognosis [44,45] whereas increasing levels of M2 macrophages [42] or decreased lymphocyte to monocyte ratios [46] predict poor outcomes. While these correlation studies have yet to be linked to causation, emerging therapeutic strategies aiming to remove macrophages and/or alter macrophage phenotypes are facilitating promising therapeutic benefits [41].

1.3 Pharmacological modulation of macrophages/TAMs

1.3.1 Bisphosphonate

Bisphosphonates are a family of compounds structurally composed of a central carbon linked by two phosphate groups, R1 and R2 side groups where R1 is H, OH, or Cl and R2 comprises diverse functional groups which determine the potency of the compounds [47]. The first generation non-nitrogen containing bisphosphonates (etidronate, clodronate, and tiludronate) are intracellularly converted to a non-hydrolyzable ATP analogue leading to apoptosis [48]. The second generation (aliphatic amine R2) and third generation (aromatic amine R2) bisphosphonates induce apoptosis by inhibiting the essential enzyme farnesyl diphosphate (FPP) synthase. Bisphosphonates have a high affinity for hydroxyapatite and are frequently used in management of bone diseases such as osteoporosis, Paget disease, and bone metastases. Moreover, pre-clinical studies in murine breast tumor models suggest that bisphosphonate may also exhibit an extraskeletal therapeutic effect [49,50]. In this case, the bisphosphonate (zoledronic acid) primarily binds to microcalcifications present in breast tumors and is subsequently phagocytosed by TAMs to both induce apoptosis and promote M2-to-M1 repolarization. To improve pharmacokinetics, reduce toxic side effects (e.g. osteonecrosis of the jaw), and alter biodistribution away from bone for extraskeletal applications, bisphosphonates are typically formulated into liposomes or nanoparticles [51,52]. Although depletion of TAMs with liposomal clodronate (clodrolip) improves survival in some pre-clinical cancer models, to our knowledge, complete regression of tumors using bisphosphonate alone has not been achieved

[51]. Some of the drugs shown to benefit from depletion of TAMs via bisphosphonates include anti-angiogenesis therapies (sorafenib and anti-VEGF antibody) and liposomal doxorubicin (Doxil) [51,53,54]. In addition to disrupting the pro-tumoral effect of TAMs, associated depletion of resident Kupffer cells has also been shown to reduce hepatic clearance of drug-loaded nanoparticles and hence prolong their plasma circulation time [54,55]. However, not all therapies benefit from depletion of macrophages/TAMs, especially immunotherapies designed to stimulate anti-tumor innate immunity [56–58]. In fact, an indiscriminate depletion of systemic macrophages such as via administration of clodronate liposomes may sometimes exacerbate the disease progression. As examples, depletion of subcapsular sinus CD169⁺ macrophages in tumor-draining lymph nodes is linked to increased tumor burden in B16F10 tumor model while the density of CD169⁺ macrophages in lymph nodes is also positively correlated with favorable prognosis in patients with colorectal and breast cancers [59–61]. These reports further suggest that TAM-targeted therapeutics that spare other potentially beneficial resident macrophages are more desirable than general macrophage depletion strategies. Clinically, bisphosphonates were among the first anti-cancer drug with reported activities on TAMs to be approved for human use, dating back to as early as 1995 for pamidronate and 2002 for zoledronic acid, where they were indicated for use in the management of multiple myeloma and bone-related metastasis (Table 1.1) [62].

Table 1.1 FDA-approved drugs whose mechanisms of action may involve modulation of macrophages/TAMs

Drug	Treatment	Year approved (US FDA)
Bisphosphonate		
Pamidronate/Aredia	Multiple myeloma, metastatic breast cancer	1995
Zoledronic acid/Zometa	Multiple myeloma, bone metastases from solid tumors	2002
Alkylating agent		
Trabectedin/Yondelis	Advanced soft-tissue sarcoma	2007 (EU) [63] 2015 (US)
	Ovarian cancer	2009 (EU) [63]
Tyrosine kinase inhibitor		
Imatinib/Gleevec	Chronic myelogenous leukemia (CML)	2001
Dasatinib/Sprycel	CML, Philadelphia chromosome-positive acute lymphoblastic leukemia (ALL)	2006
	Chronic phase CML	2007
	Chronic phase Philadelphia chromosome-positive CML	2010
Sunitinib/Sutent	Gastrointestinal stromal tumor (GIST), advanced kidney cancer	2006
	Pancreatic neuroendocrine tumors	2011
Nilotinib/Tasigna	CML	2007
Imaging agent		
Tc 99m tilmanocept/ Lymphoseek (CD206 targeting)	Lymphatic mapping in breast cancer and melanoma	2013
	Guiding Sentinel Lymph Node (SLN) Biopsy in squamous cell carcinoma of the oral cavity	2014

Source: www.fda.gov, www.cancer.gov
 These drugs were not necessarily approved due to their actions on TAMs.

1.3.2 Inhibition of growth factor signaling

1.3.2.1 CSF-1R inhibition

Colony stimulating factor 1 receptor (CSF-1R) is a tyrosine kinase receptor expressed on mononuclear phagocytes [64]. Dimerization of the receptor upon binding to CSF-1 or IL-34 leads to a cascade of signaling events which promote proliferation, function, and survival of macrophages [64,65]. Antibodies targeting CSF-1 or CSF-1R as well as CSF-1R kinase inhibitors have been developed for therapeutic modulation of resident macrophages and TAMs [66]. AFS98 and M279 anti-mouse CSF-1R antibodies, capable of blocking both CSF-1 and IL-34, are widely used to study the effect of macrophage depletion in mouse tumor models and have been shown to reduce tumor size and improve survival in MMTV-PyMT spontaneous breast tumor model when administered both early and chronically [66–68]. While intraperitoneal administration of anti CSF-1R antibody systemically depletes resident macrophages in several major organs, a minimal effect is observed in brain, lung, ovary, and uterus likely due to anatomical accessibility (blood brain barrier), tissue turnover rate, or specific stimuli within the

tissue environment [69]. On the other hand, a small molecule CSF-1R kinase inhibitor (BLZ945), which readily passes through blood brain barrier, has been shown to be effective in murine models of glioma, breast cancer, and cervical cancer [70,71]. It is worth noting that tumor recurrence in a murine glioma model following prolonged treatment with BLZ945 is attributed to increased level of IL-4 which enriches TAMs with the CD206⁺ M2-like phenotype [72]. These IL-4 stimulated TAMs secrete insulin-like growth factor-1 (IGF-1) to enhance survival of rebound glioma cells via stimulation of the phosphatidylinositol 3-kinase (PI3k) pathway. A combination therapy of BLZ945 with IGF-1R inhibitor significantly prolonged survival of mice with rebound glioma compared to monotherapy of either BLZ945 or IGF-1R inhibitor highlighting the need for rational design of combinatorial therapy for maximized response to TAM-directed anti-cancer therapy. Due to structural similarities among different receptor tyrosine kinases, tyrosine kinase inhibitors typically recognize multiple targets [73] and as such, several FDA-approved, multi-target tyrosine kinase inhibitors (Table 1.1), initially developed for other targets such as c-KIT, VEGFR, and PDGFR (reviewed in [74]), have now been shown to exhibit activity on the CSF-1R kinase domain [75–77]. New developments of more CSF-1R-specific inhibitors (e.g. PLX3397, PLX7486, BLZ945, and ARRY-382) are also being investigated in clinical trials (Table 1.2). In particular, PLX3397, developed by structure-guided design against the CSF-1R target, exhibits higher affinity and selectivity to CSF-1R than imatinib and demonstrates better efficacy in treatment of tenosynovial giant cell tumor [78]. As a result, the drug has been designated breakthrough therapy status and advanced into clinical trial phase III for the indication. Antibodies targeting CSF-1R are also entering Phase I and II clinical trials for treatment of solid tumors.

1.3.2.2 RON inhibition

RON (Recepteur d'Origine Nantais) is a receptor tyrosine kinase expressed on tissue-resident macrophages that binds to macrophage-stimulating protein (MSP) after its proteolytic activation at inflammation sites [79]. RON signaling in macrophages promotes cell spreading and phagocytosis as well as enhances M2 polarization via stimulation of arginase expression and attenuation of responses to pro-inflammatory stimuli e.g. IFN γ and LPS [80–83]. In prostate and breast cancer models, RON signaling in macrophages has been shown to impair anti-tumor functions of CD8⁺ T cells leading to promotion of tumor growth and metastatic outgrowth

respectively [84,85]. Pharmacologic blockade of RON kinase with an inhibitor, BMS-777607/ASLAN002, boosts the population of pro-inflammatory TNF- α -secreting macrophages and reduces metastatic outgrowth in the lungs in the PyMT-MSP breast tumor model [85]. Alternatively, restoration of iNOS expression in MSP-stimulated macrophages may be achieved via inhibition of PI3k, one of the downstream targets of RON activation [83]. In fact, a synergistic therapeutic effect between the RON kinase inhibitor and a PI3k inhibitor NVP-BKM120 has been reported in a mouse xenograft model of patient-derived breast tumor where cancer cells express constitutively active isoform of RON (short-form RON or sfRON) [86]. Both RON and PI3k inhibitors are being investigated in clinical trials [85,87].

Table 1.2 Selected compilation of drugs in clinical trials whose mechanisms of action may involve modulation of macrophages/TAMs

Drug/Description	Sponsors and collaborators	Phase/ Status	Tumor type	Treatment	ClinicalTrials .govIdentifier	First received
CSF1R inhibitor						
Pexidartinib/PLX3397 (Oral c-fms/KIT/FLT3 tyrosine kinase inhibitor)	Centre Leon Berard and Plexxikon, AstraZeneca	1 Ongoing	Advanced/metastatic colorectal or pancreatic cancer	With Durvalumab (Anti-PD-L1 antibody)	NCT02777710	May 12, 2016
	Plexxikon and Merck Sharp & Dohme Corp.	1/2a Ongoing	Advanced melanoma and other solid tumors	With Pembrolizumab (Anti-PD-1 antibody)	NCT02452424	May 20, 2015
	Daiichi Sankyo Inc.	3 Ongoing	Pigmented villonodular synovitis (PVNS), giant cell tumors of the tendon sheath (GCT-TS), or tenosynovial giant cell tumor (TGCT)	Monotherapy	NCT02371369	February 19, 2015
PLX7486 (Oral c-fms/Trk tyrosine kinase inhibitor, tosylate salt form)	Plexxikon	1 Ongoing	Solid tumors or tumors of any history with activating Trk point or NTRK fusion mutation	Monotherapy	NCT01804530	March 1, 2013
BLZ945 (Oral c-fms tyrosine kinase inhibitor)	Novartis Pharmaceuticals	1/2 Ongoing	Advanced solid tumors	Monotherapy and with PDR001 (Anti-PD-1 antibody)	NCT02829723	July 8, 2016
ARRY-382 (Oral c-fms tyrosine kinase inhibitor)	Array BioPharma	1b/2 Ongoing	Advanced solid tumors	With Pembrolizumab (Anti-PD-1 antibody)	NCT02880371	August 2, 2016
AMG 820 (Human IgG2 anti-CSF-1R antibody)	Amgen	1b/2 Ongoing	Advanced solid tumors	With Pembrolizumab (Anti-PD-1 antibody)	NCT02713529	March 3, 2016
Emactuzumab/RO5509554/RG7155 (Human IgG1 anti-CSF-1R antibody)	Hoffmann-La Roche	1 Ongoing	Solid cancers	With MPDL3280A (Tecentriq/anti-PD-L1 antibody)	NCT02323191	December 5, 2014
	Hoffmann-La Roche	1 Ongoing	Solid tumors	With RO7009789 (Anti-CD40 agonistic antibody)	NCT02760797	April 14, 2016
	M.D. Anderson Cancer Center and Genentech Inc.	2 Ongoing	Platinum-resistant, epithelial ovarian, fallopian tube or primary peritoneal Cancer	With paclitaxel and Bevacizumab (Avastin/anti-VEGF antibody)	NCT02923739	September 30, 2016
LY3022855/IMC-CS4 (Human IgG1 anti-CSF-1R antibody)	Eli Lilly and Company and AstraZeneca	1a/1b Ongoing	Advanced solid tumors	With Durvalumab (Anti-PD-L1 antibody) or Tremelimumab (Anti-CTLA-4 antibody)	NCT02718911	March 21, 2016
Cabiralizumab/FPA008 (Anti-CSF-1R antibody)	Five Prime Therapeutics Inc. and Bristol-Myers Squibb	1a/1b Ongoing	Advanced solid tumors	With BMS-936558 (Nivolumab/anti-PD-1 antibody)	NCT02526017	August 13, 2015
RON/MET inhibition						
ASLAN002/BMS777607 (Oral RON/MET receptor tyrosine kinase inhibitor)	Aslan Pharmaceuticals	1 Completed	Malignant solid tumors	Monotherapy	NCT01721148	November 1, 2012
CD47-SIRPα inhibitor						
Hu5F9-G4 (Human IgG4 Anti-CD47 antibody)	Forty Seven Inc.	1b/2 Ongoing	Colorectal neoplasms or solid tumors	With Cetuximab (Erbix/anti-EGFR antibody)	NCT02953782	November 1, 2016
	Forty Seven Inc.	1b/2 Ongoing	Non-Hodgkin's lymphoma or diffuse large B-cell diffuse lymphoma, indolent lymphoma	With Rituximab (Anti-CD20 antibody)	NCT02953509	November 1, 2016

CC-90002 (Anti-CD47 antibody)	Celgene	1 Ongoing	Acute myeloid leukemia or myelodysplastic syndromes	Monotherapy	NCT02641002	November 12, 2015
TTI-621 (SIRP α -Fc fusion)	Trillium Therapeutics Inc.	1 Ongoing	Solid tumors or mycosis fungoides	Monotherapy	NCT02890368	August 26, 2016
ALX148 (High affinity SIRP α variant)	Alexo Therapeutics Inc.	1 Ongoing	Metastatic cancer, solid tumor, advanced cancer, or non-Hodgkin's lymphoma	Monotherapy, with Atezolizumab (Tecentriq/anti-PD-L1 antibody) or Transtuzumab (Herceptin/anti-HER2 antibody)	NCT03013218	December 15, 2016
CCR2-CCL2 inhibitor PF-04136309/PF6309 (Small molecule CCR2 antagonist)	Pfizer	1b/2 Ongoing	Metastatic pancreatic ductal adenocarcinoma	With Nab-paclitaxel and gemcitabine	NCT02732938	February 29, 2016
MLN1202/S0916/plozalizumab (Human anti-CCR2 antibody)	Millennium Pharmaceuticals Inc.	1 Ongoing	Melanoma	With Nivolumab (Anti-PD-1 antibody)	NCT02723006	March 25, 2016
Carlumab/CNTO 888 (Human IgG1 κ anti-CCL2 antibody)	Centocor Inc.	1 Completed	Cancer	With DOXIL, gemcitabine, paclitaxel + carboplatin, or docetaxel	NCT01204996	September 16, 2010
CXCR4-CXCL12 inhibitor Mozobil/AMD-3100/plerixafor* (Small molecule CXCR4 antagonist)	CCTU-Cancer Theme, Sanofi, Stand Up To Cancer, CRUK Cambridge Institute, Lustgarten Foundation, and National Institute for Health Research (UK)	1 Ongoing	Metastatic pancreatic adenocarcinoma, ovarian serous adenocarcinoma, or metastatic colorectal cancer	Monotherapy	NCT02179970	July 1, 2014
LY2510924 (CXCR4 agonistic peptide)	Eli Lilly and Company and AstraZeneca	1 Ongoing	Solid tumors	With Durvalumab (Anti-PD-L1 antibody)	NCT02737072	April 8, 2016
CD40 agonist CP-870,893/RO7009789 (Human IgG2 anti-CD40 antibody)	Abramson Cancer Center of the University of Pennsylvania Hoffmann-La Roche	1 Ongoing	Recurrent/stage IV melanoma	with Tremelimumab (Anti-CTLA-4 antibody)	NCT01103635	April 12, 2010
	Hoffmann-La Roche	1 Ongoing	Solid cancers	with MPDL3280A (Tecentriq/anti-PD-L1 antibody)	NCT02304393	November 26, 2014
	Abramson Cancer Center of the University of Pennsylvania Hoffmann-La Roche	1 Ongoing	Pancreatic cancer	With nab-paclitaxel and gemcitabine	NCT02588443	October 21, 2015
	Hoffmann-La Roche	1 Ongoing	Advanced/metastatic solid tumors	With Vanucizumab (Bispecific anti-Ang2/VEGF-A antibody)	NCT02665416	January 15, 2016
	Hoffmann-La Roche	1 Ongoing	Solid tumors	With Emactuzumab (Anti-CSF-1R antibody)	NCT02760797	April 14, 2016
Vasculature-modulating agent Vanucizumab (Human bispecific anti-Ang2/VEGF antibody)	Hoffmann-La Roche	1 Ongoing	Neoplasms	With Atezolizumab (Anti-PD-L1 antibody)	NCT01688206	September 13, 2012
	Hoffmann-La Roche	1 Ongoing	Advanced/metastatic solid tumors	With RO7009789 (Anti-CD40 antibody)	NCT02665416	January 15, 2016
Vadimezan/5,6-dimethylxanthenone-4-acetic acid (DMXAA) (Vasculature-disrupting agent)	Swiss Group for Clinical Cancer Research	2 Completed	Lung cancer	With carboplatin and paclitaxel	NCT01057342	January 26, 2010

PI3kγ inhibitor Duvelisib/IPI-549 (Oral PI3k δ/γ inhibitor)	Infinity Pharmaceuticals Inc.	1 Ongoing	Advanced solid tumors, non-small cell lung cancer (NSCLC), melanoma, or squamous cell cancer of the head and neck	With Nivolumab (Anti-PD-1 antibody)	NCT02637531	December 16, 2015
---	-------------------------------	--------------	---	-------------------------------------	-------------	-------------------

Source: clinicaltrials.gov, www.cancer.gov

This compilation highlights the recently initiated clinical trials with emphasis on combination therapy.

“Ongoing” includes both recruiting and non-recruiting stages.

*Approved for use in combination with G-MCSF to mobilize hematopoietic stem cells to peripheral blood for collection and subsequent autologous transplantation in patients with non-Hodgkin’s lymphoma and multiple myeloma.

1.3.3 Modulation of macrophage phagocytic activity

1.3.3.1 Antibody-dependent cellular phagocytosis (ADCP)

Two important innate immune functions of macrophages are phagocytosis of foreign bodies, apoptotic cells, as well as cancer cells and processing of the engulfed materials for antigen presentation to stimulate adaptive immunity [88]. Tumor-targeted antibodies are a powerful class of anti-cancer biologics that act through direct inhibition of survival signaling, mediation of antibody-dependent cellular cytotoxicity (ADCC) by natural killer (NK) cells, induction of complement-dependent cytotoxicity (CDC) via complement cascade activation, and facilitation of antibody-dependent cellular phagocytosis (ADCP) by macrophages [89]. Clinically approved anti-cancer monoclonal antibodies such as rituximab and trastuzumab have been demonstrated to exert their therapeutic effects, primarily or in part, through macrophage-mediated ADCP [90,91]. Contrary to their capability to promote tumor invasion, TAMs are also able to phagocytose cancer cells in the presence of the opsonizing tumor-targeted antibodies [92]. Nonetheless, the therapeutic efficacy of these antibodies may be limited by counter mechanisms including antigenic modulation and trogocytosis, both of which remove antibody-antigen complexes off target cell plasma membrane [90,93]. Of note, trogocytosis has recently been shown to induce cell death complimentary to whole cell phagocytosis [94]. To further improve ADCP activity, the Fc region of tumor-targeted antibodies could be engineered to increase its interaction with activatory Fc receptors, most importantly Fc γ RIIa, on macrophages [95]. While development of clinical antibodies is primarily focused on IgG, therapeutic potentials of other Ig isotypes (IgA and IgE) are being investigated in several pre-clinical studies where monocytes/macrophages are also important in effecting the ADCC/ADCP functions [96,97].

1.3.3.2 Inhibition of CD47-SIRP α signaling

Successful development and maturation of tumors require effective evasion from such immune-surveillance activities [98]. In several tumor types, cancer cells block phagocytosis by upregulating surface expression of CD47 which interacts with signal regulatory protein alpha (SIRP α) on macrophages to transmit the “don’t eat me” signal. Inhibiting the CD47-SIRP α signaling axis with anti-CD47 antibodies or an engineered SIRP α -Fc fusion has been shown to restore macrophage ability to phagocytose cancer cells and prime a cytotoxic CD8⁺ T-cell response, leading to a significant reduction in tumor size and metastasis in several cancer models [98,99]. With promising results in pre-clinical studies, numerous clinical trials have been initiated in the past few years to investigate different therapeutic variants including anti-CD47 antibody (Hu5F9-G4 and CC-90002), engineered high affinity SIRP α (ALX148), and SIRP α -Fc fusion (TTI-621) (Table 1.2). One potential challenge in clinical translation of anti-CD47 therapies is the ubiquitous expression of CD47 on red blood cells and hematopoietic stem cells which may serve as an antibody sink to reduce efficacy while also causing transient anemia [100,101]. Alternative strategies have been investigated including targeted blocking of SIRP α with engineered high affinity CD47 ectodomain or development of bispecific antibody targeting both CD47 and tumor-associated antigen [101,102]. To minimize possible off-target toxicity, anti-CD47 antibody may be developed using the Fc scaffold of IgG4 to reduce Fc effector functions, or the engineered SIRP α without Fc fusion may be used in combination with Fc-active tumor-targeted antibodies [100,103].

1.3.4 Inhibition of inflammatory monocyte/macrophage recruitment

1.3.4.1 Inhibition of CCR2-CCL2 signaling

The number of intratumoral TAMs increases with tumor growth due to self-proliferation as well as recruitment and differentiation from circulating inflammatory Ly6C⁺CCR2⁺ monocytes [104]. The latter is mediated by elevated secretion of CCL2 (also known as monocyte chemoattractant protein-1 (MCP-1)), the ligand for CCR2, by cancer and stromal cells in tumors and associated metastases [105–107]. As a chemotactic factor, CCL2 mobilizes bone marrow-resident inflammatory monocytes into circulation and subsequently into the tumors. High expression of CCL2 in tumors and high count of CCR2⁺ monocytes in the peripheral blood are both correlated with poor prognosis in several cancer types [105,108,109]. Strategies to

pharmacologically interrupt CCR2-CCL2 signaling axis (e.g. CCR2 small molecule inhibitor, anti-CCR2 antibody, and anti-CCL2 antibody) have been developed as anti-cancer therapies [110]. In a pancreatic mouse cancer model, a small molecule CCR2 inhibitor (PF-04136309) effectively reduces recruitment of inflammatory monocytes into the tumors resulting in reduced tumor growth and fewer liver metastases [105]. Anti-CCL2 antibodies have been shown to prevent metastasis in breast and prostate cancer models [111,112]. However, in the breast cancer model, discontinuation of the treatment accelerated metastases as a result of increased tumor localization of monocytes that were originally sequestered in bone marrow during the antibody treatment [111].

1.3.4.2 Inhibition of CXCR4-CXCL12 signaling

In addition to the CCR2-CCL2 signaling axis, CXCR4-CXCL12 (also known as stromal cell-derived factor-1 (SDF-1)) interaction is another signaling axis involved in recruitment of monocytes/macrophages and implicated in promotion of tumor invasiveness/regrowth [113,114]. Mechanistically, CXCL12 is secreted by both tumor and stromal cells including TAMs, and hence, mediates both autocrine and paracrine signaling in recruiting and differentiating monocytes expressing its receptor CXCR4 into tumor-infiltrating TAMs [115]. In glioma and breast cancer models, anti-cancer treatments with radiation therapy or chemotherapy have been shown to increase the level of CXCL12 in the perivascular region of tumors which in turn promotes accumulation of CXCR4⁺ TAMs [114,115]. Secretion of vascular endothelial growth factor A (VEGF-A) by these TAMs stimulates formation of new tumor vasculature and tumor relapse, the effects of which could be inhibited by treatment with CXCR4 inhibitor (AMD3100). Given multiple signaling pathways in monocyte/macrophage recruitment, simultaneous blockades of different signaling axes may be necessary to achieve the optimal effect.

1.3.5 Immunostimulation by anti-CD40 agonistic antibody

CD40 is a member of the tumor necrotic factor (TNF) receptor family expressed on antigen-presenting cells (APCs), monocytes, B cells, as well as in some tumors [116]. Since ligation between CD40 on APCs and CD40 ligand (CD40L) on T cells stimulates these APCs to activate effector T cells for anti-tumor response, the therapeutic effect of anti-CD40 agonistic antibody was thought to act through a similar mechanism. However, in a KPC mouse model of

pancreatic ductal adenocarcinoma (PDA), depletion experiments of different immune cell populations revealed that the anti-tumor effect of the antibody could be mediated in a T cell-independent manner, requiring only the tumor infiltration of macrophages [117]. Mechanistically, systemic administration of anti-CD40 antibody raises the serum level of CCL2 and IFN γ where the former recruits inflammatory monocytes to the tumors, and the latter reprograms the recruited monocytes/macrophages for tumoricidal activities [118]. Interestingly, further optimization of anti-CD40 antibody by testing different IgG subclasses indicates that its agonistic immunostimulatory activity requires effective engagement of the antibody Fc domain with inhibitory Fc γ RIIb but not with other activatory Fc receptors (needed for ADCC/CDC) [119]. Consistent with the preclinical finding that the agonistic activity of anti-CD40 antibody is mediated more robustly when the activatory/inhibitory Fc receptor binding ratio (A/I) is lower [120], Pfizer's human anti-CD40 antibody of IgG2 subclass (CP-870,893) has been shown in clinical trials to be more agonistic in immunostimulation compared to the other candidates (e.g. dacetuzumab, Chi Lob 7/4, and HCD122), the rest of which have IgG1 subclass (Table S1.1) [116].

1.3.6 Inhibition of angiogenic signaling

One of the essential pro-tumoral functions of macrophages is promotion of angiogenesis. The TIE2⁺ subpopulation, also called TIE2-expressing monocytes/macrophages (TEMs), has been shown to predominantly contribute to this role [6]. TEMs are typically recruited from circulation into the perivascular region of tumors where their pro-angiogenic activities are stimulated upon interaction of TIE2 with the corresponding ligand angiopoietin 2 (ANG2), secreted in several tumors [121,122]. Mazzieri et al. demonstrated that therapeutic blockade of ANG2 with an anti-ANG2 antibody reduced angiogenesis and tumor growth in mammary and pancreatic tumor models by preventing association between TEMs and angiogenic blood vessels as well as suppressing expression of TIE2 in TEMs [121]. Since upregulation of ANG2 is one of the resistance mechanisms to anti-VEGF therapy, dual targeting of both ANG2 and VEGF via either combination therapy or bispecific antibody has been investigated as a strategy to circumvent the therapeutic resistance [123,124]. Interestingly, in both highly vasculature-aberrant G1261 as well as less aberrant MGG8 glioblastoma models, treatment with bispecific anti-ANG2/VEGF-A antibody (CrossMab, A2V) successfully improved survival the effect of

which was attributed to the antibody-induced M2-to-M1 reprogramming of TAMs [124]. Similarly, a vascular-disrupting agent 5,6-dimethylxanthenone-4-acetic acid (DMXAA), initially developed for disrupting tumor vasculature, has also been shown to activate immunostimulatory functions of TAMs, which in turn orchestrate anti-tumor response of CD8⁺ T cells [125].

1.3.7 Metabolic modulation of macrophages/TAMs

1.3.7.1 mTOR inhibition

Macrophages of different functional states vary in their use of metabolic pathways for energy and metabolite production to support their specialized cellular activities [126]. Mammalian target of rapamycin (mTOR) signaling through mTOR complex 1 (mTORC1) and mTORC2 serves a central role in sensing nutrients, oxygen, and metabolites to direct metabolic programming of these macrophages [127]. In addition to its direct cytotoxic effect on cancer cells [128], rapamycin, an mTORC1-specific inhibitor, has been shown to stimulate macrophages to the M1-like phenotype with an anti-tumor effect in Huh-7 hepatocarcinoma mouse model [129]. Of note, other signaling molecules upstream of mTOR (e.g. PI3k γ , protein kinase B (Akt), and phosphatase and tensin homolog deleted on chromosome 10 (PTEN)) are also involved in shaping polarization and functions of macrophages/TAMs, making them potential targets for anti-cancer therapies [130–132]. As an example, Kaneda et al. recently showed that PI3k γ inhibitor (IPI-549) retarded tumor growth in implanted human papilloma virus positive head and neck squamous cell carcinoma (HPV⁺HNSCC), lung carcinoma, and breast carcinoma models in a TAM-dependent manner by promoting TAM-immunostimulatory responses [130]. Similarly, expression of PTEN (PI3k suppressor) or silencing of Akt1 can also promote anti-tumor M1 macrophage polarization [131,132].

1.3.7.2 Modulation of PPAR γ -Gpr132-lactate signaling

The TME is enriched for lactate which is secreted by cancer cells performing glycolysis [133]. It is now known that the recognition of lactate by Gpr132 (G-protein coupled receptor) on TAMs promotes M2 polarization of these TAMs while the expression of Gpr132 is under a suppressive control of peroxisome proliferator-activated receptor (PPAR γ) transcription factor [134,135]. Several strategies have been developed to interrupt this signaling axis. For example, supply of lactate for M2-TAM polarization could be blocked using an inhibitor of lactate

dehydrogenase (oxamic acid) [134]. Alternatively, PPAR γ agonists (e.g. thiazolidinedione family of drugs) or siRNA silencing of Gpr132 have been successfully used to insensitize TAMs to lactate stimulation with a tumor-shrinking effect in EO771 breast tumor model [135].

1.3.7.3 Inhibition of metabolism of amino acids and lipids

In addition to competition for glucose, TAMs readily catabolize arginine and tryptophan which are essential amino acids required for anti-tumor T cell functions [126]. Restoration of these nutrients by inhibiting arginase, nitric oxide synthase, and indoleamine 2, 3-dioxygenase (IDO) constitutes another promising therapeutic intervention to improve T cell survival and functions [136,137]. Moreover, TAMs are also known to mediate immunosuppressive and metastasis-promoting functions in response to cancer cell/TAM-secreted lipid metabolites such as prostaglandin E₂ (PGE₂) and sphingosine-1-phosphate (S1P) [138–140]. Pharmacological inhibition of PGE₂-producing enzymes microsomal PGE₂ synthase 1 (mPGES1) and cyclooxygenase-2 (COX-2), with CAY10526 and celecoxib respectively, effectively reduced PGE₂ level in bone marrow cell/MBT-2 bladder cancer cell coculture with celecoxib being further shown to lower expression of T cell-suppressive programmed cell death ligand 1 (PD-L1) in an MBT-2 cancer model and also promote M2-to-M1 polarization of TAMs in an *Apc^{min/+}* colon cancer model [139,141].

1.3.7.4 Modulation of essential elements and vitamins

Iron metabolism is vastly different between M1- and M2-polarized macrophages [142]. M1 macrophages upregulate ferritin to promote intracellular iron retention whereas M2 macrophages upregulate ferroportin to enhance iron efflux. Consistent with the M2-like phenotype, TAMs preferentially liberate iron and provide cancer cells with this essential element for promoting proliferation. Several iron chelators are being evaluated as anti-cancer agents [143]. Iron chelation therapy has recently been shown to reverse iron-processing function of M2 macrophages from iron release towards sequestration and block tumor-promoting effect of the macrophages [144]. Conversely, external supply of iron through administration of ferumoxytol iron oxide nanoparticles has also been shown to be therapeutic at inhibiting tumor growth and metastasis by stimulating pro-inflammatory macrophage polarization and production of ROS

[145]. These seemingly contradictory results regarding iron supply and macrophage response emphasize the need for further study in this area.

In another example, macrophages may secrete a host-defense peptide, cathelicidin, shown to readily lyse proliferating B cell lymphoma cells but not normal B cells [146]. Cathelicidin production requires intracellular metabolism of 25-hydroxyvitamin D (25D) into bioactive 1,25-dihydroxyvitamin D (1,25D3) by vitamin D-1-hydroxylase CYP27B1, which is expressed at lower levels in M2 macrophages and TAMs compared to M1 macrophages. Treating M2 macrophages with 1,25D3 successfully restores cathelicidin production and cytotoxicity against the B cell lymphoma cells [146].

1.3.8 Modulation of macrophage scavenger receptors

Scavenger receptors comprise a family of receptors that broadly recognize modified low-density lipoproteins, polyanions, endogenous proteins, as well as conserved microbial structures and are important for clearing foreign particles, pathogens, and apoptotic cells from the body [147]. Several scavenger receptors (e.g. scavenger receptor class A (SR-A1), macrophage receptor with collagenous structure (MARCO), CD36, CD68, CD163, and receptor for advanced glycation endproducts (RAGE)) are expressed on macrophages, some of which are involved in regulation of tumor immunity and are therefore potential targets for therapeutic modulation [148,149]. As an example, apolipoprotein A-I mimetic peptide 4F, a competing ligand for SR-A1, has been shown to inhibit tumor growth and metastasis in ovarian and pancreatic tumor models [150]. The proposed mechanisms of action involve interrupting TAM/cancer cell crosstalk, blocking SR-A1 from scavenging ECM components that allow for cancer cell migration, and scavenging of pro-inflammatory/angiogenic lysophosphatidic acid (LPA) [151]. However, in the context of glioma model, Zhang et al. demonstrated that recognition of tumor-secreted heat shock protein 70 (HSP70) by SR-A1 is important in suppressing M2 polarization in TAMs and is needed for inhibition of glioma proliferation and angiogenesis [152]. These studies highlight the context-dependent effect in modulation of scavenger receptor activity as a result of its recognition of a broad range of ligands.

1.3.9 Chemotherapy drugs

Although chemotherapy drugs are primarily developed to induce cell death in rapidly dividing cancer cells, many also have pharmacological effects on non-cancer cell populations. In particular, trabectedin and its second generation lurbectedin are effective at killing TAMs in addition to cancer cells [153,154]. Mechanistically, trabectedin interacts with tumor necrosis factor-related apoptosis inducing ligand receptor 2 (TRAIL-R2) on mononuclear phagocytes leading to receptor clustering and subsequent caspase-8 dependent activation of apoptosis [154,155]. Its selective toxicity in TAMs over neutrophils and lymphocytes has been attributed to higher expression of the receptor in conjunction with lower expression of non-signaling decoy TRAIL-R3. In addition, trabectedin also inhibits production of chemoattractant cytokine CCL2 by TAMs and tumor cells [156]. Apart from exerting a cytotoxic effect, several chemotherapy drugs modulate macrophage responses to tumor [157,158]. In murine fibrosarcoma and mammary tumor models, microtubule-stabilizing agents such as docetaxel and paclitaxel have been shown to promote polarization of myeloid-derived suppresser cells (MDSCs) to macrophages with anti-tumor M1-phenotype via suppression of STAT3 phosphorylation [159,160]. Cyclophosphamide treatment promotes infiltration of macrophages, enhances secretion of pro-inflammatory cytokines (IL-6 and IL-12), and suppresses production of pro-tumoral M2-related cytokines (IL-4, IL-10, and IL-13) [161,162]. As a self-protective mechanism against chemotherapies, chemo-resistant cancer cells secrete IL-34 which enhances their survival as well as promotes M2 polarization of TAMs to further reinforce immunosuppressive functions [163]. In addition, chemotherapy treatments may also increase intratumoral level of CXCL12, which serves as a chemotactic factor in recruiting TIE2⁺CXCR4⁺ macrophages to the perivascular region of the tumor where they preferentially promote angiogenesis and tumor regrowth [113]. To combat these resistance mechanisms, an integration of chemotherapy and immunotherapy may allow for a more effective tumor regression. Of note, paclitaxel and gemcitabine are two chemotherapy drugs commonly investigated in a combination therapy with other TAM-modulating therapeutics due to their possible promotion of antigen release following cancer cell death (Table 1.2 and S1.1).

1.3.10 Activation of Toll-like receptors (TLRs)

Toll-like receptors (TLRs), expressed on either plasma membranes (TLR1, 2, 4, 5, 6, and 10) or endosomal membranes (TLR3, 7, 8, and 9) of APCs, recognize various PAMPs and damage-associated molecular patterns (DAMPs), constituting an indispensable system for innate immune surveillance [164]. In regard to modulation of TAMs, several TLR agonists (e.g. polyinosinic:polycytidylic acid (polyI:C) for TLR3, LPS for TLR4, imiquimod for TLR7, and CpG-oligonucleotide for TLR9) have been shown to activate NF- κ B leading to pro-inflammatory M1 polarization (reviewed in [165]). Moreover, TLR signaling may also be initiated by chemotherapy drugs via induction of immunogenic cell death (ICD) [166]. Oftentimes, engaging multiple TLRs is essential to effect a more potent anti-tumor response. As an example, a recent study by Zheng et al. reported development of a dual TLR4/5 stimulating bacterial cell therapy (BCT) based on attenuated Δ ppGpp *Salmonella typhimurium* (TLR4 agonist) with inducible production of *Vibrio vulnificus* flagellin B (FlaB, TLR5 agonist) [167]. The dual stimulation was more effective at reprogramming TAMs from CD206⁺ M2 phenotype to immunostimulating CD86⁺ M1 phenotype. Despite the anti-tumor effect of NF- κ B activation being observed in TLR agonistic therapies, an opposite finding has also been reported where inhibition of I κ B kinase β (IKK β), the main downstream activator molecule of NF- κ B, repolarizes TAMs to IL-12-secreting, NO-producing M1 phenotype with a growth inhibition effect in an ID8 ovarian tumor model [168]. These opposing reports on pro-tumoral/anti-tumoral effects of NF- κ B activation may imply involvement of other determining parameters (e.g. the presence of other signaling factors that shape TLR responses or the effects of TLR signaling on other cell populations in TME) that collectively dictate the overall response to the therapies and highlight the need to thoroughly understand the immunological context of tumor for effective tailoring of anti-cancer therapy.

1.4 Targeted drug delivery systems to macrophages/TAMs

With promising drugs for different molecular targets being identified that could potentially modulate TAMs to effect an anti-tumor response, the next challenge has been how to deliver these immunomodulating drugs effectively and selectively to TAMs while minimizing off-target side effects. Passive targeting to tumor via the enhanced permeability and retention (EPR) effect opens up the field of cancer nanomedicine with extensive development and

characterization of nanoparticle systems for tumor targeting. As a result, we also gain more understanding about parameters that influence internalization by macrophages (e.g. Kupffer cells), the main player in the mononuclear phagocyte system responsible for clearance of nanomedicine. This section describes parameters that dictate passive targeting of macrophages/TAMs as well as targeting ligands being investigated pre-clinically for active targeting of macrophages/TAMs.

1.4.1 Passive targeting to macrophages/TAMs

Due to their primary role in clearing cellular debris, pathogens, and foreign substances, macrophages possess high phagocytic capability. Micro/nanoparticles are relatively indiscriminately internalized by macrophages, although the rate and extent of uptake is affected by properties such as shape, size, rigidity, contact angle, and surface charge (Figure 1.2) [169–172]. For nanoparticles/liposomes larger than 100 nm, most studies report increased uptake with increasing particle size up to about 1 - 3 μm , after which uptake declines [169,173]. On the other hand, for nanoparticles/liposomes smaller than 100 nm, most studies report increased uptake with decreasing particle size [174–176]. Contrasting trends are also observed which may be partially attributed to differences in nanoparticle composition and macrophage source, as well as involvement of other uptake mechanisms [177–179]. In term of charge, nanoparticles with either highly positive or highly negative zeta potentials are preferentially internalized compared to the ones with near neutral or slightly negative zeta potentials [169,177]. In general, rigid and spherical nanoparticles are more readily uptaken by macrophages than soft and cylindrical nanoparticles [172,180–183].

Recently, MacParland et al. reported a comparative study on nanoparticle uptake by human monocyte-derived macrophages of different phenotypic polarization [184]. In general, M2-polarized human macrophages exhibit higher internalization of gold nanoparticles than the M1-polarized cells, and the extent of uptake is positively correlated with the expression of M2 markers CD163 and CD206. Further investigation on the nanoparticle uptake by unstimulated and stimulated M1- or M2-polarized Kupffer cells from deceased donors showed that the unstimulated Kupffer cells, possessing a mixed M1/M2 phenotype, exhibited comparable internalization of nanoparticles to the M2-polarized cells, both of which ingested more nanoparticles than the M1-polarized cells did.

While the natural tendency of M2 macrophages to more readily internalize nanoparticles could be beneficial for designing TAM-targeted therapy, the resident macrophages' penchant for internalizing nanoparticles is still an important challenge in developing TAM-targeted therapies [181,185–187]. While this ability might be exploited to target TAMs in liver cancer or metastasis, delivery of NP-based formulations to TAMs at other sites must compete with avid internalization by hepatic and splenic macrophages [180,188]. In fact, the current mainstay for depletion of TAMs in animal cancer models utilizes liposomal clodronate, which relies on passive accumulation of liposomes in the macrophages and therefore indiscriminately affects both TAMs and resident macrophages [52,189].

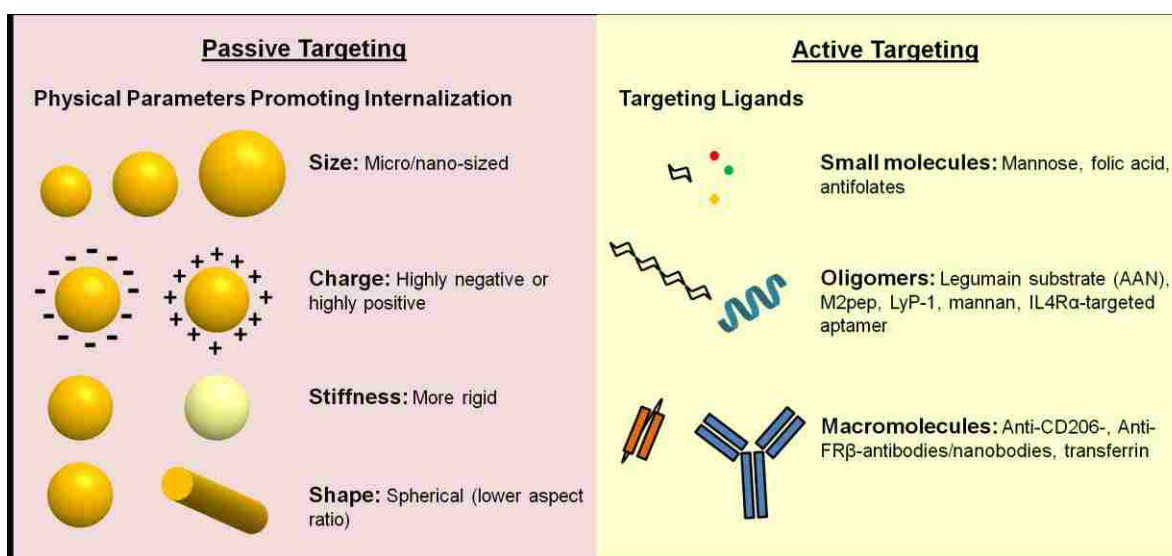


Figure 1.2 Strategies to promote passive and active targeting of macrophages/TAMs.

1.4.2 Active targeting to macrophages/TAMs

Targeting ligands are also employed to facilitate preferential delivery to TAMs via specific ligand-receptor interaction (Figure 1.2). Mannose receptor (CD206) is one of the most commonly targeted receptors for macrophage delivery due to its overexpression on M2 macrophages [190]. As a simple sugar, the native ligand mannose can be easily conjugated to carriers but binds with low affinity. Thus, anti-CD206 antibody has also been developed for

targeting TAMs [191]. Although CD206-targeted drug delivery systems can achieve high M2/M1 selectivity, they are readily sequestered in liver by resident macrophages and liver sinusoidal endothelial cells which also express high level of the receptor [192].

TAMs also overexpress folate receptor beta (FR β), which can be targeted using its ligand, folic acid [193,194]. To improve selectivity over folate receptor alpha (FR α), reduced folate carrier (RFC), and proton-coupled folate transporter (PCFT) which are expressed on both cancerous and non-cancerous tissues, various antifolate analogs have been developed a few of which exhibit significant FR β selectivity over the rest [195]. Anti-FR β Fv is also successfully used to selectively target FR β ⁺ TAMs [196]. While expression of FR β is more restricted than FR α , several studies have reported that FR β is also expressed on pro-inflammatory activated M1 macrophages [197–199].

Legumain and transferrin receptor are two other target receptors overexpressed on M2-TAMs compared to M1-TAMs but that are also present on several cancer cell types [200–202]. The proteolytic activity of legumain specific to the Ala-Ala-Asn substrate sequence has been used in the design of pro-drugs or smart drug delivery systems that target both TAMs and cancer cells [200,203,204]. Although many drug delivery systems targeting transferrin receptor have been reported, to our knowledge, all these systems are tailored toward targeting cancer cells expressing the receptor or enhancing transcytosis across blood brain barrier, and neither the effect on nor the application to affect TAMs has been reported [205–207].

In order to improve TAM selectivity over resident macrophages, a few groups have employed unique physical properties of TME to rationally design their targeting systems [190,203,208]. As an example, Zhu et al. reported the development of mannosylated PLGA nanoparticles that are masked with acid-sensitive PEG(2000) that prevents recognition by resident macrophages but is cleaved in the acidic TME to expose mannose for intratumoral TAM targeting [190]. In another study, Movahedi and Schoonooghe et al. demonstrated the use of excess unlabeled bivalent anti-MMR nanobody as a decoy to reduce background signal of ^{99m}Tc-labeled monovalent anti-MMR nanobody in liver and spleen [208]. The bivalent nanobody competitively binds to resident macrophages with higher avidity over the monovalent nanobody but has poor tumor penetration due to its bigger size, whereas the monovalent nanobody can diffuse into tumor to label M2-TAMs for imaging.

On our part, we have developed an M2 macrophage-targeting peptide (M2pep) via peptide phage display screening [209]. The peptide binds to M2 macrophages and M2-TAMs selectively over M1 and M0 macrophages as well as over other leukocytes. Further optimization of the peptide improves its serum stability and affinity, and enables enhanced targeting to M2-TAMs in syngeneic CT26 colon cancer and 4T1 breast cancer models [210,211]. Multivalent display of the peptide further improves binding avidity to M2 macrophages [212]. The small size and easy production of M2pep make it a promising and attractive targeting ligand for developing M2-TAM-targeted therapeutics.

1.5 Macrophages as a therapeutic depot

Macrophages receive considerable interest as a drug delivery carrier due to their tumor-homing property, high phagocytic capability of drug-loaded nanoparticles, and ability to directly kill cancer cells given the right immuno-stimulating environment [213]. For examples, peritoneal macrophages may be harvested, incubated with drugs, typically in nanoparticle/liposome formulations, for loading, and then infused back to animals/patients [214,215], or nanoparticles with appropriate size and/or ligand may be directly injected *in vivo* and get uptaken by resident macrophages/TAMs in the body for subsequent sustained release [188,216,217]. While both strategies significantly improve the circulation half-life of the drugs, the long-term survival of the macrophage host is limited by toxicity of the drug, and hence, most of the drugs are loaded in the nanoparticle or liposome formulations to reduce acute toxicity to the macrophage carrier [214,216]. Interestingly, Tanei et al. observed increased expression of p-glycoprotein efflux pump in albumin-bound paclitaxel nanoparticle-loaded macrophages compared to the unloaded control and attributed this as one of the possible mechanisms to preserve macrophage viability as well as to enable drug release to the surrounding e.g. TME [188]. In the case where drug is not toxic to macrophages, appropriate formulation enables sustained release of the loaded drug from macrophages for up to at least 2 weeks as demonstrated by Dou et al. for indinavir nanoparticle-loaded macrophages [218,219]. With proper nanoparticle encapsulation strategies to achieve intracellular stability, it is even possible to load biologics such as proteins into macrophages [220,221]. Equally important to effective drug loading is the ability of drug-laden macrophages to migrate to tumor. A study by Chang and Guo et al. shows that the size of nanoparticles internalized by macrophages can significantly alter locomotivity of the macrophages, with

smaller nanoparticles (30 and 50 nm) having higher uptake into macrophages than larger nanoparticles (100 and 500 nm) but also more readily retarding the migration rate of the macrophages; this study suggests that 100 nm nanoparticles provide a good balance for effective drug loading and macrophage migration [174]. To increase control over drug activity from macrophage carriers, macrophage have been loaded with temperature-responsive liposomes for triggered release [216], with gold-silica nanoshells for photothermal therapy [215], and with iron oxide nanoparticles for dual tracking and trafficking using electromagnetic actuation [214,222,223].

Recently, an additional role of TAMs as a processing factory for antibody-drug conjugates (ADCs) has been reported [224]. Specifically, Li et al. observed an anti-tumor activity of non-targeted humanized IgG conjugated to protease-cleavable monomethyl auristatin E (hIgG-vaMMAE) in L-82 anaplastic large cell lymphoma and MCF-7 breast cancer xenograft models and further demonstrated, in a panel of xenograft models, that the efficacy is positively correlated with the extent of F4/80⁺ TAM infiltrate. Mechanistic investigation revealed the two key parameters for the TAM-mediated, antigen-independent, anti-tumor activity; (1) binding and internalization of ADCs to Fc γ R on TAMs for processing and release of drug and (2) membrane permeability of drug to mediate the by-stander effect once released from TAMs. This report provides the first evidence on the possible contribution of TAMs on efficacy of ADCs and presents an underexplored opportunity of TAM-targeted ADC engineering.

Instead of loading drugs into macrophages, it is also possible to genetically engineer them to produce therapeutic proteins. As an example, Palma and Mazziere et al. transduced hematopoietic/progenitor stem cells (HPSCs) with lentiviral vector encoding *Ifna1* under control of *Tie2* promoter/enhancer elements. When transplanted into tumor-bearing mice, a subpopulation of these cells matured into TEMs and homed to the tumor where their TIE2 expression was further heightened resulting in localized production of IFN α that provided an anti-tumor effect and without systemic toxicity [225].

Since macrophages may exhibit both pro-tumoral and anti-tumoral activities in TME, it is important to fully understand the *in vivo* fate/functional state of these macrophages as well as ideally be able to promote and maintain the anti-tumor functional state of the macrophage carrier in order to maximize this cell-directed therapy. Although the early days of research were devoted to loading macrophages with cytotoxic drugs, it should be possible to load drugs/nanoparticles

that may enhance *in vivo* anti-tumor properties of these macrophages or other immune cells. In light with the recent report on M1-inducing property of clinically approved iron oxide nanoparticles [145], it would be interesting to study how the iron oxide nanoparticle-loaded macrophages, already developed for diagnostic purpose, may exhibit enhanced anti-tumor properties. Finally, further development of the technology for delivery of biologics such as peptide or proteins drugs would greatly expand the utility of this technology in cancer therapy.

1.6 Perspectives on TAM-targeted therapeutics

With deeper understanding of cancer immunology, diverse strategies for modulation of TAMs are being uncovered and explored for therapeutic applications. Due to the complexity of tumors, combination therapy is typically needed to maximize an anti-tumor response. Thus, a clear understanding of the modes of drug action as well as mechanisms of resistance is needed in order to design an efficacious combination therapy that minimizes antagonistic effects. For example, identification of PI3k up-regulation in tumor as a resistance mechanism for CSF-1R kinase inhibitor in recurrent glioma suggests that a combination therapy between PI3k and CSF-1R inhibitors could be more beneficial [72]. Conversely, the therapeutics aiming to block macrophage recruitment signals (e.g. CCL2 or CXCL12 inhibition) may not be compatible with the ones that require the presence of macrophages for anti-tumor actions (e.g. anti-CD40 antibody) [118]. In regard to well-appreciated immunosuppressive roles of TAMs, a consensus was seen on the potential benefits of TAM-targeted therapies in potentiating immune checkpoint blockade therapies (anti PD-1/PD-L1/CTLA-4 antibodies) as evidenced in the race among pharmaceutical companies to investigate such combination therapies (Table 1.2). Improvement in gene sequencing and analysis technologies greatly facilitates the adoption of precision medicine where patients could be examined for genetic makeup and matched with appropriate therapeutic regimens. Documenting patients' genetic profile and the corresponding therapeutic outcome are also beneficial in correlation studies to better predict patient response as well as in refining drug development. In the case of CSF-1R inhibition therapy, certain single nucleotide polymorphisms (SNPs) in CSF-1R have been identified that reduce the potency of emactuzumab [226]. Nonetheless, the study may help in the future design of the next-generation CSF-1R blockade therapy. To reap the benefit of a steady rise in molecularly targeted therapies that are

promising for clinical translation, it is more than ever important to be resource-efficient. This may be possible through careful validation of pre-clinical studies and innovative design of clinical trials as seen, for example, in the I-SPY 2 trial (NCT01042379) [227]. With numerous therapeutic targets being identified and drug candidates being explored for modulation of TAMs, drug delivery technologies will soon come into play to further enhance therapeutic efficacy of these drugs, for example, by improving pharmacokinetics, stability, selectivity, or intracellular delivery while limiting systemic toxicity. Together with advancement in gene-editing technology, effective silencing of genes that promote pro-tumoral functions of TAMs (e.g. STAT3, SIRP α , PI3k, or Gpr132) may one day be a practicable therapeutic option. Finally, a cost barrier is another factor that could impede the clinical translation especially when multiple antibodies are used in a combination therapy as currently investigated in several trials. The problem may be alleviated with improvement in manufacturing efficiency or development of cheaper alternatives such as small molecule drugs or peptide analogs.

It is clear from the last century of research that the mononuclear phagocyte system and macrophages play an essential role in normal physiological processes and disease development. Targeting TAMs has proven enormously successful as TAM targeting agents are rapidly advancing to the clinic, both in combination with traditional therapeutics and with other immunomodulatory agents. With the increasing depth of TAM targeting agents within preclinical development and novel mechanistic TAM pathways/targeting agents arising everyday in basic research, it is clear that TAM targeted therapies will be an important addition to the anti-cancer armamentarium.

1.7 Acknowledgments

This work was supported by NIH 1R01CA177272. Chayanon Ngambenjwong was supported by an Anandamahidol Foundation Fellowship. Heather H. Gustafson was supported by the Cardiovascular Pathology Training Grant (5 T32 HL 007312-37).

1.8 References

- [1] D.A. Hume, The mononuclear phagocyte system., *Curr. Opin. Immunol.* 18 (2006) 49–53. doi:10.1016/j.coi.2005.11.008.
- [2] E. Mass, I. Ballesteros, M. Farlik, F. Halbritter, P. Gunther, L. Crozet, et al., Specification

- of tissue-resident macrophages during organogenesis., *Science*. 353 (2016). doi:10.1126/science.aaf4238.
- [3] C. Schulz, E. Gomez Perdiguero, L. Chorro, H. Szabo-Rogers, N. Cagnard, K. Kierdorf, et al., A lineage of myeloid cells independent of Myb and hematopoietic stem cells., *Science*. 336 (2012) 86–90. doi:10.1126/science.1219179.
- [4] T.A. Wynn, A. Chawla, J.W. Pollard, Macrophage biology in development, homeostasis and disease., *Nature*. 496 (2013) 445–455. doi:10.1038/nature12034.
- [5] F. Ginhoux, S. Jung, Monocytes and macrophages: developmental pathways and tissue homeostasis., *Nat. Rev. Immunol.* 14 (2014) 392–404. doi:10.1038/nri3671.
- [6] C.E. Lewis, A.S. Harney, J.W. Pollard, The Multifaceted Role of Perivascular Macrophages in Tumors., *Cancer Cell*. 30 (2016) 365. doi:10.1016/j.ccell.2016.07.009.
- [7] A. Mantovani, F. Marchesi, A. Malesci, L. Laghi, P. Allavena, Tumour-associated macrophages as treatment targets in oncology., *Nat. Rev. Clin. Oncol.* (2017). doi:10.1038/nrclinonc.2016.217.
- [8] I.I. Mechnikov, Immunity in Infective Diseases, *Rev. Infect. Dis.* 10 (1988) 223–227. <http://dx.doi.org/10.1093/clinids/10.1.223>.
- [9] R.C. Paolicelli, G. Bolasco, F. Pagani, L. Maggi, M. Scianni, P. Panzanelli, et al., Synaptic pruning by microglia is necessary for normal brain development., *Science*. 333 (2011) 1456–1458. doi:10.1126/science.1202529.
- [10] D. Nayak, T.L. Roth, D.B. McGavern, Microglia development and function., *Annu. Rev. Immunol.* 32 (2014) 367–402. doi:10.1146/annurev-immunol-032713-120240.
- [11] T. Ganz, Macrophages and systemic iron homeostasis., *J. Innate Immun.* 4 (2012) 446–453. doi:10.1159/000336423.
- [12] V. Hvidberg, M.B. Maniecki, C. Jacobsen, P. Hojrup, H.J. Moller, S.K. Moestrup, Identification of the receptor scavenging hemopexin-heme complexes., *Blood*. 106 (2005) 2572–2579. doi:10.1182/blood-2005-03-1185.
- [13] M. Kohyama, W. Ise, B.T. Edelson, P.R. Wilker, K. Hildner, C. Mejia, et al., Role for Spi-C in the development of red pulp macrophages and splenic iron homeostasis, *Nature*. 457 (2009) 318–321. <http://dx.doi.org/10.1038/nature07472>.
- [14] M. Merad, M.G. Manz, H. Karsunky, A. Wagers, W. Peters, I. Charo, et al., Langerhans cells renew in the skin throughout life under steady-state conditions., *Nat. Immunol.* 3 (2002) 1135–1141. doi:10.1038/ni852.
- [15] T. Hussell, T.J. Bell, Alveolar macrophages: plasticity in a tissue-specific context., *Nat. Rev. Immunol.* 14 (2014) 81–93. doi:10.1038/nri3600.
- [16] J.D. Stockand, S.C. Sansom, Glomerular mesangial cells: electrophysiology and regulation of contraction., *Physiol. Rev.* 78 (1998) 723–744.

- [17] B. Ajami, J.L. Bennett, C. Krieger, K.M. McNagny, F.M. V Rossi, Infiltrating monocytes trigger EAE progression, but do not contribute to the resident microglia pool., *Nat. Neurosci.* 14 (2011) 1142–1149. doi:10.1038/nn.2887.
- [18] M.B. Brown, M. von Chamier, A.B. Allam, L. Reyes, M1/M2 macrophage polarity in normal and complicated pregnancy., *Front. Immunol.* 5 (2014) 606. doi:10.3389/fimmu.2014.00606.
- [19] S.J. Renaud, C.H. Graham, The role of macrophages in utero-placental interactions during normal and pathological pregnancy., *Immunol. Invest.* 37 (2008) 535–564. doi:10.1080/08820130802191375.
- [20] L.C. Davies, S.J. Jenkins, J.E. Allen, P.R. Taylor, Tissue-resident macrophages., *Nat. Immunol.* 14 (2013) 986–995. doi:10.1038/ni.2705.
- [21] Y. Lavin, A. Mortha, A. Rahman, M. Merad, Regulation of macrophage development and function in peripheral tissues., *Nat. Rev. Immunol.* 15 (2015) 731–744. doi:10.1038/nri3920.
- [22] Y. Lavin, D. Winter, R. Blecher-Gonen, E. David, H. Keren-Shaul, M. Merad, et al., Tissue-Resident Macrophage Enhancer Landscapes Are Shaped by the Local Microenvironment, *Cell.* 159 (2014) 1312–1326. doi:10.1016/j.cell.2014.11.018.
- [23] Y. Okabe, R. Medzhitov, Tissue-specific signals control reversible program of localization and functional polarization of macrophages., *Cell.* 157 (2014) 832–844. doi:10.1016/j.cell.2014.04.016.
- [24] T. Kawai, S. Akira, The role of pattern-recognition receptors in innate immunity: update on Toll-like receptors., *Nat. Immunol.* 11 (2010) 373–384. doi:10.1038/ni.1863.
- [25] K. Takeda, S. Akira, TLR signaling pathways., *Semin. Immunol.* 16 (2004) 3–9.
- [26] I. Malyshev, Y. Malyshev, Current Concept and Update of the Macrophage Plasticity Concept: Intracellular Mechanisms of Reprogramming and M3 Macrophage “Switch” Phenotype., *Biomed Res. Int.* 2015 (2015) 341308. doi:10.1155/2015/341308.
- [27] K. Takeda, T. Tanaka, W. Shi, M. Matsumoto, M. Minami, S. Kashiwamura, et al., Essential role of Stat6 in IL-4 signalling., *Nature.* 380 (1996) 627–630. doi:10.1038/380627a0.
- [28] S. Gordon, F.O. Martinez, Alternative activation of macrophages: mechanism and functions., *Immunity.* 32 (2010) 593–604. doi:10.1016/j.immuni.2010.05.007.
- [29] F.O. Martinez, L. Helming, S. Gordon, Alternative activation of macrophages: an immunologic functional perspective., *Annu. Rev. Immunol.* 27 (2009) 451–483. doi:10.1146/annurev.immunol.021908.132532.
- [30] S.J. Van Dyken, R.M. Locksley, Interleukin-4- and interleukin-13-mediated alternatively activated macrophages: roles in homeostasis and disease., *Annu. Rev. Immunol.* 31 (2013) 317–343. doi:10.1146/annurev-immunol-032712-095906.

- [31] P. Italiani, D. Boraschi, From Monocytes to M1/M2 Macrophages: Phenotypical vs. Functional Differentiation., *Front. Immunol.* 5 (2014) 514. doi:10.3389/fimmu.2014.00514.
- [32] P.J. Murray, J.E. Allen, S.K. Biswas, E.A. Fisher, D.W. Gilroy, S. Goerdts, et al., Macrophage activation and polarization: nomenclature and experimental guidelines., *Immunity.* 41 (2014) 14–20. doi:10.1016/j.immuni.2014.06.008.
- [33] F.O. Martinez, S. Gordon, The M1 and M2 paradigm of macrophage activation: time for reassessment, *F1000Prime Rep.* 6 (2014) 13. doi:10.12703/P6-13.
- [34] D. Zhou, C. Huang, Z. Lin, S. Zhan, L. Kong, C. Fang, et al., Macrophage polarization and function with emphasis on the evolving roles of coordinated regulation of cellular signaling pathways., *Cell. Signal.* 26 (2014) 192–197. doi:10.1016/j.cellsig.2013.11.004.
- [35] E. Elinav, R. Nowarski, C.A. Thaiss, B. Hu, C. Jin, R.A. Flavell, Inflammation-induced cancer: crosstalk between tumours, immune cells and microorganisms, *Nat Rev Cancer.* 13 (2013) 759–771. <http://dx.doi.org/10.1038/nrc3611>.
- [36] R. Evans, P. Alexander, Cooperation of immune lymphoid cells with macrophages in tumour immunity., *Nature.* 228 (1970) 620–622.
- [37] H.-W. Wang, J.A. Joyce, Alternative activation of tumor-associated macrophages by IL-4: priming for protumoral functions., *Cell Cycle.* 9 (2010) 4824–4835. doi:10.4161/cc.9.24.14322.
- [38] D.F. Quail, J.A. Joyce, Microenvironmental regulation of tumor progression and metastasis., *Nat. Med.* 19 (2013) 1423–1437. doi:10.1038/nm.3394.
- [39] C. Caux, R.N. Ramos, G.C. Prendergast, N. Bendriss-Vermare, C. Ménétrier-Caux, A Milestone Review on How Macrophages Affect Tumor Growth, *Cancer Res.* 76 (2016) 6439 LP-6442. <http://cancerres.aacrjournals.org/content/76/22/6439.abstract>.
- [40] R. Ostuni, F. Kratochvill, P.J. Murray, G. Natoli, Macrophages and cancer: from mechanisms to therapeutic implications, *Trends Immunol.* 36 (2017) 229–239. doi:10.1016/j.it.2015.02.004.
- [41] D.F. Quail, J.A. Joyce, Molecular Pathways: Deciphering Mechanisms of Resistance to Macrophage-Targeted Therapies, *Clin. Cancer Res.* (2016). <http://clincancerres.aacrjournals.org/content/early/2016/11/24/1078-0432.CCR-16-0133.abstract>.
- [42] Z.-Y. Yuan, R.-Z. Luo, R.-J. Peng, S.-S. Wang, C. Xue, High infiltration of tumor-associated macrophages in triple-negative breast cancer is associated with a higher risk of distant metastasis., *Onco. Targets. Ther.* 7 (2014) 1475–1480. doi:10.2147/OTT.S61838.
- [43] B. Ruffell, N.I. Affara, L.M. Coussens, Differential macrophage programming in the tumor microenvironment., *Trends Immunol.* 33 (2012) 119–126. doi:10.1016/j.it.2011.12.001.

- [44] J. Ma, L. Liu, G. Che, N. Yu, F. Dai, Z. You, The M1 form of tumor-associated macrophages in non-small cell lung cancer is positively associated with survival time., *BMC Cancer*. 10 (2010) 112. doi:10.1186/1471-2407-10-112.
- [45] J. Mei, Z. Xiao, C. Guo, Q. Pu, L. Ma, C. Liu, et al., Prognostic impact of tumor-associated macrophage infiltration in non-small cell lung cancer: A systemic review and meta-analysis., *Oncotarget*. 7 (2016) 34217–34228. doi:10.18632/oncotarget.9079.
- [46] L. Gu, H. Li, L. Chen, X. Ma, X. Li, Y. Gao, et al., Prognostic role of lymphocyte to monocyte ratio for patients with cancer: evidence from a systematic review and meta-analysis, *Oncotarget*. 7 (2016) 31926–31942. doi:10.18632/oncotarget.7876.
- [47] M.T. Drake, B.L. Clarke, S. Khosla, Bisphosphonates: Mechanism of Action and Role in Clinical Practice, *Mayo Clin. Proc.* 83 (2008) 1032–1045. <http://www.ncbi.nlm.nih.gov/pmc/articles/PMC2667901/>.
- [48] A.J. Roelofs, K. Thompson, S. Gordon, M.J. Rogers, Molecular mechanisms of action of bisphosphonates: current status., *Clin. Cancer Res.* 12 (2006) 6222s–6230s. doi:10.1158/1078-0432.CCR-06-0843.
- [49] S. Junankar, G. Shay, J. Jurczyk, N. Ali, J. Down, N. Pocock, et al., Real-time intravital imaging establishes tumor-associated macrophages as the extraskeletal target of bisphosphonate action in cancer., *Cancer Discov.* 5 (2015) 35–42. doi:10.1158/2159-8290.CD-14-0621.
- [50] M. Coscia, E. Quaglino, M. Iezzi, C. Curcio, F. Pantaleoni, C. Riganti, et al., Zoledronic acid repolarizes tumour-associated macrophages and inhibits mammary carcinogenesis by targeting the mevalonate pathway., *J. Cell. Mol. Med.* 14 (2010) 2803–2815. doi:10.1111/j.1582-4934.2009.00926.x.
- [51] S.M. Zeisberger, B. Odermatt, C. Marty, A.H.M. Zehnder-Fjallman, K. Ballmer-Hofer, R.A. Schwendener, Clodronate-liposome-mediated depletion of tumour-associated macrophages: a new and highly effective antiangiogenic therapy approach., *Br. J. Cancer.* 95 (2006) 272–281. doi:10.1038/sj.bjc.6603240.
- [52] T.L. Rogers, I. Holen, Tumour macrophages as potential targets of bisphosphonates., *J. Transl. Med.* 9 (2011) 177. doi:10.1186/1479-5876-9-177.
- [53] W. Zhang, X.-D. Zhu, H.-C. Sun, Y.-Q. Xiong, P.-Y. Zhuang, H.-X. Xu, et al., Depletion of tumor-associated macrophages enhances the effect of sorafenib in metastatic liver cancer models by antimetastatic and antiangiogenic effects., *Clin. Cancer Res.* 16 (2010) 3420–3430. doi:10.1158/1078-0432.CCR-09-2904.
- [54] Y. Hattori, K. Shibuya, K. Kojima, A. Miatmoko, K. Kawano, K.-I. Ozaki, et al., Zoledronic acid enhances antitumor efficacy of liposomal doxorubicin., *Int. J. Oncol.* 47 (2015) 211–219. doi:10.3892/ijo.2015.2991.
- [55] Y. Ohara, T. Oda, K. Yamada, S. Hashimoto, Y. Akashi, R. Miyamoto, et al., Effective delivery of chemotherapeutic nanoparticles by depleting host Kupffer cells., *Int. J. Cancer.*

- 131 (2012) 2402–2410. doi:10.1002/ijc.27502.
- [56] K.D. Moynihan, C.F. Opel, G.L. Szeto, A. Tzeng, E.F. Zhu, J.M. Engreitz, et al., Eradication of large established tumors in mice by combination immunotherapy that engages innate and adaptive immune responses., *Nat. Med.* 22 (2016) 1402–1410. doi:10.1038/nm.4200.
- [57] M.P. Chao, A.A. Alizadeh, C. Tang, J.H. Myklebust, B. Varghese, S. Gill, et al., Anti-CD47 antibody synergizes with rituximab to promote phagocytosis and eradicate non-Hodgkin lymphoma, *Cell*. 142 (2010) 699–713. doi:10.1016/j.cell.2010.07.044.
- [58] B. Lehmann, M. Biburger, C. Brückner, A. Ipsen-Escobedo, S. Gordan, C. Lehmann, et al., Tumor location determines tissue-specific recruitment of tumor-associated macrophages and antibody-dependent immunotherapy response, *Sci. Immunol.* 2 (2017). <http://immunology.sciencemag.org/content/2/7/eaah6413.abstract>.
- [59] F. Pucci, C. Garris, C.P. Lai, A. Newton, C. Pfirschke, C. Engblom, et al., SCS macrophages suppress melanoma by restricting tumor-derived vesicle-B cell interactions., *Science*. 352 (2016) 242–246. doi:10.1126/science.aaf1328.
- [60] K. Ohnishi, Y. Komohara, Y. Saito, Y. Miyamoto, M. Watanabe, H. Baba, et al., CD169-positive macrophages in regional lymph nodes are associated with a favorable prognosis in patients with colorectal carcinoma., *Cancer Sci.* 104 (2013) 1237–1244. doi:10.1111/cas.12212.
- [61] T. Shiota, Y. Miyasato, K. Ohnishi, M. Yamamoto-Ibusuki, Y. Yamamoto, H. Iwase, et al., The Clinical Significance of CD169-Positive Lymph Node Macrophage in Patients with Breast Cancer, *PLoS One*. 11 (2016) e0166680. <http://dx.doi.org/10.1371/journal.pone.0166680>.
- [62] M.D. Michaelson, M.R. Smith, Bisphosphonates for treatment and prevention of bone metastases., *J. Clin. Oncol.* 23 (2005) 8219–8224. doi:10.1200/JCO.2005.02.9579.
- [63] <http://www.fda.gov/NewsEvents/Newsroom/PressAnnouncements/ucm468832.htm>.
- [64] K. Otero, I.R. Turnbull, P.L. Poliani, W. Vermi, E. Cerutti, T. Aoshi, et al., Macrophage colony-stimulating factor induces the proliferation and survival of macrophages via a pathway involving DAP12 and beta-catenin., *Nat. Immunol.* 10 (2009) 734–743. doi:10.1038/ni.1744.
- [65] H. Lin, E. Lee, K. Hestir, C. Leo, M. Huang, E. Bosch, et al., Discovery of a cytokine and its receptor by functional screening of the extracellular proteome., *Science*. 320 (2008) 807–811. doi:10.1126/science.1154370.
- [66] D.A. Hume, K.P.A. MacDonald, Therapeutic applications of macrophage colony-stimulating factor-1 (CSF-1) and antagonists of CSF-1 receptor (CSF-1R) signaling., *Blood*. 119 (2012) 1810–1820. doi:10.1182/blood-2011-09-379214.
- [67] M. Lohela, A.-J. Casbon, A. Olow, L. Bonham, D. Branstetter, N. Weng, et al., Intravital imaging reveals distinct responses of depleting dynamic tumor-associated macrophage

- and dendritic cell subpopulations., *Proc. Natl. Acad. Sci. U. S. A.* 111 (2014) E5086-95. doi:10.1073/pnas.1419899111.
- [68] L. Fend, N. Accart, J. Kintz, S. Cochin, C. Reymann, F. Le Pogam, et al., Therapeutic effects of anti-CD115 monoclonal antibody in mouse cancer models through dual inhibition of tumor-associated macrophages and osteoclasts., *PLoS One.* 8 (2013) e73310. doi:10.1371/journal.pone.0073310.
- [69] K.P.A. MacDonald, J.S. Palmer, S. Cronau, E. Seppanen, S. Olver, N.C. Raffelt, et al., An antibody against the colony-stimulating factor 1 receptor depletes the resident subset of monocytes and tissue- and tumor-associated macrophages but does not inhibit inflammation., *Blood.* 116 (2010) 3955–3963. doi:10.1182/blood-2010-02-266296.
- [70] S.M. Pyonteck, L. Akkari, A.J. Schuhmacher, R.L. Bowman, L. Sevenich, D.F. Quail, et al., CSF-1R inhibition alters macrophage polarization and blocks glioma progression., *Nat. Med.* 19 (2013) 1264–1272. doi:10.1038/nm.3337.
- [71] D.C. Strachan, B. Ruffell, Y. Oei, M.J. Bissell, L.M. Coussens, N. Pryer, et al., CSF1R inhibition delays cervical and mammary tumor growth in murine models by attenuating the turnover of tumor-associated macrophages and enhancing infiltration by CD8+ T cells., *Oncoimmunology.* 2 (2013) e26968. doi:10.4161/onci.26968.
- [72] D.F. Quail, R.L. Bowman, L. Akkari, M.L. Quick, A.J. Schuhmacher, J.T. Huse, et al., The tumor microenvironment underlies acquired resistance to CSF-1R inhibition in gliomas., *Science.* 352 (2016) aad3018. doi:10.1126/science.aad3018.
- [73] W. Jeong, J.H. Doroshow, S. Kummar, US FDA Approved Oral Kinase Inhibitors for the Treatment of Malignancies, *Curr. Probl. Cancer.* 37 (2013) 110–144. doi:10.1016/j.crrproblcancer.2013.06.001.
- [74] F. Broekman, E. Giovannetti, G.J. Peters, Tyrosine kinase inhibitors: Multi-targeted or single-targeted?, *World J. Clin. Oncol.* 2 (2011) 80–93. doi:10.5306/wjco.v2.i2.80.
- [75] M. Kogan, T. Fischer-Smith, R. Kaminsky, G. Lehmicke, J. Rappaport, CSF-1R up-regulation is associated with response to pharmacotherapy targeting tyrosine kinase activity in AML cell lines, *Anticancer Res.* 32 (2012) 893–899. <http://www.ncbi.nlm.nih.gov/pmc/articles/PMC3601026/>.
- [76] N. Brownlow, A.E. Russell, H. Saravanapavan, M. Wiesmann, J.M. Murray, P.W. Manley, et al., Comparison of nilotinib and imatinib inhibition of FMS receptor signaling, macrophage production and osteoclastogenesis, *Leukemia.* 22 (2007) 649–652. <http://dx.doi.org/10.1038/sj.leu.2404944>.
- [77] N. Brownlow, C. Mol, C. Hayford, S. Ghaem-Maghami, N.J. Dibb, Dasatinib is a potent inhibitor of tumour-associated macrophages, osteoclasts and the FMS receptor, *Leukemia.* 23 (2008) 590–594. <http://dx.doi.org/10.1038/leu.2008.237>.
- [78] W.D. Tap, Z.A. Wainberg, S.P. Anthony, P.N. Ibrahim, C. Zhang, J.H. Healey, et al., Structure-Guided Blockade of CSF1R Kinase in Tenosynovial Giant-Cell Tumor, *N. Engl.*

- J. Med. 373 (2015) 428–437. doi:10.1056/NEJMoa1411366.
- [79] A. Chaudhuri, Regulation of Macrophage Polarization by RON Receptor Tyrosine Kinase Signaling., *Front. Immunol.* 5 (2014) 546. doi:10.3389/fimmu.2014.00546.
- [80] M.A. Lutz, P.H. Correll, Activation of CR3-mediated phagocytosis by MSP requires the RON receptor, tyrosine kinase activity, phosphatidylinositol 3-kinase, and protein kinase C zeta., *J. Leukoc. Biol.* 73 (2003) 802–814.
- [81] D.R. Sharda, S. Yu, M. Ray, M.L. Squadrito, M. De Palma, T.A. Wynn, et al., Regulation of macrophage arginase expression and tumor growth by the Ron receptor tyrosine kinase., *J. Immunol.* 187 (2011) 2181–2192. doi:10.4049/jimmunol.1003460.
- [82] A.C. Morrison, C.B. Wilson, M. Ray, P.H. Correll, Macrophage-stimulating protein, the ligand for the stem cell-derived tyrosine kinase/RON receptor tyrosine kinase, inhibits IL-12 production by primary peritoneal macrophages stimulated with IFN-gamma and lipopolysaccharide., *J. Immunol.* 172 (2004) 1825–1832.
- [83] Y.Q. Chen, J.H. Fisher, M.H. Wang, Activation of the RON receptor tyrosine kinase inhibits inducible nitric oxide synthase (iNOS) expression by murine peritoneal exudate macrophages: phosphatidylinositol-3 kinase is required for RON-mediated inhibition of iNOS expression., *J. Immunol.* 161 (1998) 4950–4959.
- [84] D. Gurusamy, J.K. Gray, P. Pathrose, R.M. Kulkarni, F.D. Finkleman, S.E. Waltz, Myeloid-Specific Expression of Ron Receptor Kinase Promotes Prostate Tumor Growth, *Cancer Res.* 73 (2013) 1752–1763. doi:10.1158/0008-5472.CAN-12-2474.
- [85] H. Eyob, H.A. Ekiz, Y.S. DeRose, S.E. Waltz, M.A. Williams, A.L. Welm, Inhibition of Ron kinase blocks conversion of micrometastases to overt metastases by boosting anti-tumor immunity, *Cancer Discov.* 3 (2013) 751–760. doi:10.1158/2159-8290.CD-12-0480.
- [86] M. Bieniasz, P. Radhakrishnan, N. Faham, J.-P. De La O, A.L. Welm, Preclinical Efficacy of Ron Kinase Inhibitors Alone and in Combination with PI3K Inhibitors for Treatment of sfRon-Expressing Breast Cancer Patient-Derived Xenografts., *Clin. Cancer Res.* 21 (2015) 5588–5600. doi:10.1158/1078-0432.CCR-14-3283.
- [87] S.-M. Maira, S. Pecchi, A. Huang, M. Burger, M. Knapp, D. Sterker, et al., Identification and characterization of NVP-BKM120, an orally available pan-class I PI3-kinase inhibitor., *Mol. Cancer Ther.* 11 (2012) 317–328. doi:10.1158/1535-7163.MCT-11-0474.
- [88] Y. Lavin, M. Merad, Macrophages: gatekeepers of tissue integrity., *Cancer Immunol. Res.* 1 (2013) 201–209. doi:10.1158/2326-6066.CIR-13-0117.
- [89] N. Gul, M. van Egmond, Antibody-Dependent Phagocytosis of Tumor Cells by Macrophages: A Potent Effector Mechanism of Monoclonal Antibody Therapy of Cancer., *Cancer Res.* 75 (2015) 5008–5013. doi:10.1158/0008-5472.CAN-15-1330.
- [90] T.R.W. Tipton, A. Roghanian, R.J. Oldham, M.J. Carter, K.L. Cox, C.I. Mockridge, et al., Antigenic modulation limits the effector cell mechanisms employed by type I anti-CD20 monoclonal antibodies., *Blood.* 125 (2015) 1901–1909. doi:10.1182/blood-2014-07-

588376.

- [91] Y. Shi, X. Fan, H. Deng, R.J. Brezski, M. Ryczyn, R.E. Jordan, et al., Trastuzumab triggers phagocytic killing of high HER2 cancer cells in vitro and in vivo by interaction with Fc γ receptors on macrophages., *J. Immunol.* 194 (2015) 4379–4386. doi:10.4049/jimmunol.1402891.
- [92] K.D. Grugan, F.L. McCabe, M. Kinder, A.R. Greenplate, B.C. Harman, J.E. Ekert, et al., Tumor-associated macrophages promote invasion while retaining Fc-dependent anti-tumor function., *J. Immunol.* 189 (2012) 5457–5466. doi:10.4049/jimmunol.1201889.
- [93] R.P. Taylor, M.A. Lindorfer, Analyses of CD20 monoclonal antibody-mediated tumor cell killing mechanisms: rational design of dosing strategies., *Mol. Pharmacol.* 86 (2014) 485–491. doi:10.1124/mol.114.092684.
- [94] R. Velmurugan, D.K. Challa, S. Ram, R.J. Ober, E.S. Ward, Macrophage-Mediated Trophocytosis Leads to Death of Antibody-Opsonized Tumor Cells., *Mol. Cancer Ther.* 15 (2016) 1879–1889. doi:10.1158/1535-7163.MCT-15-0335.
- [95] J.O. Richards, S. Karki, G.A. Lazar, H. Chen, W. Dang, J.R. Desjarlais, Optimization of antibody binding to Fc γ RIIa enhances macrophage phagocytosis of tumor cells., *Mol. Cancer Ther.* 7 (2008) 2517–2527. doi:10.1158/1535-7163.MCT-08-0201.
- [96] A.M. Brandsma, T. Ten Broeke, M. Nederend, L.A.P.M. Meulenbroek, G. van Tetering, S. Meyer, et al., Simultaneous Targeting of Fc γ Rs and Fc α RI Enhances Tumor Cell Killing., *Cancer Immunol. Res.* 3 (2015) 1316–1324. doi:10.1158/2326-6066.CIR-15-0099-T.
- [97] D.H. Josephs, H.J. Bax, T. Dodev, M. Georgouli, M. Nakamura, G. Pellizzari, et al., Anti-folate receptor- α IgE but not IgG recruits macrophages to attack tumors via TNF- α /MCP-1 signaling, *Cancer Res.* (2017). <http://cancerres.aacrjournals.org/content/early/2017/01/14/0008-5472.CAN-16-1829.abstract>.
- [98] S.B. Willingham, J.-P. Volkmer, A.J. Gentles, D. Sahoo, P. Dalerba, S.S. Mitra, et al., The CD47-signal regulatory protein alpha (SIRP α) interaction is a therapeutic target for human solid tumors., *Proc. Natl. Acad. Sci. U. S. A.* 109 (2012) 6662–6667. doi:10.1073/pnas.1121623109.
- [99] K. Weiskopf, A.M. Ring, C.C.M. Ho, J.-P. Volkmer, A.M. Levin, A.K. Volkmer, et al., Engineered SIRP α variants as immunotherapeutic adjuvants to anticancer antibodies., *Science.* 341 (2013) 88–91. doi:10.1126/science.1238856.
- [100] J. Liu, L. Wang, F. Zhao, S. Tseng, C. Narayanan, L. Shura, et al., Pre-Clinical Development of a Humanized Anti-CD47 Antibody with Anti-Cancer Therapeutic Potential., *PLoS One.* 10 (2015) e0137345. doi:10.1371/journal.pone.0137345.
- [101] C.C.M. Ho, N. Guo, J.T. Sockolosky, A.M. Ring, K. Weiskopf, E. Ozkan, et al., “Velcro” engineering of high affinity CD47 ectodomain as signal regulatory protein alpha

- (SIRPalpha) antagonists that enhance antibody-dependent cellular phagocytosis., *J. Biol. Chem.* 290 (2015) 12650–12663. doi:10.1074/jbc.M115.648220.
- [102] E. Dheilily, V. Moine, L. Broyer, S. Salgado-Pires, Z. Johnson, A. Papaioannou, et al., Selective Blockade of the Ubiquitous Checkpoint Receptor CD47 Is Enabled by Dual-Targeting Bispecific Antibodies, *Mol. Ther.* (2017). doi:10.1016/j.ymthe.2016.11.006.
- [103] K. Weiskopf, K.L. Anderson, D. Ito, P.J. Schnorr, H. Tomiyasu, A.M. Ring, et al., Eradication of Canine Diffuse Large B-Cell Lymphoma in a Murine Xenograft Model with CD47 Blockade and Anti-CD20., *Cancer Immunol. Res.* 4 (2016) 1072–1087. doi:10.1158/2326-6066.CIR-16-0105.
- [104] R.A. Franklin, W. Liao, A. Sarkar, M. V Kim, M.R. Bivona, K. Liu, et al., The cellular and molecular origin of tumor-associated macrophages., *Science.* 344 (2014) 921–925. doi:10.1126/science.1252510.
- [105] D.E. Sanford, B.A. Belt, R.Z. Panni, A. Mayer, A.D. Deshpande, D. Carpenter, et al., Inflammatory monocyte mobilization decreases patient survival in pancreatic cancer: a role for targeting the CCL2/CCR2 axis., *Clin. Cancer Res.* 19 (2013) 3404–3415. doi:10.1158/1078-0432.CCR-13-0525.
- [106] G. Ren, X. Zhao, Y. Wang, X. Zhang, X. Chen, C. Xu, et al., CCR2-dependent recruitment of macrophages by tumor-educated mesenchymal stromal cells promotes tumor development and is mimicked by TNFalpha., *Cell Stem Cell.* 11 (2012) 812–824. doi:10.1016/j.stem.2012.08.013.
- [107] B.-Z. Qian, J. Li, H. Zhang, T. Kitamura, J. Zhang, L.R. Campion, et al., CCL2 recruits inflammatory monocytes to facilitate breast-tumour metastasis., *Nature.* 475 (2011) 222–225. doi:10.1038/nature10138.
- [108] C. Engblom, C. Pfirschke, M.J. Pittet, The role of myeloid cells in cancer therapies., *Nat. Rev. Cancer.* 16 (2016) 447–462. doi:10.1038/nrc.2016.54.
- [109] J. Ji, T. Eggert, A. Budhu, M. Forgues, A. Takai, H. Dang, et al., Hepatic stellate cell and monocyte interaction contributes to poor prognosis in hepatocellular carcinoma., *Hepatology.* 62 (2015) 481–495. doi:10.1002/hep.27822.
- [110] S.Y. Lim, A.E. Yuzhalin, A.N. Gordon-Weeks, R.J. Muschel, Targeting the CCL2-CCR2 signaling axis in cancer metastasis., *Oncotarget.* 7 (2016) 28697–28710. doi:10.18632/oncotarget.7376.
- [111] L. Bonapace, M.-M. Coissieux, J. Wyckoff, K.D. Mertz, Z. Varga, T. Junt, et al., Cessation of CCL2 inhibition accelerates breast cancer metastasis by promoting angiogenesis., *Nature.* 515 (2014) 130–133. doi:10.1038/nature13862.
- [112] P.S. Kirk, T. Koreckij, H.M. Nguyen, L.G. Brown, L.A. Snyder, R.L. Vessella, et al., Inhibition of CCL2 signaling in combination with docetaxel treatment has profound inhibitory effects on prostate cancer growth in bone., *Int. J. Mol. Sci.* 14 (2013) 10483–10496. doi:10.3390/ijms140510483.

- [113] R. Hughes, B.-Z. Qian, C. Rowan, M. Muthana, I. Keklikoglou, O.C. Olson, et al., Perivascular M2 Macrophages Stimulate Tumor Relapse after Chemotherapy, *Cancer Res.* 75 (2015) 3479–3491. doi:10.1158/0008-5472.CAN-14-3587.
- [114] S.-C. Wang, C.-F. Yu, J.-H. Hong, C.-S. Tsai, C.-S. Chiang, Radiation therapy-induced tumor invasiveness is associated with SDF-1-regulated macrophage mobilization and vasculogenesis., *PLoS One.* 8 (2013) e69182. doi:10.1371/journal.pone.0069182.
- [115] L. Sanchez-Martin, A. Estechea, R. Samaniego, S. Sanchez-Ramon, M.A. Vega, P. Sanchez-Mateos, The chemokine CXCL12 regulates monocyte-macrophage differentiation and RUNX3 expression., *Blood.* 117 (2011) 88–97. doi:10.1182/blood-2009-12-258186.
- [116] R.H. Vonderheide, M.J. Glennie, Agonistic CD40 antibodies and cancer therapy., *Clin. Cancer Res.* 19 (2013) 1035–1043. doi:10.1158/1078-0432.CCR-12-2064.
- [117] G.L. Beatty, E.G. Chiorean, M.P. Fishman, B. Saboury, U.R. Teitelbaum, W. Sun, et al., CD40 Agonists Alter Tumor Stroma and Show Efficacy Against Pancreatic Carcinoma in Mice and Humans, *Science.* 331 (2011) 1612–1616. doi:10.1126/science.1198443.
- [118] K.B. Long, W.L. Gladney, G.M. Tooker, K. Graham, J.A. Fraietta, G.L. Beatty, IFN γ and CCL2 Cooperate to Redirect Tumor-Infiltrating Monocytes to Degrade Fibrosis and Enhance Chemotherapy Efficacy in Pancreatic Carcinoma., *Cancer Discov.* 6 (2016) 400–413. doi:10.1158/2159-8290.CD-15-1032.
- [119] F. Li, J. V Ravetch, Inhibitory Fc γ receptor engagement drives adjuvant and anti-tumor activities of agonistic CD40 antibodies., *Science.* 333 (2011) 1030–1034. doi:10.1126/science.1206954.
- [120] A.L. White, H.T.C. Chan, A. Roghanian, R.R. French, C.I. Mockridge, A.L. Tutt, et al., Interaction with Fc γ R1B is critical for the agonistic activity of anti-CD40 monoclonal antibody., *J. Immunol.* 187 (2011) 1754–1763. doi:10.4049/jimmunol.1101135.
- [121] R. Mazzeri, F. Pucci, D. Moi, E. Zonari, A. Ranghetti, A. Berti, et al., Targeting the ANG2/TIE2 axis inhibits tumor growth and metastasis by impairing angiogenesis and disabling rebounds of proangiogenic myeloid cells., *Cancer Cell.* 19 (2011) 512–526. doi:10.1016/j.ccr.2011.02.005.
- [122] S.B. Coffelt, A.O. Tal, A. Scholz, M. De Palma, S. Patel, C. Urbich, et al., Angiopoietin-2 regulates gene expression in TIE2-expressing monocytes and augments their inherent proangiogenic functions., *Cancer Res.* 70 (2010) 5270–5280. doi:10.1158/0008-5472.CAN-10-0012.
- [123] O. Coutelle, L.M. Schiffmann, M. Liwschitz, M. Brunold, V. Goede, M. Hallek, et al., Dual targeting of Angiopoietin-2 and VEGF potentiates effective vascular normalisation without inducing empty basement membrane sleeves in xenograft tumours., *Br. J. Cancer.* 112 (2015) 495–503. doi:10.1038/bjc.2014.629.

- [124] J. Kloepper, L. Riedemann, Z. Amoozgar, G. Seano, K. Susek, V. Yu, et al., Ang-2/VEGF bispecific antibody reprograms macrophages and resident microglia to anti-tumor phenotype and prolongs glioblastoma survival., *Proc. Natl. Acad. Sci. U. S. A.* 113 (2016) 4476–4481. doi:10.1073/pnas.1525360113.
- [125] A.S. Jassar, E. Suzuki, V. Kapoor, J. Sun, M.B. Silverberg, L. Cheung, et al., Activation of tumor-associated macrophages by the vascular disrupting agent 5,6-dimethylxanthenone-4-acetic acid induces an effective CD8+ T-cell-mediated antitumor immune response in murine models of lung cancer and mesothelioma., *Cancer Res.* 65 (2005) 11752–11761. doi:10.1158/0008-5472.CAN-05-1658.
- [126] B. Ghesquiere, B.W. Wong, A. Kuchnio, P. Carmeliet, Metabolism of stromal and immune cells in health and disease., *Nature.* 511 (2014) 167–176. doi:10.1038/nature13312.
- [127] T. Weichhart, M. Hengstschlager, M. Linke, Regulation of innate immune cell function by mTOR., *Nat. Rev. Immunol.* 15 (2015) 599–614. doi:10.1038/nri3901.
- [128] V.S. Rodrik-Outmezguine, M. Okaniwa, Z. Yao, C.J. Novotny, C. McWhirter, A. Banaji, et al., Overcoming mTOR resistance mutations with a new-generation mTOR inhibitor., *Nature.* 534 (2016) 272–276. doi:10.1038/nature17963.
- [129] W. Chen, T. Ma, X. Shen, X. Xia, G. Xu, X. Bai, et al., Macrophage-induced tumor angiogenesis is regulated by the TSC2-mTOR pathway., *Cancer Res.* 72 (2012) 1363–1372. doi:10.1158/0008-5472.CAN-11-2684.
- [130] M.M. Kaneda, K.S. Messer, N. Ralainirina, H. Li, C.J. Leem, S. Gorjestani, et al., PI3K γ is a molecular switch that controls immune suppression, *Nature.* 539 (2016) 437–442. <http://dx.doi.org/10.1038/nature19834>.
- [131] A. Arranz, C. Doxaki, E. Vergadi, Y. Martinez de la Torre, K. Vaporidi, E.D. Lagoudaki, et al., Akt1 and Akt2 protein kinases differentially contribute to macrophage polarization., *Proc. Natl. Acad. Sci. U. S. A.* 109 (2012) 9517–9522. doi:10.1073/pnas.1119038109.
- [132] E. Sahin, S. Haubenwallner, M. Kuttke, I. Kollmann, A. Halfmann, A.M. Dohnal, et al., Macrophage PTEN regulates expression and secretion of arginase I modulating innate and adaptive immune responses., *J. Immunol.* 193 (2014) 1717–1727. doi:10.4049/jimmunol.1302167.
- [133] O.R. Colegio, N.-Q. Chu, A.L. Szabo, T. Chu, A.M. Rhebergen, V. Jairam, et al., Functional polarization of tumour-associated macrophages by tumour-derived lactic acid., *Nature.* 513 (2014) 559–563. doi:10.1038/nature13490.
- [134] P. Chen, H. Zuo, H. Xiong, M.J. Kolar, Q. Chu, A. Saghatelian, et al., Gpr132 sensing of lactate mediates tumor-macrophage interplay to promote breast cancer metastasis., *Proc. Natl. Acad. Sci. U. S. A.* 114 (2017) 580–585. doi:10.1073/pnas.1614035114.
- [135] W.Y. Cheng, H. Huynh, P. Chen, S. Pena-Llopis, Y. Wan, Macrophage PPAR γ inhibits Gpr132 to mediate the anti-tumor effects of rosiglitazone., *Elife.* 5 (2016).

doi:10.7554/eLife.18501.

- [136] S. Kusmartsev, D.I. Gabrilovich, STAT1 signaling regulates tumor-associated macrophage-mediated T cell deletion., *J. Immunol.* 174 (2005) 4880–4891.
- [137] D.H. Munn, E. Shafizadeh, J.T. Attwood, I. Bondarev, A. Pashine, A.L. Mellor, Inhibition of T cell proliferation by macrophage tryptophan catabolism., *J. Exp. Med.* 189 (1999) 1363–1372.
- [138] S. Beloribi-Djefafia, S. Vasseur, F. Guillaumond, Lipid metabolic reprogramming in cancer cells, *Oncogenesis.* 5 (2016) e189. <http://dx.doi.org/10.1038/oncogenesis.2015.49>.
- [139] V. Prima, L.N. Kaliberova, S. Kaliberov, D.T. Curiel, S. Kusmartsev, COX2/mPGES1/PGE2 pathway regulates PD-L1 expression in tumor-associated macrophages and myeloid-derived suppressor cells., *Proc. Natl. Acad. Sci. U. S. A.* (2017). doi:10.1073/pnas.1612920114.
- [140] M. Jung, B. Oren, J. Mora, C. Mertens, S. Dziumbila, R. Popp, et al., Lipocalin 2 from macrophages stimulated by tumor cell-derived sphingosine 1-phosphate promotes lymphangiogenesis and tumor metastasis., *Sci. Signal.* 9 (2016) ra64. doi:10.1126/scisignal.aaf3241.
- [141] Y. Nakanishi, M. Nakatsuji, H. Seno, S. Ishizu, R. Akitake-Kawano, K. Kanda, et al., COX-2 inhibition alters the phenotype of tumor-associated macrophages from M2 to M1 in *ApcMin/+* mouse polyps., *Carcinogenesis.* 32 (2011) 1333–1339. doi:10.1093/carcin/bgr128.
- [142] S. V Torti, F.M. Torti, Ironing out cancer., *Cancer Res.* 71 (2011) 1511–1514. doi:10.1158/0008-5472.CAN-10-3614.
- [143] S. V Torti, F.M. Torti, Iron and cancer: more ore to be mined., *Nat. Rev. Cancer.* 13 (2013) 342–355. doi:10.1038/nrc3495.
- [144] C. Mertens, E.A. Akam, C. Rehwald, B. Brüne, E. Tomat, M. Jung, Intracellular Iron Chelation Modulates the Macrophage Iron Phenotype with Consequences on Tumor Progression, *PLoS One.* 11 (2016) e0166164. <http://dx.doi.org/10.1371/journal.pone.0166164>.
- [145] S. Zanganeh, G. Hutter, R. Spitler, O. Lenkov, M. Mahmoudi, A. Shaw, et al., Iron oxide nanoparticles inhibit tumour growth by inducing pro-inflammatory macrophage polarization in tumour tissues., *Nat. Nanotechnol.* 11 (2016) 986–994. doi:10.1038/nnano.2016.168.
- [146] H. Bruns, M. Buttner, M. Fabri, D. Mougiakakos, J.T. Bittenbring, M.H. Hoffmann, et al., Vitamin D-dependent induction of cathelicidin in human macrophages results in cytotoxicity against high-grade B cell lymphoma., *Sci. Transl. Med.* 7 (2015) 282ra47. doi:10.1126/scitranslmed.aaa3230.
- [147] J. Canton, D. Neculai, S. Grinstein, Scavenger receptors in homeostasis and immunity, *Nat Rev Immunol.* 13 (2013) 621–634. <http://dx.doi.org/10.1038/nri3515>.

- [148] X. Yu, C. Guo, P.B. Fisher, J.R. Subjeck, X.-Y. Wang, Scavenger Receptors: Emerging Roles in Cancer Biology and Immunology., *Adv. Cancer Res.* 128 (2015) 309–364. doi:10.1016/bs.acr.2015.04.004.
- [149] A.-M. Georgoudaki, K.E. Prokopec, V.F. Boura, E. Hellqvist, S. Sohn, J. Ostling, et al., Reprogramming Tumor-Associated Macrophages by Antibody Targeting Inhibits Cancer Progression and Metastasis., *Cell Rep.* 15 (2016) 2000–2011. doi:10.1016/j.celrep.2016.04.084.
- [150] C. Neyen, A. Plüddemann, S. Mukhopadhyay, E. Maniati, M. Bossard, S. Gordon, et al., Macrophage Scavenger Receptor A promotes tumour progression in murine models of ovarian and pancreatic cancer, *J. Immunol.* 190 (2013) 3798–3805. doi:10.4049/jimmunol.1203194.
- [151] C. Neyen, S. Mukhopadhyay, S. Gordon, T. Hagemann, An apolipoprotein A-I mimetic targets scavenger receptor A on tumor-associated macrophages: A prospective anticancer treatment?, *Oncoimmunology.* 2 (2013) e24461. doi:10.4161/onci.24461.
- [152] H. Zhang, W. Zhang, X. Sun, R. Dang, R. Zhou, H. Bai, et al., Class A1 scavenger receptor modulates glioma progression by regulating M2-like tumor-associated macrophage polarization, *Oncotarget.* 7 (2016) 50099–50116. doi:10.18632/oncotarget.10318.
- [153] M.V. Cespedes, M.J. Guillen, P.P. Lopez-Casas, F. Sarno, A. Gallardo, P. Alamo, et al., Lurbinectedin induces depletion of tumor-associated macrophages, an essential component of its in vivo synergism with gemcitabine, in pancreatic adenocarcinoma mouse models., *Dis. Model. Mech.* 9 (2016) 1461–1471. doi:10.1242/dmm.026369.
- [154] G. Germano, R. Frapolli, C. Belgiovine, A. Anselmo, S. Pesce, M. Liguori, et al., Role of macrophage targeting in the antitumor activity of trabectedin., *Cancer Cell.* 23 (2013) 249–262. doi:10.1016/j.ccr.2013.01.008.
- [155] M. Liguori, C. Buracchi, F. Pasqualini, F. Bergomas, S. Pesce, M. Sironi, et al., Functional TRAIL receptors in monocytes and tumor-associated macrophages: A possible targeting pathway in the tumor microenvironment., *Oncotarget.* 7 (2016) 41662–41676. doi:10.18632/oncotarget.9340.
- [156] P. Allavena, M. Signorelli, M. Chieppa, E. Erba, G. Bianchi, F. Marchesi, et al., Anti-inflammatory properties of the novel antitumor agent yondelis (trabectedin): inhibition of macrophage differentiation and cytokine production., *Cancer Res.* 65 (2005) 2964–2971. doi:10.1158/0008-5472.CAN-04-4037.
- [157] A. Mantovani, P. Allavena, The interaction of anticancer therapies with tumor-associated macrophages., *J. Exp. Med.* 212 (2015) 435–445. doi:10.1084/jem.20150295.
- [158] M. De Palma, C.E. Lewis, Macrophage regulation of tumor responses to anticancer therapies., *Cancer Cell.* 23 (2013) 277–286. doi:10.1016/j.ccr.2013.02.013.
- [159] D.W. Mullins, C.J. Burger, K.D. Elgert, Paclitaxel enhances macrophage IL-12

- production in tumor-bearing hosts through nitric oxide., *J. Immunol.* 162 (1999) 6811–6818.
- [160] K.N. Kodumudi, K. Woan, D.L. Gilvary, E. Sahakian, S. Wei, J.Y. Djeu, A novel chemoimmunomodulating property of docetaxel: suppression of myeloid-derived suppressor cells in tumor bearers., *Clin. Cancer Res.* 16 (2010) 4583–4594. doi:10.1158/1078-0432.CCR-10-0733.
- [161] J.L. Guerriero, D. Ditsworth, J.M. Catanzaro, G. Sabino, M.B. Furie, R.R. Kew, et al., DNA alkylating therapy induces tumor regression through an HMGB1-mediated activation of innate immunity., *J. Immunol.* 186 (2011) 3517–3526. doi:10.4049/jimmunol.1003267.
- [162] K. Bryniarski, M. Szczepanik, M. Ptak, M. Zemelka, W. Ptak, Influence of cyclophosphamide and its metabolic products on the activity of peritoneal macrophages in mice., *Pharmacol. Rep.* 61 (2009) 550–557.
- [163] M. Baghdadi, H. Wada, S. Nakanishi, H. Abe, N. Han, W.E. Putra, et al., Chemotherapy-Induced IL34 Enhances Immunosuppression by Tumor-Associated Macrophages and Mediates Survival of Chemoresistant Lung Cancer Cells., *Cancer Res.* 76 (2016) 6030–6042. doi:10.1158/0008-5472.CAN-16-1170.
- [164] S. Kaczanowska, A.M. Joseph, E. Davila, TLR agonists: our best frenemy in cancer immunotherapy, *J. Leukoc. Biol.* 93 (2013) 847–863. doi:10.1189/jlb.1012501.
- [165] X. Tang, C. Mo, Y. Wang, D. Wei, H. Xiao, Anti-tumour strategies aiming to target tumour-associated macrophages., *Immunology.* 138 (2013) 93–104. doi:10.1111/imm.12023.
- [166] S. Gebremeskel, B. Johnston, Concepts and mechanisms underlying chemotherapy induced immunogenic cell death: impact on clinical studies and considerations for combined therapies, *Oncotarget.* 6 (2015) 41600–41619. <http://www.ncbi.nlm.nih.gov/pmc/articles/PMC4747176/>.
- [167] J.H. Zheng, V.H. Nguyen, S.-N. Jiang, S.-H. Park, W. Tan, S.H. Hong, et al., Two-step enhanced cancer immunotherapy with engineered Salmonella typhimurium secreting heterologous flagellin, *Sci. Transl. Med.* 9 (2017). <http://stm.sciencemag.org/content/9/376/eaak9537.abstract>.
- [168] T. Hagemann, T. Lawrence, I. McNeish, K.A. Charles, H. Kulbe, R.G. Thompson, et al., “Re-educating” tumor-associated macrophages by targeting NF- κ B, *J. Exp. Med.* 205 (2008) 1261 LP-1268. <http://jem.rupress.org/content/205/6/1261.abstract>.
- [169] Y. Tabata, Y. Ikada, Effect of the size and surface charge of polymer microspheres on their phagocytosis by macrophage., *Biomaterials.* 9 (1988) 356–362.
- [170] J.A. Champion, S. Mitragotri, Role of target geometry in phagocytosis., *Proc. Natl. Acad. Sci. U. S. A.* 103 (2006) 4930–4934. doi:10.1073/pnas.0600997103.
- [171] C. He, Y. Hu, L. Yin, C. Tang, C. Yin, Effects of particle size and surface charge on

- cellular uptake and biodistribution of polymeric nanoparticles., *Biomaterials*. 31 (2010) 3657–3666. doi:10.1016/j.biomaterials.2010.01.065.
- [172] N.G. Sosale, K.R. Spinler, C. Alvey, D.E. Discher, Macrophage engulfment of a cell or nanoparticle is regulated by unavoidable opsonization, a species-specific “Marker of Self” CD47, and target physical properties., *Curr. Opin. Immunol.* 35 (2015) 107–112. doi:10.1016/j.coi.2015.06.013.
- [173] S. Chono, T. Tanino, T. Seki, K. Morimoto, Uptake characteristics of liposomes by rat alveolar macrophages: influence of particle size and surface mannose modification., *J. Pharm. Pharmacol.* 59 (2007) 75–80. doi:10.1211/jpp.59.1.0010.
- [174] Y.-N. Chang, H. Guo, J. Li, Y. Song, M. Zhang, J. Jin, et al., Adjusting the balance between effective loading and vector migration of macrophage vehicles to deliver nanoparticles., *PLoS One*. 8 (2013) e76024. doi:10.1371/journal.pone.0076024.
- [175] M.J.D. Clift, B. Rothen-Rutishauser, D.M. Brown, R. Duffin, K. Donaldson, L. Proudfoot, et al., The impact of different nanoparticle surface chemistry and size on uptake and toxicity in a murine macrophage cell line, *Toxicol. Appl. Pharmacol.* 232 (2008) 418–427. doi:http://dx.doi.org/10.1016/j.taap.2008.06.009.
- [176] R.A. Schwendener, P.A. Lagocki, Y.E. Rahman, The effects of charge and size on the interaction of unilamellar liposomes with macrophages., *Biochim. Biophys. Acta*. 772 (1984) 93–101.
- [177] S.S. Yu, C.M. Lau, S.N. Thomas, W.G. Jerome, D.J. Maron, J.H. Dickerson, et al., Size- and charge-dependent non-specific uptake of PEGylated nanoparticles by macrophages., *Int. J. Nanomedicine*. 7 (2012) 799–813. doi:10.2147/IJN.S28531.
- [178] H. Herd, N. Daum, A.T. Jones, H. Huwer, H. Ghandehari, C.-M. Lehr, Nanoparticle geometry and surface orientation influence mode of cellular uptake., *ACS Nano*. 7 (2013) 1961–1973. doi:10.1021/nn304439f.
- [179] T.M. Allen, G.A. Austin, A. Chonn, L. Lin, K.C. Lee, Uptake of liposomes by cultured mouse bone marrow macrophages: influence of liposome composition and size., *Biochim. Biophys. Acta*. 1061 (1991) 56–64.
- [180] J. Key, A.L. Palange, F. Gentile, S. Aryal, C. Stigliano, D. Di Mascolo, et al., Soft Discoidal Polymeric Nanoconstructs Resist Macrophage Uptake and Enhance Vascular Targeting in Tumors., *ACS Nano*. 9 (2015) 11628–11641. doi:10.1021/acsnano.5b04866.
- [181] Z. Li, L. Sun, Y. Zhang, A.P. Dove, R.K. O’Reilly, G. Chen, Shape Effect of Glyco-Nanoparticles on Macrophage Cellular Uptake and Immune Response., *ACS Macro Lett.* 5 (2016) 1059–1064. doi:10.1021/acsmacrolett.6b00419.
- [182] Y. Qiu, Y. Liu, L. Wang, L. Xu, R. Bai, Y. Ji, et al., Surface chemistry and aspect ratio mediated cellular uptake of Au nanorods., *Biomaterials*. 31 (2010) 7606–7619. doi:10.1016/j.biomaterials.2010.06.051.
- [183] M. Bartneck, H.A. Keul, S. Singh, K. Czaja, J. Bornemann, M. Bockstaller, et al., Rapid

- uptake of gold nanorods by primary human blood phagocytes and immunomodulatory effects of surface chemistry., *ACS Nano*. 4 (2010) 3073–3086. doi:10.1021/nn100262h.
- [184] S.A. MacParland, K.M. Tsoi, B. Ouyang, X.-Z. Ma, J. Manuel, A. Fawaz, et al., Phenotype Determines Nanoparticle Uptake by Human Macrophages from Liver and Blood., *ACS Nano*. 11 (2017) 2428–2443. doi:10.1021/acsnano.6b06245.
- [185] E. Blanco, H. Shen, M. Ferrari, Principles of nanoparticle design for overcoming biological barriers to drug delivery., *Nat. Biotechnol.* 33 (2015) 941–951. doi:10.1038/nbt.3330.
- [186] C.-Y. Tsai, S.-L. Lu, C.-W. Hu, C.-S. Yeh, G.-B. Lee, H.-Y. Lei, Size-dependent attenuation of TLR9 signaling by gold nanoparticles in macrophages., *J. Immunol.* 188 (2012) 68–76. doi:10.4049/jimmunol.1100344.
- [187] H.L. Herd, K.T. Bartlett, J.A. Gustafson, L.D. McGill, H. Ghandehari, Macrophage silica nanoparticle response is phenotypically dependent., *Biomaterials*. 53 (2015) 574–582. doi:10.1016/j.biomaterials.2015.02.070.
- [188] T. Tanei, F. Leonard, X. Liu, J.F. Alexander, Y. Saito, M. Ferrari, et al., Redirecting Transport of Nanoparticle Albumin-Bound Paclitaxel to Macrophages Enhances Therapeutic Efficacy against Liver Metastases., *Cancer Res.* 76 (2016) 429–439. doi:10.1158/0008-5472.CAN-15-1576.
- [189] N. Van Rooijen, A. Sanders, Liposome mediated depletion of macrophages: mechanism of action, preparation of liposomes and applications., *J. Immunol. Methods*. 174 (1994) 83–93.
- [190] S. Zhu, M. Niu, H. O’Mary, Z. Cui, Targeting of Tumor-Associated Macrophages Made Possible by PEG-Sheddable, Mannose-Modified Nanoparticles, *Mol. Pharm.* 10 (2013) 3525–3530. doi:10.1021/mp400216r.
- [191] X. Sun, D. Gao, L. Gao, C. Zhang, X. Yu, B. Jia, et al., Molecular imaging of tumor-infiltrating macrophages in a preclinical mouse model of breast cancer., *Theranostics*. 5 (2015) 597–608. doi:10.7150/thno.11546.
- [192] J.M. Irache, H.H. Salman, C. Gamazo, S. Espuelas, Mannose-targeted systems for the delivery of therapeutics., *Expert Opin. Drug Deliv.* 5 (2008) 703–724. doi:10.1517/17425247.5.6.703.
- [193] Y. Hattori, J. Yamashita, C. Sakaida, K. Kawano, E. Yonemochi, Evaluation of antitumor effect of zoledronic acid entrapped in folate-linked liposome for targeting to tumor-associated macrophages., *J. Liposome Res.* 25 (2015) 131–140. doi:10.3109/08982104.2014.954128.
- [194] A. Puig-Kroger, E. Sierra-Filardi, A. Dominguez-Soto, R. Samaniego, M.T. Corcuera, F. Gomez-Aguado, et al., Folate receptor beta is expressed by tumor-associated macrophages and constitutes a marker for M2 anti-inflammatory/regulatory macrophages., *Cancer Res.* 69 (2009) 9395–9403. doi:10.1158/0008-5472.CAN-09-2050.

- [195] L.K. Golani, A. Wallace-Povirk, S.M. Deis, J. Wong, J. Ke, X. Gu, et al., Tumor Targeting with Novel 6-Substituted Pyrrolo [2,3-d] Pyrimidine Antifolates with Heteroatom Bridge Substitutions via Cellular Uptake by Folate Receptor α and the Proton-Coupled Folate Transporter and Inhibition of de Novo Purine Nucleotide Biosynthesis, *J. Med. Chem.* 59 (2016) 7856–7876. doi:10.1021/acs.jmedchem.6b00594.
- [196] T. Nagai, M. Tanaka, Y. Tsuneyoshi, B. Xu, S.A. Michie, K. Hasui, et al., Targeting tumor-associated macrophages in an experimental glioma model with a recombinant immunotoxin to folate receptor beta., *Cancer Immunol. Immunother.* 58 (2009) 1577–1586. doi:10.1007/s00262-009-0667-x.
- [197] W. Xia, A.R. Hilgenbrink, E.L. Matteson, M.B. Lockwood, J.-X. Cheng, P.S. Low, A functional folate receptor is induced during macrophage activation and can be used to target drugs to activated macrophages., *Blood.* 113 (2009) 438–446. doi:10.1182/blood-2008-04-150789.
- [198] W. Han, R. Zaynagetdinov, F.E. Yull, V. V Polosukhin, L.A. Gleaves, H. Tanjore, et al., Molecular imaging of folate receptor beta-positive macrophages during acute lung inflammation., *Am. J. Respir. Cell Mol. Biol.* 53 (2015) 50–59. doi:10.1165/rcmb.2014-0289OC.
- [199] Y. Furusho, M. Miyata, T. Matsuyama, T. Nagai, H. Li, Y. Akasaki, et al., Novel Therapy for Atherosclerosis Using Recombinant Immunotoxin Against Folate Receptor beta-Expressing Macrophages., *J. Am. Heart Assoc.* 1 (2012) e003079. doi:10.1161/JAHA.112.003079.
- [200] Y. Lin, C. Wei, Y. Liu, Y. Qiu, C. Liu, F. Guo, Selective ablation of tumor-associated macrophages suppresses metastasis and angiogenesis., *Cancer Sci.* 104 (2013) 1217–1225. doi:10.1111/cas.12202.
- [201] G. Corna, L. Campana, E. Pignatti, A. Castiglioni, E. Tagliafico, L. Bosurgi, et al., Polarization dictates iron handling by inflammatory and alternatively activated macrophages., *Haematologica.* 95 (2010) 1814–1822. doi:10.3324/haematol.2010.023879.
- [202] W. Wu, Y. Luo, C. Sun, Y. Liu, P. Kuo, J. Varga, et al., Targeting cell-impermeable prodrug activation to tumor microenvironment eradicates multiple drug-resistant neoplasms., *Cancer Res.* 66 (2006) 970–980. doi:10.1158/0008-5472.CAN-05-2591.
- [203] Z. Liu, M. Xiong, J. Gong, Y. Zhang, N. Bai, Y. Luo, et al., Legumain protease-activated TAT-liposome cargo for targeting tumours and their microenvironment., *Nat. Commun.* 5 (2014) 4280. doi:10.1038/ncomms5280.
- [204] S. Ruan, C. Hu, X. Tang, X. Cun, W. Xiao, K. Shi, et al., Increased Gold Nanoparticle Retention in Brain Tumors by in Situ Enzyme-Induced Aggregation., *ACS Nano.* 10 (2016) 10086–10098. doi:10.1021/acsnano.6b05070.
- [205] C.H.J. Choi, C.A. Alabi, P. Webster, M.E. Davis, Mechanism of active targeting in solid tumors with transferrin-containing gold nanoparticles., *Proc. Natl. Acad. Sci. U. S. A.* 107 (2010) 1235–1240. doi:10.1073/pnas.0914140107.

- [206] A.J. Clark, M.E. Davis, Increased brain uptake of targeted nanoparticles by adding an acid-cleavable linkage between transferrin and the nanoparticle core, *Proc. Natl. Acad. Sci. U. S. A.* 112 (2015) 12486–12491. doi:10.1073/pnas.1517048112.
- [207] T. Kang, M. Jiang, D. Jiang, X. Feng, J. Yao, Q. Song, et al., Enhancing Glioblastoma-Specific Penetration by Functionalization of Nanoparticles with an Iron-Mimic Peptide Targeting Transferrin/Transferrin Receptor Complex., *Mol. Pharm.* 12 (2015) 2947–2961. doi:10.1021/acs.molpharmaceut.5b00222.
- [208] K. Movahedi, S. Schoonoghe, D. Laoui, I. Houbracken, W. Waelput, K. Breckpot, et al., Nanobody-based targeting of the macrophage mannose receptor for effective in vivo imaging of tumor-associated macrophages., *Cancer Res.* 72 (2012) 4165–4177. doi:10.1158/0008-5472.CAN-11-2994.
- [209] M. Cieslewicz, J. Tang, J.L. Yu, H. Cao, M. Zavaljevski, K. Motoyama, et al., Targeted delivery of proapoptotic peptides to tumor-associated macrophages improves survival., *Proc. Natl. Acad. Sci. U. S. A.* 110 (2013) 15919–15924. doi:10.1073/pnas.1312197110.
- [210] C. Ngambenjawong, H.H. Gustafson, J.M. Pineda, N.A. Kacherovsky, M. Cieslewicz, S.H. Pun, Serum Stability and Affinity Optimization of an M2 Macrophage-Targeting Peptide (M2pep)., *Theranostics.* 6 (2016) 1403–1414. doi:10.7150/thno.15394.
- [211] C. Ngambenjawong, J.M.B. Pineda, S.H. Pun, Engineering an Affinity-Enhanced Peptide through Optimization of Cyclization Chemistry., *Bioconjug. Chem.* 27 (2016) 2854–2862. doi:10.1021/acs.bioconjchem.6b00502.
- [212] C. Ngambenjawong, M. Cieslewicz, J.G. Schellinger, S.H. Pun, Synthesis and evaluation of multivalent M2pep peptides for targeting alternatively activated M2 macrophages, *J. Control. Release.* 224 (2016) 103–111. doi:http://dx.doi.org/10.1016/j.jconrel.2015.12.057.
- [213] S. Lee, S. Kivimae, A. Dolor, F.C. Szoka, Macrophage-based cell therapies: The long and winding road., *J. Control. Release.* 240 (2016) 527–540. doi:10.1016/j.jconrel.2016.07.018.
- [214] J. Choi, H.-Y. Kim, E.J. Ju, J. Jung, J. Park, H.-K. Chung, et al., Use of macrophages to deliver therapeutic and imaging contrast agents to tumors., *Biomaterials.* 33 (2012) 4195–4203. doi:10.1016/j.biomaterials.2012.02.022.
- [215] S.J. Madsen, S.-K. Baek, A.R. Makkouk, T. Krasieva, H. Hirschberg, Macrophages as cell-based delivery systems for nanoshells in photothermal therapy., *Ann. Biomed. Eng.* 40 (2012) 507–515. doi:10.1007/s10439-011-0415-1.
- [216] Y. Ikehara, T. Niwa, L. Biao, S.K. Ikehara, N. Ohashi, T. Kobayashi, et al., A carbohydrate recognition-based drug delivery and controlled release system using intraperitoneal macrophages as a cellular vehicle., *Cancer Res.* 66 (2006) 8740–8748. doi:10.1158/0008-5472.CAN-06-0470.
- [217] M.A. Miller, Y.-R. Zheng, S. Gadde, C. Pfirschke, H. Zope, C. Engblom, et al., Tumour-

- associated macrophages act as a slow-release reservoir of nano-therapeutic Pt(IV) pro-drug., *Nat. Commun.* 6 (2015) 8692. doi:10.1038/ncomms9692.
- [218] H. Dou, C.J. Destache, J.R. Morehead, R.L. Mosley, M.D. Boska, J. Kingsley, et al., Development of a macrophage-based nanoparticle platform for antiretroviral drug delivery., *Blood.* 108 (2006) 2827–2835. doi:10.1182/blood-2006-03-012534.
- [219] H. Dou, C.B. Grotepas, J.M. McMillan, C.J. Destache, M. Chaubal, J. Werling, et al., Macrophage delivery of nanoformulated antiretroviral drug to the brain in a murine model of neuroAIDS., *J. Immunol.* 183 (2009) 661–669. doi:10.4049/jimmunol.0900274.
- [220] Y. Zhao, M.J. Haney, N.L. Klyachko, S. Li, S.L. Booth, S.M. Higginbotham, et al., Polyelectrolyte Complex Optimization for Macrophage Delivery of Redox Enzyme Nanoparticles, *Nanomedicine (Lond).* 6 (2011) 25–42. doi:10.2217/nnm.10.129.
- [221] N.L. Klyachko, M.J. Haney, Y. Zhao, D.S. Manickam, V. Mahajan, P. Suresh, et al., Macrophages offer a paradigm switch for CNS delivery of therapeutic proteins., *Nanomedicine (Lond).* 9 (2014) 1403–1422. doi:10.2217/nnm.13.115.
- [222] M. Muthana, A.J. Kennerley, R. Hughes, E. Fagnano, J. Richardson, M. Paul, et al., Directing cell therapy to anatomic target sites in vivo with magnetic resonance targeting., *Nat. Commun.* 6 (2015) 8009. doi:10.1038/ncomms9009.
- [223] J. Han, J. Zhen, V. Du Nguyen, G. Go, Y. Choi, S.Y. Ko, et al., Hybrid-Actuating Macrophage-Based Microrobots for Active Cancer Therapy., *Sci. Rep.* 6 (2016) 28717. doi:10.1038/srep28717.
- [224] F. Li, M. Ulrich, M. Jonas, I.J. Stone, G. Linares, X. Zhang, et al., Tumor associated macrophages can contribute to antitumor activity through FcγR-mediated processing of antibody-drug conjugates., *Mol. Cancer Ther.* (2017). doi:10.1158/1535-7163.MCT-17-0019.
- [225] M. De Palma, R. Mazziere, L.S. Politi, F. Pucci, E. Zonari, G. Sitia, et al., Tumor-targeted interferon-α delivery by Tie2-expressing monocytes inhibits tumor growth and metastasis., *Cancer Cell.* 14 (2008) 299–311. doi:10.1016/j.ccr.2008.09.004.
- [226] L.P. Pradel, C.-H. Ooi, S. Romagnoli, M.A. Cannarile, H. Sade, D. Ruttinger, et al., Macrophage Susceptibility to Emactuzumab (RG7155) Treatment., *Mol. Cancer Ther.* 15 (2016) 3077–3086. doi:10.1158/1535-7163.MCT-16-0157.
- [227] L.A. Carey, E.P. Winer, I-SPY 2 — Toward More Rapid Progress in Breast Cancer Treatment, *N. Engl. J. Med.* 375 (2016) 83–84. doi:10.1056/NEJMe1603691.

1.9 Supplementary information

Table S1.1 Extended compilation of drugs in clinical trials whose mechanisms of action may involve modulation of macrophages/TAMs

Drug/Description	Sponsors and collaborators	Phase/ Status	Tumor type	Treatment	ClinicalTrials.govIdentifier	First received
CSF-1R inhibitor						
Pexidartinib/PLX3397 (Oral CSF-1R/KIT/FLT3 tyrosine kinase inhibitor)	QuantumLeap Healthcare Collaborative	2 Ongoing	Breast cancer	Evaluation of multiple novel agents	NCT01042379	December 31, 2009
	Plexxikon	2 Completed	Hodgkin's lymphoma	Monotherapy	NCT01217229	October 4, 2010
	Plexxikon	1/2 Ongoing	Acute myeloid leukemia	Monotherapy	NCT01349049	May 4, 2011
	Plexxikon	2 Completed	Recurrent glioblastoma	Monotherapy	NCT01349036	May 4, 2011
	Plexxikon	2 Completed	Prostate cancer	Monotherapy	NCT01499043	December 20, 2011
	Plexxikon	1b Ongoing	Advanced solid tumor	with paclitaxel	NCT01525602	January 31, 2012
	Hope Rugo, MD (University of California, San Francisco), Susan G. Komen Breast Cancer Foundation, Plexxikon	1b/2 Ongoing	Metastatic breast cancer	With eribulin	NCT01596751	May 7, 2012
	Plexxikon	1b/2 Ongoing	Newly diagnosed glioblastoma	With radiation therapy and temozolomide	NCT01790503	February 7, 2013
	Plexxikon	1b Terminated	V600-mutated BRAF melanoma	With vemurafenib (BRAF inhibitor)	NCT01826448	April 1, 2013
	The Christie NHS Foundation Trust	2 Ongoing	Malignant melanoma	Monotherapy	NCT02071940	May 8, 2013
	Daiichi Sankyo Inc.	3 Ongoing	Pigmented villonodular synovitis (PVNS), giant cell tumors of the tendon sheath (GCT-TS), tenosynovial giant cell tumor (TGCT)	Monotherapy	NCT02371369	February 19, 2015
	National Cancer Institute (NCI)	1/2 Ongoing	Plexiform neurofibroma, precursor cell lymphoblastic leukemia-lymphoma, acute prolymphocytic leukemia, sarcoma		NCT02390752	March 17, 2015
	Plexxikon	1/2 Ongoing	Gastrointestinal stromal tumors	With PLX9486 (KIT inhibitor)	NCT02401815	March 19, 2015
	Plexxikon, Merck Sharp & Dohme Corp.	1/2a Ongoing	Advanced melanoma and other solid tumors	With Pembrolizumab (Anti-PD-1 antibody)	NCT02452424	May 20, 2015
	Barbara Ann Karmanos Cancer Institute, National Cancer Institute (NCI)	1 Ongoing	Prostate adenocarcinoma	With antiandrogen therapy and radiation therapy	NCT02472275	June 11, 2015
	Gary Schwartz (Columbia University), Plexxikon	1/2 Ongoing	Sarcoma (Phase 1), malignant peripheral nerve sheath tumors (Phase 2)	With sirolimus (Rapamycin, mTOR inhibitor)	NCT02584647	October 21, 2015
	Centre Leon	1	Advanced/metastatic colorectal or	With	NCT02777710	May 12,

	Berard, Plexxikon, AstraZeneca Plexxikon	Ongoing	pancreatic cancer	Durvalumab (Anti-PD-L1 antibody)		2016
		1/2 Ongoing	Malignant melanoma	Monotherapy	NCT02975700	November 21, 2016
PLX7486 (Oral, fms/Trk tyrosine kinase inhibitor, tosylate salt form)	Plexxikon	1 Ongoing	Solid tumors, tumors of any history with activating Trk point or NTRK fusion mutation	Monotherapy	NCT01804530	March 1, 2013
BLZ945 (Oral c-fms tyrosine kinase inhibitor)	Novartis Pharmaceuticals	1/2 Ongoing	Advanced solid tumors	Monotherapy and with PDR001 (Anti-PD-1 antibody)	NCT02829723	July 8, 2016
ARRY-382 (Oral c-FMS inhibitor)	Array BioPharma	1 Completed	Metastatic cancer	Monotherapy	NCT01316822	December 1, 2010
	Array BioPharma	1b/2 Ongoing	Advanced solid tumors	With Pembrolizumab (Anti-PD-1 antibody)	NCT02880371	August 2, 2016
AMG 820 (Human IgG2 anti CSF-1R antibody)	Amgen	1 Completed	Advanced solid tumor	Monotherapy	NCT01444404	September 1, 2011
	Amgen	1b/2 Ongoing	Advanced solid tumor	With Pembrolizumab (Anti-PD-1 antibody)	NCT02713529	March 3, 2016
Emactuzumab/RO55095 54/RG7155 (Human IgG1 anti-CSF-1R antibody)	Hoffmann-La Roche	1 Ongoing	Advanced solid tumors	Monotherapy and with paclitaxel	NCT01494688	December 2, 2011
	Hoffmann-La Roche	1 Ongoing	Solid cancers	With MPDL3280A (Tecentriq/anti-PD-L1 antibody)	NCT02323191	December 5, 2014
	Hoffmann-La Roche	1 Ongoing	Solid tumors	With RO7009789 (Anti-CD40 agonistic antibody)	NCT02760797	April 14, 2016
	M.D. Anderson Cancer Center, Genentech Inc.	2 Ongoing	Platinum-resistant, epithelial ovarian, fallopian tube or primary peritoneal Cancer	With paclitaxel and Bevacizumab (Avastin/anti-VEGF antibody)	NCT02923739	September 30, 2016
LY3022855/IMC-CS4 (Human IgG1 anti-CSF-1R antibody)	Eli Lilly and Company	1 Ongoing	Neoplasms	Monotherapy	NCT01346358	April 29, 2011
	Eli Lilly and Company	1 Ongoing	Breast or prostate cancer	Monotherapy	NCT02265536	September 24, 2014
	Eli Lilly and Company, AstraZeneca	1a/1b Ongoing	Advanced solid tumors	With Durvalumab (Anti-PD-L1 antibody) or Tremelimumab (Anti-CTLA-4 antibody)	NCT02718911	March 21, 2016
Cabiralizumab/FPA008 (Anti-CSF-1R antibody)	Five Prime Therapeutics Inc.	1/2 Ongoing	PVNS (Phase 1), TGCT (Phase 2)	Monotherapy	NCT02471716	June 1, 2015
	Five Prime Therapeutics Inc., Bristol-Myers Squibb	1a/1b Ongoing	Advanced solid tumors	With BMS-936558 (Nivolumab/anti-PD-1 antibody)	NCT02526017	August 13, 2015
RON/MET inhibitor IMC-RON8/Narnatumab (Human anti-RON antibody)	Eli Lilly and Company	1 Completed	Cancer	Monotherapy	NCT01119456	May 6, 2010
ASLAN002/BMS77760 7 (Oral RON/MET receptor tyrosine kinase inhibitor)	Bristol-Myers Squibb	1/2 Completed	Advanced solid tumor	Monotherapy	NCT00605618	January 18, 2008
	Aslan Pharmaceuticals	1 Completed	Malignant solid tumor	Monotherapy	NCT01721148	November

						1, 2012
CD47-SIRPα inhibitor Hu5F9-G4 (Human IgG4 anti-CD47 antibody)	Forty Seven Inc.	1 Ongoing	Solid tumors	Monotherapy	NCT02216409	August 12, 2014
	Forty Seven Inc.	1 Ongoing	Acute myeloid leukemia	Monotherapy	NCT02678338	January 27, 2016
	Forty Seven Inc.	1b/2 Ongoing	Colorectal neoplasms, solid tumors	With Cetuximab (Erbix/anti-EGFR antibody)	NCT02953782	November 1, 2016
	Forty Seven Inc.	1b/2 Ongoing	Non-Hodgkin's lymphoma, diffuse large B-cell diffuse lymphoma, indolent lymphoma	With Rituximab (Anti-CD20 antibody)	NCT02953509	November 1, 2016
CC-90002 (Anti-CD47 antibody)	Celgene	1 Ongoing	Hematologic neoplasms	Monotherapy	NCT02367196	February 13, 2015
	Celgene	1 Ongoing	Acute myeloid leukemia, myelodysplastic syndromes	Monotherapy	NCT02641002	November 12, 2015
TTI-621 (SIRP α -Fc fusion)	Trillium Therapeutics Inc.	1 Ongoing	Hematologic malignancies	Monotherapy	NCT02663518	January 19, 2016
	Trillium Therapeutics Inc.	1 Ongoing	Solid tumors, mycosis fungoides	Monotherapy	NCT02890368	August 26, 2016
ALX148 (High affinity SIRP α variant)	Alexo Therapeutics Inc.	1 Ongoing	Metastatic cancer, solid tumor, advanced cancer, non-Hodgkin's lymphoma	Monotherapy, with Atezolizumab (Tecentriq/anti-PD-L1 antibody) or Transtuzumab (Herceptin/anti-HER2 antibody)	NCT03013218	December 15, 2016
CCR2-CCL2 inhibitor PF-04136309/PF6309 (Small molecule CCR2 antagonist)	Washington University School of Medicine, National Cancer Institute (NCI)	1 Completed	Pancreatic neoplasm	With oxaliplatin, irinotecan, leucovorin, and fluorouracil	NCT01413022	July 29, 2011
	Pfizer	1b/2 Ongoing	Metastatic pancreatic ductal adenocarcinoma	With Nab-paclitaxel and gemcitabine	NCT02732938	February 29, 2016
MLN1202/S0916/plozalizumab (Human anti-CCR2 antibody)	Southwest Oncology Group	2 Completed	Metastatic cancer (bone), adult solid tumors	Monotherapy	NCT01015560	November 17, 2009
	Millennium Pharmaceuticals Inc.	1 Ongoing	Melanoma	With Nivolumab (Anti-PD-1 antibody)	NCT02723006	March 25, 2016
Carlumab/CNTO 888 (Human IgG1 κ anti-CCL2 antibody)	Centocor Inc.	1 Completed	Cancer	Monotherapy	NCT00537368	September 28, 2007
	Centocor Research & Development Inc.	2 Completed	Prostate cancer	Monotherapy	NCT00992186	September 29, 2009
	Centocor Inc.	1 Completed	Cancer	With DOXIL, gemcitabine, paclitaxel + carboplatin, or docetaxel	NCT01204996	September 16, 2010
CXCR4-CXCL12 inhibitor Mozobil/AMD-3100/plerixafor* (Small molecule CXCR4 antagonist)	CCTU-Cancer Theme, Sanofi, Stand Up To Cancer, CRUK Cambridge Institute, Lustgarten Foundation,	1 Ongoing	Metastatic pancreatic adenocarcinoma, ovarian serous adenocarcinoma, metastatic colorectal cancer	Monotherapy	NCT02179970	July 1, 2014

LY2510924 (CXCR4 agonistic peptide)	National Institute for Health Research (United Kingdom) Eli Lilly and Company	2 Ongoing	Metastatic clear cell renal cell carcinoma	With sunitinib	NCT01391130	July 7, 2011
	Eli Lilly and Company	2	Extensive stage small cell lung carcinoma	With carboplatin and etoposide	NCT01439568	September 21, 2011
	M.D. Anderson Cancer Center, Eli Lilly and Company, High Impact Clinical Research Support Program Eli Lilly and Company, AstraZeneca	1 Ongoing 1 Ongoing	Leukemia Solid tumors	With idarubicin and cytarabine With Durvalumab (Anti-PD-L1 antibody)	NCT02652871 NCT02737072	January 8, 2016 April 8, 2016
CD 40 agonist CP-870,893/RO7009789 (Human IgG2 anti-CD40 antibody)	Hoffmann-La Roche	1 Completed	Neoplasms	With paclitaxel and carboplatin	NCT00607048	January 22, 2008
	Hoffmann-La Roche,	1 Completed	Pancreatic neoplasm	With gemcitabine	NCT00711191	June 26, 2008
	University of Pennsylvania NCI, Oncovir Inc., Pfizer	1 Completed	Melanoma	With NY-ESO-1 157-165 (165V) and gp1002 80-288 (288V) peptides and Oncovir poly IC:LC	NCT01008527	November 2, 2009
	Abramson Cancer Center of the University of Pennsylvania	1 Ongoing	Recurrent/stage IV melanoma	With Tremelimumab (Anti-CTLA-4 antibody)	NCT01103635	April 12, 2010
	Abramson Cancer Center of the University of Pennsylvania	1 Completed	Adenocarcinoma pancreas	With gemcitabine	NCT01456585	October 19, 2011
	Abramson Cancer Center of the University of Pennsylvania	1 Completed	Solid tumors	Monotherapy	NCT02157831	June 4, 2014
	Abramson Cancer Center of the University of Pennsylvania	1 Completed	Advanced solid tumors	Monotherapy	NCT02225002	August 22, 2014
	Hoffmann-La Roche	1 Ongoing	Solid cancers	With MPDL3280A (Tecentriq/anti-PD-L1 antibody)	NCT02304393	November 26, 2014
	Abramson Cancer Center of the University of Pennsylvania	1 Ongoing	Pancreatic cancer	With nab-paclitaxel and gemcitabine	NCT02588443	October 21, 2015
	Hoffmann-La Roche	1 Ongoing	Advanced/metastatic solid tumors	With Vanucizumab (Bi-specific anti-Ang2/VEGF-A antibody)	NCT02665416	January 15, 2016
ADC-1013/JNJ-64457107 (Human IgG1 anti-CD40 antibody)	Hoffmann-La Roche	1 Ongoing	Solid tumors	With Emactuzumab (Anti-CSF-1R antibody)	NCT02760797	April 14, 2016
	Alligator Bioscience AB	1 Ongoing	Neoplasm, solid tumors	Monotherapy	NCT02379741	February 16, 2015
	Janssen Research & Development,	1 Ongoing	Advanced solid neoplasms	Monotherapy	NCT02829099	July 7, 2016

HCD122 (Human IgG1 anti-CD40 antibody)	LLC Novartis Pharmaceuticals, XOMA (US)	1 Terminated	Chronic lymphocytic leukemia	Monotherapy	NCT00108108	April 14, 2005
	LLC Novartis Pharmaceuticals	2 Completed	Multiple myeloma	Monotherapy	NCT00231166	September 30, 2005
	Novartis Pharmaceuticals, XOMA (US)	1a/2 Completed	Non-Hodgkin's lymphoma, Hodgkin's lymphoma	Monotherapy	NCT00670592	April 30, 2008
SGN-40/Dacetuzumab (Human IgG1 anti-CD40 antibody)	LLC Novartis Pharmaceuticals	1b Completed	Follicular lymphoma	Monotherapy	NCT01275209	January 10, 2011
	Seattle Genetics Inc., Genentech Inc.	1 Completed	Multiple myeloma	Monotherapy	NCT00079716	March 11, 2004
	Seattle Genetics Inc., Genentech Inc.	1 Completed	Non-Hodgkin's lymphoma	Monotherapy	NCT00103779	February 14, 2005
	Seattle Genetics Inc., Genentech Inc.	1/2 Completed	Chronic lymphocytic leukemia	Monotherapy	NCT00283101	January 25, 2006
	Seattle Genetics Inc., Genentech Inc.	2 Completed	Non-Hodgkin's lymphoma, diffuse large B-cell lymphoma	Monotherapy	NCT00435916	February 14, 2007
	Seattle Genetics Inc., Genentech Inc.	1 Completed	Multiple myeloma	With lenalidomide and dexamethasone	NCT00525447	August 31, 2007
	Genentech Inc., Seattle Genetics Inc.	1 Completed	Non-Hodgkin's lymphoma	With Rituximab (Anti-CD20 antibody)	NCT00556699	November 9, 2007
	Seattle Genetics Inc., Genentech Inc.	2 Terminated	Non-Hodgkin's lymphoma, diffuse large B-cell lymphoma	With Rituximab (Anti-CD20 antibody), etoposide, carboplatin, ifostamide	NCT00529503	September 11, 2007
	Seattle Genetics Inc., Genentech Inc.	1 Completed	Non-Hodgkin's lymphoma, diffuse large B-cell lymphoma	With Rituximab (Anti-CD20 antibody) and gemcitabine	NCT00655837	April 4, 2008
Chi Lob 7/4 (Chimeric IgG1 anti-CD40 antibody)	Genentech Inc., Seattle Genetics Inc.	1 Completed	Multiple myeloma	With bortezomib	NCT00664898	April 21, 2008
	Cancer Research UK	1 Completed	Advanced malignancies	Monotherapy	NCT01561911	March 21, 2012
	SEA-CD40 (Non-fucosylated human IgG1 anti-CD40 antibody)	Seattle Genetics Inc.	1 Ongoing	Cancer, carcinoma, neoplasm, metastasis, Hodgkin's disease, lymphoma	Monotherapy	NCT02376699
APX005M (Human IgG1 anti-CD40 antibody)	Apexigen Inc.	1 Ongoing	Cancer, carcinoma, neoplasm, metastasis	Monotherapy	NCT02482168	June 11, 2015
	Apexigen Inc.	1 Ongoing	Melanoma	With Pembrolizumab (Anti-PD-1 antibody)	NCT02706353	March 8, 2016
Vasculature-modulating agent MEDI3617 (Human anti-ANG2 antibody)	MedImmune LLC	1/1b Completed	Advanced solid tumors, advanced recurrent ovarian tumors	Monotherapy and with Bevacizumab (Anti-VEGF-A antibody), paclitaxel, paclitaxel + carboplatin, or gemcitabine + carboplatin	NCT01248949	November 23, 2010
	F. Stephen Hodi MD,	1 Ongoing	Metastatic melanoma	With Tremelinumab	NCT02141542	May 15,

	MedImmune LLC			(Anti-CTLA-4 antibody)		2014
Vanucizumab (Human bispecific anti-Ang2/VEGF antibody)	Hoffmann-La Roche	1 Ongoing	Neoplasms	With Atezolizumab (Anti-PD-L1 antibody)	NCT01688206	September 13, 2012
	Hoffmann-La Roche	2 Ongoing	Colorectal cancer	With fluorouracil, oxaliplatin, and folinic acid (compare performance to Bevacizumab (Anti-VEGF-A antibody))	NCT02141295	May 15, 2014
	Hoffmann-La Roche	1 Ongoing	Advanced/metastatic solid tumors	With RO7009789 (Anti-CD40 agonistic antibody) Monotherapy	NCT02665416	January 15, 2016
Vadimezan/5,6-dimethylxanthenone-4-acetic acid (DMXAA) (Vasculature-disrupting agent) Partial list)	Antisoma Research	2 Completed	Prostate cancer		NCT00111618	May 24, 2005
	Novartis Pharmaceuticals	3 Terminated	NSCLC	With carboplatin and paclitaxel	NCT00662597	April 17, 2008
	Novartis Pharmaceuticals	3 Terminated	NSCLC	With docetaxel	NCT00738387	August 19, 2008
	Swiss Group for Clinical Cancer Research	2 Completed	Lung cancer	With carboplatin and paclitaxel	NCT01057342	January 26, 2010
PI3ky inhibitor Duvelisib/IPI-549 (Oral PI3k δ/γ inhibitor)	Infinity Pharmaceuticals Inc.	1 Ongoing	Advanced solid tumors, non-small cell lung cancer (NSCLC), melanoma, squamous cell cancer of the head and neck	With Nivolumab (Anti-PD-1 antibody)	NCT02637531	December 16, 2015

Source: clinicaltrials.gov, www.cancer.gov

"Ongoing" includes both recruiting and non-recruiting stages.

*Approved for use in combination with G-MCSF to mobilize hematopoietic stem cells to peripheral blood for collection and subsequent autologous transplantation in patients with non-Hodgkin's lymphoma and multiple myeloma.

Chapter 2

SYNTHESIS AND EVALUATION OF MULTIVALENT M2PEP PEPTIDES FOR TARGETING ALTERNATIVELY ACTIVATED M2 MACROPHAGES

Chayanon Ngambenjawong, Maryelise Cieslewicz, Joan G. Schellinger, Suzie H. Pun

Abstract

The tumor microenvironment in the majority of cancers is known to favor polarization of tumor-associated macrophages (TAMs) to alternatively activated M2 phenotype, promoting disease progression and reducing patient survival. Effective therapy targeting this M2 macrophage population is thus a promising adjuvant to approved cancer therapies. One of the challenges in targeting M2-like TAMs is a lack of high affinity targeting ligand with good selectivity over anti-tumor M1-like TAMs. We have previously identified an M2 macrophage-targeting peptide (M2pep) that binds preferentially to murine M2 macrophages and M2-like TAMs. A fusion peptide of M2pep with pro-apoptotic peptide KLA (M2pepKLA) was further used to reduce TAM population *in vivo* but high concentrations and frequent dosing were required due to low binding affinity of M2pep for M2 macrophage. The goal of this study was to develop more potent TAM depletion constructs by increasing the valency of both the M2pep targeting and KLA drug domains. Divalent and tetravalent displays of M2pep ([M2pep]₂-Biotin and [M2pep]₄-Biotin) were synthesized and evaluated for improvement in binding avidity to the murine macrophages. High avidity and selective binding of [M2pep]₂-Biotin to M2 macrophages was achieved with at least 10-fold lower concentration than required for monovalent M2pep activity. Increasing M2pep valency to four, however, resulted in a reduction in both binding activity and selectivity. Surprisingly, both divalent and tetravalent M2pep, without conjugation of any cytotoxic drug cargo, exhibited M2 macrophage-selective toxicity not observed in monovalent M2pep treatment. We next synthesized divalent M2pep with monovalent and divalent KLA ([M2pep]₂-[KLA] and [M2pep]₂-[KLA]₂) to evaluate its enhanced potency compared to M2pepKLA. While both constructs were significantly more toxic than M2pepKLA to primary, bone marrow-derived M2 macrophage, desired selectivity was retained only with [M2pep]₂-[KLA]. Finally, we evaluated all multivalent M2pep and M2pepKLA analogs using a syngeneic CT-26 tumor cell suspension. In this setting, [M2pep]₄-Biotin and [M2pep]₂-[KLA]₂ exhibited selective toxicity to both M2-like TAMs and malignant cells but not to M1-like TAMs. Therefore, these constructs are promising anti-cancer constructs with dual-modality mechanisms: malignant cell killing and TAM-based immunomodulation.²

² Reprinted with permission from Ngambenjawong et al. (2016) J Control Release 28(224):103-111. Copyright© 2016 Elsevier

2.1 Introduction

Advances in the field of immunology and cancer biology have led to recent developments of clinically-effective cancer immunotherapies [1,2]. The complex tumor microenvironment, including the crosstalk between immune and cancer cells, is now actively investigated as a source of potential new drug targets [3]. The tumor associated macrophage (TAM) is a particularly enigmatic participant in this microenvironment. TAMs may be recruited from nearby tissue resident macrophages or from monocytes in circulation [4,5]. Due to macrophage plasticity, TAMs exist as a heterogeneous population and may be broadly categorized as classically activated M1 or alternatively activated M2 macrophages [6]. Notably, these two polarizing phenotypes also exhibit opposing functions toward cancer immunity [7]. M2-like TAMs are known to be pro-tumorigenic, promoting a local immunosuppressive environment, angiogenesis, and metastasis via secretion of TGF- β , VEGF, and MMP proteases. In contrast, M1-like TAMs bolster anti-tumor immunity by directly killing cancer cells through secretion of reactive nitric oxide and by stimulating immune response in tumor microenvironment. Clinically, high accumulation of TAMs observed in biopsy specimens has been correlated with both positive and negative disease prognosis depending on the cancer type [4,8]. This contradictory observation may be attributed to the difference in relative abundance of M2 versus M1-like TAM populations, and hence in more recent studies, analysis of more defined macrophage subpopulations and/or M1/M2 ratio is usually included [9–11]. In several types of cancers including breast, ovarian, pancreatic, and brain cancers where high density of TAMs has been correlated to poor disease prognosis, the majority of these TAMs express the M2 phenotype [9,12–14].

M2-like TAMs are therefore a potential therapeutic target, and selective depletion of this macrophage subpopulation is expected to improve patient outcome. Experimentally, bisphosphonate formulations such as clodronate liposomes and zoledronic acid have been used to eliminate macrophages; however, these approaches are not M2-specific and affect tissue-resident macrophages [15,16]. Targeted blocking of macrophage colony stimulating factor 1 receptor (CSF-1R) with anti-CSF-1R antibodies showed some promise toward M2-like TAM depletion or repolarization [17,18]. Nonetheless, systemic depletion of macrophages was observed following the treatment, and CSF-1R blocking resulted in a rise in plasma CSF-1 concentration which could mediate a rebound effect in macrophage population after therapy cessation. In addition,

association between CSF-1R inhibition and increased incidence of breast cancer metastasis was also reported [19]. Another challenge for targeting M2-like TAMs arises from their recruitment to hypoxic tumor regions [20–22] which are less accessible to diffusion limited macromolecular drugs [23]. Hence, alternative M2 macrophage-targeting therapeutics are still needed that 1) readily gain access to and selectively deplete M2-like TAMs, 2) do not mediate an adverse cytokine storm effect, and 3) spare systemic macrophages to improve dose-limiting toxicity profile.

Toward this goal, we have identified a peptide targeting ligand for murine M2 macrophages using peptide phage display [24]. This peptide selectively binds both M2-like TAMs and primary, polarized M2 macrophages over other leukocytes including their M1 counterparts. Fusion of M2pep to pro-apoptotic KLA peptide (M2pepKLA) was further shown to mediate TAM depletion *in vivo*. However, its efficacy was limited by relatively low binding affinity of M2pep ($K_d \sim 100 \mu\text{M}$) typical of phage display-discovered peptides. Therefore, an opportunity exists to further improve M2pepKLA by increasing receptor binding affinity of the ligand and cytotoxic potency of the cargo.

In this study, we aimed to improve our M2pep-based therapeutics for more selective and potent depletion of M2-like TAMs by 1) investigating multivalent display of M2pep to increase binding avidity to M2 macrophages and 2) investigating multivalent display of KLA as a way to enhance cargo cytotoxicity. Multivalency is used to increase binding avidity to target receptors [25–28] and also has been shown by us and others to enhance cytotoxicity of KLA [29–32]. In the first part of this study, we report the synthesis of divalent and tetravalent M2pep ([M2pep]₂-Biotin and [M2pep]₄-Biotin, respectively) and the binding of these constructs to primary M1 and M2 macrophages. In the second part of this study, we report synthesis and cytotoxicity evaluation of two multivalent M2pepKLA analogs; 1) [M2pep]₂-[KLA] and 2) [M2pep]₂-[KLA]₂, having M2pep-to-KLA ratio of 2:1 and 1:1 respectively. Finally, we demonstrate cytotoxicity and selectivity of multivalent M2pep and M2pepKLA analogs in a mixed cell population derived from syngeneic CT-26 tumors.

2.2 Materials and methods

2.2.1 Materials

Fmoc-protected amino acids and 1-[Bis(dimethylamino)methylene]-1H-1,2,3-triazolo[4,5-b]pyridinium 3-oxid hexafluorophosphate (HATU) were purchased from AAPPTec (Louisville, KY) and AnaSpec (Fremont, CA). NovaPEG Rink Amide, Biotin NovaTag, and 2-chlorotriyl chloride resins were purchased from Merck Millipore (Billerica, MA). Collagenase (C0130), 3-maleimidopropionic acid, 3-(maleimido)propionic acid N-hydroxysuccinimide ester (NHS-maleimide), and tris(2-carboxyethyl)phosphine hydrochloride (TCEP) were purchased from Sigma-Aldrich (St. Louis, MO). 1,11-Bismaleimidotriethyleneglycol (BM(PEG)₃), pacific blue anti-mouse F4/80 antibody, and LIVE/DEAD fixable far red cell stain kit were purchased from Life Technologies (Grand Island, NY). PerCP anti-mouse/human CD11b antibody and anti-mouse CD16/32 antibody (Fc receptor block) were purchased from BioLegend (San Diego, CA). FITC anti-mouse Ly-6G antibody was purchased from BD Pharmingen (San Diego, CA). Streptavidin FITC was purchased from eBioscience (San Diego, CA). Mouse macrophage colony-stimulating factor (M-CSF), interleukin-4 (IL-4), and interferon- γ (IFN- γ) were purchased from R&D Systems (Minneapolis, MN). Lipopolysaccharide (LPS) was purchased from InvivoGen (San Diego, CA). Dispase II was purchased from Roche (Indianapolis, IN). All other reagents were purchased from Fisher Scientific (Pittsburgh, PA) and were of reagent grade or better.

2.2.2 Multivalent peptide synthesis

2.2.2.1 Peptide synthesis

M2pepBiotin (YEQDPWGVKWWYGGGSKKKKBiotin) was purchased from Elim Biopharm (Hayward, CA). M2pepKKKC (YEQDPWGVKWWYGGGSKKKC), scrambled M2pepKKKC (WEDYQWPVYKGWGGGSKKKC), M2pepKLA (YEQDPWGVKWWYGGGSKlklakklaklak), M2pepGCGKLA (YEQDPWGVKWWYGCGSKlklakklaklak), and KLA (klaklakklaklak) were synthesized on NovaPEG rink amide resin using an automated PS3 peptide synthesizer (Protein Technologies, Phoenix, AZ) following standard Fmoc solid phase peptide synthesis strategy. The peptide sequences are written from N-terminus to C-terminus, and lower case letters denote d-amino acids. When Fmoc deprotection or amino acid coupling was performed off the peptide

synthesizer, the following conditions were applied: peptide resin was swelled in DCM for 15 min followed by Fmoc deprotection using 20 (v/v)% piperidine in DMF for 30 min (repeat 1 time). Amino acids were coupled by incubating peptide resin in 4 eq. of amino acid and 3.9 eq. of HATU dissolved in 0.4 M N-methylmorpholine in DMF for 3 h. Maleimide-functionalized KLA (KLA-Mal) was synthesized by on-resin coupling of KLA with 3-maleimidopropionic acid at the N terminus. Peptides were cleaved from the NovaPEG rink amide resin by incubation in TFA/triisopropylsilane (TIPS)/1,2-ethanedithiol (EDT)/1,3-dimethoxybenzene (90:2.5:2.5:5 v/v/v/v) for 2.5 h. EDT was included in the cleavage solution only for the cysteine-containing peptides. The cleaved peptides were precipitated in cold ether twice and purified to >95% purity by RP-HPLC (Agilent 1200, Santa Clara, CA) using Phenomenex Fusion-RP C18 semi-preparative column (Torrance, CA) with water (0.1% TFA) and acetonitrile (0.1% TFA) as mobile phases. Molecular weights of the purified peptides were confirmed by either MALDI-TOF MS or ESI-MS (Bruker Daltonics, Billerica, MA).

2.2.2.2 Synthesis of [Mal]₂-Biotin and [Mal]₂-Cys(Trt) divalent linkers

To synthesize the [Mal]₂-Biotin divalent linker, the Fmoc protecting group on Biotin NovaTag resin was first manually deprotected and coupled with Fmoc-Lys(Fmoc)-OH following the previously-described protocol. Fmoc protecting groups were then deprotected and coupled with 3-maleimidopropionic acid (4 eq. relative to NH₂ groups). The linker was cleaved in 20 (v/v)% TFA in DCM for 2 h, precipitated in cold ether twice, dried under vacuum, and used directly without purification. To synthesize the [Mal]₂-Cys(Trt) divalent linker, Fmoc-Cys(Trt)-OH was coupled to 2-chlorotrityl chloride resin by incubating the resin in 4 eq. of the amino acid and 8 eq. of DIPEA in DMF for 3 h. Remaining unreacted sites were quenched by double 10 min incubations in DCM/MeOH/DIPEA (17:2:1 v/v/v). Fmoc-Lys(Fmoc)-OH and 3-maleimiopropionic acid were then coupled to the resin as noted for [Mal]₂-Biotin. The linker was cleaved in acetic acid/trifluoroethanol/DCM (1:1:8 v/v/v) for 1 h, precipitated in cold ether twice, dried under vacuum, and used directly without further purification.

2.2.2.3 Synthesis of [Mal]₄-Biotin tetravalent linker

Tetravalent linker precursor (GKGKGKKGK) was synthesized on NovaPEG rink amide resin using the automated peptide synthesizer. Biotin was manually coupled to N-terminus of the peptide on resin following which the biotinylated tetravalent linker precursor (Biotin-GKGKGKKGK) was cleaved in TFA/DCM (1:1 v/v) for 3 h, precipitated in cold ether twice, and purified by RP-HPLC. Biotin-GKGKGKKGK was coupled with NHS-maleimide (8 eq.) and DIPEA (24 eq.) in DMF for 24 h at room temperature. As the reaction proceeded, the product ([Mal]₄-Biotin) formed which became less soluble in DMF and precipitated out of the solvent. The precipitated product was washed twice with cold ether and used directly without further purification.

2.2.2.4 Synthesis of [M2pep]₂-Biotin and [M2pep]₄-Biotin

To synthesize [M2pep]₂-Biotin, 0.04 eq. of TCEP (10 mg/mL in dH₂O) was added to a 1 mM solution of M2pepKKKC in PBS (pH 6.5, 1 mM EDTA)/ACN (1:1 v/v). The flask was capped with a rubber septum, and the solution was purged with argon for 10 min. During purging, [Mal]₂-Biotin was dissolved in methanol (10 mg/mL), and the appropriate volume (0.4 eq.) was added to the flask. Purging was continued for another 10 min after which the needle was removed, and the septum was sealed with parafilm. The reaction was left to proceed for 24 h at room temperature. The solution mixture was then evaporated under reduced pressure, resolubilized in a minimal volume of H₂O/DMF (2:1 v/v). M2pepKKKC dimer formed during coupling reaction was reduced with TCEP (10 eq. relative to the starting amount of M2pepKKKC) for 30 min before the solution was desalted with a Sep-Pak C18 cartridge (Waters, Milford, MA) and purified by RP-HPLC. To synthesize [M2pep]₄-Biotin, the same protocol as the synthesis of [M2pep]₂-Biotin was used with some modifications as follows: 0.02 eq. of TCEP and 0.2 eq. of [Mal]₄-Biotin were used in the synthesis. [Mal]₄-Biotin was dissolved in DMSO to make a stock solution.

2.2.2.5 Synthesis of [M2pep]₂-Cys(Trt) and deprotection of Trt protecting group

[M2pep]₂-Cys(Trt) was synthesized in the same manner as the synthesis of [M2pep]₂-Biotin. Subsequent deprotection of Trt protecting group from the peptide was done in

TFA/TIPS/DMF (75:2.5:22.5 v/v/v) for 1 h and precipitated in cold ether. Successful deprotection was confirmed by ESI-MS.

2.2.2.6 Synthesis of [M2pep]₂-[KLA] and [M2pep]₂-[KLA]₂

[M2pep]₂-[KLA] was synthesized by conjugating KLA-Mal to [M2pep]₂-Cys using the same conjugation conditions as the synthesis of [M2pep]₂-Biotin except that 2 eq. of KLA-Mal was used in the synthesis. [M2pep]₂-[KLA]₂ was also synthesized in the same manner using 1 eq. of M2pepGCGKLA and 0.4 eq. of BM(PEG)₃. BM(PEG)₃ was dissolved in DMSO for use.

2.2.3 Generation of bone marrow-derived macrophages

All animal handling protocols were approved by the University of Washington Institutional Animal Care and Use Committee. Femurs and tibias were harvested from female c57bl6/027 mice with the age between 6-8 weeks. The bones were flushed with RPMI 1640 medium to collect bone marrow cells. Roughly 5 million cells per dish were seeded on 100 mm petri dish in RPMI 1640 medium containing 20% donor horse serum, 1% antibiotic-antimycotic (AbAm), and 20 ng/mL M-CSF. After 7 d of culture, M-CSF was replaced with either 25 ng/mL IFN- γ and 100 ng/mL LPS for M1 macrophage activation or 25 ng/mL IL-4 for M2 macrophage activation. The culture was continued for 2 d before the activated macrophages were scraped off the petri dishes for study.

2.2.4 Binding study

Activated macrophages were plated on a black round bottom 96-well plate at the density of 50,000 cells/well. Biotinylated multivalent M2pep analogs in 100 μ L PBS containing 1% BSA were added to each well and incubated on ice for 20 min. Unbound peptides were washed off, and the bound peptides were probed by incubation with streptavidin FITC for 15 min on ice. Excess streptavidin FITC was washed off, and the macrophages were resuspended for analysis with a MACSQuant Flow Cytometer (Miltenyi Biotec, San Diego, CA). Propidium iodide (PI) was added to the samples prior to data acquisition to discriminate dead cells. Flow cytometry data were analyzed on FlowJo Analysis Software (Tree Star, Ashland, OR). Median fluorescence intensity values of FITC in the live macrophage population were normalized to the values of the

control samples that were treated with only streptavidin FITC without peptide. Each condition was tested in triplicates and each experiment was also conducted three independent times.

2.2.5 In vitro cytotoxicity study

Activated macrophages were seeded in suspension on a black round bottom 96-well plate at the density of 50,000 cells/well. Multivalent M2pep or M2pepKLA analogs at varying concentrations in 100 μ L RPMI 1640 medium were added to each well and incubated in a tissue culture (TC) incubator for 2 h at 37 °C, 5% CO₂. The macrophages were washed and resuspended in PBS for flow cytometry analysis. PI was added to probe for the extent of cell death. Cell viability data were presented as percentage of live macrophages normalized to the mean percentage of the live untreated control samples. The study was conducted in three independent experiments.

2.2.6 Ex vivo cytotoxicity study

CT-26 colon carcinoma cells were maintained in RPMI 1640 medium containing 10% fetal bovine serum and 1% AbAm. Tumors were inoculated by injection of 10⁶ CT-26 cells into the left flanks of female BALB/c mice with the age between 6-8 weeks and left for 2 weeks to develop tumors. Each tumor was then processed into single cell suspension by mincing into small pieces, homogenizing on gentleMACS Dissociator (Miltenyi Biotec, San Diego, CA), and incubating in 5 mL RPMI 1640 medium with 100 μ L collagenase (10,000 CDU/mL stock solution) and 100 μ L dispase II (32 mg/mL stock solution) for 40 min in the TC incubator. The dissociated single cells were then collected through 70 μ m cell strainer and plated on a black round bottom 96-well plate at the density of 200,000 cells/well. The cells were treated with multivalent M2pep and M2pepKLA analogs for 2 h in the TC incubator. To quantify cell viability of each subpopulation, the cells were first stained with LIVE/DEAD fixable far red cell stain and then with an antibody cocktail solution (anti-CD11b, anti-Ly-6G, and anti-F4/80 antibodies). After staining, the cells were fixed with 4% paraformaldehyde and analyzed with flow cytometer. The detailed list of antibodies and example flow cytometry gating schematics were included in Figure S2.1.

2.3 Results and discussion

2.3.1 Multivalent targeting ligands

2.3.1.1 Synthesis of multivalent M2pep

Divalent and tetravalent M2pep were synthesized with a biotin tag ([M2pep]₂-Biotin and [M2pep]₄-Biotin, respectively) by conjugation of M2pepKKKC to maleimide functionalized linkers, [Mal]₂-Biotin and [Mal]₄-Biotin, via thiol-maleimide chemistry (Scheme 2.1 and S2.1). [Mal]₂-Biotin was synthesized from the Biotin NovaTag resin whereby Fmoc-Lys(Fmoc)-OH was first coupled to the resin, deprotected to expose two free amines, and then coupled with 3-maleimidopropionic acid. Cleavage of the linker from the resin and precipitation in ether afforded an amber viscous product. [Mal]₄-Biotin was synthesized from GKGKGKGGK scaffold with N-terminal biotin. The scaffold was first synthesized on the automated peptide synthesizer, cleaved off the resin, and purified by RP-HPLC. The purified precursor was then reacted with NHS-maleimide in solution, and a white solid product was obtained from ether precipitation of the reaction solution. In both cases, the linkers were of sufficient purity for M2pepKKKC conjugation to give [M2pep]₂-Biotin and [M2pep]₄-Biotin in good yields. Successful synthesis of the linkers and multivalent M2pep was confirmed by mass spectrometry (Table S1). The synthesis strategy for the multivalent linkers reported here allows for tunable display of targeting peptides at other valencies by simply extending the oligolysine peptide precursor. In addition, biotin may be replaced with other functional compounds for different applications, and spacing between each targeting peptide may also be adjusted by increasing the number of amino acids between adjacent lysines or using oligoPEG as a molecular spacer.



Scheme 2.1 (A) Multivalent M2pep analogs. (B) Chemical structures of molecular linkers used in the synthesis.

2.3.1.2 Binding and cytotoxicity studies of multivalent M2pep with primary cultured macrophage

The mono-, di- and tetra-valent M2pep ligands were tested for binding selectivity to target cells using primary bone marrow-derived macrophages polarized to M1 or M2 state with IFN- γ /LPS or IL-4, respectively. Significant and selective binding of monovalent M2pep to M2 macrophages versus M1 macrophages was detected at 50 μ M but not at lower concentration (≤ 5 μ M) due to the relatively high K_D of the peptide (~ 90 μ M, reported previously [24]) (Figure 2.1A). On the other hand, divalent [M2pep]₂-Biotin exhibited significantly enhanced binding to M2 macrophages with good selectivity over M1 macrophages even at 1 μ M, with M2 binding increasing with concentration. Unexpectedly, tetravalent [M2pep]₄-Biotin bound less to cultured M2 macrophages compared to [M2pep]₂-Biotin, and its selectivity over M1 macrophages was significantly compromised. Internalization of these M2pep constructs were investigated by confocal microscopy and shown to correlate with the result from the binding study (Figure S2.2).

Cytotoxicity of the multivalent peptides but not M2pepBiotin was observed during the binding study and was therefore quantified by PI staining with flow cytometry analysis (Figure 2.1B). Interestingly, both [M2pep]₂-Biotin and [M2pep]₄-Biotin were selectively toxic to M2 macrophages over M1 macrophages at low micromolar concentrations while no toxicity to either cell type was observed for M2pepBiotin even at 50 μ M. Although not investigated in this study, it was possible that tetravalent M2pep display on the Biotin-GKGKGGK base linker may not be in the optimal configuration for M2pep peptides to engage in binding to multiple M2pep receptors. Reduced binding with increasing valency beyond its optimal number was previously observed in other multivalent systems and was proposed to be attributed to steric hindrance from overcrowding of targeting ligands or over-occupation of surface receptors per individual targeting construct [33–35]. Hence, future investigation into M2pep display configuration, multivalency-associated cytotoxicity, and the effect of spacer length and flexibility may be needed to further improve M2 macrophage-binding with higher M2pep valencies. The use of flexible linkers such as oligoPEG is especially attractive as they have been shown to facilitate optimal multivalent binding over a greater span of linker lengths compared to rigid linkers which have a more stringent spacing requirement for optimal binding [36].

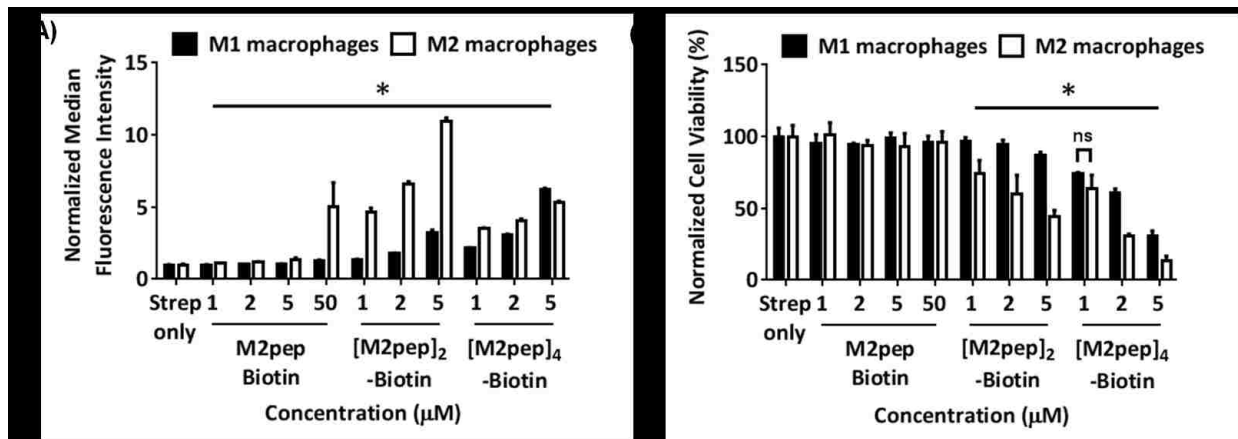


Figure 2.1 (A) *In vitro* binding of M2pepBiotin, [M2pep]₂-Biotin, and [M2pep]₄-Biotin to M1 and M2 macrophages. (B) Cell viability of macrophages following peptide incubation during binding study. Data were normalized to values from streptavidin only samples and presented as mean \pm standard deviation. Stars denote statistically significant difference between M1 and M2 macrophages under the same treatment concentration. * $P < 0.05$.

Next, we further investigated cytotoxicity of the multivalent M2pep ligands by incubating the peptides at different concentrations for 2 h at 37 °C before assessing cell viability by PI staining (Figure 2.2). Values of the effective concentration which caused a 50 percent reduction in cell viability (EC_{50}) were then calculated from the toxicity curves. Selectivity ratio in toxicity between M1 and M2 macrophages was defined as $EC_{50}^{M1}/EC_{50}^{M2}$. A relatively short incubation time was chosen because cytotoxicity was observed with a 20 min incubation of the peptides with cells on ice during the binding study. [M2pep]₄-Biotin was found to be the most potent at inducing cytotoxicity to M2 macrophages ($EC_{50} = 1.12 \mu\text{M}$) with the highest selectivity ratio of 9.92. [M2pep]₂-Biotin showed lower cytotoxicity to M2 macrophages but still retaining M2 macrophage selectivity (Selectivity ratio = 2.56). On the other hand, EC_{50} of M2pepBiotin was not reached even at 40 μM . We further confirmed M2pep sequence specificity on macrophage toxicity by incubating macrophages with M2pepKKKC and scrambled M2pepKKKC. Both peptides partially dimerized in solution to form dimers as confirmed by ESI-MS, but toxicity was only observed in the M2pepKKKC-treated samples (Figure S2.3). In addition, we also confirmed that the cytotoxicity was not due to the linkers used (Figure S2.4). The selective and potent toxicity of [M2pep]₄-Biotin to M2 macrophage is surprising considering that selective binding to this population compared to M1 was not observed. M1 macrophages may simply be more resistant to this M2pep-mediated signaling pathway, or the association between tetravalent M2pep and M1 macrophages may be partially non-specific such that not all the peptide binds to the appropriate M2pep receptor to trigger the cytotoxic signal.

It would be interesting to explore in future studies how a more flexible or longer linker between M2pepKKKC affects macrophage cytotoxicity. This knowledge, together with the identification of M2pep receptor, may help us elucidate the mechanism of cytotoxicity (e.g. due to crosslinking of multiple M2pep receptors on cells resulting in intracellular signaling, multivalency-induced change in conformation of individual M2pep receptors that may possess multiple M2pep-binding domains on the same receptor, or some other mechanisms). In recent years, there is a growing interest in developing drug-free macromolecular therapeutics employing the concept of receptor crosslinking-induced cell death [37]. One of the best known examples is the work by the Kopecek group which investigated into the use of coiled-coil interaction between CCE and CCK peptides to crosslink CCE-conjugated Fab' fragments of anti-CD20 antibody with CCK-grafted polymer. Crosslinking of CD20 in this manner was shown to

induce apoptosis in Raji B cells *in vitro* with promising preclinical results in SCID mice bearing human B-lymphoma xenografts [38]. Crosslinking of multiple M2pep receptors may thus represent a strategy to induce cell death in M2 macrophages without the need for cytotoxic drug cargos. However, a more in-depth understanding of M2pep receptor and its interaction with M2pep is required to better optimize the drug free, M2 macrophage-depleting therapeutics.

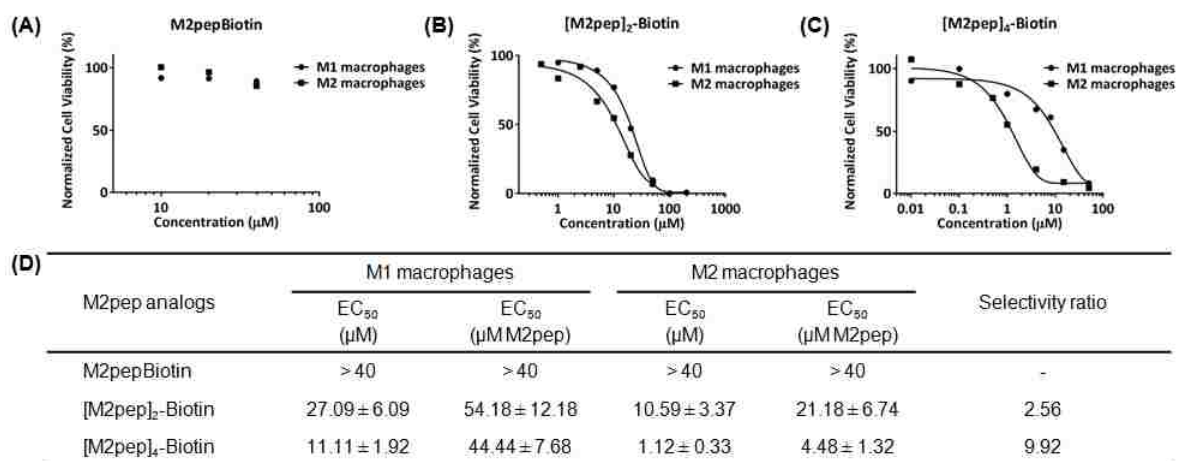


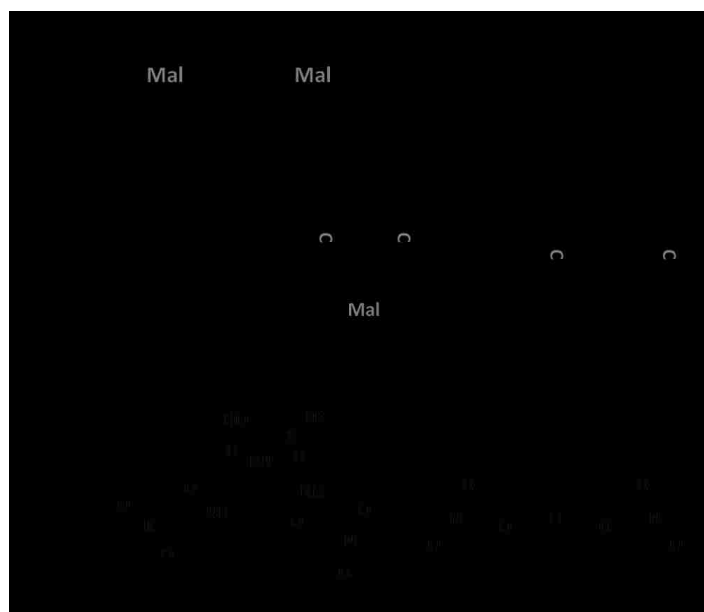
Figure 2.2 Representative cytotoxicity curves of (A) M2pepBiotin, (B) [M2pep]₂-Biotin, and (C) [M2pep]₄-Biotin on M1 and M2 macrophages. (D) Tabulated EC₅₀ values of multivalent M2pep presented as mean \pm standard deviation from 3 independent experiments.

2.3.2 Multivalent pro-apoptotic KLA cargo

2.3.2.1 Synthesis of multivalent KLA constructs

Since divalent M2pep was shown here to significantly improve selective binding to M2 macrophages, we next synthesized [M2pep]₂-[KLA] (Scheme 2 and S2) to evaluate how the enhanced binding would potentiate the pro-apoptotic peptide KLA toxicity to the macrophages compared to monovalent M2pepKLA. [Mal]₂-Cys(Trt) was first synthesized from a 2-chlorotriyl chloride resin via manual coupling of Fmoc-Cys(Trt)-OH, Fmoc-Lys(Fmoc)-OH, and 3-maleimidopropionic acid respectively. Mild cleavage condition enabled us to obtain [Mal]₂-Cys(Trt) which was conjugated to M2pepKKKC via thiol-maleimide chemistry. The Trt protecting group on the [M2pep]₂-Cys(Trt) was then removed by TFA treatment exposing a free thiol for subsequent conjugation with KLA-Mal. In addition, divalent M2pep with divalent KLA ([M2pep]₂-[KLA]₂) was also synthesized to evaluate if increasing the number of KLA would

further enhance the overall potency. M2pepGCGKLA was synthesized from the automated peptide synthesizer with cysteine replacing glycine in the spacer region of the original M2pepKLA sequence. M2pepGCGKLA was then dimerized using the BM(PEG)₃ linker. Successful synthesis of both M2pepKLA analogs was confirmed by ESI-MS (Table S2.1).



Scheme 2. (A) Multivalent M2pepKLA analogs. (B) Chemical structures of molecular linkers used in the synthesis.

2.3.2.2 Cytotoxicity study of multivalent M2pepKLA

Next, the cytotoxicity of M2pepKLA, [M2pep]₂-[KLA], and [M2pep]₂-[KLA]₂ to M1 and M2 macrophages was determined using cultured primary cells. The fusion peptide between KLA and tetravalent M2pep was not investigated in this study since [M2pep]₄-Biotin did not exhibit M2 macrophage-selective binding. Toxicity curves, calculated EC₅₀ values, and selectivity ratios are reported in Figure 2.3. Conjugation of KLA to M2pep imparts cytotoxicity to M2 macrophages with an EC₅₀ value of 4.29 μM and a selectivity ratio of 1.78. Remarkably, conjugation of a single KLA to the dimerized targeting ligand ([M2pep]₂-[KLA]) increases cytotoxicity by 10-fold (EC₅₀ = 1.08 μM versus 10.58 μM for [M2pep]₂-Biotin) compared to dimeric ligand alone and by 4-fold over M2pepKLA while improving selectivity (Selectivity

ratio = 3.44). Thus, the increased binding avidity of the divalent M2pep ligand also increases potency when this ligand is used for internalization of KLA.

Dimerization of KLA ([M2pep]₂-[KLA]₂) did not further improve the overall potency compared to [M2pep]₂-[KLA] but rather reduced M2 macrophage selectivity. This reduced selectivity is possibly in accordance with the improved cell penetration property of dimeric KLA recently reported by Hyun et al. [31]. Hence, this study demonstrates a significant contribution of cationic KLA on M2pep selectivity especially in the multivalent format and cautions the use of cationic antimicrobial peptides as a cytotoxic cargo in ligand-targeted therapeutics due to non-specific cell interaction. As alternatives to improve M2 macrophage-targeting selectivity, we suggest exploration of other potent drug cargos with inherently lower internalizing activity or alternatively reversibly altering charges on KLA with dimethylmaleic anhydride or benzoic imine to reduce non-specific uptake of the peptide [39–41].

In addition, we performed a cytotoxicity study with annexin V/PI staining to investigate the mechanism of macrophage death upon the treatment of multivalent M2pep and M2pepKLA constructs (Figure S2.5). Interestingly, all multivalent constructs induced an increase in the annexin V-positive/PI-positive (late apoptosis/secondary necrosis) population over time whereas the annexin V-positive/PI-negative (early apoptosis) population comprised a relatively low percentage with no appreciable change over time. This implies that additional non-apoptosis mechanism may be contributing to macrophage death. It is worth noting that cationic antimicrobial peptides have been shown to induce non-apoptotic cell death by directly disrupting cell membrane [42] which could be a possible mechanism for our case.

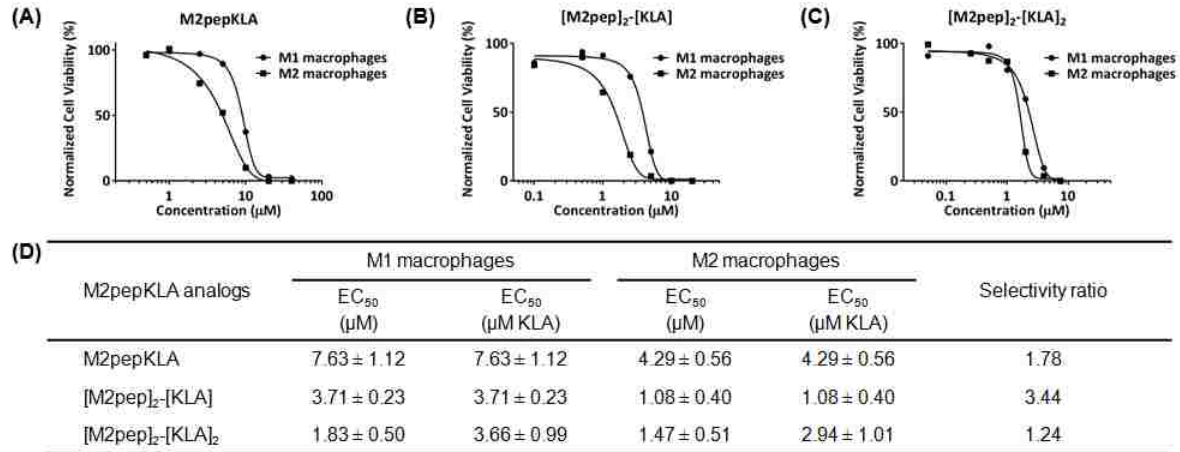


Figure 2.3 Representative cytotoxicity curves of (A) M2pepKLA, (B) $[\text{M2pep}]_2\text{-[KLA]}$, and (C) $[\text{M2pep}]_2\text{-[KLA]}_2$ on M1 and M2 macrophages. (D) Tabulated EC_{50} values of multivalent M2pepKLA presented as mean \pm standard deviation from 3 independent experiments.

2.3.3 *Ex vivo* evaluation of multivalent constructs with TAMs

Next, we evaluated multivalent M2pep and M2pepKLA constructs for potency and selectivity to TAMs in mixed tumor cell suspensions. Tumors were harvested from syngeneic CT-26 colon carcinoma tumors of Balb/c mice after two weeks of inoculation and processed into single cell suspension for viability studies using flow cytometry (Figure 2.4A). The cell suspension included CT-26 cells, TAMs, and other tumor-associated cells (e.g. other leukocytes, endothelial cells, fibroblasts) in physiologically relevant ratios and thus represented more closely what cells the peptides would encounter in the tumor *in vivo*. Here, we evaluated the cytotoxic effect of multivalent M2pep and M2pepKLA analogs on 1) CD11b^- population (primarily CT-26 malignant cells), 2) M1-like TAM population, and 3) M2-like TAM population following the flow cytometry gating strategy shown in Figure 2.4B and Figure S2.1. The cell viability data were first normalized to total cell count and then presented as percentage relative to their respective live populations in the untreated control. In general, all multivalent M2pep constructs, with or without KLA, were cytotoxic to the tumor cell suspension at high concentrations (Fig. 4C, 4D). Selective toxicity to M2-like TAMs over M1-like TAMs was observed but not over CD11b^- population. Toxicity on CD11b^- population was in accordance with our previously reported study that M2pep bound strongly to this cell population *ex vivo* although interaction and internalization in these cells *in vivo* was not observed [24]. Hence, we expect the cytotoxic effect on this population to be less *in vivo*.

As observed *in vitro*, multimerization of M2pep resulted in cytotoxicity, with [M2pep]₄-Biotin being the most potent analog. Of the KLA-containing constructs, [M2pep]₂-[KLA]₂ was most potent and exhibited better M2 to M1 selectivity compared with [M2pep]₂-[KLA]. In tumor microenvironment where there is a complex mix of different cell populations, targeting activity of the therapeutics may be significantly altered and not fully correlated to the *in vitro* results. The death or stimulation of one cell population may also trigger release of cytokines that affect viability of the others making selective depletion of a desired population an even more challenging task. In addition, negatively-charged extracellular matrix components such as hyaluronan, which is abundant in the tumor microenvironment [43], may interact with the positively-charged KLA and help restore the M2 selectivity relative to M1-like TAMs observed *ex vivo*. However, this electrostatic interaction may impede diffusion of the drug into the deeper hypoxic region, thus limiting its *in vivo* efficacy [44]. Here, our *ex vivo* study suggested [M2pep]₂-[KLA]₂ and [M2pep]₄-Biotin as promising candidates in term of potency for future *in vivo* evaluation although complementary strategies that facilitate tumor penetration may be needed. Dual killing of both cancer cells and M2-like TAMs observed *ex vivo*, if translated to an *in vivo* setting, would be desirable for cancer therapy.

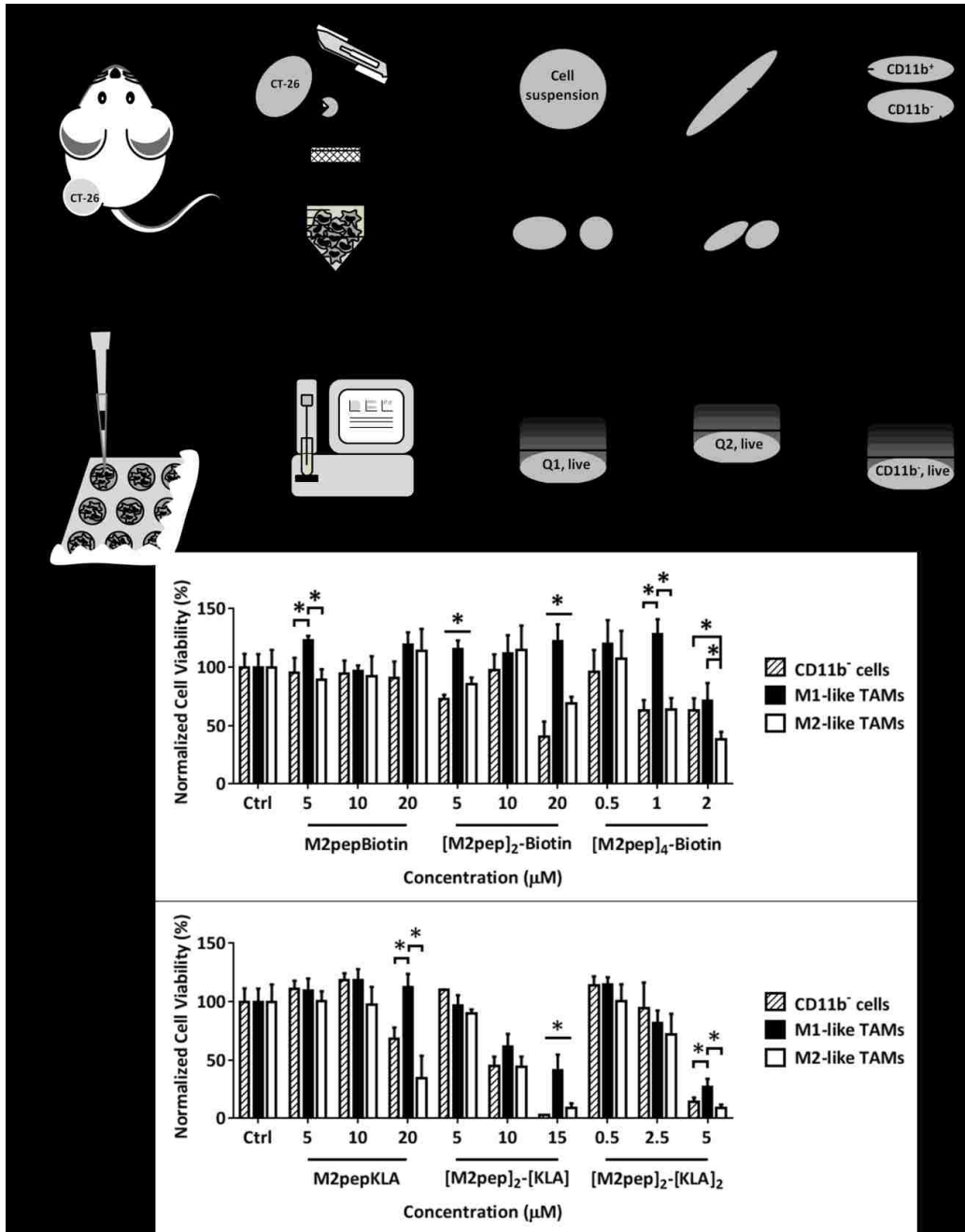


Figure 2.4 (A) Tumor processing for *ex vivo* cytotoxicity evaluation: (i) CT-26 tumors were inoculated in Balb/c mice. (ii) The tumors were harvested and processed into single cell suspension. (iii) Cell suspension was seeded and treated with different M2pep and M2pepKLA analogs. (iv) The cells were stained and analyzed by flow cytometry. (B) Flow cytometry gating strategy for cell viability analysis of tumor sub-populations. *Ex vivo* cytotoxicity of multivalent M2pep (C) and M2pepKLA (D) constructs on each sub-population in CT-26 tumor-derived cell suspension. Unless labeled in pairs, stars denote statistical significance among all populations. * $P < 0.05$.

2.4 Conclusions

In this work, divalent display of M2pep was shown to improve M2 macrophage-binding activity *in vitro*. On the other hand, tetravalent display of M2pep had reduced binding compared to divalent M2pep and was accompanied with loss in selectivity over M1 macrophages. Surprisingly, divalent and tetravalent displays of M2pep were found to exhibit M2 macrophage-selective cytotoxicity both *in vitro* and *ex vivo*. Conjugation of divalent M2pep to KLA significantly improved M2 macrophage-cytotoxicity and selectivity *in vitro*. In the *ex vivo* study, [M2pep]₂-[KLA]₂ and tetravalent [M2pep]₄-Biotin were the most potent making them promising candidates for future *in vivo* study. Additionally, further improvement in multivalency-induced macrophage death by M2pep may also have a potential as a drug-free, anti-cancer construct via M2-like TAM depletion.

2.5 Acknowledgments

This work was supported by NIH 1R01CA177272. Chayanon Ngambenjwong was supported by an Anandamahidol Foundation Fellowship. Maryelise Cieslewicz was supported by a National Science Foundation Graduate Fellowship.

2.6 References

- [1] D.M. Pardoll, Spinning molecular immunology into successful immunotherapy, *Nat. Rev. Immunol.* 2 (2002) 227–238. doi:10.1038/nri774.
- [2] P. Sharma, K. Wagner, J.D. Wolchok, J.P. Allison, Novel cancer immunotherapy agents with survival benefit: recent successes and next steps, *Nat Rev Cancer.* 11 (2011) 805–812. <http://dx.doi.org/10.1038/nrc3153>.
- [3] J. a. Joyce, Therapeutic targeting of the tumor microenvironment, *Cancer Cell.* 7 (2005) 513–520. doi:10.1016/j.ccr.2005.05.024.
- [4] Y. Komohara, M. Jinushi, M. Takeya, Clinical significance of macrophage heterogeneity in human malignant tumors, *Cancer Sci.* 105 (2014) 1–8. doi:10.1111/cas.12314.
- [5] Q. Lahmar, J. Keirsse, D. Laoui, K. Movahedi, E. Van Overmeire, J. a. Van Ginderachter, Tissue-resident versus monocyte-derived macrophages in the tumor microenvironment, *Biochim. Biophys. Acta - Rev. Cancer.* (2015). doi:10.1016/j.bbcan.2015.06.009.

- [6] S.K. Biswas, A. Mantovani, Macrophage plasticity and interaction with lymphocyte subsets: cancer as a paradigm, *Nat. Immunol.* 11 (2010) 889–896. doi:10.1038/ni.1937.
- [7] C. Lamagna, M. Aurrand-Lions, B. a Imhof, Dual role of macrophages in tumor growth and angiogenesis, *J. Leukoc. Biol.* 80 (2006) 705–713. doi:10.1189/jlb.1105656.
- [8] Q. Zhang, L. Liu, C. Gong, H. Shi, Y. Zeng, X. Wang, et al., Prognostic significance of tumor-associated macrophages in solid tumor: a meta-analysis of the literature, *PLoS One.* 7 (2012) e50946. doi:10.1371/journal.pone.0050946.
- [9] E.K. Colvin, Tumor-associated macrophages contribute to tumor progression in ovarian cancer, *Front. Oncol.* 4 (2014) 137. doi:10.3389/fonc.2014.00137.
- [10] R. Cornelissen, L. a. Lievense, A.P. Maat, R.W. Hendriks, H.C. Hoogsteden, A.J. Bogers, et al., Ratio of Intratumoral Macrophage Phenotypes Is a Prognostic Factor in Epithelioid Malignant Pleural Mesothelioma, *PLoS One.* 9 (2014) e106742. doi:10.1371/journal.pone.0106742.
- [11] F. Pantano, P. Berti, F.M. Guida, G. Perrone, B. Vincenzi, M.M.C. Amato, et al., The role of macrophages polarization in predicting prognosis of radically resected gastric cancer patients, *J. Cell. Mol. Med.* 17 (2013) 1415–1421. doi:10.1111/jcmm.12109.
- [12] H. Kurahara, H. Shinchu, Y. Mataka, K. Maemura, H. Noma, F. Kubo, et al., Significance of M2-polarized tumor-associated macrophage in pancreatic cancer, *J. Surg. Res.* 167 (2011) 211–219. doi:10.1016/j.jss.2009.05.026.
- [13] C. Medrek, F. Pontén, K. Jirström, K. Leandersson, The presence of tumor associated macrophages in tumor stroma as a prognostic marker for breast cancer patients, *BMC Cancer.* 12 (2012) 306. doi:10.1186/1471-2407-12-306.
- [14] W. Zhou, S.Q. Ke, Z. Huang, W. Flavahan, X. Fang, J. Paul, et al., Periostin secreted by glioblastoma stem cells recruits M2 tumour-associated macrophages and promotes malignant growth, *Nat. Cell Biol.* 17 (2015) 170–182. doi:10.1038/ncb3090.
- [15] S.M. Zeisberger, B. Odermatt, C. Marty, a H.M. Zehnder-Fjällman, K. Ballmer-Hofer, R. a Schwendener, Clodronate-liposome-mediated depletion of tumour-associated macrophages: a new and highly effective antiangiogenic therapy approach, *Br. J. Cancer.* 95 (2006) 272–281. doi:10.1038/sj.bjc.6603240.
- [16] S. Junankar, G. Shay, J. Jurczyk, N. Ali, J. Down, N. Pocock, et al., Real-Time Intravital Imaging Establishes Tumor-Associated Macrophages as the Extraskelatal Target of Bisphosphonate Action in Cancer, *Cancer Discov.* 5 (2014) 35–42. doi:10.1158/2159-8290.CD-14-0621.

- [17] C.H. Ries, M. a. Cannarile, S. Hoves, J. Benz, K. Wartha, V. Runza, et al., Targeting tumor-associated macrophages with anti-CSF-1R antibody reveals a strategy for cancer therapy, *Cancer Cell*. 25 (2014) 846–859. doi:10.1016/j.ccr.2014.05.016.
- [18] S.M. Pyonteck, L. Akkari, A.J. Schuhmacher, R.L. Bowman, L. Sevenich, D.F. Quail, et al., CSF-1R inhibition alters macrophage polarization and blocks glioma progression, *Nat. Med.* 19 (2013) 1264–1272. doi:10.1038/nm.3337.
- [19] A. Swierczak, A.D. Cook, J.C. Lenzo, C.M. Restall, J.P. Doherty, R.L. Anderson, et al., The Promotion of Breast Cancer Metastasis Caused by Inhibition of CSF-1R/CSF-1 Signaling Is Blocked by Targeting the G-CSF Receptor, *Cancer Immunol. Res.* (2014) 765–777. doi:10.1158/2326-6066.CIR-13-0190.
- [20] A. Casazza, D. Laoui, M. Wenes, S. Rizzolio, N. Bassani, M. Mambretti, et al., Impeding Macrophage Entry into Hypoxic Tumor Areas by Sema3A/Nrp1 Signaling Blockade Inhibits Angiogenesis and Restores Antitumor Immunity, *Cancer Cell*. 24 (2013) 695–709. doi:10.1016/j.ccr.2013.11.007.
- [21] C. Murdoch, A. Giannoudis, C.E. Lewis, Mechanisms regulating the recruitment of macrophages into hypoxic areas of tumors and other ischemic tissues, *Blood*. 104 (2004) 2224–2234. doi:10.1182/blood-2004-03-1109.
- [22] D. Laoui, E. Van Overmeire, G. Di Conza, C. Aldeni, J. Keirsse, Y. Morias, et al., Tumor hypoxia does not drive differentiation of tumor-associated macrophages but rather fine-tunes the M2-like macrophage population, *Cancer Res.* 74 (2014) 24–30. doi:10.1158/0008-5472.CAN-13-1196.
- [23] M.R. Dreher, W. Liu, C.R. Michelich, M.W. Dewhirst, F. Yuan, A. Chilkoti, Tumor vascular permeability, accumulation, and penetration of macromolecular drug carriers, *J. Natl. Cancer Inst.* 98 (2006) 335–344. doi:10.1093/jnci/djj070.
- [24] M. Cieslewicz, J. Tang, J.L. Yu, H. Cao, M. Zavaljevski, K. Motoyama, et al., Targeted delivery of proapoptotic peptides to tumor-associated macrophages improves survival, *Proc. Natl. Acad. Sci. U. S. A.* 110 (2013) 15919–24. doi:10.1073/pnas.1312197110.
- [25] C. Fasting, C. a. Schalley, M. Weber, O. Seitz, S. Hecht, B. Kokschi, et al., Multivalency as a chemical organization and action principle, *Angew. Chemie - Int. Ed.* 51 (2012) 10472–10498. doi:10.1002/anie.201201114.
- [26] L. Locke, M. Mayo, A. Yoo, M. Williams, S. Berr, PET imaging of tumor associated macrophages using mannose coated 64 Cu liposomes, *Biomaterials*. 33 (2012). doi:10.1016/j.biomaterials.2012.07.022.
- [27] S. Zhu, M. Niu, H. O'Mary, Z. Cui, Targeting of Tumor-Associated Macrophages Made Possible by PEG-Sheddable, Mannose-Modified Nanoparticles, *Mol. Pharm.* 10 (2013) 3525–3530. doi:10.1021/mp400216r.

- [28] M. Niu, Y.W. Naguib, A.M. Aldayel, Y. Shi, S.D. Hursting, M.A. Hersh, et al., Biodistribution and in Vivo Activities of Tumor-Associated Macrophage-Targeting Nanoparticles Incorporated with Doxorubicin, *Mol. Pharm.* 11 (2014) 4425–4436. doi:10.1021/mp500565q.
- [29] D.S.H. Chu, M.J. Bocek, J. Shi, A. Ta, C. Ngambenjawong, R.C. Rostomily, et al., Multivalent display of pendant pro-apoptotic peptides increases cytotoxic activity, *J. Control. Release.* 205 (2015) 155–161. doi:10.1016/j.jconrel.2015.01.013.
- [30] L. Agemy, Targeted nanoparticle enhanced proapoptotic peptide as potential therapy for glioblastoma, *Proc. Natl. Acad. Sci. U. S. A.* 108 (2011) 17450–17455. doi:10.1073/pnas.1114518108/-/DCSupplemental.www.pnas.org/cgi/doi/10.1073/pnas.1114518108.
- [31] S. Hyun, S. Lee, S. Kim, S. Jang, J. Yu, Y. Lee, Apoptosis Inducing, Conformationally Constrained, Dimeric Peptide Analogs of KLA with Submicromolar Cell Penetrating Abilities, *Biomacromolecules.* 15 (2014) 3746–3752. doi:10.1021/bm501026e.
- [32] L. Adar, Y. Shamay, G. Journo, A. David, Pro-apoptotic peptide-polymer conjugates to induce mitochondrial-dependent cell death, *Polym. Adv. Technol.* 22 (2011) 199–208. doi:10.1002/pat.1829.
- [33] D. Voulgaraki, R. Mitnacht-Kraus, M. Letarte, M. Foster-Cuevas, M.H. Brown, a. N. Barclay, Multivalent recombinant proteins for probing functions of leucocyte surface proteins such as the CD200 receptor, *Immunology.* 115 (2005) 337–346. doi:10.1111/j.1365-2567.2005.02161.x.
- [34] B.D. Polizzotti, K.L. Kiick, Effects of polymer structure on the inhibition of cholera toxin by linear polypeptide-based glycopolymers, *Biomacromolecules.* 7 (2006) 483–490. doi:10.1021/bm050672n.
- [35] D. V. Schaffer, D. a. Lauffenburger, Optimization of cell surface binding enhances efficiency and specificity of molecular conjugate gene delivery, *J. Biol. Chem.* 273 (1998) 28004–28009. doi:10.1074/jbc.273.43.28004.
- [36] H.L. Handl, R. Sankaranarayanan, J.S. Josan, J. Vagner, E. a Mash, R.J. Gillies, et al., Synthesis and evaluation of bivalent NDP-alpha-MSH(7) peptide ligands for binding to the human melanocortin receptor 4 (hMC4R), *Bioconjug. Chem.* 18 (2007) 1101–1109. doi:10.1021/bc0603642.
- [37] T.-W. Chu, J. Kopeček, Drug-free macromolecular therapeutics – a new paradigm in polymeric nanomedicines, *Biomater. Sci.* (2015) 908–922. doi:10.1039/C4BM00442F.
- [38] K. Wu, J. Yang, J. Liu, J. Kopeček, Coiled-coil based drug-free macromolecular therapeutics: In vivo efficacy, *J. Control. Release.* 157 (2012) 126–131. doi:10.1016/j.jconrel.2011.08.002.

- [39] L. Jiang, L. Li, X. He, Q. Yi, B. He, J. Cao, et al., Overcoming drug-resistant lung cancer by paclitaxel loaded dual-functional liposomes with mitochondria targeting and pH-response, *Biomaterials*. 52 (2015) 126–139. doi:<http://dx.doi.org/10.1016/j.biomaterials.2015.02.004>.
- [40] H. Cheng, J.-Y. Zhu, X.-D. Xu, W.-X. Qiu, Q. Lei, K. Han, et al., Activable cell-penetrating peptide (ACPP) conjugated prodrug for tumor targeted drug delivery, *ACS Appl. Mater. Interfaces*. (2015) 150710083756006. doi:10.1021/acsami.5b04517.
- [41] C. Ding, J. Gu, X. Qu, Z. Yang, Preparation of multifunctional drug carrier for tumor-specific uptake and enhanced intracellular delivery through the conjugation of weak acid labile linker, *Bioconjug. Chem.* 20 (2009) 1163–1170. doi:10.1021/bc800563g.
- [42] E.J. Paredes-Gamero, M.N.C. Martins, F.A.M. Cappabianco, J.S. Ide, A. Miranda, Characterization of dual effects induced by antimicrobial peptides: Regulated cell death or membrane disruption, *Biochim. Biophys. Acta - Gen. Subj.* 1820 (2012) 1062–1072. doi:<http://dx.doi.org/10.1016/j.bbagen.2012.02.015>.
- [43] N. Itano, L. Zhuo, K. Kimata, Impact of the hyaluronan-rich tumor microenvironment on cancer initiation and progression, *Cancer Sci.* 99 (2008) 1720–1725. doi:10.1111/j.1349-7006.2008.00885.x.
- [44] N. Bertrand, J. Wu, X. Xu, N. Kamaly, O.C. Farokhzad, Cancer nanotechnology: The impact of passive and active targeting in the era of modern cancer biology, *Adv. Drug Deliv. Rev.* 66 (2014) 2–25. doi:10.1016/j.addr.2013.11.009.

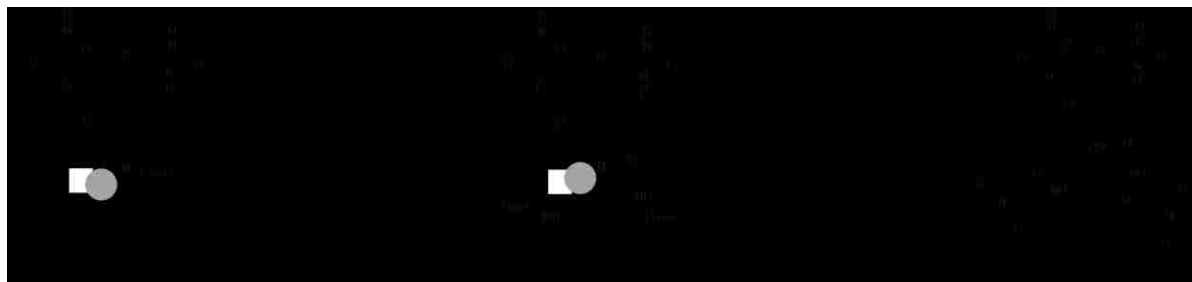
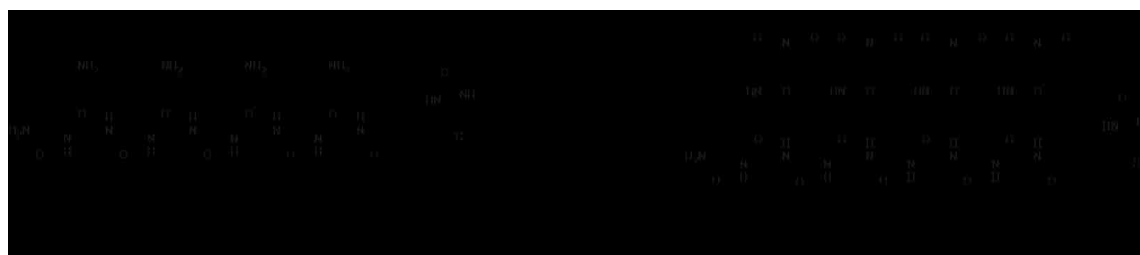
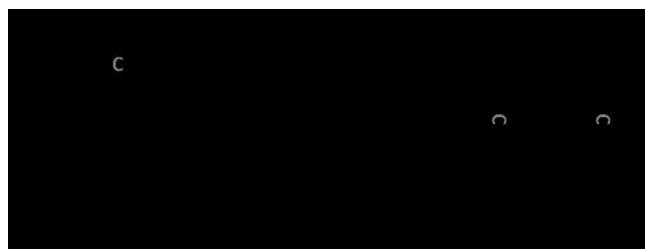
2.7 Supplementary information

Table S2.1 Molecular weight of peptides

Peptide	Molecular weight (Da)	
	Calculated	Measured
M2pepBiotin	2,524.86	[M+H] ⁺ = 2,524.36
M2pepKKKC	2,401.71	[M+H] ⁺ = 2,402.33
Scrambled M2pepKKKC	2,401.71	[M+H] ⁺ = 2,402.28
[Mal] ₂ -Biotin	877.02	[M+H] ⁺ = 877.30
[Mal] ₂ -Cys(Trt)	793.88	[M-H] ⁻ = 792.7
[M2pep] ₂ -Biotin	5,680.44 [M+5H] ⁵⁺ = 1,137.1, [M+6H] ⁶⁺ = 947.7, [M+7H] ⁷⁺ = 812.5, [M+8H] ⁸⁺ = 711.1, [M+9H] ⁹⁺ = 632.2	[M+5H] ⁵⁺ = 1,137.1, [M+6H] ⁶⁺ = 947.9, [M+7H] ⁷⁺ = 812.7, [M+8H] ⁸⁺ = 711.4, [M+9H] ⁹⁺ = 632.9
[M2pep] ₂ -Cys(Trt)	5,597.3 [M+5H] ⁵⁺ = 1,120.5, [M+6H] ⁶⁺ = 933.9, [M+7H] ⁷⁺ = 800.6, [M+8H] ⁸⁺ = 700.7	[M+5H] ⁵⁺ = 1,120.5, [M+6H] ⁶⁺ = 934.0, [M+7H] ⁷⁺ = 800.9, [M+8H] ⁸⁺ = 701.0
[M2pep] ₂ -Cys	5,354.99 [M+5H] ⁵⁺ = 1,072.0, [M+6H] ⁶⁺ = 893.5, [M+7H] ⁷⁺ = 766.0, [M+8H] ⁸⁺ = 670.4	[M+5H] ⁵⁺ = 1,072.0, [M+6H] ⁶⁺ = 893.7, [M+7H] ⁷⁺ = 766.2, [M+8H] ⁸⁺ = 670.7
[Mal] ₄ -Biotin	1,588.70 [M+2Na] ²⁺ = 817.3, [M+H ₂ O+2Na] ²⁺ = 826.3, [M+2H ₂ O+2Na] ²⁺ = 835.4	[M+2Na] ²⁺ = 817.8, [M+H ₂ O+2Na] ²⁺ = 826.4*, [M+2H ₂ O+2Na] ²⁺ = 835.5*
[M2pep] ₄ -Biotin	11,195.54 [M+10H] ¹⁰⁺ = 1,120.6, [M+11H] ¹¹⁺ = 1,018.8, [M+12H] ¹²⁺ = 934.0, [M+13H] ¹³⁺ = 862.2, [M+14H] ¹⁴⁺ = 800.7	[M+10H] ¹⁰⁺ = 1,120.8, [M+11H] ¹¹⁺ = 1,019.1, [M+12H] ¹²⁺ = 934.3, [M+13H] ¹³⁺ = 862.7, [M+14H] ¹⁴⁺ = 801.4
M2pepKLA	3,420.03	[M+H] ⁺ = 3,420.75
M2pepGCGKLA	3,466.12	[M+H] ⁺ = 3,466.30
KLA-Mal	1,674.12	[M+H] ⁺ = 1,673.68
[M2pep] ₂ -[KLA]	7,029.11 [M+7H] ⁷⁺ = 1,005.2, [M+8H] ⁸⁺ = 879.6, [M+9H] ⁹⁺ = 782.0, [M+10H] ¹⁰⁺ = 703.9	[M+7H] ⁷⁺ = 1,005.6, [M+8H] ⁸⁺ = 880.1, [M+9H] ⁹⁺ = 782.5, [M+10H] ¹⁰⁺ = 704.5
[M2pep] ₂ -[KLA] ₂	7,284.37 [M+7H] ⁷⁺ = 1,041.6, [M+8H] ⁸⁺ = 911.6, [M+9H] ⁹⁺ = 810.4, [M+10H] ¹⁰⁺ = 729.4, [M+11H] ¹¹⁺ = 663.2	[M+7H] ⁷⁺ = 1,041.7, [M+8H] ⁸⁺ = 911.9, [M+9H] ⁹⁺ = 810.8, [M+10H] ¹⁰⁺ = 730.3, [M+11H] ¹¹⁺ = 663.7

[M+H]⁺ data were measured by MALDI-TOF MS. All other data were measured by ESI-MS.

* The sample was dissolved in H₂O and left overnight before analysis so some hydrolysis was observed

Scheme S2.1 Synthesis of [M2pep]₂-Biotin and [M2pep]₄-Biotin**S2.1A** Synthetic scheme of [Mal]₂-Biotin**S2.1B** Synthetic scheme of [Mal]₄-Biotin**S2.1C** Synthetic scheme of [M2pep]₂-Biotin**S2.1D** Synthetic scheme of [M2pep]₄-Biotin

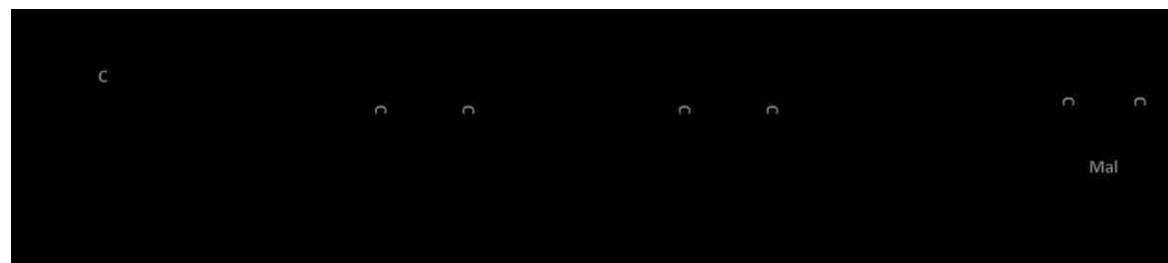
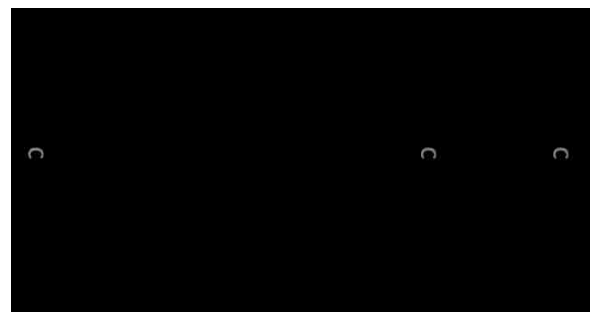
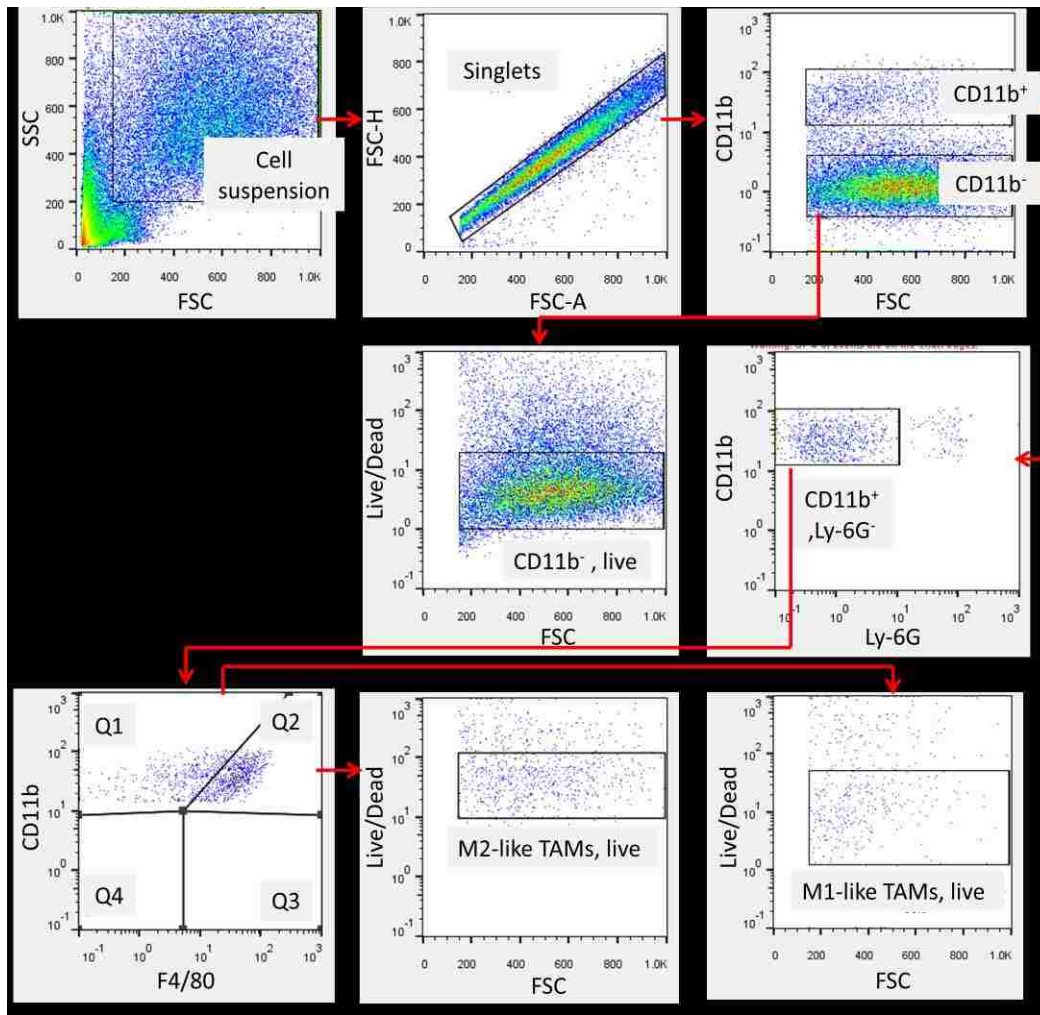
Scheme S2.2 Synthesis of [M2pep]₂-[KLA] and [M2pep]₂-[KLA]₂**S2.2A** Synthetic scheme of [Mal]₂-Cys(Trt)**S2.2B** Synthetic scheme of [M2pep]₂-[KLA]**S2.2C** Synthetic scheme of [M2pep]₂-[KLA]₂

Figure S2.1 Flow cytometry gating strategy for *ex vivo* cytotoxicity study.



Antibody	Clone	Vendor	Conjugation
CD16/CD32	93	BioLegend	
CD11b	M1/70	BioLegend	PerCP
Ly-6G	1A8	BD Pharmingen	FITC
F4/80	BM8	Life Technologies	Pacific blue
Live/Dead		Life Technologies	Far red

Figure S2.2 Internalization of multivalent M2pep. Macrophages were incubated with peptides for 2 h at 37 °C, fixed with 4% PFA, incubated with streptavidin FITC, and imaged under confocal microscopy (Leica TCS SP8X). Blue = DAPI, Green = Streptavidin FITC.

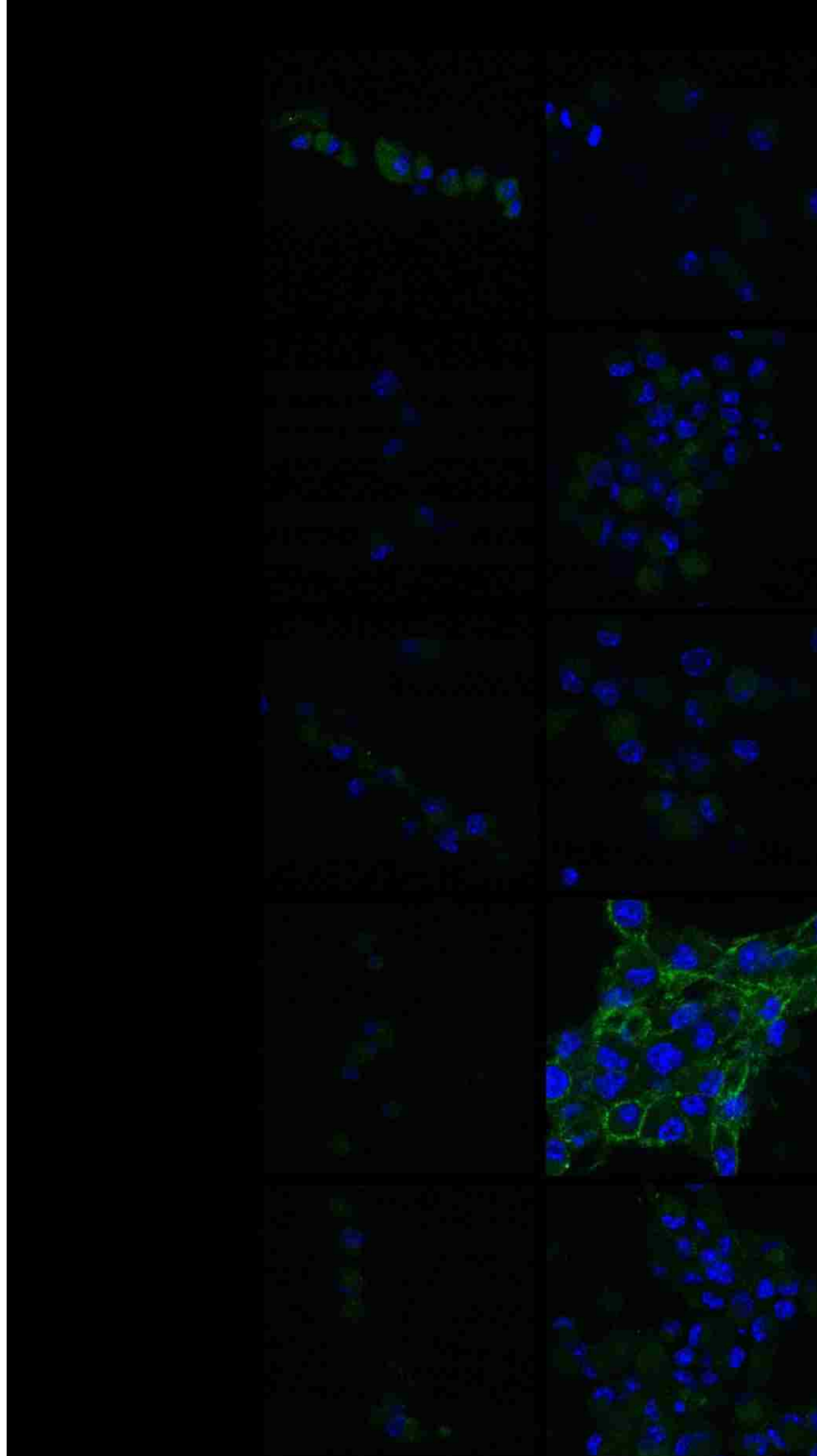


Figure S2.3 (A) Cytotoxicity of M2pepKKKC was sequence-specific. (B) ESI-MS spectrum of M2pepKKKC showing partial dimerization.

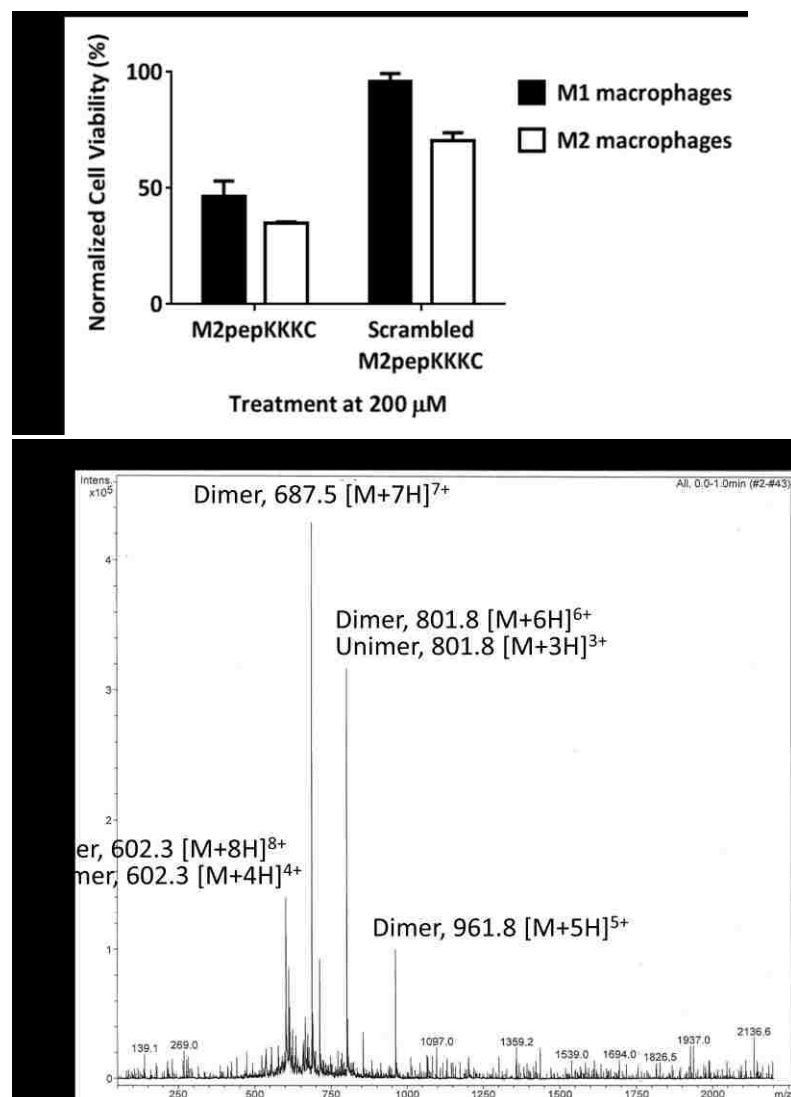


Figure S2.4 (A) Chemical structures of control free amine/acetylated, divalent/tetravalent linkers. (B) Toxicity study of the control linkers.

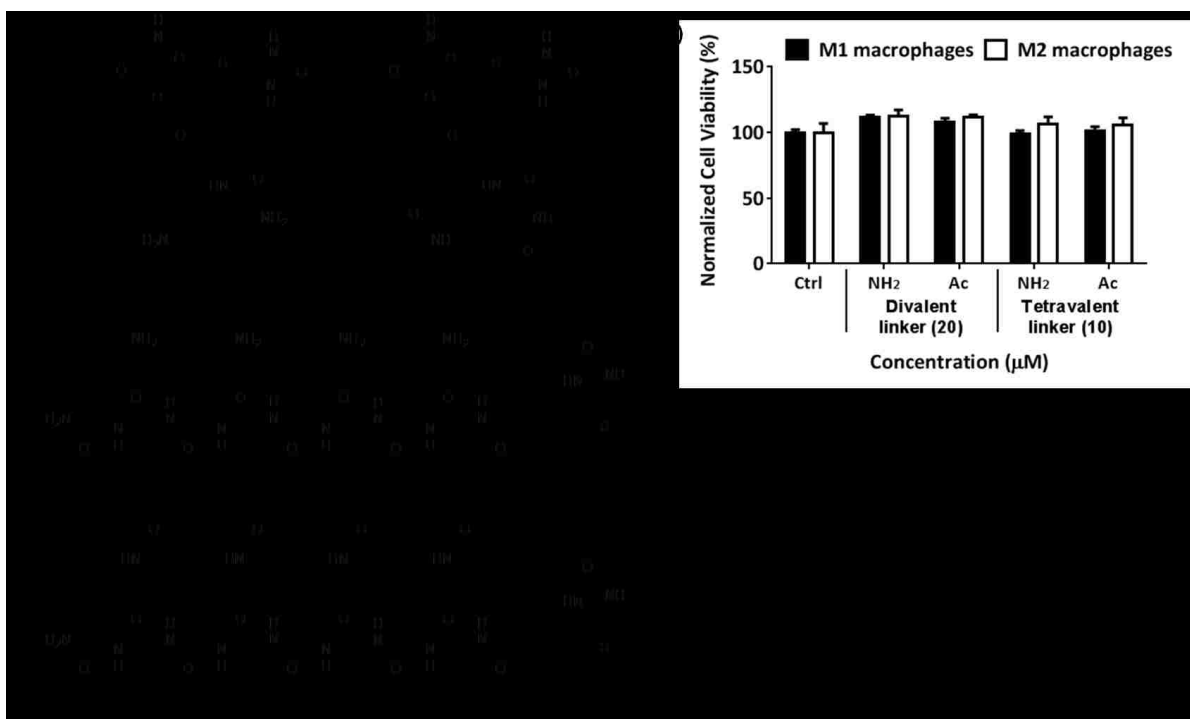
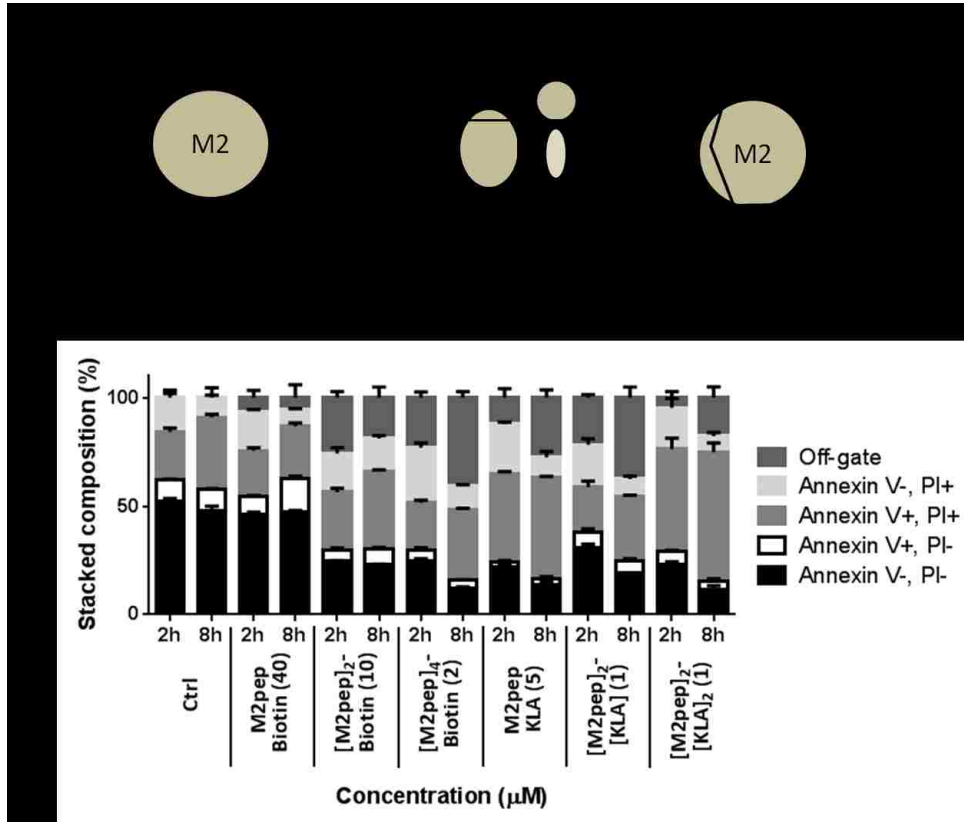


Figure S2.5 Apoptosis assay by annexin V/PI staining. M2 macrophages were incubated with peptides for 2 h at 37 °C and stained with annexin V-eFlour450 (eBioscience) per manufacturer's instructions. PI was then added before analysis with flow cytometry. (A) Schematic showing analysis of different states of cell death. (B) Apoptosis assay on M2 macrophages treated with multivalent M2pep and M2pepKLA for 2 and 8 h.



Chapter 3

SERUM STABILITY AND AFFINITY OPTIMIZATION OF AN M2 MACROPHAGE-TARGETING PEPTIDE (M2PEP)

Chayanon Ngambenjawong, Heather H. Gustafson, Julio M. Pineda, Nataly A. Kacherovsky, Maryelise Cieslewicz, Suzie H. Pun

Abstract

Tumor associated macrophages (TAMs) are a major stromal component of the tumor microenvironment in several cancers. TAMs are a potential target for adjuvant cancer therapies due to their established roles in promoting proliferation of cancer cells, angiogenesis, and metastasis. We previously discovered an M2 macrophage-targeting peptide (M2pep) which was successfully used to target and deliver a pro-apoptotic KLA peptide to M2-like TAMs in a CT-26 colon carcinoma model. However, the effectiveness of *in vivo* TAM-targeting using M2pep is limited by its poor serum stability and low binding affinity. In this study, we synthesized M2pep derivatives with the goals of increasing serum stability and binding affinity. Serum stability evaluation of M2pepBiotin confirmed its rapid degradation attributed to exolytic cleavage from the N-terminus and endolytic cleavages at the W10/W11 and S16/K17 sites. N-terminal acetylation of M2pepBiotin protected the peptide against the exolytic degradation while W10w and K(17,18,19)k substitutions were able to effectively protect endolytic degradation at their respective cleavage sites. However, no tested amino acid changes at the W10 position resulted in both protease resistance at that site and retention of binding activity. Therefore, cyclization of M2pep was investigated. Cyclized M2pep better resisted serum degradation without compromising binding activity to M2 macrophages. During the serum stability optimization process, we also discovered that K9R and W10Y substitutions significantly enhanced binding affinity of M2pep. In an *in vitro* binding study of different M2pep analogs pre-incubated in mouse serum, cyclic M2pep with K9R and W10Y modifications (cyclic M2pep(RY)) retained the highest binding activity to M2 macrophages over time due to its improved serum stability. Finally, we evaluated the *in vivo* accumulation of sulfo-Cy5-labeled M2pep and cyclic M2pep(RY) in both the CT-26 and 4T1 breast carcinoma models. Cyclic M2pep(RY) outperformed M2pep in both tumor localization and selective accumulation in M2-like TAMs. In conclusion, we report cyclic M2pep(RY) as our lead M2pep analog with improved serum stability and M2 macrophage-binding activity. Its enhanced utility as an *in vivo* M2-like-TAM-targeting agent was demonstrated in two tumor models, and is expected to be applicable for other tumor models or in models of M2 macrophage-related diseases.³

³ Reprinted from Ngambenjawong et al. (2016) *Theranostics* 6(9):1403-1404. Copyright© 2016 Ivyspring International Publisher for non-commercial purpose in compliance with Creative Commons Attribution (CC BY-NC) License

3.1 Introduction

Despite advancement in medical research, cancer remains one of the leading causes of death in the United States [1]. One of the main limitations in cancer therapies is non-specific side effects, which significantly compromise patients' quality of life and restrict the effective dosage that can be administered [2]. Improvement in nanotechnology and molecular biology enables development of therapeutics that can more precisely target the diseased organs or cells, thus alleviating the side effects [3]. Ligand-mediated active targeting is a powerful strategy used to enhance cellular internalization, and hence potency, of drug-loaded nanoparticles or biomacromolecular therapeutics to cells overexpressing the corresponding receptors [2–4]. This active targeting strategy is used in ligand-decorated nanoparticles that are progressing in different stages of clinical trials as well as the recent FDA approvals of antibody-drug conjugates; Brentuximab vedotin and Trastuzumab emtansine [3,5,6].

The increased use of active targeting strategies for drug delivery or imaging applications especially in cancer is in part due to advances in molecular engineering and combinatorial screening techniques that have lead to new targeting ligands for different cell targets [7,8]. Antibodies, proteins, oligonucleotides, peptides, and small molecules have all been successfully used as targeting moieties in several targeted drug delivery systems. The inherent advantages and disadvantages of each of these ligand classes has been reviewed in recent literature [3,8–10]. For tumor targeting applications, peptide targeting ligands offer significant advantages over antibodies due to their smaller size which can enhance tumor penetration, in addition to their lower immunogenicity and higher scalability. Small molecule screening is usually more tedious and less successful compared to the discovery of targeting peptides, which is greatly accelerated by robust phage display screening technology. Moreover, diverse functional groups of amino acids also allow for more flexible conjugation chemistry to cargo of interest. Nonetheless, using peptides as targeting moiety may have disadvantages from lower target affinity and serum stability, which in several cases have been successfully improved via multivalent display of the peptides and rational modifications respectively [8,11–13].

We have been interested in targeted drug delivery for local immunomodulation in solid tumors [13,14]. The immune-suppressive microenvironment of tumors has been reported to contribute toward immune evasion and tumor progression [15,16]. One strategy for tumor immunomodulation is selective depletion of tumor-associated macrophages (TAMs), which are

known to mostly express an anti-inflammatory “M2” phenotype and contribute to tumor progression, angiogenesis, and metastasis [17]. We have previously performed phage display biopanning to identify an M2 macrophage-targeting peptide (M2pep) that binds preferentially to murine anti-inflammatory M2 macrophages/M2-like TAMs over other leukocytes including pro-inflammatory M1 macrophages/M1-like TAMs, which are known to promote anti-tumor immunity [14]. A fusion peptide comprised of M2pep with a pro-apoptotic peptide KLA was shown to successfully mediate selective depletion of M2-TAMs in a syngeneic CT-26 colon carcinoma model [14]. However, poor serum half-life and low target binding affinity ($K_D \sim 90 \mu\text{M}$) of M2pep are two major obstacles limiting its therapeutic efficacy.

In this study, we aim to improve serum stability and binding affinity of M2pep through rational peptide engineering. Following successful optimization of M2pep, we demonstrate its enhanced performance in *in vivo* targeting of M2-like TAMs in both the syngeneic CT-26 colon carcinoma model as well as in the 4T1 breast carcinoma model.

3.2 Materials and Methods

3.2.1 Materials

Protected amino acids and 2-(6-chloro-1H-benzotriazole-1-yl)-1,1,3,3-tetramethylaminium hexafluorophosphate (HCTU) were purchased from AAPPTec (Louisville, KY) and AnaSpec (Fremont, CA). NovaPEG Rink Amide was purchased from Merck Millipore (Billerica, MA). Collagenase (C0130), dispase II, triisopropylsilane (TIPS), 1,2-ethanedithiol (EDT), 1,3-dimethoxybenzene (DMB), tris(2-carboxyethyl)phosphine hydrochloride (TCEP), copper(II) sulfate pentahydrate ($\text{CuSO}_4 \cdot 5\text{H}_2\text{O}$), tris(3-hydroxypropyl)triazolylmethylamine (THPTA), and sodium ascorbate were purchased from Sigma-Aldrich (St. Louis, MO). Sulfo-Cy5-alkyne was purchased from Lumiprobe (Hallandale Beach, FL). Streptavidin FITC was purchased from eBioscience (San Diego, CA). Pacific blue anti-mouse F4/80 antibody (Clone BM8) was purchased from Life Technologies (Grand Island, NY). PerCP anti-mouse/human CD11b antibody (Clone M1/70) and anti-mouse CD16/32 antibody (Fc receptor block, clone 93) were purchased from BioLegend (San Diego, CA). FITC anti-mouse Ly-6G antibody (Clone 1A8) was purchased from BD Pharmingen (San Diego, CA). Mouse macrophage colony-stimulating factor (M-CSF), interleukin-4 (IL-4), and interferon- γ (IFN- γ) were purchased from R&D Systems (Minneapolis, MN). Lipopolysaccharide (LPS) was purchased from InvivoGen

(San Diego, CA). Normal mouse serum (Catalog number 10410) and other reagents were purchased from Thermo Fisher Scientific (Waltham, MA).

3.2.2 Peptide synthesis

3.2.2.1 Biotinylated peptides

Peptide synthesis was performed on an automated PS3 peptide synthesizer (Protein Technologies, Phoenix, AZ) following the standard Fmoc solid phase peptide synthesis chemistry. When needed, amino acids were manually coupled by incubation in a solution of amino acid and HCTU dissolved in 0.4 M N-methylmorpholine in DMF for 3 h. The coupling reaction was checked for completion by Kaiser Test as previously described [18]. Fmoc protecting groups were removed by two 30 min incubations in 20% (v/v) piperidine in DMF. Biotinylated peptides were synthesized from the biotinylated resin manually as follows: Fmoc-Lys(Mtt)-OH was first coupled to the NovaPEG rink amide resin. The Mtt-protecting group was removed by 3-min incubations in 1.8% (v/v) TFA in DCM until completion (15 - 20 times) as indicated by the disappearance of the yellow color (Mtt cation) in the drained deprotection solution. Biotin was then coupled to the resin, and the subsequent amino acid extension was continued on the peptide synthesizer. Peptides were acetylated at the N-terminus in acetic anhydride/triethylamine/DCM (1:1:5 v/v/v) for 2 h. Peptides were cleaved in TFA/TIPS/EDT/DMB (90:2.5:2.5:5 v/v/v/v) for 2.5 h. EDT was included in the cleavage solution only for the cysteine-containing peptides. The cleaved peptides were precipitated in cold ether twice and purified by RP-HPLC (Agilent 1200, Santa Clara, CA) using Phenomenex Fusion-RP C18 semi-preparative column (Torrance, CA) in H₂O (0.1% TFA) as a mobile phase A and ACN (0.1% TFA) as a mobile phase B. Disulfide cyclization of the purified peptides was performed by incubation in deaerated 0.1 M ammonium bicarbonate buffer (4 mg/mL peptide concentration) for 2 days. The peptides were then desalted using the HyperSepTM C18 cartridge and confirmed for purity with RP-HPLC. Molecular weights of the purified peptides were confirmed by matrix-assisted laser desorption/ionization time-of-flight mass spectrometry (MALDI-TOF MS, Bruker Daltonics, Billerica, MA).

3.2.2.2 Sulfo-Cy5-labeled peptides

Azide-functionalized peptides were synthesized following the procedure described above replacing Fmoc-Lys(Mtt)-OH with Fmoc-D-Lys(N₃)-OH at the C-terminus. Sulfo-Cy5 labeling via copper(I)-catalyzed azide-alkyne cycloaddition (CuAAC) was performed by reacting 1 eq. of peptide with 1.3 eq. of sulfo-Cy5-alkyne in the presence of 5 eq. of CuSO₄•5H₂O, THPTA, and sodium ascorbate. CuSO₄•5H₂O and THPTA were pre-mixed for a few minutes before adding to the peptide solution, and sodium ascorbate was added last. The final peptide concentration was 1 mM in H₂O/DMF (1:1 v/v). The conjugation reaction was maintained at 37 °C for 1.5 h after which any solid precipitate was centrifuged. The supernatant was initially cleaned up by eluting through Sep-Pak C18 cartridge, concentrated by rotary evaporator, and then purified by RP-HPLC. Peptide was cyclized after sulfo-Cy5 labeling.

3.2.3 Serum stability study

The peptide of interest (30 µL of 10 mg/mL stock solution in dH₂O) was added to normal mouse serum (300 µL) and incubated at 37 °C in an incubator. At each time point, an aliquot of 40 µL was drawn and an equal volume of ACN was added to the aliquot to precipitate serum proteins. The cloudy mixture was centrifuged at 10,000 rpm for 5 min and then supernatant removed. A solution of 1:1 H₂O/ACN (80 µL) was added to the pellet and sonicated for 10 min to further extract the remaining peptides. This resuspended mixture was then centrifuged, and the supernatant was pooled with the former and vacuum-dried on a Speedvac machine. The dried pellet was solubilized in H₂O (50 µL) by sonication for 10 min. The mixture was then centrifuged, and the supernatant was drawn and analyzed by MALDI-TOF MS.

3.2.4 Bone marrow harvest

All animal handling protocols were approved by the University of Washington Institutional Animal Care and Use Committee. Bone marrow harvest was performed following the previously reported protocol [14]. Briefly, femur and tibia were excised from 6-8 week-old female c57bl6/027 mice. Cuts were made on the ends of each bone, and RPMI 1640 medium was used to flush out bone marrow cells via 18G needle. The cells were cultured on petri dishes in RPMI 1640 medium supplemented with 20% donor horse serum, 1% antibiotic-antimycotic (AbAm), and 20 ng/mL M-CSF. After 7 d of culture, macrophages were activated by replacing

M-CSF with 25 ng/mL IFN- γ and 100 ng/mL LPS for M1 macrophage or 25 ng/mL IL-4 for M2 macrophage. The macrophages were activated for 2 d and then scraped off the petri dishes with cell lifter for binding studies.

3.2.5 Binding study

Peptide solutions at different concentrations for binding study were prepared by dilutions from the stock solution (10 mg/mL in dH₂O) with PBS containing 1% BSA (PBSA). M1 and M2 macrophages (50,000 cells/well) were seeded on a black 96-well plate and incubated in the peptide solutions on ice for 20 min. Unbound peptides were washed off with PBSA twice. The macrophages were subsequently incubated with streptavidin-FITC for 15 min on ice to probe for the bound peptides. Excess streptavidin-FITC was washed off with PBSA twice, and the macrophages were then resuspended in PBS for analysis by MACSQuant Flow Cytometer (Miltenyi Biotec, San Diego, CA). Propidium iodide was added to the samples before the data acquisition to discriminate dead cells. Flow cytometry data were analyzed with FlowJo Analysis Software (Tree Star, Ashland, OR). Binding study of peptides post serum incubation was similarly performed with the following additions: The peptides (5 mM stock solution in H₂O) were diluted in serum to a final concentration of 0.5 mM and incubated at 37 °C in an incubator. At each time point, an aliquot of the peptides was drawn and diluted in PBS to the final concentration for the binding study. The diluted aliquot was heated at 80 °C for 30 min to inactivate serum proteins, stored in a -20 °C freezer, and thawed for use in the binding study after aliquots at all time points were collected.

3.2.6 In vivo biodistribution study in CT-26 and 4T1 tumor models

CT-26 colon carcinoma cells and 4T1 mammary carcinoma cells were maintained in DMEM medium supplemented with 10% fetal bovine serum (FBS) and 1% Penicillin Streptomycin. Subcutaneous tumors were formed by the injection of 10⁶ CT-26 or 4T1 cells into the right flank or mammary fat pad, respectively, of 6 week-old female BALB/c mice. Tumor-bearing mice were used 2 weeks post inoculation at a maximum tumor diameter of 1.5 cm. The mice were injected retro-orbitally with 150 μ L of PBS control or sulfo-Cy5-labeled peptides (2.24 nmol in PBS with 10% DMSO). At 20 min after peptide injection, mice were anesthetized with a ketamine/xylazine cocktail and perfused with PBS. Organs were harvested and imaged on

the Caliper Xenogen IVIS (PerkinElmer, Hopkinton, MA). The fluorescence intensity emitted from each organ was subsequently quantified utilizing Xenogen's Living Image software. Following imaging, each tumor was then processed into single cell suspension by mincing into small pieces, homogenizing on gentleMACS Dissociator (Miltenyi Biotec, San Diego, CA), and incubating in 5 mL RPMI 1640 medium with 100 μ L collagenase (10,000 CDU/mL stock solution) and 100 μ L dispase II (32 mg/mL stock solution) for 40 min in the TC incubator. The dissociated single cells were collected through 70 μ m cell strainer and plated on a black round bottom 96-well plate at the density of 200,000 cells/well. Incubation of the cells with Fc receptor block was performed prior to staining with CD11b, Ly-6G, and F4/80 antibodies. Finally, the cells were fixed with 4% paraformaldehyde and analyzed with flow cytometer.

3.2.7 Statistical analysis

Normalized median fluorescent intensity values in the binding studies were presented as mean \pm SD of triplicate in the same experiment. Statistical significance in binding between M1 and M2 macrophages or binding between M2pep and its modified analogs was evaluated by Student's unpaired t-test. For clarity of presentation, only statistical significance at 50 μ M concentration was labeled to elucidate the general trend in binding activity. Analysis of the binding of M2pep analogs post-serum incubation at the 24-h time point was performed by One-way ANOVA with Tukey's post-hoc tests. Accumulation of M2pep analogs in different organs were compared by Student's unpaired t-test. Finally, intratumoral biodistribution of each M2pep analog in different tumor subpopulations as well as comparison of accumulation in M2-like TAMs of the M2pep analogs were analyzed by one-way ANOVA with Tukey's post-hoc tests. All data analysis was processed on GraphPad Prism 6 (GraphPad Software Inc., La Jolla, CA). $P < 0.5$ was considered as statistically significant.

3.3 Results and Discussion

Table 3.1 Amino acid sequences and molecular weights of M2pep analogs

Name	Sequence	Mw (Calculated)	Mw (Observed)	Note
Linear M2pepBiotin analogs				
M2pepBiotin	YEQDPWGVKWWYGGGSKK(K-Biotin)	2,524.86	2,524.21	Original sequence
AcM2pepBiotin	Ac-YEQDPWGVKWWYGGGSKKK(K-Biotin)	2,694.77	2,693.32	
W10w	Ac-YEQDPWGVK ^w WYGGGSKKK(K-Biotin)	2,694.77	2,694.04	
W(10,11)w	Ac-YEQDPWGVK ^w WYGGGSKKK(K-Biotin)	2,694.77	2,693.83	
W10P	Ac-YEQDPWGVK ^P WYGGGskkk(K-Biotin)	2,605.67	2,605.47	
W10Y	Ac-YEQDPWGVK ^Y WYGGGskkk(K-Biotin)	2,671.73	2,671.02	
K9R	Ac-YEQDPWGV ^R WYGGGSKKK(K-Biotin)	2,722.78	2,721.22	
AcM2pep(RY)Biotin	Ac-YEQDPWGV ^{RY} WYGGGskkk(K-Biotin)	2,699.74	2,699.45	Supplementary info.
W10(P,D,T,R,H) (Crude mixture)	Ac-YEQDPWGVK(P,D,T,R,H)WYGGGskkk(K-Biotin)	P: 2,605.67 D: 2,623.64 T: 2,609.66 R: 2,664.74 H: 2,645.70	P: 2,604.96 D: 2,624.78 T: not detected R: 2,664.17 H: 2,646.17	Supplementary info.
Y12y	Ac-YEQDPWGV ^{RY} WyGGGskkk(K-Biotin)	2,699.74	2,698.65	.
P5Hyp	Ac-YEQD(Hyp)WGV ^{RY} WyGGGskkk(K-Biotin)	2,715.74	2,715.00	
R0	Ac-RYEQDPWGV ^{RY} WyGGGskkk(K-Biotin)	2,855.93	2,856.18	
Cyclic M2pepBiotin analogs				
Cyclic M2pep(RY)Biotin	CGYEQDPWGV ^{RY} WYGckkk(K-Biotin)	2,718.16	2,717.59	GGGS spacer to GC
cRYWY	CGDPWGV ^{RY} WYGckkk(K-Biotin)	2,297.74	2,297.25	GGGS spacer to GC Deletion of Y1E2Q3
cRYW	CGDPWGV ^{RY} WYGckkk(K-Biotin)	2,134.56	2,134.00	GGGS spacer to GC Deletion of Y1E2Q3, Y12
Sulfo-Cy5-labeled peptides				
M2pep-sulfoCy5	YEQDPWGVKWWYGGGSKKK(k(N ₃)-sulfoCy5)	3,132.74	3,132.17	
Cyclic M2pep(RY)-sulfoCy5	CGYEQDPWGV ^{RY} WYGckkk(k(N ₃)-sulfoCy5)	3,197.86	3,198.13	

All peptides are amidated at the C terminus. Ac denotes N-terminal acetylation. Small letters denote D-amino acids. Amino acid positions are in reference to the original M2pepBiotin sequence. Modifications to the original M2pepBiotin are highlighted in red. Mw observed from MALDI-TOF MS is reported as [M+H]⁺.

3.3.1 The effect of N-terminal acetylation on serum stability and binding activity of M2pepBiotin

In vivo applications of peptides as therapeutic or imaging agents are usually limited by their short serum half life, typically on the order of a few minutes, due to degradation by serum proteases as well as clearance via kidneys and liver [19–21]. In regard to serum stability, several strategies including N-terminal acetylation, C-terminal amidation, D-amino acid substitution, and peptide stapling/macrocyclization have been utilized to impart peptide resistance against peptidase degradation [19,22]. In this study, serum stability of M2pep was first evaluated to

determine peptidase-susceptible sites. A series of rationally-engineered peptides were then synthesized and evaluated for their serum stability and binding activity (Table 3.1).

To evaluate serum stability of M2pep, the peptide was incubated in mouse serum, and aliquots of the serum at various time points were withdrawn for analysis of degradation patterns by MALDI-TOF MS. M2pepBiotin was quickly degraded in mouse serum and was no longer detected after 4 h of serum incubation (Figure 3.1A). Instead, a serum peptide (652.15 Da) became the predominant signal detected from this time point onwards. Analysis of the degraded peptide fragments revealed that the peptide degradation is both exolytic from the N-terminus and endolytic within the peptide (Figure 3.1B). Poor serum stability of this peptide therefore warranted investigation into more serum-resistant M2pep analogs.

N-terminal acetylation of peptides is a common peptide modification strategy shown to effectively prevent N-terminal peptide degradation by exopeptidases [23,24]. Hence, M2pep was acetylated at the N-terminus by reaction with acetic anhydride before cleavage from resin. The acetylated peptide, AcM2pepBiotin, was indeed resistant to N-terminal degradation (Figure 3.1C). However, this modification did not improve the overall serum stability of the peptide since the peptide remained susceptible to endolytic degradation. With the N-terminal protection, the peptide degradation patterns became clearer showing two distinct peptide fragments corresponding to endolytic cleavages at W10/W11 and S16/K17 sites with the latter occurring with relatively faster kinetics.

Next, the binding specificity of AcM2pepBiotin to M2 versus M1 macrophage was evaluated using primary bone marrow-derived macrophages polarized to the M1 or M2 phenotypes as we previously described [14]. AcM2pepBiotin retained binding selectivity to M2 macrophages over M1 macrophages although with slight, but not statistically significant, reduction in binding activity compared to M2pep at the concentrations tested (Figure 3.1D). Hence, we decided to acetylate all our subsequent peptides to protect against exolytic degradation and focused our next modifications at the W10/W11 and S16/K17 endolytic cleavage sites.

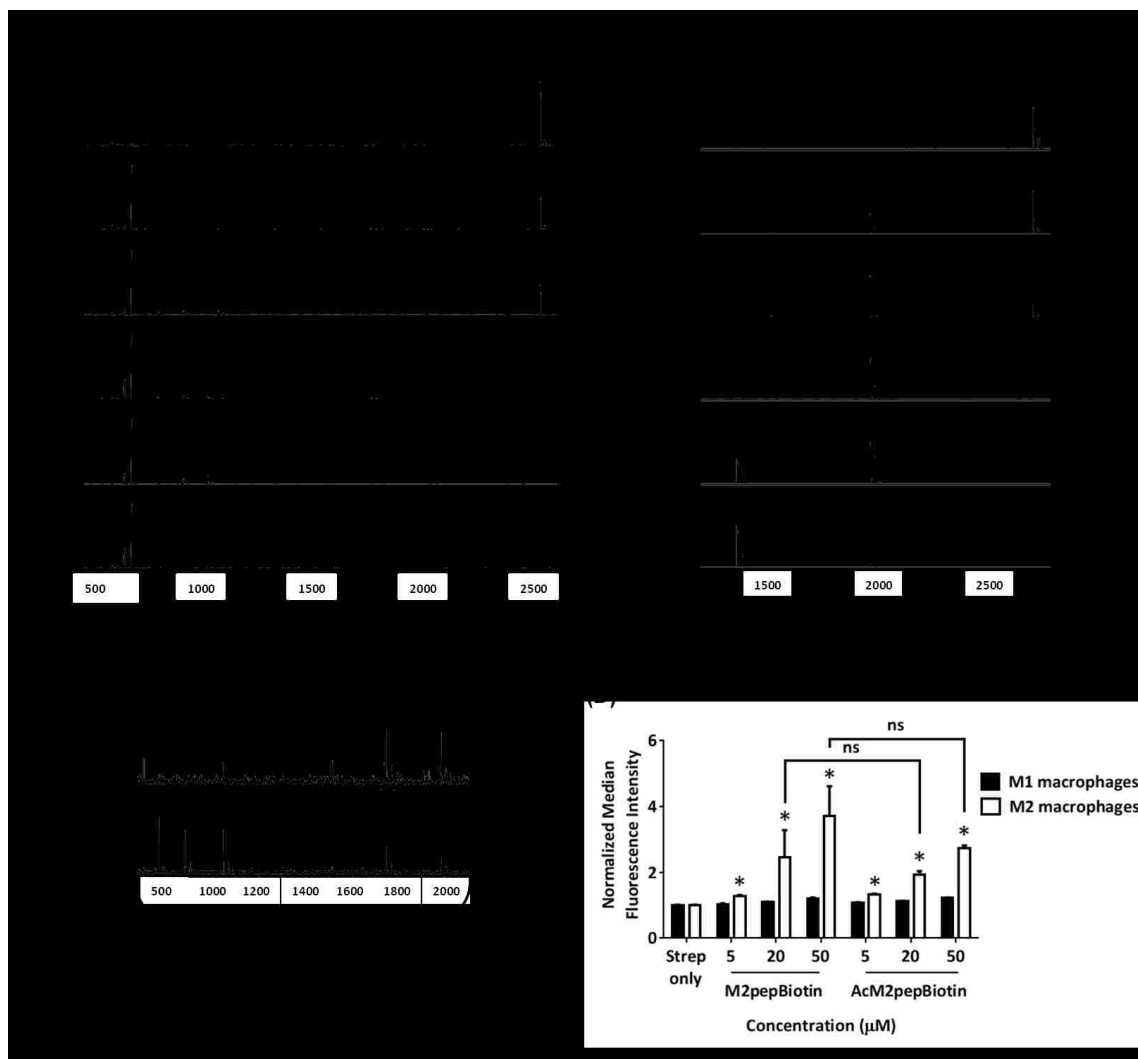


Figure 3.1 (A) MALDI-TOF MS spectra of M2pepBiotin at different serum incubation times. (B) Zoomed-in MALDI-TOF MS spectra of M2pepBiotin at 1 and 2 h. (C) MALDI-TOF MS spectra of AcM2pepBiotin at different serum incubation times. Adjacent to the primary peaks are their respective Na^+ adducts. (D) Binding of AcM2pepBiotin versus M2pepBiotin to M1 and M2 macrophages. Stars denote statistical significance between M1 and M2 macrophages in the same treatment group. * $P < 0.05$, ns = not statistically significant.

3.3.2 The effect of D-amino acid substitutions on serum stability and binding activity of AcM2pepBiotin

As reported previously, our high throughput sequencing of phage that bound to M2 macrophages showed a consensus motif of DPWXXXXW where X denoted other amino acids with less or no consensus [25]. Hence, we deduced that the motif may be essential for binding to

the M2pep receptor and targeted our next peptide modification to the W10 position which lies in the non-consensus region. Since D-amino acids are not normally present in nature and substitution with D-amino acids into peptide sequences often confer serum stability [11], we explored the effect of D-tryptophan substitution at the W10 position (W10w). Despite its effective protection against endolytic cleavage at the W10/W11 site (Figure 3.2A), the W10w substitution abrogated binding activity of the peptide (Figure 3.2B). In addition, D-tryptophan substitutions to both W10 and W11 (W(10,11)w) also did not restore the binding activity of M2pep.

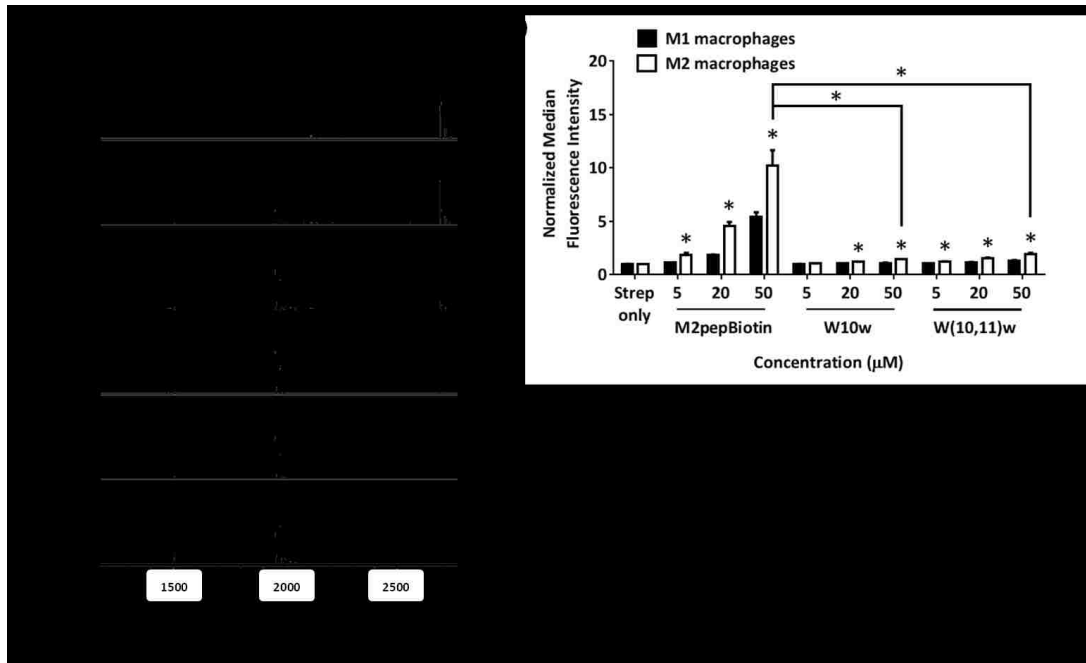


Figure 3.2 (A) MALDI-TOF MS spectra of W10w analog at different serum incubation times. Adjacent to the primary peaks are their respective Na^+ adducts. (B) Binding of M2pepBiotin compared to W10w and W(10,11)w analogs to M1 and M2 macrophages. Unless labeled in pairs, stars denote statistical significance between M1 and M2 macrophages in the same treatment group. * $P < 0.05$.

3.3.3 The effect of L-amino acid substitutions on serum stability and binding activity of AcM2pepBiotin

Next, we investigated how substitutions of W10 with other L-amino acids may help protect against degradation at the W10/W11 site. We first synthesized a W10P analog due to the apparent serum stability at the P5W6 site in AcM2pepBiotin and also a W10Y analog since tyrosine, like tryptophan, is an amino acid with a bulky aromatic side chain [26]. For both analogs, the trilycine spacer was also replaced with D-lysines to evaluate if this replacement would improve serum stability at the S16/K17 site. In addition, we also studied a K9R analog. K9 is the only lysine in the targeting region and being able to replace this lysine with arginine would allow us to synthesize AcM2pep with C-terminal lysine for facile and site-selective conjugation to drug cargos with activated NHS ester. D-lysine substitution at the trilycine spacer improved serum stability at S16/K17 site while W10P, W10Y, and K9R substitutions did not confer protection at the W10/W11 site (Figure 3A). Interestingly, binding studies showed that both K9 and W10 amino acid positions are essential for binding activity of AcM2pepBiotin (Figure 3B). In this case, K9R and W10Y substitutions significantly increased binding activity of AcM2pepBiotin while a W10P substitution abrogated the binding activity. Combining K9R and W10Y substitutions together (AcM2pep(RY)Biotin) did not improve the binding activity any further compared to the K9R analog and also did not improve serum stability at the W10/W11 site (Figure S3.1). Given high natural abundance of pi-cation interactions between Lys/Arg and Phe/Tyr/Trp in many proteins [27], K9 may be involved in the interaction with the aromatic amino acids either on the M2pep itself or on the target receptor, and the higher binding affinity of the K9R analog may thus be attributed to the stronger pi-cation interaction of the relatively more hydrophobic arginine with the corresponding aromatic amino acid [28,29]. Additional investigation into W10(D,R,H) substitutions also did not give a positive result in term of improving serum stability (Figure S3.2).

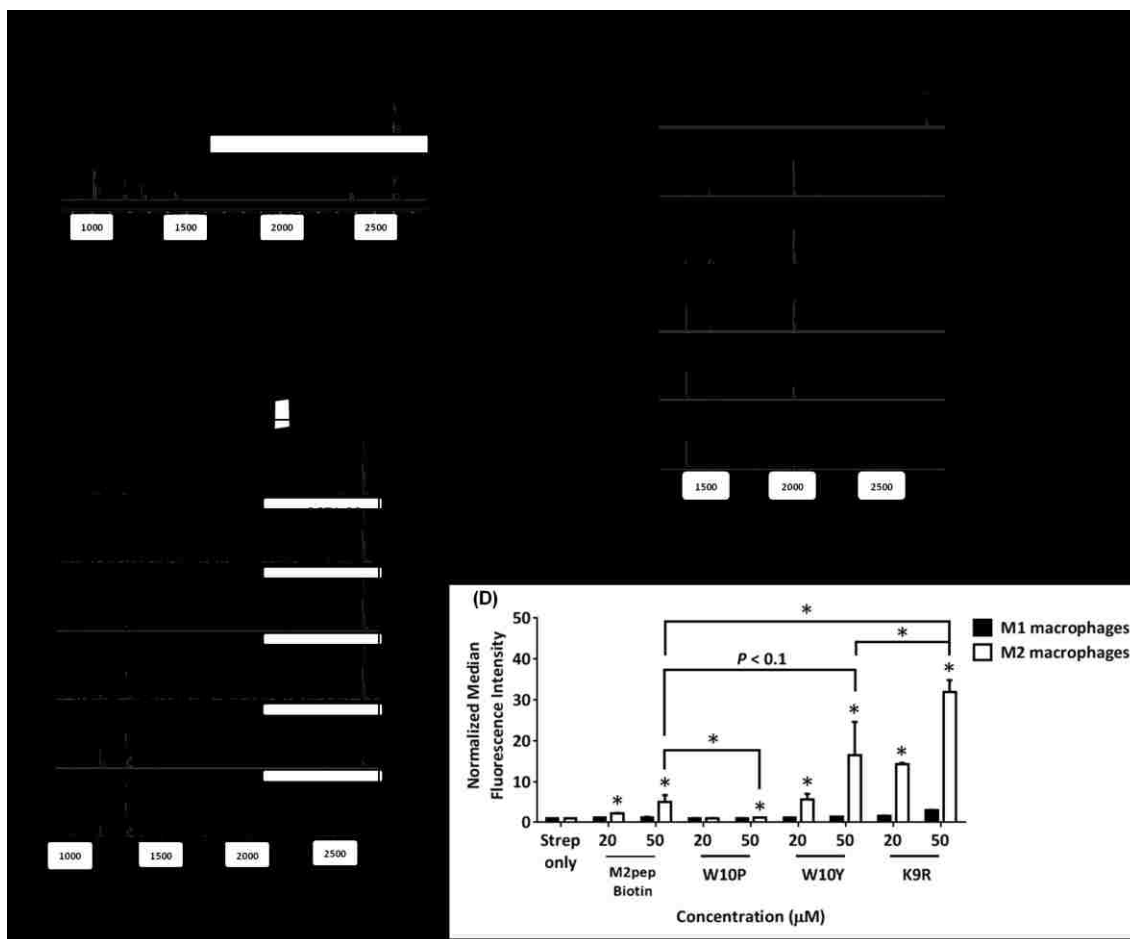


Figure 3.3 MALDI-TOF MS spectra of M2pep analogs: (A) W10P, (B) W10Y, and (C) K9R at different serum incubation times. Adjacent to the primary peaks are their respective Na⁺ adducts. (D) Binding of the M2pep analogs to M1 and M2 macrophages. Unless labeled in pairs, stars denote statistical significance between M1 and M2 macrophages in the same treatment group. * $P < 0.05$.

3.3.4 The effect of cyclization on serum stability and binding activity of M2pepBiotin

Head-to-tail cyclization of peptides may impose structural rigidity to the peptides and in several cases, leads to improvement in bioactivity and serum stability [30]. Hence, we modified linear M2pep(RY)Biotin with two flanking cysteines to enable disulfide cyclization of the peptide. The synthesized peptide (cyclic M2pep(RY)Biotin) had markedly improved serum stability over the linear AcM2pep(RY)Biotin (Figure 3.4A). Unlike the linear, acetylated M2pep derivatives which were degraded within 2 to 8 hrs post-serum incubation, cyclic M2pep(RY)Biotin remained detectable by MALDI-TOF MS even after serum incubation for 48

h. No endolytic cleavage was observed at the W10/W11 site in cyclic M2pep(RY)Biotin for up to at least 8 h. At 24 and 48 h, however, signals corresponding to N-terminal degradation and W10/W11 endolytic cleavage were observed. This degradation might be attributed to reduction of the disulfide bond over time, which converts the peptide to the protease-accessible linear form (Figure 3.4B). Interestingly, cleavage of biotin from the peptide was also observed at later time points and was not appreciated previously due to poor serum stability of the other analogs. Furthermore, cyclic M2pep(RY)Biotin has comparable binding activity to the linear AcM2pep(RY)Biotin, the highest affinity linear M2pep analog (Figure 3.4C). The binding curve of cyclic M2pep(RY)Biotin was shown in Figure S3.3. Hence, in this study, we showed that cyclization of M2pep(RY)Biotin significantly imparted serum stability over all linear AcM2pep analogs while retaining high binding activity comparable to AcM2pep(RY)Biotin. In the future, more stable cyclization strategies, such as incorporation of azide- and alkyne-functionalized amino acids for cyclization via CuAAC, may be investigated to further improve serum stability of this peptide.

In an effort to truncate the cyclic M2pep(RY)Biotin sequence, we investigated the effect of deleting amino acids that lie outside the DPWXXXXW motif by synthesizing two cyclic M2pep(RY)Biotin analogs; 1) cRYWY having deletion of Y1, E2, and Q3 and 2) cRYW containing deletions of Y1, E2, Q3, and also Y12. Both cRYWY and cRYW analogs have significantly lower binding activity compared to cyclic M2pep(RY)Biotin implying that Y1, E2, and Q3 may be important for binding to M2 macrophages (Figure 3.4D). However, Y12 may not be a critical residue since cRYWY and cRYW analogs have similar binding activity.

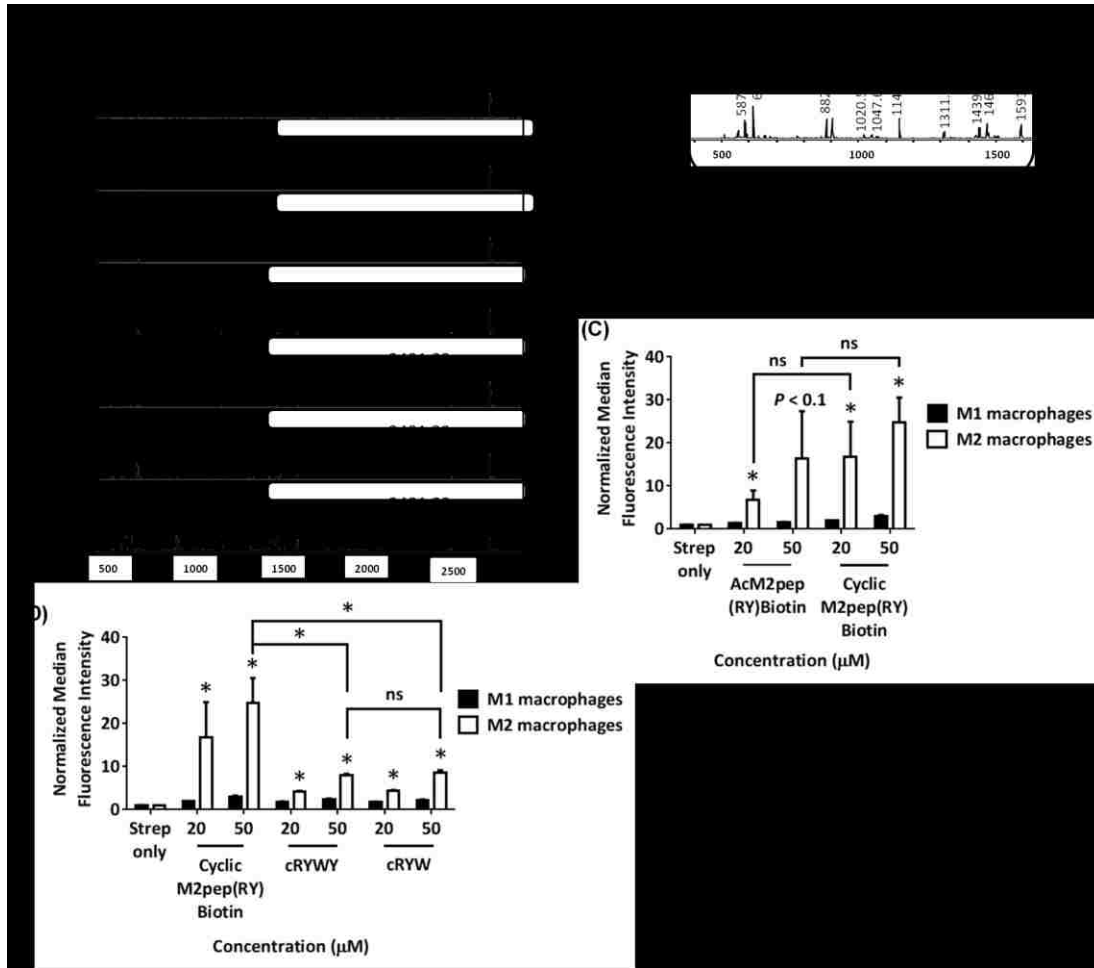


Figure 3.4 (A) MALDI-TOF MS spectra of cyclic M2pep(RY)Biotin at different serum incubation times. (B) Zoomed-in MALDI-TOF MS spectra of cyclic M2pep(RY)Biotin at 48 h. (C) Binding of cyclic M2pep(RY)Biotin and AcM2pep(RY)Biotin to M1 and M2 macrophages. (D) Binding of cyclic M2pep(RY)Biotin, cRYWY, and cRYW to M1 and M2 macrophages. Unless labeled in pairs, stars denote statistical significance between M1 and M2 macrophages in the same treatment group. * $P < 0.05$, ns = not statistically significant.

3.3.5 The effect of Y12y on serum stability and binding activity of AcM2pep(RY)Biotin

Since Y12 is not required for binding activity, we next synthesized linear AcM2pep(RY)Biotin with a D-tyrosine substitution at the Y12 position (Y12y) to evaluate if this substitution confers protection to the nearby W10/W11 cleavage site. However, the Y12y analog did not improve serum stability at the W10/W11 site (Figure 3.5A) and also unexpectedly reduced binding activity of the peptide (Figure 3.5B). Thus, while deletion of Y12 does not affect binding, substitution with a D-amino acid reduces binding affinity. Since AcM2pepBiotin

shows trends of slightly reduced binding compared with M2pepBiotin (Figure 3.1D), we investigated the effect of introducing an arginine (R0) at the start of the AcM2pep(RY)Biotin sequence to offset for loss in amine from acetylation of M2pep. In addition, we also substituted P5 with hydroxyproline (HyP), which has been shown previously to improve binding activity of another proline-containing peptide [31]. Both analogs were synthesized with the Y12y substitution, and binding study was evaluated in comparison to the Y12y analog. The R0 analog did not improve binding activity any further while P5Hyp significantly ablated the binding activity (Figure 3.5C).

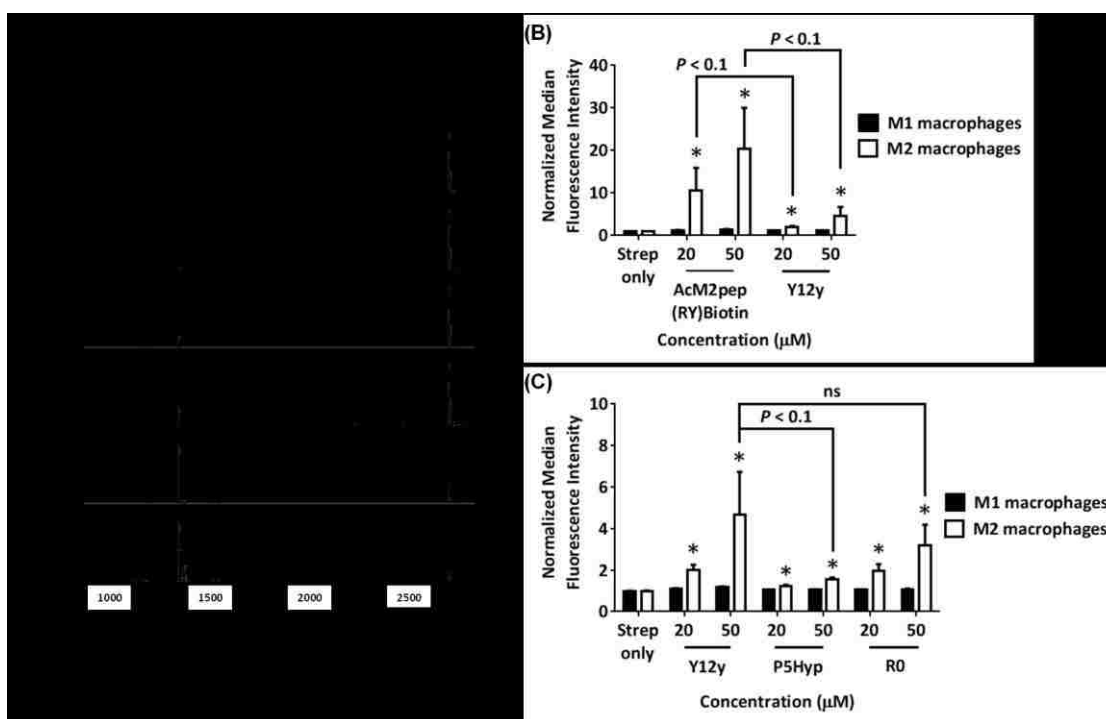


Figure 3.5 (A) MALDI-TOF MS spectra of Y12y analog at different serum incubation times. (B) Binding of AcM2pep(RY) and Y12y to M1 and M2 macrophages. (C) Binding study Y12y, P5Hyp, and R0 analogs to M1 and M2 macrophages. Stars denote statistical significance between M1 and M2 macrophages in the same treatment group. * $P < 0.05$, ns = not statistically significant.

3.3.6 Binding of M2pep analogs post serum incubation

For TAM targeting applications, M2pep analogs will be exposed to serum during systemic circulation. Therefore, we next studied how the serum stability of M2pep analogs affects subsequent binding to target cells. Peptides were incubated with mouse serum at 37 °C to mimic peptidase exposure in systemic circulation, and aliquots of the serum were withdrawn at various time points for binding studies with polarized macrophages. In general, binding activity of the M2pep analogs corresponded with the peptides' serum stability (Figure 3.6). Binding studies were performed at 150 μ M of M2pepBiotin and 50 μ M of AcM2pep(RY)Biotin and cyclic M2pep(RY)Biotin such that all the analogs had similar extent of binding at 0 h. M2pepBiotin had the fastest and greatest decline in binding activity while cyclic M2pep(RY)Biotin had the least decline which was also partially accounted by the cleavage of biotin. At 24 h, cyclic M2pep(RY)Biotin retained the highest binding activity compared to M2pepBiotin and AcM2pep(RY)Biotin reaffirming the highest serum stability of this M2pep analog observed in the previous study.

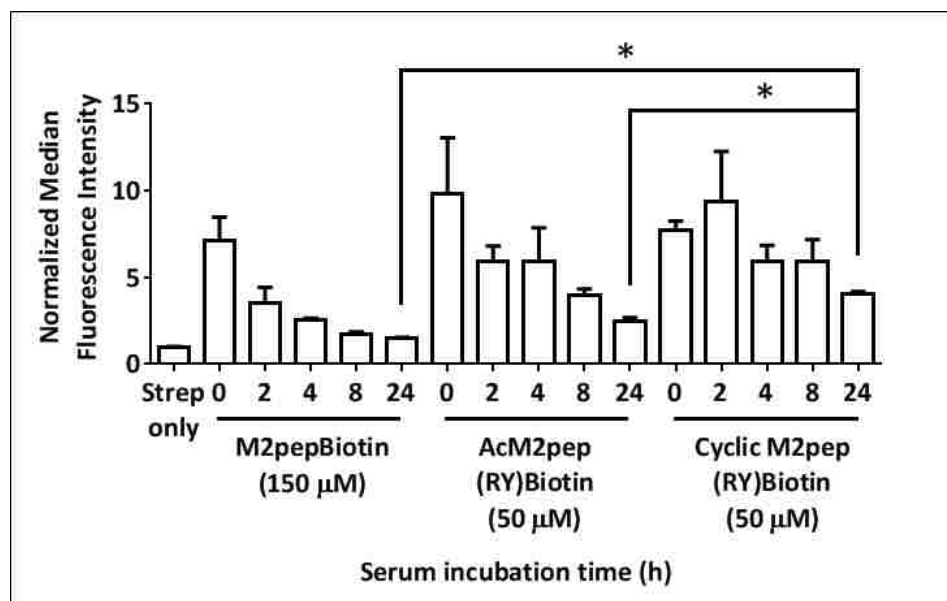


Figure 3.6 M2 macrophage-binding study of M2pepBiotin, AcM2pep(RY)Biotin, and cyclic M2pep(RY)Biotin pre-incubated in serum for different durations. * $P < 0.05$.

3.3.7 Biodistribution of M2pep analogs in CT-26 and 4T1 tumor models

Finally, we assessed the effectiveness of cyclic M2pep(RY) as an *in vivo* TAM-targeting ligand in a syngeneic CT-26 colon carcinoma and a 4T1 breast carcinoma tumor model. The biodistribution study was first performed in the CT-26 tumor model which we previously used to evaluate the original M2pep [14]. CT-26 tumor-bearing mice were intravenously administered with PBS control, M2pep-sulfoCy5, or cyclic M2pep(RY)-sulfoCy5 and perfused 20 min after. Organs were then harvested and imaged under the Xenogen IVIS. Subsequently, the tumors were processed into cell suspension, stained with antibodies, and analyzed for intratumoral distribution by flow cytometry. The gating strategy is depicted in Figure S3.4. In general, higher accumulation of cyclicM2pep(RY)-sulfoCy5 than M2pep-sulfoCy5 in tumors and other organs was observed with an exception of liver and kidneys (Figure 3.7A(i-ii)). The highest fluorescent signal was observed in kidneys where the peptides were filtered and excreted. Intratumorally, cyclic M2pep(RY)-sulfoCy5 promoted significantly higher uptake in M2-like TAMs compared to M2pep-sulfoCy5 while selectivity to M2-like TAMs over M1-like TAMs and non-TAM CD11b⁻ cells was observed in both peptide treatments (Figure 3.7A(iii)).

Following successful application of cyclic M2pep(RY) for targeting M2-like TAMs in CT-26 model, we further evaluated its effectiveness as an *in vivo* targeting ligand in the 4T1 breast tumor model since high accumulation of M2-like TAMs in breast cancer has been correlated to poor disease prognosis [32]. As observed in the CT-26 tumor model, cyclic M2pep(RY)-sulfoCy5 localized to 4T1 tumors to a greater extent compared to M2pep-sulfoCy5 (Figure 3.7B(i-ii)), and also accumulated preferentially in M2-like TAMs (Figure 3.7B(iii)). Hence, we have demonstrated through the studies of two tumor models that cyclic M2pep(RY) can be effectively used as an *in vivo* M2-TAM-targeting ligand due to its superior serum stability and enhanced binding affinity over the original M2pep. Its utility is expected to extend across multiple tumor models. In perspective, cyclic M2pep(RY)-mediated delivery of therapeutic cargos or imaging agents to M2-like TAMs could enable scientists to develop a more potent and selective M2-like TAM immunomodulation regimen or to better monitor their behavior over the course of tumor development.

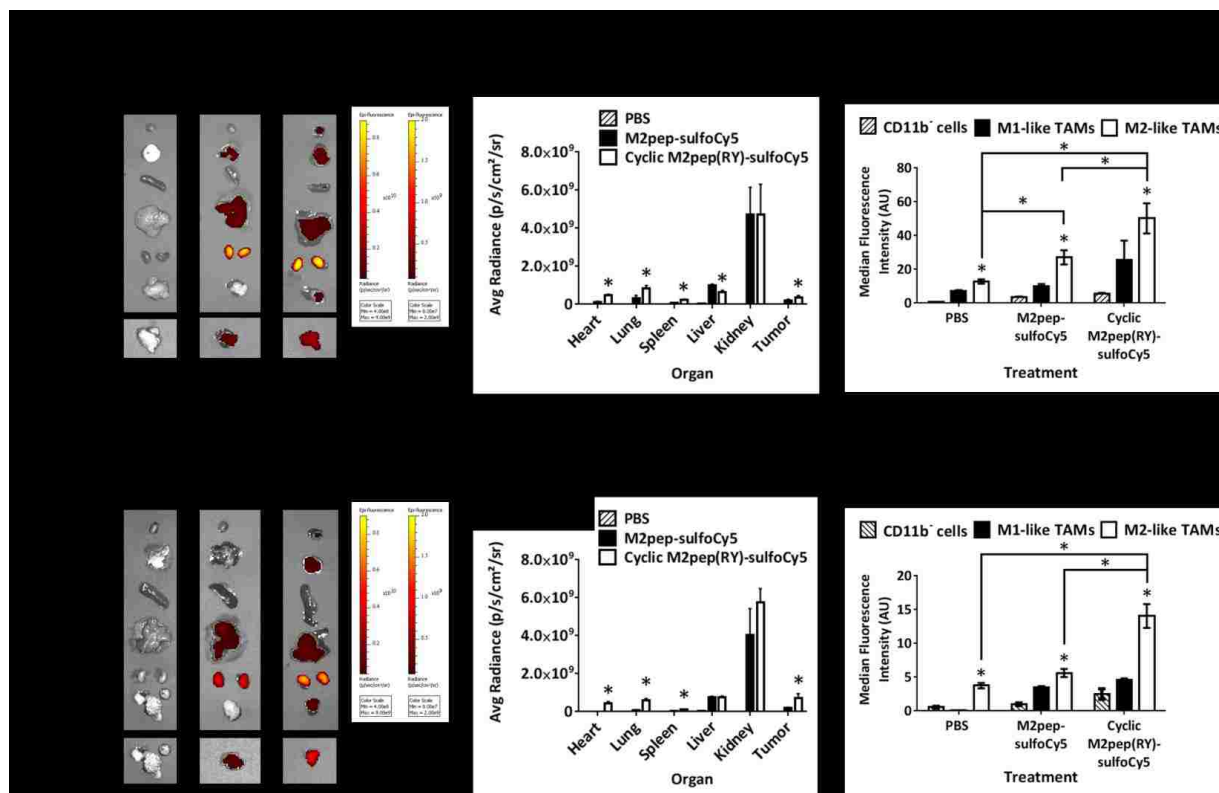


Figure 3.7 *In vivo* biodistribution study of M2pep-sulfoCy5 versus cyclic M2pep(RY)-sulfoCy5 in (A) CT-26 tumor model ($n = 5$) and (B) 4T1 tumor model ($n = 3$); (i) Representative xenogen images of the harvested organs (Δ indicates the corresponding pair of the tumor images and the scale bar), (ii) Quantified fluorescence intensity in each organ (Stars denote statistical significance relative to PBS and M2pep-sulfoCy5-treated groups. $P < 0.05$), and (iii) Intratumoral accumulation in CD11b⁻ cells, M1-like TAMs, and M2-like TAMs. Unless labeled in pairs, stars denote statistical significance relative to both CD11b⁻ cells and M1-like TAMs in the same treatment group. * $P < 0.05$.

3.4 Conclusions

M2pep was successfully optimized for serum stability via cyclization of the peptide as well as replacement of trilycine spacer to D-lysines. Binding activity of M2pep was further enhanced via K9R and W10Y substitutions. The optimized cyclic M2pep(RY) performed significantly better than M2pep at tumor localization and M2-like TAM accumulation in both CT-26 and 4T1 tumor models confirming its superior utility as an *in vivo* M2-like TAM-targeting ligand.

3.5 Acknowledgments

This work was supported by NIH 1R01CA177272. Chayanon Ngambenjawong was supported by an Anandamahidol Foundation Fellowship. Heather H. Gustafson was supported by the Cardiovascular Pathology Training Grant (5 T32 HL 007312-37). Julio M. Pineda was supported by a Mary Gates Research Scholarship. Maryelise Cieslewicz was supported by a National Science Foundation Graduate Fellowship. We thank David S.H. Chu for consultation on serum stability study of peptides.

3.6 References

- [1] R.L. Siegel, K.D. Miller, A. Jemal, Cancer Statistics, 2015, *CA Cancer J Clin.* 65 (2015) 5–29. doi:10.3322/caac.21254.
- [2] T.M. Allen, Ligand-targeted therapeutics in anticancer therapy., *Nat. Rev. Cancer.* 2 (2002) 750–763. doi:10.1038/nrc903.
- [3] V. Sanna, N. Pala, M. Sechi, Targeted therapy using nanotechnology: Focus on cancer, *Int. J. Nanomedicine.* 9 (2014) 467–483. doi:10.2147/IJN.S36654.
- [4] D.W. Bartlett, H. Su, I.J. Hildebrandt, W. a Weber, M.E. Davis, Impact of tumor-specific targeting on the biodistribution and efficacy of siRNA nanoparticles measured by multimodality in vivo imaging., *Proc. Natl. Acad. Sci. U. S. A.* 104 (2007) 15549–15554. doi:10.1073/pnas.0707461104.
- [5] R.V.J. Chari, M.L. Miller, W.C. Widdison, Antibody-drug conjugates: An emerging concept in cancer therapy, *Angew. Chemie - Int. Ed.* 53 (2014) 3796–3827. doi:10.1002/anie.201307628.
- [6] M. Srinivasarao, C. V. Galliford, P.S. Low, Principles in the design of ligand-targeted cancer therapeutics and imaging agents, *Nat. Rev. Drug Discov.* 14 (2015) 203–219. doi:10.1038/nrd4519.
- [7] G. a. Khoury, J. Smadbeck, C. a. Kieslich, C. a. Floudas, Protein folding and de novo protein design for biotechnological applications, *Trends Biotechnol.* 32 (2014) 99–109. doi:10.1016/j.tibtech.2013.10.008.
- [8] K.C. Brown, Peptidic tumor targeting agents: the road from phage display peptide selections to clinical applications., *Curr. Pharm. Des.* 16 (2010) 1040–1054.
- [9] M.K. Yu, J. Park, S. Jon, Targeting strategies for multifunctional nanoparticles in cancer imaging and therapy, *Theranostics.* 2 (2012) 3–44. doi:10.7150/thno.3463.
- [10] N. Bertrand, J. Wu, X. Xu, N. Kamaly, O.C. Farokhzad, Cancer nanotechnology: The impact of passive and active targeting in the era of modern cancer biology, *Adv. Drug Deliv. Rev.* 66 (2014) 2–25. doi:10.1016/j.addr.2013.11.009.
- [11] J.-W. Kim, T.-D. Kim, B.S. Hong, O.Y. Kim, W.-H. Yoon, C.-B. Chae, et al., A serum-stable branched dimeric anti-VEGF peptide blocks tumor growth via anti-angiogenic activity., *Exp. Mol. Med.* 42 (2010) 514–523. doi:10.3858/emm.2010.42.7.052.

- [12] M. Akcan, M.R. Stroud, S.J. Hansen, R.J. Clark, N.L. Daly, D.J. Craik, et al., Chemical re-engineering of chlorotoxin improves bioconjugation properties for tumor imaging and targeted therapy, *J. Med. Chem.* 54 (2011) 782–787. doi:10.1021/jm101018r.
- [13] C. Ngambenjawong, M. Cieslewicz, J.G. Schellinger, S.H. Pun, Synthesis and evaluation of multivalent M2pep peptides for targeting alternatively activated M2 macrophages, *J. Control. Release.* 224 (2016) 103–111. doi:http://dx.doi.org/10.1016/j.jconrel.2015.12.057.
- [14] M. Cieslewicz, J. Tang, J.L. Yu, H. Cao, M. Zavaljevski, K. Motoyama, et al., Targeted delivery of proapoptotic peptides to tumor-associated macrophages improves survival., *Proc. Natl. Acad. Sci. U. S. A.* 110 (2013) 15919–24. doi:10.1073/pnas.1312197110.
- [15] T.F. Gajewski, H. Schreiber, Y.-X. Fu, Innate and adaptive immune cells in the tumor microenvironment, *Nat Immunol.* 14 (2013) 1014–1022. doi:10.1038/ni.2703.
- [16] T.L. Whiteside, The tumor microenvironment and its role in promoting tumor growth, *Oncogene.* 27 (2008) 5904–5912. doi:10.1038/onc.2008.271.
- [17] C. Lamagna, M. Aurrand-Lions, B. a Imhof, Dual role of macrophages in tumor growth and angiogenesis., *J. Leukoc. Biol.* 80 (2006) 705–713. doi:10.1189/jlb.1105656.
- [18] J.-S. Zheng, S. Tang, Y.-K. Qi, Z.-P. Wang, L. Liu, Chemical synthesis of proteins using peptide hydrazides as thioester surrogates, *Nat. Protoc.* 8 (2013) 2483–2495. http://dx.doi.org/10.1038/nprot.2013.152.
- [19] R. Cochran, F. Cochran, Phage display and molecular imaging: expanding fields of vision in living subjects., *Biotechnol. Genet. Eng. Rev.* 27 (2010) 57–94.
- [20] D.P. McGregor, Discovering and improving novel peptide therapeutics, *Curr. Opin. Pharmacol.* 8 (2008) 616–619. doi:http://dx.doi.org/10.1016/j.coph.2008.06.002.
- [21] L. Pollaro, C. Heinis, Strategies to prolong the plasma residence time of peptide drugs, *Medchemcomm.* 1 (2010) 319–324. doi:10.1039/C0MD00111B.
- [22] L.D. Walensky, G.H. Bird, Hydrocarbon-Stapled Peptides: Principles, Practice, and Progress, *J. Med. Chem.* 57 (2014) 6275–6288. doi:10.1021/jm4011675.
- [23] a Sahu, a M. Soulika, D. Morikis, L. Spruce, W.T. Moore, J.D. Lambris, Binding kinetics, structure-activity relationship, and biotransformation of the complement inhibitor compstatin., *J. Immunol.* 165 (2000) 2491–2499. doi:10.4049/jimmunol.165.5.2491.
- [24] L.T. Nguyen, J.K. Chau, N. a Perry, L. de Boer, S. a J. Zaat, H.J. Vogel, Serum stabilities of short tryptophan- and arginine-rich antimicrobial peptide analogs, *PLoS One.* 5 (2010) 1–8. doi:10.1371/journal.pone.0012684.
- [25] G.W. Liu, B.R. Livesay, N. a Kacherovsky, M. Cieslewicz, E. Lutz, A. Waalkes, et al., Efficient Identification of Murine M2 Macrophage Peptide Targeting Ligands by Phage Display and Next-Generation Sequencing, *Bioconjug. Chem.* 26 (2015) 1811–1817. doi:10.1021/acs.bioconjchem.5b00344.
- [26] D. Bordo, P. Argos, Suggestions for “safe” residue substitutions in site-directed mutagenesis, *J. Mol. Biol.* 217 (1991) 721–729. doi:10.1016/0022-2836(91)90528-E.
- [27] J.P. Gallivan, D. a Dougherty, Cation-pi interactions in structural biology., *Proc. Natl. Acad. Sci. U. S. A.* 96 (1999) 9459–9464. doi:10.1073/pnas.96.17.9459.

- [28] D. a. Dougherty, Cation- π Interactions Involving Aromatic Amino Acids, *J. Nutr.* 137 (2007) 1504S–1508. <http://jn.nutrition.org/cgi/content/long/137/6/1504S>.
- [29] R.M. Hughes, K.R. Wiggins, S. Khorasanizadeh, M.L. Waters, Recognition of trimethyllysine by a chromodomain is not driven by the hydrophobic effect., *Proc. Natl. Acad. Sci. U. S. A.* 104 (2007) 11184–11188. doi:10.1073/pnas.0610850104.
- [30] R.J. Clark, H. Fischer, L. Dempster, N.L. Daly, K.J. Rosengren, S.T. Nevin, et al., Engineering stable peptide toxins by means of backbone cyclization: stabilization of the alpha-conotoxin MII., *Proc. Natl. Acad. Sci. U. S. A.* 102 (2005) 13767–13772. doi:10.1073/pnas.0504613102.
- [31] A.F. Kolodziej, Z. Zhang, K. Overoye-Chan, V. Jacques, P. Caravan, Peptide optimization and conjugation strategies in the development of molecularly targeted magnetic resonance imaging contrast agents., *Methods Mol. Biol.* 1088 (2014) 185–211. doi:10.1007/978-1-62703-673-3_13.
- [32] D. Laoui, K. Movahedi, E. Van Overmeire, J. Van den Bossche, E. Schouppe, C. Mommer, et al., Tumor-associated macrophages in breast cancer: distinct subsets, distinct functions., *Int. J. Dev. Biol.* 55 (2011) 861–867. doi:10.1387/ijdb.113371dl.

3.7 Supplementary information

Figure S3.1 (A) Binding of AcM2pep(RY)Biotin, K9R, and W10Y analogs to M1 and M2 macrophages. (B) MALDI-TOF MS spectra of AcM2pep(RY)Biotin at different serum incubation times. Adjacent to the primary peaks are their respective Na⁺ adducts. Unless labeled in pairs, stars denote statistical significance between M1 and M2 macrophages in the same treatment group. * $P < 0.05$, ns = not statistically significant.

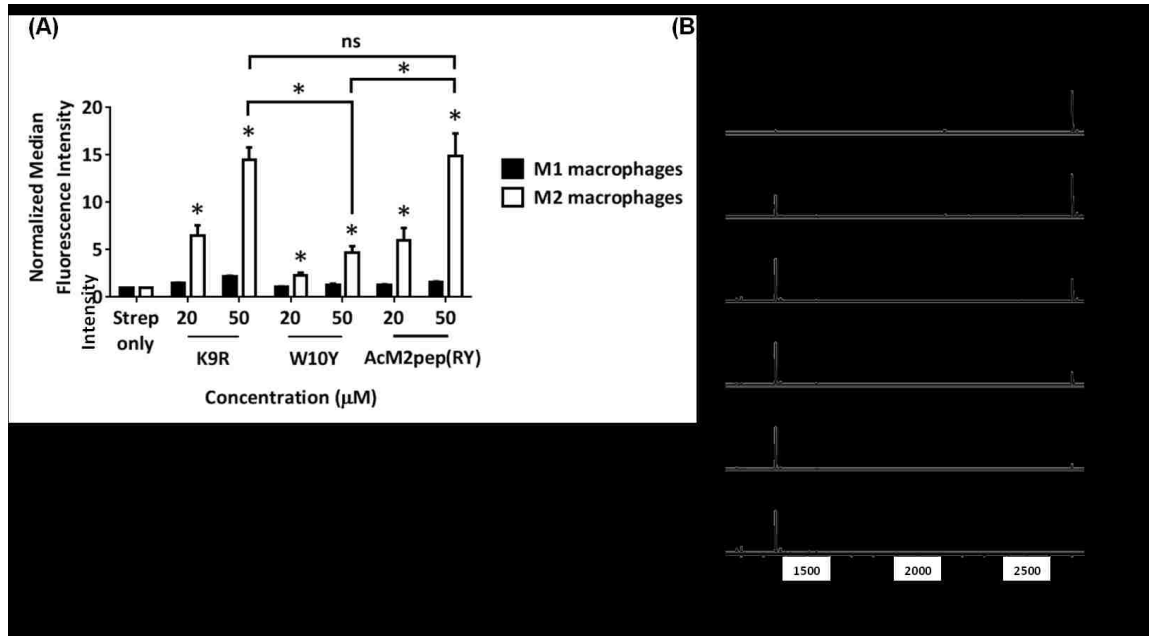


Figure S3.2 MALDI-TOF MS spectra of crude W10(P,D,T,R,H) analog at different serum incubation times. The crude mixture was synthesized using the split-and-mix strategy at the W10 position. Briefly, WYGGGSkkk(K-Biotin) was synthesized on the automatic peptide synthesizer. The peptide on resin was then split into 5 portions, separately coupled with Pro, Asp, Thr, Arg, and His, manually pooled together, and put on the peptide synthesizer to continue the synthesis of the remaining sequence. The crude mixture was used without RP-HPLC purification.

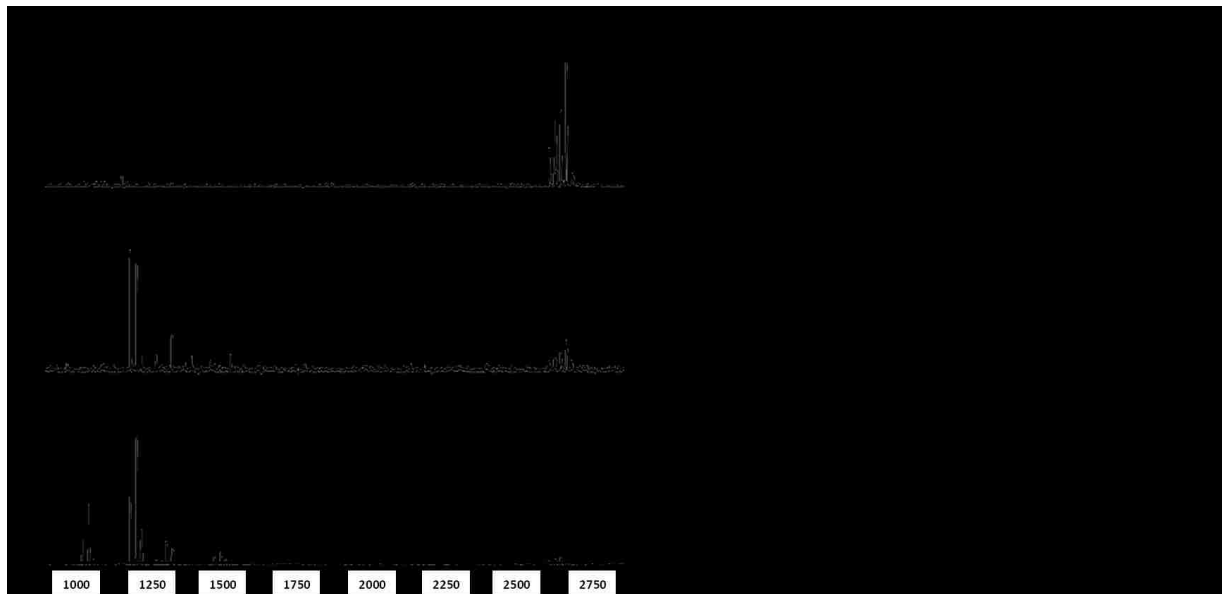


Figure S3.3 Binding curves of M2pepBiotin and cyclic M2pep(RY)Biotin on M2 macrophages. The K_D value for M2pepBiotin reported here is slightly higher than the previously reported value due to some differences in experimental methodology. In this study, M2 macrophages were not fixed after incubation with peptides and were stained with propidium iodide to only quantify binding on live cells.

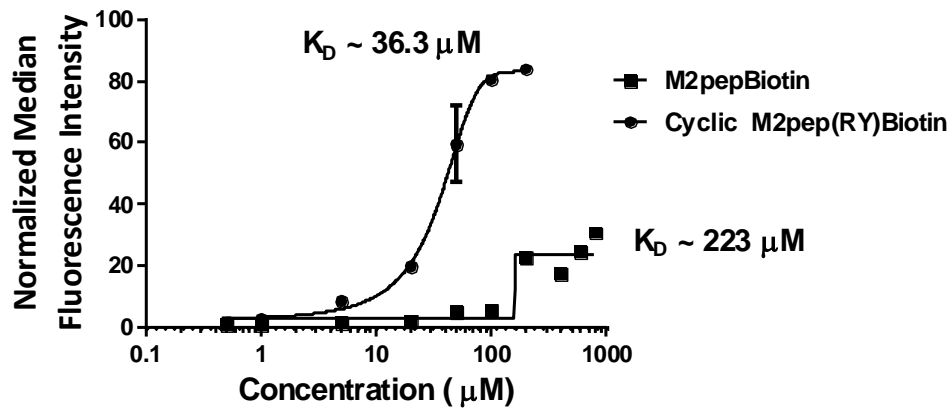
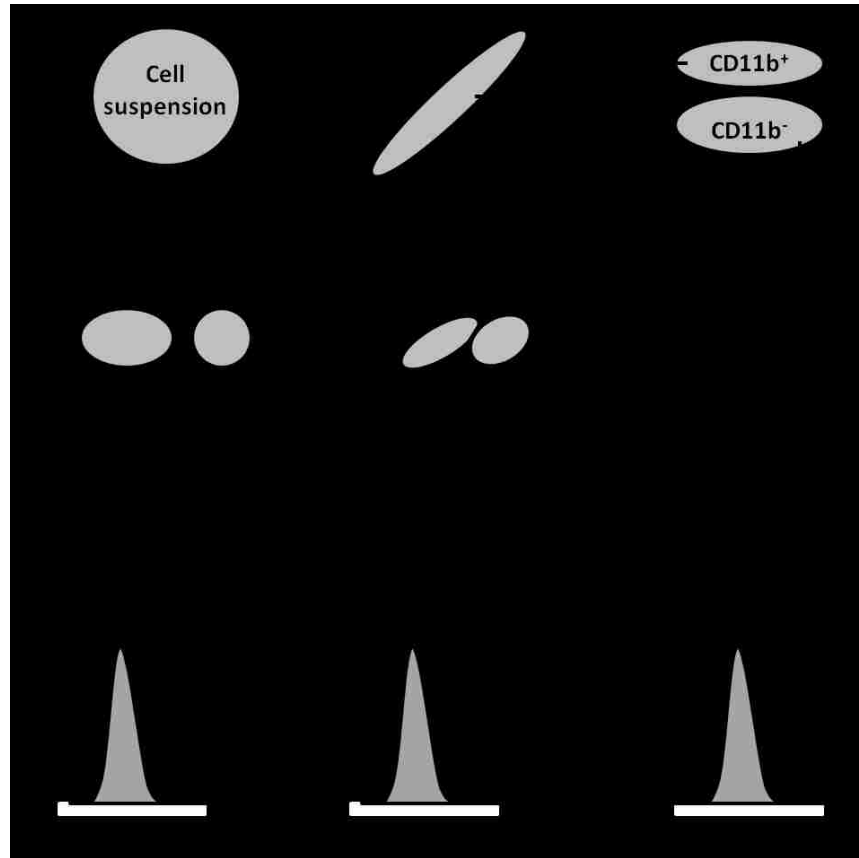


Figure S3.4 Schematics elucidating the gating strategy for analysis of intratumoral biodistribution of M2pep analogs in 1) CD11b⁻ population, 2) M1-like TAMs, and 3) M2-like TAMs.



Chapter 4

**ENGINEERING AN AFFINITY-ENHANCED PEPTIDE THROUGH
OPTIMIZATION OF CYCLIZATION CHEMISTRY**

Chayanon Ngambenjawong, Julio Marco B. Pineda, Suzie H. Pun

Abstract

Peptide cyclization is a strategy used to improve stability and/or activity of peptides. The most commonly used cyclization method is disulfide bridge formation of cysteine-containing peptides as typically found in nature. Over the years, an increasing number of alternative chemistries for peptide cyclization with improved efficiency, kinetics, orthogonality, and stability have been reported. However, there has been less appreciation for the opportunity to fine-tune peptide activity via the diverse chemical entities introduced at the site of linkage by different cyclization strategies. Here, we demonstrate how cyclization optimization of an M2 “anti-inflammatory” macrophage-binding peptide (M2pep) resulted in a significant increase in binding affinity of the optimized analog to M2 macrophages while maintaining binding selectivity compared to M1 “pro-inflammatory” macrophages. In this study, we report synthesis and evaluation of four cyclic M2pep(RY) analogs with diverse cyclization strategies; 1) Asp-[Amide]-Lys, 2) Azido-Lys-[Triazole (Copper(I)-catalyzed alkyne-azide cycloaddition (CuAAC))]-Propargyl-Gly, 3) Cys-[Decafluorobiphenyl (DFBP)]-Cys, and 4) Cys-[Decafluorobiphenyl sulfone (DFS)]-Cys, whereby the chemical entity/linker at the linkage site is shown in the square bracket and is between the residues involved in cyclization. These peptides are compared to a disulfide-cyclized M2pep(RY) that we previously reported as a serum-stable, affinity enhanced analog to the original linear M2pep. DFBP-cyclized M2pep(RY) exhibits the highest binding activity to M2 macrophages with apparent dissociation constant (K_D) about 2.03 μM compared to 36.3 μM for the original disulfide-cyclized M2pep(RY) and 220 μM for the original linear peptide. DFS-cyclized M2pep(RY) also binds more strongly than the original cyclized analog whereas Amide- and Triazole-cyclized M2pep(RY) analogs bind less strongly. We verified that DFBP alone has negligible binding to M2 macrophages and the incorporation of diphenylalanine to the original sequence improves binding activity at the expense of solubility and increased toxicity. In conclusion, we report development of cyclic M2pep(RY) analogs with diverse cyclization strategies leading to the discovery of DFBP-cyclized M2pep(RY) with enhanced M2 macrophage-binding activity.⁴

⁴ Reprinted with permission from Ngambenjawong et al. (2016) *Bioconjug Chem* 27(12):2854-2862. Copyright© 2016 American Chemical Society

4.1 Introduction

Peptides are an important class of biomolecules for biomedical applications. The diversity of available amino acids and their different side chains allow for unique peptide sequences with specific bio-recognition to target receptors. The discovery of targeting peptides has been greatly accelerated by high-throughput combinatorial screening technologies such as peptide phage display library and one-bead-one-compound (OBOC) peptide library as well as by advanced computational design [1,2]. Hence, peptides have been increasingly used as targeting ligands for diagnostics and drug delivery systems and also as therapeutic entities. Peptides have advantages of being smaller in size than proteins, allowing for application-dependent advantages such as higher diffusivity and lower manufacturing cost [3,4]. However, peptides are also more susceptible to proteolytic degradation in serum and fast renal clearance [3]. In addition, peptide sequences are sometimes too short to engage with the target receptors with sufficient affinity [5]. As a result, most first generation peptides discovered from library screening need to be engineered or further optimized to improve serum stability and binding affinity before successful clinical translation [6,7]. Common approaches in peptide optimization include alanine scanning and/or truncation analysis to identify key residues for subsequent biased library selection [8–11], incorporating unnatural or D-amino acids [12], altering the amide backbone [13–15], and stapling or cyclizing peptides to enhance stability, activity, and in some cases, cellular permeability [16,17].

Conventional as well as newly developed bioconjugation chemistries have broadened the repertoire of cyclization strategies beyond disulfide bridge formation between cysteine pair(s) or lactamization between lysine and aspartic acid/glutamic acid [18,19]. Copper(I)-catalyzed alkyne-azide cycloaddition (CuAAC) between non-natural amino acids with azide and alkyne side chains allows for orthogonal cyclization of cysteine-containing peptides without affecting the free cysteine residue which is sometimes important for peptide biological activity [19,20]. Ruthenium-catalyzed ring-closing olefin metathesis (RCM) and molybdenum-catalyzed ring-closing alkyne metathesis (RCAM) enable orthogonal formation of bicyclic peptides containing non-natural amino acids with alkene and alkyne side chains, respectively, in a one-pot reaction [21]. A family of perfluoroaryl compounds such as decafluorobiphenyl (DFBP) and decafluorobiphenyl sulfone (DFS) has been developed for selective cyclization of cysteine-

containing peptides with fast reaction kinetics whereas DFS has also been successfully used to cyclize lysine-containing peptides that are absent in cysteine residues [22–24].

Optimization of peptide activity via cyclization has focused on selecting the right amino acid positions for modification as well as the appropriate length of the linker [19,21,25]. However, there have been few studies investigating the effect of cyclization chemistry on peptide bioactivity or stability, which may be an important parameter since the linker chemistry may affect peptide/receptor binding affinity or provide structural reinforcement to the peptide. In this study, we demonstrate that cyclization strategies significantly affect peptide activity using an M2 macrophage-binding peptide (M2pep) as an example [26]. We previously reported a disulfide-cyclized M2pep(RY) as a serum stable, affinity-enhanced M2pep analog [27]. This peptide binds to murine M2 (IL4-polarized, “anti-inflammatory”) macrophages with an apparent dissociation constant (K_D) of about 36.3 μ M and with high selectivity over M1 (IFN- γ and LPS-polarized, “pro-inflammatory”) macrophages. The disulfide-cyclized M2pep(RY) peptide was also successfully used to target tumor-promoting M2-like tumor associated macrophages (M2-TAMs) in CT-26 colon carcinoma and 4T1 breast cancer mouse models making it a useful targeting platform for development of M2-TAM-targeting diagnostics or therapeutics for cancer treatments [27]. Here, we report synthesis of four additional cyclic M2pep(RY) analogs (Figure 4.1) with focus on the development of on-resin synthesis strategy for eventual manufacturing scalability. The effect of cyclization strategies on biological activity of these analogs were also compared through binding studies with M1 and M2 murine macrophages.



Figure 4.1 Schematics of M2pep and cyclic M2pep(RY) analogs. RY substitution to the original M2pep sequence for affinity improvement is shown in green [27]. Modified amino acids for cyclization and serum stability improvement are shown in red.

4.2 Results and Discussion

4.2.1 Peptide synthesis

In this work, five cyclic M2pep(RY) peptides were synthesized using various cyclization chemistries (Figure 4.1). Successful synthesis of all peptides was verified by MALDI-ToF MS (Table S4.1). On-resin cyclization of Amide-, Triazole-, and DFBP-cyclized M2pep(RY)Biotin proceeded efficiently based on HPLC traces during purification. Full schematics for on-resin synthesis of these analogs as well as their associated HPLC traces and methods are shown in Figure S4.1. Successful CuAAC-mediated cyclization of Triazole-cyclized M2pep(RY)Biotin was confirmed by insensitivity to TCEP-mediated azide reduction and inactivity to subsequent CuAAC reaction with propargyl alcohol (Figure S4.2). Attempts in on-resin cyclization of DFS-cyclized M2pep(RY)Biotin following the developed strategy for on-resin synthesis of DFBP-cyclized M2pep(RY)Biotin were not successful and instead, a major side product of -346 Da was observed (Figure S4.3A). Nonetheless, in-solution cyclization of DFS-cyclized M2pep(RY)Biotin was optimized to proceed in high yield with minimal formation of an unidentified “-20 Da” side product (Figure S4.3B). In addition, we found that addition of TCEP

to the DFBP and DFS cyclization reactions in solution significantly increases yield of the desired product by suppressing formation of the disulfide-cyclized peptide. Three of the cyclized variants (Disulfide, DFBP, and DFS analogs) can be readily synthesized from the same linear precursor, thus saving time for the optimization process. Although not investigated in this study, it should also be possible to synthesize Amide- and Triazole-cyclized analogs from a common linear precursor (e.g. GYEQDPWGVRYWYGX₂kkk(K-Biotin-resin) where X₂ is azidolysine), followed by coupling with Boc-Propargylglycine-OH for CuAAC-mediated cyclization and coupling with Boc-Asp(OAll)-OH followed by reduction of azide to amine [28] and OAll deprotection before on-resin lactamization, respectively.

4.2.2 In vitro binding study

M1 and M2 polarized murine macrophages were incubated with various concentrations of biotinylated M2pep analogs and probed for peptide binding using streptavidin-FITC with flow cytometry analysis. Binding curves were acquired by determining the median fluorescence intensity (MFI) of streptavidin-FITC associated with cells at various peptide concentrations, and apparent K_D values were calculated based on half-maximal MFI of each individual peptide analog. All M2pep analogs bind preferentially to M2 macrophages over M1 macrophages (Figure 4.2). For comparison, previously-reported binding curves for M2pepBiotin and Disulfide-cyclized M2pep(RY)biotin are also included [27]. Disulfide-, Amide-, and Triazole-cyclized M2pep(RY)Biotin have similar K_D values, between 30-40 μM, although varying maximum MFI values were observed for each construct. Strikingly, DFBP- and DFS-cyclized M2pep(RY)Biotin have significantly improved affinity with about 15-30 fold lower K_D values (2.03 μM and 1.42 μM, respectively) than the other cyclic analogs. Comparing these two analogs, DFS-cyclized M2pep(RY)Biotin has lower maximal MFI than the DFBP analog. The maximum MFI correlates to the maximal extent at which peptides can engage with surface receptors on plasma membrane of target cells. It is surprising to us that different cyclic analogs exhibit different maximal MFI values even though they are expected to bind to the same target receptor on M2 macrophages. However, since the identity of the M2pep receptor remains unknown, we are not able to make further conclusions regarding the mechanism of binding of these peptide constructs. Nonetheless, our binding data demonstrate that optimization of cyclization chemistry is important in maximizing the cyclic peptide activity.

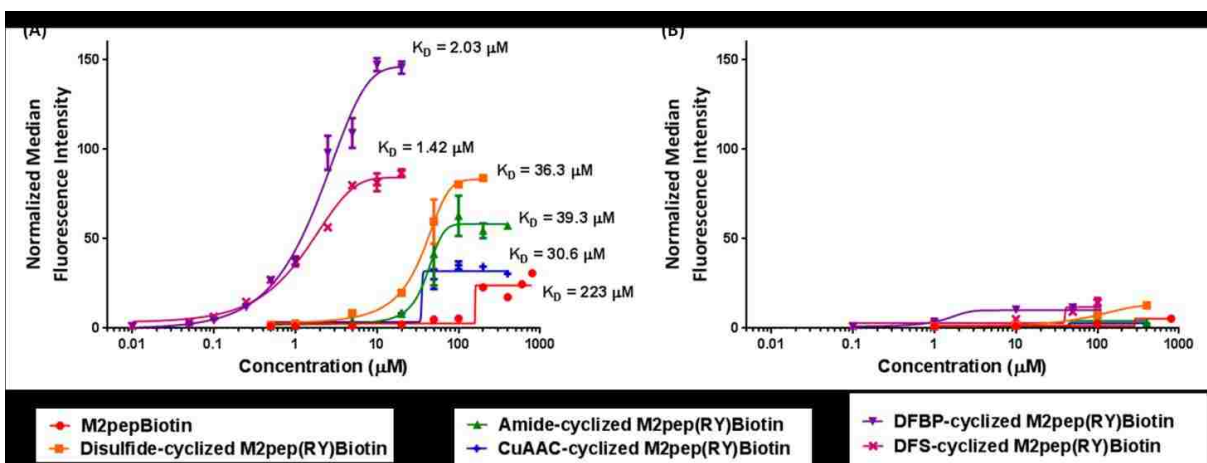


Figure 4.2 Binding curves of M2pep analogs on (A) M2 macrophages and (B) M1 macrophages.

Due to the low K_D and high maximal MFI obtained for DFBP-cyclized M2pep(RY)Biotin, we next verified whether the RY modification, originally reported to improve binding affinity of M2pep [27], remains a relevant modification for this cyclic analog. DFBP-cyclized M2pepBiotin without RY modification was synthesized and evaluated for binding activity. Binding studies confirmed that the RY modification enhances binding activity of the cyclized-M2pep peptide to M2 murine macrophages by about 4-fold compared to the original sequence (Figure 4.3). Hence, we confirmed the discovery of DFBP-cyclized M2pep(RY)Biotin as an affinity-enhanced M2 macrophage-targeting peptide which could be useful for future development of diagnostics or drug delivery systems targeting M2 macrophages or M2-like tumor-associated macrophages.

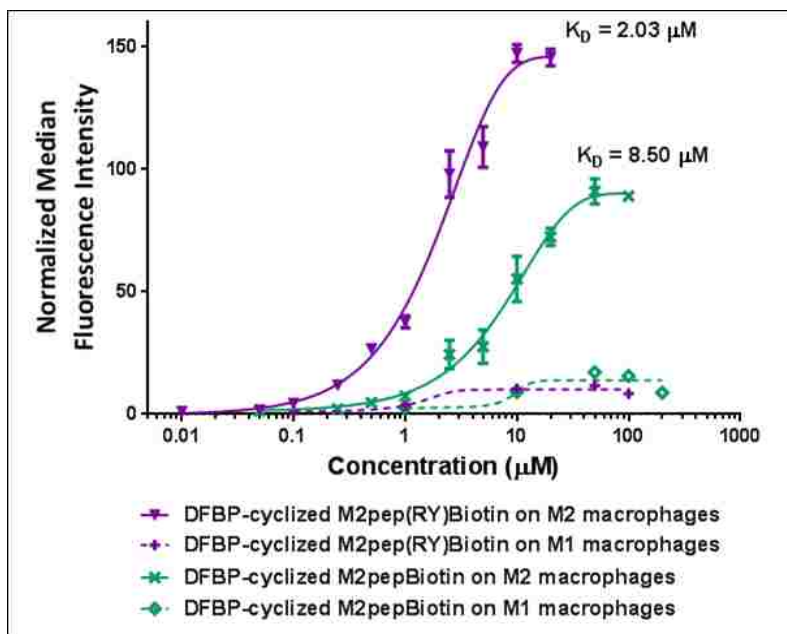


Figure 4.3 Binding curves of DFBP-cyclized M2pep(RY)Biotin and DFBP-cyclized M2pepBiotin with M1 and M2 macrophages.

In order to understand the affinity enhancement of DFBP-cyclized M2pep(RY)Biotin, we first assessed the effect of DFBP on macrophage binding by synthesizing a DFBP-functionalized linear control peptide (Biotin-Ahx-GRGRGRG(C-DFBP)G) where DFBP is conjugated to a single cysteine and the GR region serves as a spacer and solubility enhancer for DFBP (Figure 4.4A). This peptide binds very weakly to macrophages even at 100 µM whereas DFBP-cyclized M2pep(RY)Biotin exhibits strong binding activity even at 1 µM (Figure 4.4B). This data suggests that DFBP itself does not increase binding to the unknown M2pep receptor and that DFBP may instead increase binding by an alternative mechanism such as via altering or stabilizing peptide conformation. Since DFBP is a small hydrophobic molecule, we speculated that DFBP might bind to some hydrophobic pockets on BSA present in our binding solutions and promote enhanced binding via a multivalent effect. This possibility was eliminated based on binding studies of DFBP-cyclized M2pep(RY)Biotin performed in both PBS and PBSA (PBS with 1% albumin) that showed no difference in binding (Figure 4.4C).

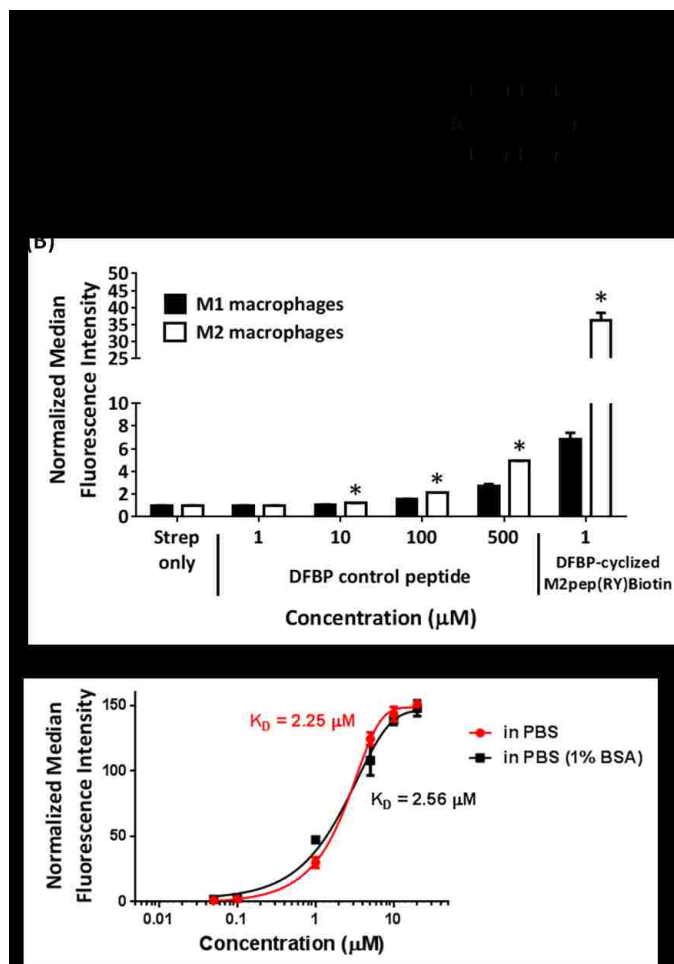


Figure 4.4 (A) DFBP-functionalized linear control peptide. (B) Binding study of DFBP-functionalized linear control peptide on M1 and M2 macrophages. Stars denote statistical significance between M2 and M1 macrophages. $*P < 0.05$. (C) Binding study of DFBP-cyclized M2pep(RY)Biotin in PBS and PBSA on M2 macrophages.

Next, we investigated whether the higher binding activity of DFBP-cyclized M2pep(RY)Biotin could be recapitulated by an addition of a dipeptide with aromatic side chain into the original disulfide-cyclized M2pep(RY)Biotin peptide. Two additional disulfide-cyclized M2pep(RY)Biotin analogs were synthesized incorporating either diphenylalanine (FF-cyclized M2pep(RY)Biotin) or dipentafluorophenylalanine (F(F5)F(F5)-cyclized M2pep(RY)Biotin) before the N-terminal cysteine to assess the effect of aromatic ring and fluorine substitution on binding activity to macrophages (Figure 4.5A). Introduction of these dipeptides significantly reduces solubility of the peptide analogs with the F(F5)F(F5)-cyclized analog being less soluble than the FF-cyclized analog. Notably, despite being highly fluorinated, DFBP-cyclized

M2pep(RY)Biotin has higher solubility than FF-cyclized M2pep(RY)Biotin. Addition of diphenylalanine indeed improves binding activity of the peptide on M2 macrophages implying that the presence of aromatic structure near the site of cyclization may contribute to the enhanced binding (Figure 4.5B). F(F5)F(F5)-cyclized M2pep(RY)Biotin was very toxic to macrophages even at low micromolar concentrations (Figure S4), so we were not able to accurately construct a binding curve for this analog. Nonetheless, based on the binding data at the lower concentrations (Figure 4.5C), this analog seems to exhibit similar binding activity as FF-cyclized M2pep(RY)Biotin with M2 macrophages implying that fluorine substitution may not have a significant effect towards binding activity. However, since FF-cyclized M2pep(RY)Biotin still has lower binding activity than DFBP-cyclized M2pep(RY)Biotin, there are likely additional factors involved in the enhanced binding phenomenon observed with the DFBP-cyclized peptide.

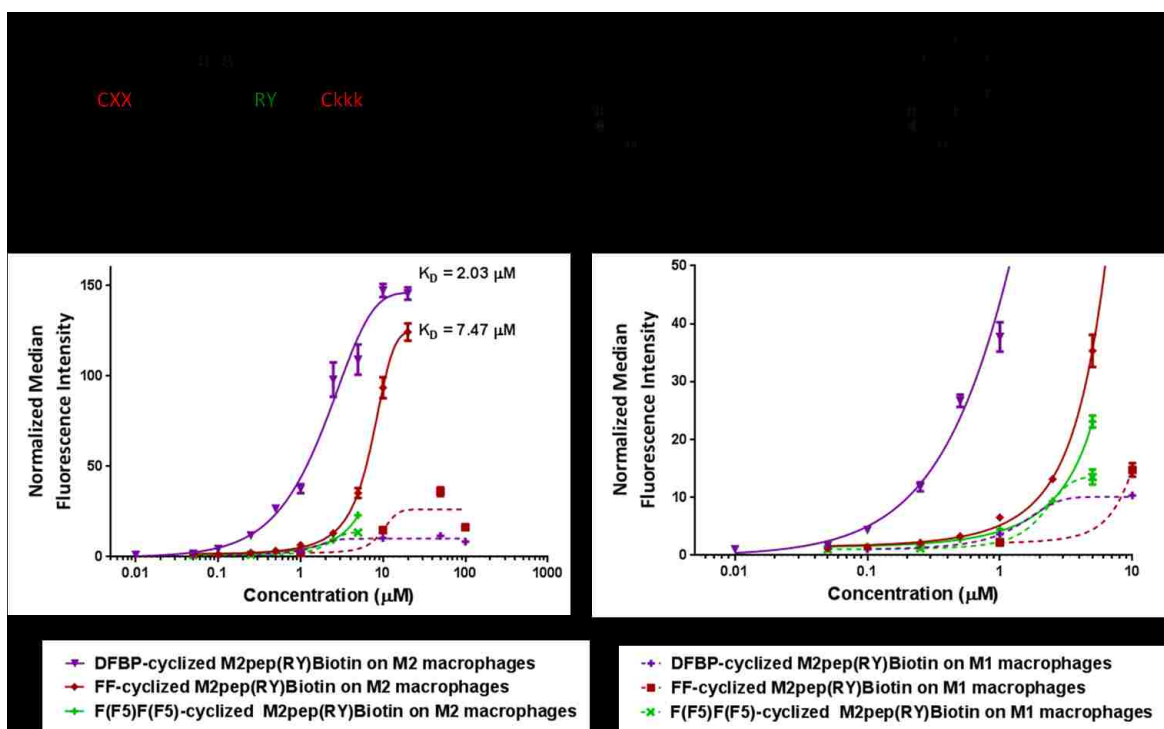


Figure 4.5 (A) FF- and F(F5)F(F5)-cyclized M2pep(RY)Biotin. (B) Binding curves of DFBP-, FF-, and F(F5)F(F5)-cyclized M2pep(RY)Biotin with M1 and M2 macrophages. (C) Enlarged binding curves at the lower concentration range.

4.2.3 Circular Dichroism (CD) measurement

Improvement in peptide activity via cyclization can sometimes be attributed to reinforcement in the peptide's secondary structure [29]. Hence, we performed a preliminary assessment on peptide conformation of the M2pep peptides via CD measurement. None of the CD spectra of these M2pep analogs matches characteristic spectra of 100% α -helix, β -sheet, or random coil structures [30] implying that the peptides may only be partially structured or unstructured (Figure 4.6A-D). The effect of RY modification results in an inversion from a predominantly negative CD signal with two minima at about 200 and 225 nm to a predominantly positive signal with two maxima at about 200 and 230 nm (Figure 4.6A). A decline in the CD signal at 200 and 230 nm maxima for DFBP- and DFS-cyclized M2pep(RY)Biotin analogs was observed (Figure 4.6C) compared to the other cyclic M2pep(RY)Biotin analogs which may account for the affinity improvement of the former. However, this trend is not observed in FF-cyclized M2pep(RY)Biotin which also exhibits enhanced affinity. Unlike stapled peptides of helical nature whose secondary structure reinforcement may be estimated in term of helicity content, it is more challenging to elucidate the conformational reinforcement of non-helical peptides like cyclic M2pep(RY) analogs. Future characterization studies on identification of M2pep receptor as well as its interaction with M2pep peptides will be needed in order to better understand the observed enhanced affinity to M2 macrophage.

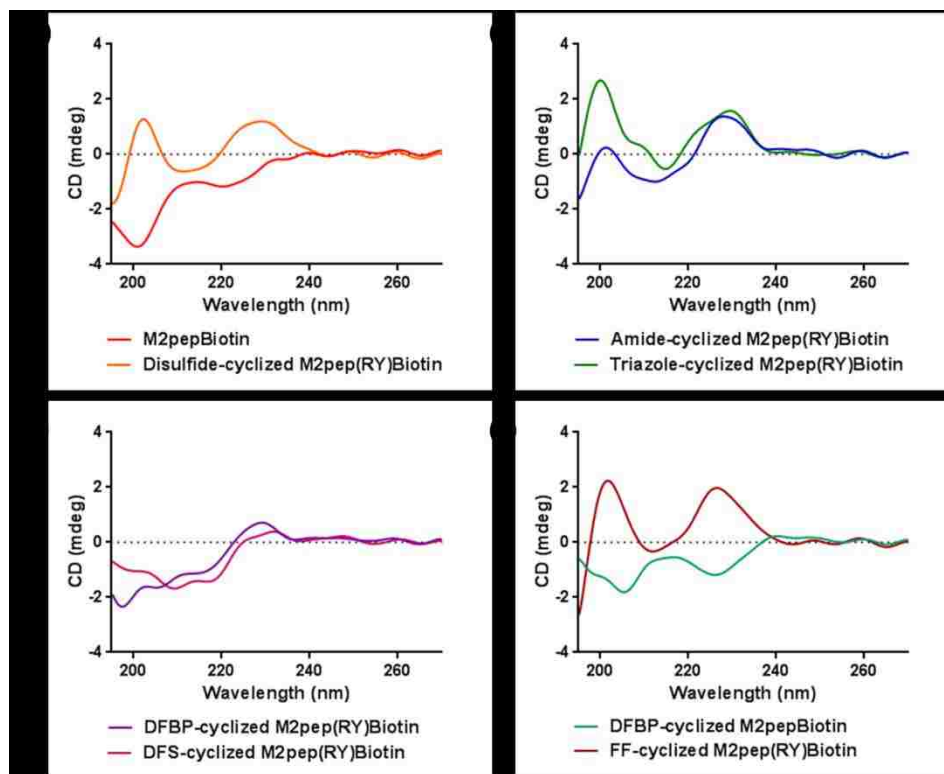


Figure 4.6 CD spectra of (A) M2pepBiotin and Disulfide-cyclized M2pep(RY)Biotin, (B) Amide- and Triazole-cyclized M2pep(RY)Biotin, (C) DFBP- and DFS-cyclized M2pep(RY)Biotin, and (D) DFBP-cyclized M2pepBiotin and FF-cyclized M2pep(RY)Biotin.

4.2.4 *In vitro* serum stability study

The original M2pepBiotin is degraded in mouse serum within 4 h via N-terminal degradation and endolytic cleavages at the W/W site in the binding region and at the S/K site in the spacer region [27]. By replacing L-lysines in the spacer region with D-lysines and cyclizing the binding region of the peptide, we demonstrate significant improvement in serum stability of M2pep [27]. Nonetheless, the cyclized peptide was eventually degraded by prolonged incubation in mouse serum for more than 1 day. Since cyclization of the first generation cyclized M2pep(RY)Biotin was based on a disulfide bridge which may be prone to linearization over time due to changes in the redox environment, we investigated whether the alternative cyclization chemistries can further improve serum stability over disulfide cyclization. Serum stability of the newly-synthesized cyclic M2pep(RY)Biotin peptides were evaluated by incubation in mouse serum and analysis for the presence of peptides at different time points by MALDI-ToF MS. As

observed for Disulfide-cyclized M2pep(RY)Biotin [27], Amide-, Triazole-, and DFBP-cyclized M2pep(RY)Biotin were stable in serum for at least 24 h after which degradation products were observed (Figure 4.7A-C). Multiple attempts to quantify the extent of degradation were unsuccessful due to variability in the amount of extracted peptides following the protein precipitation with ACN, thus preventing quantitative comparisons regarding serum stability. Nonetheless, by identifying the degradation products, it is clear that degradation was initiated at either Y/W or W/Y which corresponds to the W/W site of the original M2pepBiotin. Even though endolytic cleavage at the Y/W/Y site seems to be the rate-determining step towards peptide degradation of cyclic M2pep(RY)Biotin, the new generation analogs are expected to be more favorable than the disulfide-cyclized analog due to insensitivity to reduction. Surprisingly for DFS-cyclized M2pep(RY)Biotin, formation of the “-20 Da” side product was observed over time (Figure 4.7D). This side product was also observed when cyclization reaction with DFS was left for too long (Figure S4.3) but was not observed in the purified peptide stock solution in water, PBS, or PBSA for at least one day (Figure S4.5). Similarly, the Pentelute lab has recently reported an observation on oxidative degradation when DFS is used to cyclize cysteine-containing peptides [24]. The group has also demonstrated superior stability when DFS is instead used to cyclize lysine-containing peptides. Hence, studies by others as well as ours emphasize the need to evaluate any newly developed cyclization chemistries for stability towards physicochemical and physiological stresses such as redox environment and enzymatic degradation. Since we have shown here a higher serum stability of DFBP-cyclized M2pep(RY)Biotin as well as a similar improvement in binding affinity of DFBP- and DFS-cyclized M2pep(RY), it is possible to utilize the DFS-stapled peptide phage library reported by the Derda lab [23] for initial screening of high affinity peptide candidates before synthesizing the peptide with DFBP cyclization for the follow-up evaluation. All in all, different cyclization chemistries as well as robust and flexible synthetic strategies greatly expand our toolbox for peptide optimization that is needed for the development of new effective targeting agents or therapeutics.

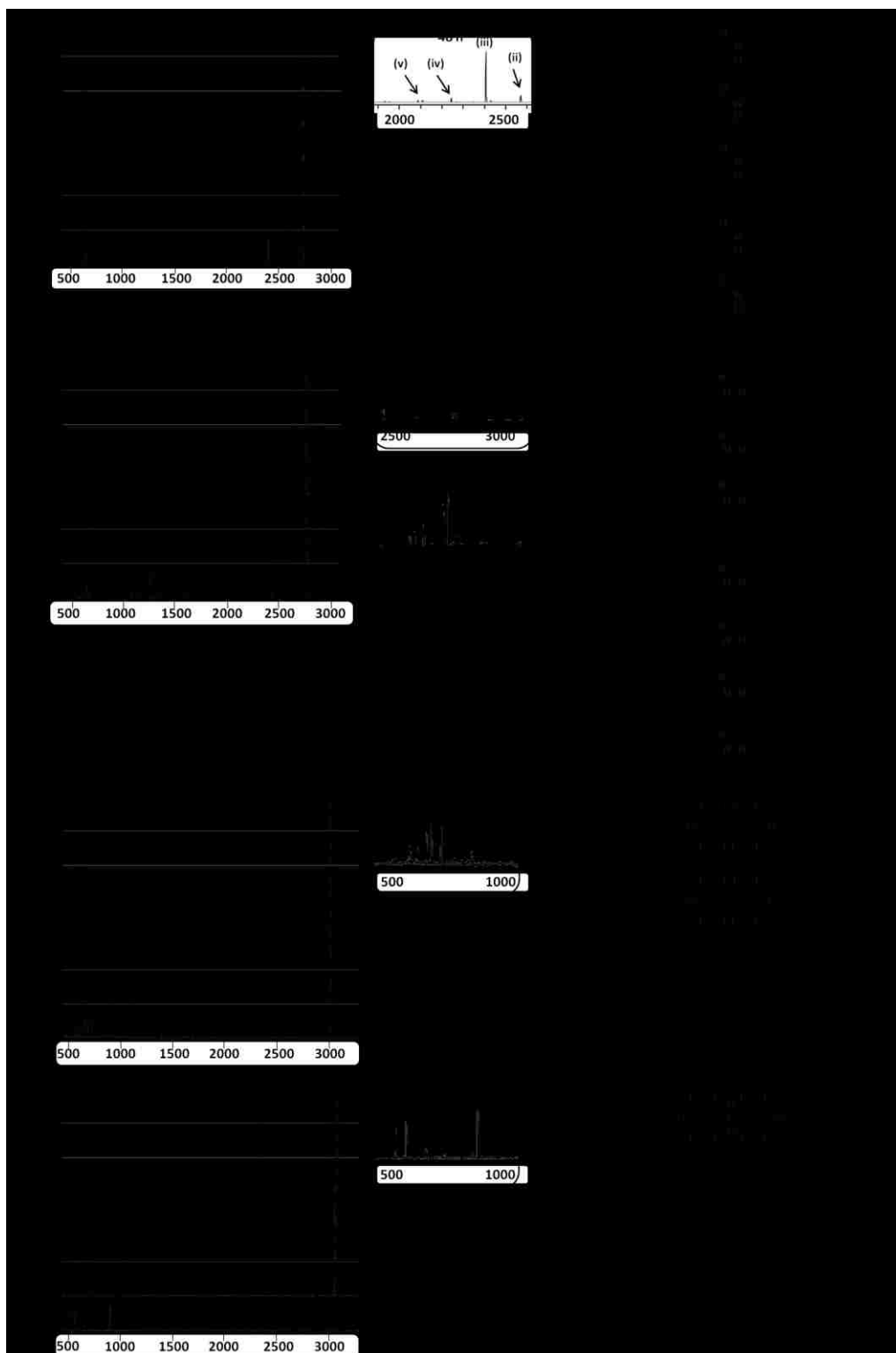


Figure 4.7 Serum stability of (A) Amide-, (B) Triazole-, (C) DFBP-, and (D) DFS-cyclized M2pep(RY)Biotin. Left: MALDI-ToF MS spectra. Middle: Selected enlarged regions of the spectra. Right: Identified degraded peptide fragments.

4.3 Conclusions

We have reported synthesis and evaluation of cyclic M2pep(RY)Biotin analogs with different cyclization chemistries. Our binding studies of these cyclic M2pep(RY)Biotin on macrophages identify DFBP-cyclized M2pep(RY)Biotin as an affinity-enhanced M2 macrophage-binding analog and highlight the possibility of optimizing peptide activity via modulation of cyclization chemistry. The on-resin synthesis strategy of DFBP-cyclized peptide reported here allows for manufacturing scalability, an important consideration in the development of peptide therapeutics.

4.4 Materials and Methods

4.4.1 Materials

Protected amino acids, 2-(6-chloro-1H-benzotriazole-1-yl)-1,1,3,3-tetramethylammonium hexafluorophosphate (HCTU), (benzotriazol-1-yloxy)tripyrrolidinophosphonium hexafluorophosphate (PyBOP), and 1-hydroxybenzotriazole hydrate (HOBt) were purchased from AAPPTec (Louisville, KY), AnaSpec (Fremont, CA), and Chem-Implex International (Wood Dale, IL). Triisopropylsilane (TIPS), 1,2-ethanedithiol (EDT), 1,3-dimethoxybenzene (DMB), tetrakis(triphenylphosphine)palladium(0) (Pd(PPh₃)₄), sodium diethyldithiocarbamate trihydrate, copper(II) sulfate pentahydrate (CuSO₄•5H₂O), and tris(2-carboxyethyl)phosphine hydrochloride (TCEP) were purchased from Sigma-Aldrich (St. Louis, MO). Tris[(1-benzyl-1H-1,2,3-triazol-4-yl)methyl]amine (TBTA) was purchased from TCI America (Portland, OR). Normal mouse serum (Catalog number 10410), phenylsilane, decafluorobiphenyl, and other reagents were purchased from Thermo Fisher Scientific (Waltham, MA). Quant*Tag Biotin quantification kit was purchased from Vector Laboratories (Burlingame, CA). Imidazole-1-sulfonyl azide hydrochloride and decafluorobiphenyl sulfone (DFS) were synthesized following the previously reported protocols [31,32]. For the synthesis of DFS, an additional purification step was performed by dissolving the partially purified light yellow product in DMF and precipitating in H₂O twice before lyophilizing to obtain the product as white powder.

4.4.2 Synthesis of biotinylated M2pep analogs

4.4.2.1 General peptide synthesis strategy

Peptides were synthesized using a PS3 automated peptide synthesizer (Protein Technologies, Phoenix, AZ) via standard Fmoc/tbu solid-phase peptide synthesis unless noted in Table 4.1. Manual coupling of amino acids was performed by incubating the peptide resin in a solution of amino acid (4 eq.) and HCTU (3.9 eq.) in 0.4 M N-methylmorpholine in DMF for 3 h. Fmoc deprotection was performed by two 30-min incubations in 20% (v/v) piperidine in DMF. Biotinylated resin was prepared from NovaPEG rink amide resin as reported previously [27] and was used for the synthesis of all biotinylated peptides. Peptides were cleaved off the resin by incubating in a cleavage cocktail containing TFA/DMB/TIPS/EDT (90:5:2.5:2.5 v/v/v/v) for 2.5 h followed by double precipitation in cold ether. EDT was included in the cleavage cocktail only for peptides containing a free cysteine after cleavage. The crude peptides were purified by RP-HPLC (Agilent 1200, Santa Clara, CA) to 95% purity using a Phenomenex Fusion-RP C18 semi-preparative column (Torrance, CA) at the flow rate of 5 mL/min with H₂O (0.1% TFA) and ACN (0.1% TFA) as a mobile phase. Molecular weights of the purified peptides were confirmed by MALDI-ToF Mass Spectrometry (MS).

Table 4.1 Protected amino acids used for cyclization

Linear precursor: X₁GYEQDPWGVRYWYGX₂kkk(K-Biotin)

M2pep analogs	Protected X ₁	Protected X ₂
Disulfide-cyclized M2pep(RY)Biotin	Fmoc-Cys(tbu)-OH	Fmoc-Cys(tbu)-OH
Amide-cyclized M2pep(RY)Biotin	Fmoc-Asp(OAll)-OH	Fmoc-Lys(Alloc)-OH
Triazole-cyclized M2pep(RY)Biotin	Boc-Lys(Fmoc)-OH	Fmoc-Propargyl-Gly-OH
DFBP-cyclized M2pep(RY)Biotin	Fmoc-Cys(Stbu)-OH	Fmoc-Cys(Mmt)-OH
DFS-cyclized M2pep(RY)Biotin	Fmoc-Cys(tbu)-OH	Fmoc-Cys(tbu)-OH

4.4.2.2 Disulfide-cyclized M2pep(RY)Biotin

The purified linear precursor (10-20 mg) was dissolved in H₂O (1-3 mL) and added to a deaerated 0.1 M ammonium bicarbonate buffer (pH 8) at a final peptide concentration of 0.14 mg/mL. The solution was left to stir for 2 days for oxidation, then acidified with TFA and desalted with a HyperSep™ C18 cartridge. The desalted cyclized peptide was concentrated with rotary evaporator and lyophilized.

4.4.2.3 Amide-cyclized M2pep(RY)Biotin

The N-terminus-Fmoc-protected precursor peptide on resin was incubated in a solution of Pd(PPh₃)₄ (0.2 eq.) and phenylsilane (20 eq.) in DCM for 20 min twice to selectively deprotect OAll and Alloc protecting groups. The resin in the deprotection solution was purged with nitrogen for 5 min prior to each incubation. Following deprotection, the resin was washed with 5 mM sodium diethyldithiocarbamate solution in DMF to remove the palladium catalyst. On-resin lactamization follows the optimized protocol by Thakkar *et al.* [33] by incubating the resin in a solution of HOBt (5 eq.), PyBOP (5 eq.), and DIPEA (10 eq.) in DCM/DMF/MNP (3:2:2 v/v/v) with 1% (v/v) triton X100 for 24 h. A small amount of peptide on resin was cleaved to monitor for completion of the cyclization via MALDI-ToF MS. Upon completion, the cyclized peptide was Fmoc-deprotected, cleaved, and purified by RP-HPLC.

4.4.2.4 Triazole-cyclized M2pep(RY)Biotin

The epsilon amine on the N-terminal lysine of the precursor peptide on resin was Fmoc-deprotected and converted to azide by an overnight incubation in a solution of imidazole-1-sulfonyl azide hydrochloride (3 eq.), CuSO₄•5H₂O (0.01 eq. pre-dissolved in a small amount of H₂O), and DIPEA (9 eq.) in DMSO as reported previously [34]. The completion of the diazotransfer reaction was monitored by the Kaiser test for the absence of amine. Alternatively, Fmoc-Lys(N₃)-OH may be used instead of Boc-Lys(Fmoc)-OH. On-resin CuAAC cyclization was performed by incubating the peptide resin in a solution of tetrakis(acetonitrile)copper(I) hexafluorophosphate (1 eq.), TBTA (1 eq.), and DIPEA (2 eq.) in DMF for 24 h. The resin was then washed with 5 mM sodium diethyldithiocarbamate solution in DMF, and the cyclized peptide was cleaved and purified by RP-HPLC.

4.4.2.5 DFBP-cyclized M2pep(RY)Biotin

In-solution cyclization of the linear peptide precursor with DFBP follows the previously described protocol [22] modified with an addition of TCEP to suppress disulfide formation during DFBP cyclization. In brief, the crude peptide precursor (20 mg) was dissolved in DMF (2.5 mL) in a 5-mL microcentrifuge tube. A fresh TCEP stock solution in H₂O (5 eq.) was added to the peptide solution, and an additional volume of H₂O was added to make up a total H₂O volume of 0.5 mL. The reaction was left for 10 min followed by an addition of 50 mM tris base in DMF (1.5 mL). DFBP predissolved in DMF (2 eq.) was then added, and the reaction was vortexed vigorously. On the next day, the reaction was diluted with 3-fold volume of H₂O (0.1% TFA) and desalted with a Sep-Pak C18 cartridge. The desalted cyclized peptide solution was concentrated and purified by RP-HPLC.

On-resin cyclization of DFBP utilizes two cysteines with orthogonal protecting groups (Table 4.1). First, the Stbu protecting group was deprotected by an overnight incubation in a solution of DTT (10 eq.) and TEA (20 eq.) in DMF. The free cysteine was functionalized by incubating in a solution of DFBP (4 eq.) and TEA (8 eq.) in DMF for 3 h. Mmt protecting group was then removed by 20-min incubations in TFA/TIPS/DCM (2:5:93 v/v/v) until yellow-colored solution disappeared (3-4 incubations). The DFBP cyclization was then proceeded by incubating the peptide resin in a TEA solution (8 eq.) in DMF for 24 h. The cyclized peptide was cleaved and purified by RP-HPLC. All deprotection and DFBP functionalization steps were monitored by the modified on-resin Ellman's assay following the previously reported protocol [35].

4.4.2.6 DFS-cyclized M2pep(RY)Biotin

In-solution cyclization of the linear peptide precursor with DFS was performed as described for DFBP cyclization with an exception that the reaction was quenched by an addition of 3-fold volume of H₂O (0.1% TFA) after a 10-min incubation to prevent formation of a side product.

4.4.3 Bone marrow harvest and macrophage culture

All animal handling protocols were approved by the University of Washington Institutional Animal Care and Use Committee. Bone marrow-derived cells were harvested from female c57bl/6 mice as previously described [36]. In brief, femurs and tibias of the mice were

excised and flushed with RPMI 1640 medium via an 18G needle. The cells were cultured on petri dishes containing RPMI 1640 medium supplemented with 20% donor horse serum, 1% antibiotic-antimycotic (AbAm), and 20 ng/mL M-CSF. After 7 d in culture, the medium was replaced with an activation medium whereby M-CSF was replaced with 25 ng/mL IFN- γ and 100 ng/mL LPS for M1 activation or with 25 ng/mL IL-4 for M2 activation. For M1 activation medium, AbAm was replaced with 1% penicillin-streptomycin (Pen-Strep). After 2 d of activation, the activated macrophages were scraped off the petri dishes for binding studies.

4.4.4 In vitro binding study

Biotinylated peptide stock solutions were prepared in H₂O at 10 mg/mL concentration and quantified for the exact concentration using Quant*Tag Biotin quantification kit. The stock solutions were diluted in PBS with 1% BSA (PBSA) to different concentrations for binding studies. Activated macrophages were seeded on a black 96-well plate (50,000 cells/well) and incubated with the peptide solutions for 20 min on ice. The cells were washed twice with PBSA and subsequently incubated with streptavidin-FITC for 15 min on ice. After two additional washes, the cells were resuspended in PBS for analysis via MACSQuant Flow Cytometer (Miltenyi Biotec, San Diego, CA). Propidium iodide (PI) was added before running each sample to assess for cell viability. Data analysis was processed on FlowJo Analysis Software (Tree Star, Ashland, OR). Construction of binding curves and determination of apparent K_D were performed using GraphPad Prism 6 (GraphPad Software Inc., La Jolla, CA) based on an average normalized median fluorescence intensity value of triplicate samples in the same experiment.

4.4.5 CD measurement

M2pep analogs were prepared in H₂O at 50 μ M concentration. CD measurement of the peptides was performed on Jasco 720 Circular Dichroism Spectrophotometer (Jasco Inc., Easton, MD) at 25 °C with an average from 8 scans. The CD spectra were corrected for baseline and smoothed on Spectra Manager Software (Jasco Inc., Easton, MD).

4.4.6 In vitro serum stability study

Different M2pep analogs (30 μ L from 10 mg/mL stock solution in H₂O) were incubated in normal mouse serum (300 μ L) at 37 °C in an incubator. An aliquot of the serum (40 μ L) was

drawn at different time intervals and precipitated with an equal volume of cold ACN. The mixture was centrifuged at 15,000 rpm for 5 min, and the supernatant was collected. A solution of H₂O/ACN (1:1 v/v, 80 μ L) was added to the pellet with a 10-min sonication to further extract residual peptides. The mixture was then centrifuged. The supernatant was pooled with the former and dried under vacuum on a Speedvac machine. The peptide pellet was resuspended in H₂O (50 μ L) with a 10-min sonication before analysis by MALDI-ToF MS.

4.5 Acknowledgments

This work was supported by NIH 1R01CA177272. Chayanon Ngambenjwong was supported by an Anandamahidol Foundation Fellowship. Julio Marco B. Pineda was supported by a Mary Gates Research Scholarship. We thank Professor Niels H. Anderson and Kalkena Sivanesam for consultation on interpretation of the CD spectra.

4.6 References

- [1] C. Falciani, L. Lozzi, A. Pini, L. Bracci, Bioactive Peptides from Libraries, *Chem. Biol.* 12 (2005) 417–426. doi:http://dx.doi.org/10.1016/j.chembiol.2005.02.009.
- [2] Y. Kliger, Computational approaches to therapeutic peptide discovery., *Biopolymers.* 94 (2010) 701–710. doi:10.1002/bip.21458.
- [3] X.-X. Zhang, H.S. Eden, X. Chen, Peptides in cancer nanomedicine: drug carriers, targeting ligands and protease substrates., *J. Control. Release.* 159 (2012) 2–13. doi:10.1016/j.jconrel.2011.10.023.
- [4] P. Vlieghe, V. Lisowski, J. Martinez, M. Khrestchatsky, Synthetic therapeutic peptides: science and market, *Drug Discov. Today.* 15 (2010) 40–56. doi:http://dx.doi.org/10.1016/j.drudis.2009.10.009.
- [5] F. Nilsson, L. Tarli, F. Viti, D. Neri, The use of phage display for the development of tumour targeting agents, *Adv. Drug Deliv. Rev.* 43 (2000) 165–196. doi:http://dx.doi.org/10.1016/S0169-409X(00)00068-5.
- [6] K.C. Brown, Peptidic tumor targeting agents: the road from phage display peptide selections to clinical applications., *Curr. Pharm. Des.* 16 (2010) 1040–1054.
- [7] A.F. Kolodziej, Z. Zhang, K. Overoye-Chan, V. Jacques, P. Caravan, Peptide optimization and conjugation strategies in the development of molecularly targeted magnetic resonance imaging contrast agents., *Methods Mol. Biol.* 1088 (2014) 185–211. doi:10.1007/978-1-62703-673-3_13.
- [8] M.D. Boersma, J.D. Sadowsky, Y.A. Tomita, S.H. Gellman, Hydrophile scanning as a

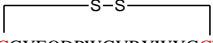
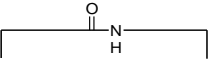
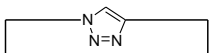
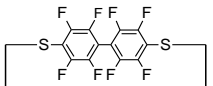
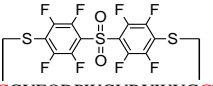
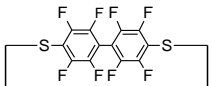
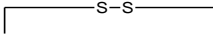
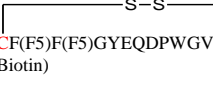
- complement to alanine scanning for exploring and manipulating protein-protein recognition: application to the Bim BH3 domain., *Protein Sci.* 17 (2008) 1232–1240. doi:10.1110/ps.032896.107.
- [9] T. Hatanaka, S. Ohzono, M. Park, K. Sakamoto, S. Tsukamoto, R. Sugita, et al., Human IgA-binding peptides selected from random peptide libraries: affinity maturation and application in IgA purification., *J. Biol. Chem.* 287 (2012) 43126–43136. doi:10.1074/jbc.M112.389742.
- [10] B.M. Larimer, W.D. Thomas, G.P. Smith, S.L. Deutscher, Affinity maturation of an ERBB2-targeted SPECT imaging peptide by in vivo phage display., *Mol. Imaging Biol. MIB Off. Publ. Acad. Mol. Imaging.* 16 (2014) 449–458. doi:10.1007/s11307-014-0724-5.
- [11] B. Santoso, B.W. Murray, Maleimide-based method for elaboration of cysteine-containing peptide phage libraries., *Methods Mol. Biol.* 1248 (2015) 267–276. doi:10.1007/978-1-4939-2020-4_18.
- [12] S. Chen, D. Gfeller, S.A. Buth, O. Michielin, P.G. Leiman, C. Heinis, Improving binding affinity and stability of peptide ligands by substituting glycines with D-amino acids., *Chembiochem.* 14 (2013) 1316–1322. doi:10.1002/cbic.201300228.
- [13] I.E. Valverde, A. Bauman, C.A. Kluba, S. Vomstein, M.A. Walter, T.L. Mindt, 1,2,3-Triazoles as amide bond mimics: triazole scan yields protease-resistant peptidomimetics for tumor targeting., *Angew. Chem. Int. Ed. Engl.* 52 (2013) 8957–8960. doi:10.1002/anie.201303108.
- [14] K.S. Harris, J.L. Casey, A.M. Coley, J.A. Karas, J.K. Sabo, Y.Y. Tan, et al., Rapid optimization of a peptide inhibitor of malaria parasite invasion by comprehensive N-methyl scanning., *J. Biol. Chem.* 284 (2009) 9361–9371. doi:10.1074/jbc.M808762200.
- [15] T.A. Hilimire, R.P. Bennett, R.A. Stewart, P. Garcia-Miranda, A. Blume, J. Becker, et al., N-Methylation as a Strategy for Enhancing the Affinity and Selectivity of RNA-binding Peptides: Application to the HIV-1 Frameshift-Stimulating RNA., *ACS Chem. Biol.* 11 (2016) 88–94. doi:10.1021/acscchembio.5b00682.
- [16] M. Goldflam, C.G. Ullman, Recent Advances Toward the Discovery of Drug-Like Peptides De novo, *Front. Chem.* 3 (2015) 69. doi:10.3389/fchem.2015.00069.
- [17] L.D. Walensky, G.H. Bird, Hydrocarbon-Stapled Peptides: Principles, Practice, and Progress, *J. Med. Chem.* 57 (2014) 6275–6288. doi:10.1021/jm4011675.
- [18] C.J. White, A.K. Yudin, Contemporary strategies for peptide macrocyclization, *Nat Chem.* 3 (2011) 509–524. <http://dx.doi.org/10.1038/nchem.1062>.
- [19] Y.H. Lau, P. de Andrade, Y. Wu, D.R. Spring, Peptide stapling techniques based on different macrocyclisation chemistries, *Chem. Soc. Rev.* 44 (2015) 91–102. doi:10.1039/C4CS00246F.
- [20] M. V Trivedi, J.S. Laurence, T.J. Siahaan, The role of thiols and disulfides in protein

- chemical and physical stability, *Curr. Protein Pept. Sci.* 10 (2009) 614–625. <http://www.ncbi.nlm.nih.gov/pmc/articles/PMC3319691/>.
- [21] P.M. Cromm, S. Schaubach, J. Spiegel, A. Furstner, T.N. Grossmann, H. Waldmann, Orthogonal ring-closing alkyne and olefin metathesis for the synthesis of small GTPase-targeting bicyclic peptides, *Nat Commun.* 7 (2016). <http://dx.doi.org/10.1038/ncomms11300>.
- [22] A.M. Spokoyny, Y. Zou, J.J. Ling, H. Yu, Y.-S. Lin, B.L. Pentelute, A Perfluoroaryl-Cysteine SNAr Chemistry Approach to Unprotected Peptide Stapling, *J. Am. Chem. Soc.* 135 (2013) 5946–5949. doi:10.1021/ja400119t.
- [23] S. Kalhor-Monfared, M.R. Jafari, J.T. Patterson, P.I. Kitov, J.J. Dwyer, J.M. Nuss, et al., Rapid biocompatible macrocyclization of peptides with decafluoro-diphenylsulfone, *Chem. Sci.* 7 (2016) 3785–3790. doi:10.1039/C5SC03856A.
- [24] G. Lautrette, F. Touti, H.G. Lee, P. Dai, B.L. Pentelute, Nitrogen Arylation for Macrocyclization of Unprotected Peptides., *J. Am. Chem. Soc.* 138 (2016) 8340–8343. doi:10.1021/jacs.6b03757.
- [25] A. Oddo, T.T. Thomsen, H.M. Britt, A. Løbner-Olesen, P.W. Thulstrup, J.M. Sanderson, et al., Modulation of Backbone Flexibility for Effective Dissociation of Antibacterial and Hemolytic Activity in Cyclic Peptides, *ACS Med. Chem. Lett.* (2016). doi:10.1021/acsmchemlett.5b00400.
- [26] M. Cieslewicz, J. Tang, J.L. Yu, H. Cao, M. Zavaljevski, K. Motoyama, et al., Targeted delivery of proapoptotic peptides to tumor-associated macrophages improves survival., *Proc. Natl. Acad. Sci. U. S. A.* 110 (2013) 15919–15924. doi:10.1073/pnas.1312197110.
- [27] C. Ngambenjawong, H.H. Gustafson, J.M. Pineda, N.A. Kacherovsky, M. Cieslewicz, S.H. Pun, Serum Stability and Affinity Optimization of an M2 Macrophage-Targeting Peptide (M2pep), *Theranostics.* 6 (2016) 1403–1414. doi:10.7150/thno.15394.
- [28] C.R. Lohani, B. Rasera, B. Scott, M. Palmer, S.D. Taylor, α -Azido Acids in Solid-Phase Peptide Synthesis: Compatibility with Fmoc Chemistry and an Alternative Approach to the Solid Phase Synthesis of Daptomycin Analogs, *J. Org. Chem.* 81 (2016) 2624–2628. doi:10.1021/acs.joc.5b02882.
- [29] M. Pelay-Gimeno, A. Glas, O. Koch, T.N. Grossmann, Structure-Based Design of Inhibitors of Protein-Protein Interactions: Mimicking Peptide Binding Epitopes., *Angew. Chem. Int. Ed. Engl.* 54 (2015) 8896–8927. doi:10.1002/anie.201412070.
- [30] N. Greenfield, G.D. Fasman, Computed circular dichroism spectra for the evaluation of protein conformation., *Biochemistry.* 8 (1969) 4108–4116.
- [31] E.D. Goddard-Borger, R. V Stick, An efficient, inexpensive, and shelf-stable diazotransfer reagent: imidazole-1-sulfonyl azide hydrochloride., *Org. Lett.* 9 (2007) 3797–3800. doi:10.1021/ol701581g.
- [32] L. Xu, J. Cheng, M.L. Trudell, Chromium(VI) Oxide Catalyzed Oxidation of Sulfides to

- Sulfones with Periodic Acid, *J. Org. Chem.* 68 (2003) 5388–5391. doi:10.1021/jo030031n.
- [33] A. Thakkar, T.B. Trinh, D. Pei, Global Analysis of Peptide Cyclization Efficiency, *ACS Comb. Sci.* 15 (2013) 120–129. doi:10.1021/co300136j.
- [34] V. Castro, J.B. Blanco-Canosa, H. Rodriguez, F. Albericio, Imidazole-1-sulfonyl Azide-Based Diazo-Transfer Reaction for the Preparation of Azido Solid Supports for Solid-Phase Synthesis, *ACS Comb. Sci.* 15 (2013) 331–334. doi:10.1021/co4000437.
- [35] J.P. Badyal, A.M. Cameron, N.R. Cameron, D.M. Coe, R. Cox, B.G. Davis, et al., A simple method for the quantitative analysis of resin bound thiol groups, *Tetrahedron Lett.* 42 (2001) 8531–8533. doi:http://dx.doi.org/10.1016/S0040-4039(01)01820-2.
- [36] J. Weischenfeldt, B. Porse, Bone Marrow-Derived Macrophages (BMM): Isolation and Applications., *CSH Protoc.* 2008 (2008) pdb.prot5080.

4.7 Supplementary information

Table S4.1 Molecular weights of the synthesized peptides

Name	Sequence	Mw (Calculated)	Mw (Observed)	Note
M2pepBiotin	YEQDPWGVKWWYGGGSKK(K-Biotin)	2,524.86	2,524.21	Original sequence
Disulfide-cyclized M2pep(RY)Biotin	 CGYEQDPWGVRYWYGCkkk(K-Biotin)	2,718.16	2,717.75	
Amide-cyclized M2pep(RY)Biotin	 DGYEQDPWGVRYWYGCkkk(K-Biotin)	2,739.13	2,739.78	
Triazole-cyclized M2pep(RY)Biotin	 X ₁ GYEQDPWGVRYWYGX ₂ kkk(K-Biotin)	2,762.97	2,763.02	X ₁ = azidolysine X ₂ = propargylglycine
DFBP-cyclized M2pep(RY)Biotin	 CGYEQDPWGVRYWYGCkkk(K-Biotin)	3,014.28	3,014.58	
DFS-cyclized M2pep(RY)Biotin	 CGYEQDPWGVRYWYGCkkk(K-Biotin)	3,078.34	3,078.75	
DFBP-cyclized M2pepBiotin	 CGYEQDPWGVKWWYGCkkk(K-Biotin)	3,009.31	3,010.29	
FF-cyclized M2pep(RY)Biotin	 CFFGYEQDPWGVRYWYGCkkk(K-Biotin)	3,012.52	3,011.63	
F(F5)F(F5)-cyclized M2pep(RY)Biotin	 CF(F5)F(F5)GYEQDPWGVRYWYGCkkk(K-Biotin)	3,192.49	3,192.64	F(F5) = pentafluorophenylalanine
(C-DFBP)(GR) ₃ -Biotin	Biotin-Ahx-GRGRGRG(C-DFBP)G	1,527.55	1,527.47	Ahx = 6-aminohexanoic acid
CC-M2pep(RY)Azide	CGYEQDPWGVRYWYGCkkk(K-N ₃)	2,519.87	2,519.44	See Figure S4.2

Peptide sequences are written from N-terminus to C-terminus.

All peptides are amidated at the C terminus. Small letters denote D-amino acids.

Amino acid residues involved in cyclization are in red.

Mw observed from MALDI-TOF MS is reported as [M+H]⁺.

Figure S4.1 On-resin synthesis schematics, representative HPLC purification traces, and methods of (A) Amide-, (B) Triazole-, and (C) DFBP-cyclized M2pep(RY)Biotin. HPLC purification was performed using a Phenomenex Fusion-RP C18 semi-preparative column (Torrance, CA) at the flow rate of 5 mL/min with H₂O (0.1% TFA) and ACN (0.1% TFA) as a mobile phase. Yields for all peptides are about 10-13 mg per 0.1 mmol scale synthesis.

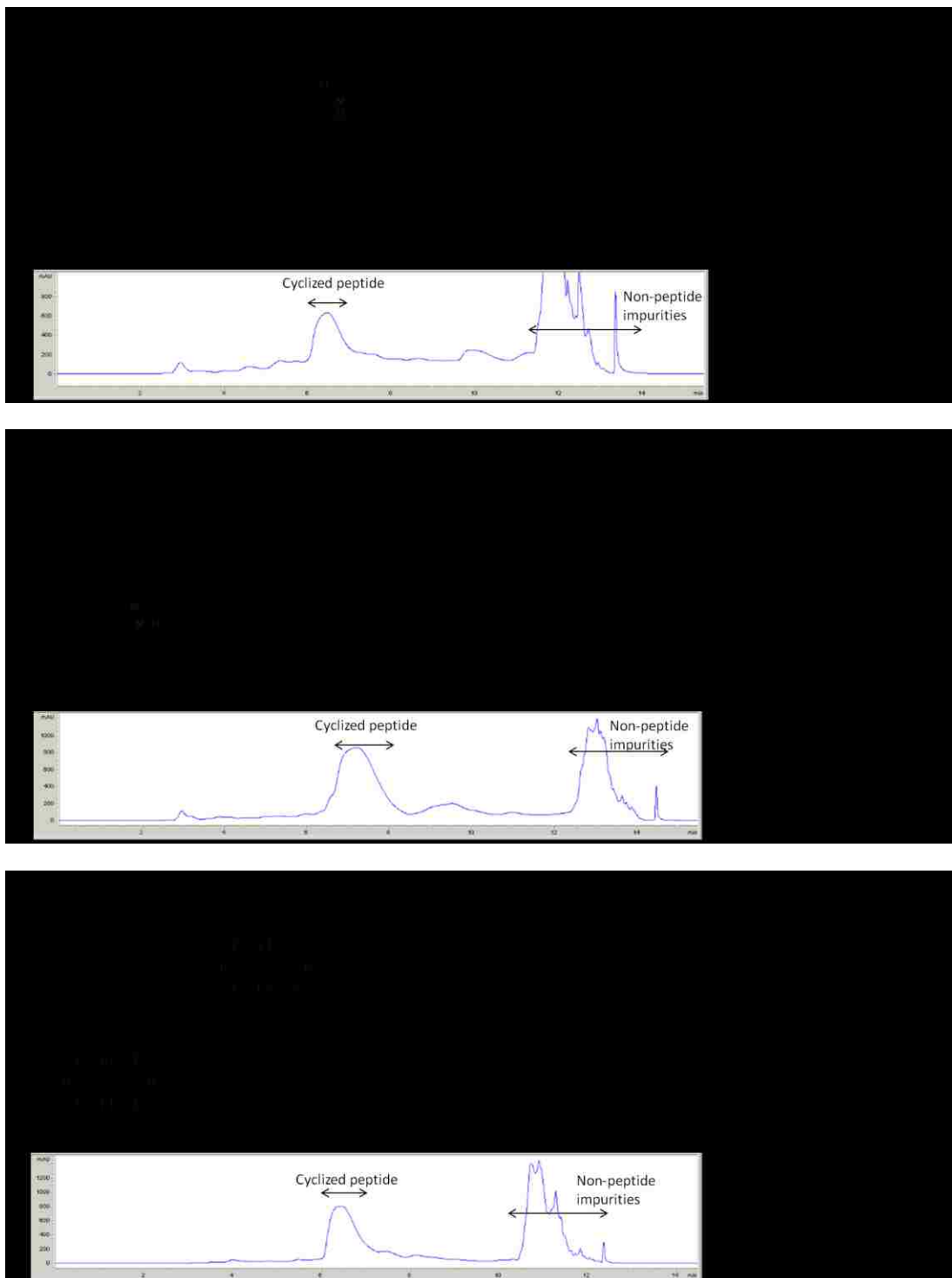


Figure S4.2 Confirmation of successful CuAAC reaction of Triazole-cyclized M2pep(RY)Biotin by (A) TCEP-mediated reduction of azide and (B) CuAAC reaction with propargyl alcohol.



Figure S4.3 (A) Unsuccessful attempt on on-resin synthesis of DFS-cyclized M2pep(RY)Biotin following the on-resin synthesis protocol developed for DFBP-cyclized M2pep(RY)Biotin. “-346 Da” side product is a major peak observed by MALDI-ToF MS. (B) Optimization of in-solution cyclization of DFS-cyclized M2pep(RY)Biotin varying reaction time and with TCEP addition. Left: HPLC traces of each reaction condition. Right: Their corresponding MALDI-ToF MS spectra.

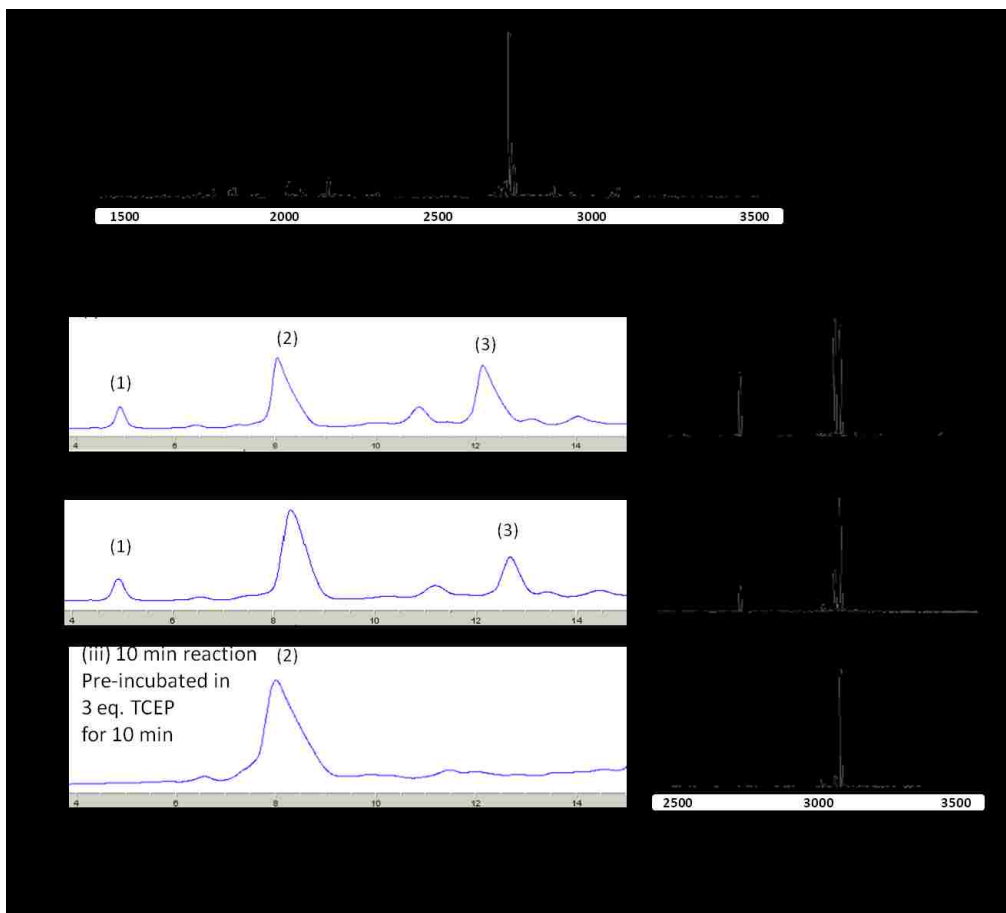


Figure S4.4 Cell viability of (A) DFBP-, (B) FF-, and (C) F(F5)F(F5)-cyclized M2pep(RY)Biotin on M2 (left) and M1 (right) macrophages during binding studies.

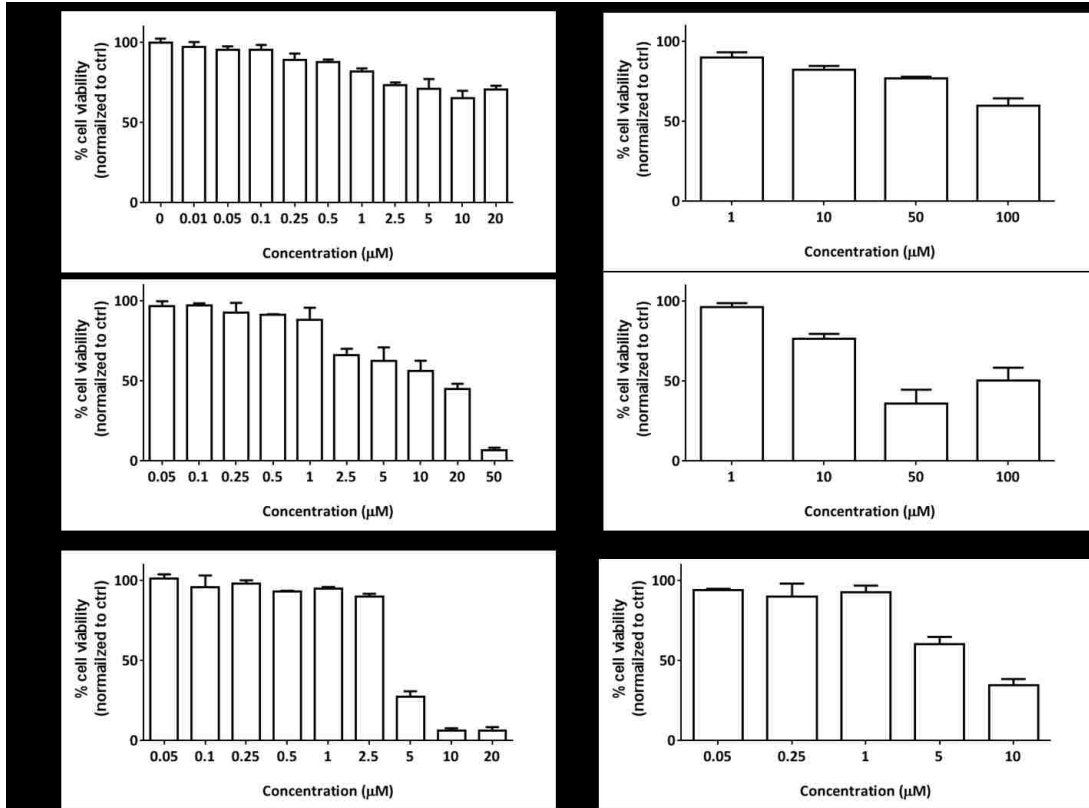
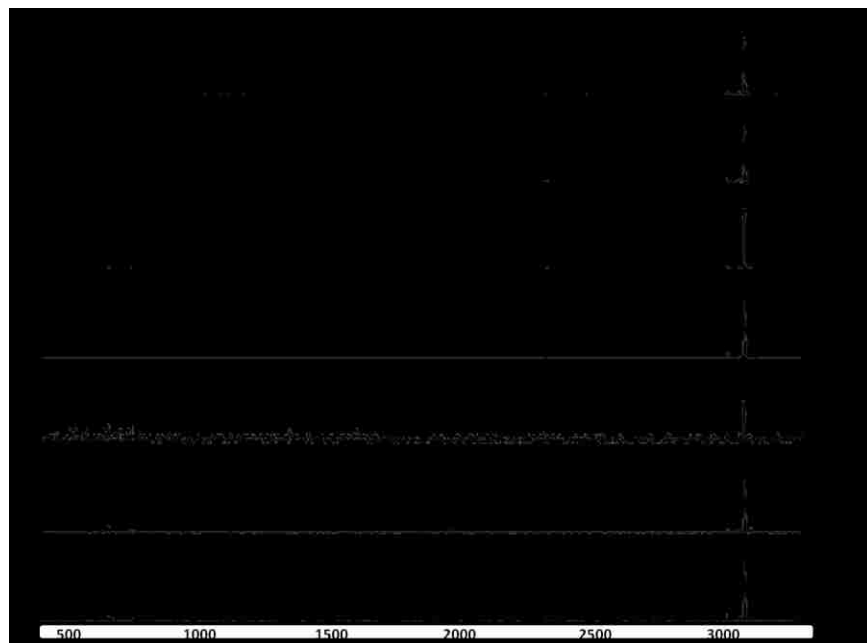


Figure S4.5 Stability of DFS-cyclized M2pep(RY)Biotin in water, PBS, PBS with 1% BSA (PBBSA), and PBS/ACN.



Chapter 5

**REVERSIBLY-SWITCHABLE pH-DEPENDENT PEPTIDE LIGAND BINDING
VIA 3,5-DIIODOTYROSINE SUBSTITUTIONS**

Chayanon Ngambenjawong, Julio M. Pineda, Suzie H. Pun

Abstract

Cell type-specific targeting ligands utilized in drug delivery applications typically recognize receptors that are overexpressed on the cells of interest. Nonetheless, these receptors may also be expressed, to varying extent, on off-target cells contributing to unintended side effects. To improve the selectivity profile of targeting ligands in cancer therapy, stimuli-responsive masking of these ligands with acid-, redox-, or enzyme-cleavable molecules has been reported whereby the targeting ligands are exposed in specific environments, e.g. acidic tumor hypoxia. One possible drawback of these systems lies in their one-time, permanent trigger which enables the “de-masked” ligands to bind off-target cells if released back into the systemic circulation. A promising strategy to address the aforementioned problem is to design ligands that show selective binding based on ionization state, which may be microenvironment-dependent. In this study, we report a systematic strategy to engineer low pH-selective targeting peptides using an M2 macrophage-targeting peptide (M2pep) as an example. 3,5-Diiodotyrosine mutagenesis into native tyrosine residues of M2pep confers pH-dependent binding behavior specific to acidic environment (pH 6) when the amino acid is protonated into the native tyrosine-like state. At physiological pH of 7.4, the hydroxyl group of 3,5-diiodotyrosine on the peptide is deprotonated leading to interruption of the peptide native binding property. Our engineered pH-responsive M2pep (Ac-Y-Î-Î) binds target M2 macrophages more selectively at pH 6 than at pH 7.4. In addition, 3,5-diiodotyrosine substitutions also improve serum stability of the peptide. Finally, we demonstrate pH-dependent reversibility in target binding via a post-binding peptide elution study. The strategy presented here should be applicable for engineering pH-dependent functionality of other targeting peptides with potential applications in physiology-dependent *in vivo* targeting applications (e.g. targeting hypoxic tumor/inflammation) or in *in vitro* receptor identification.⁵

⁵ Manuscript in preparation for submission

5.1 Introduction

Targeting ligands are an important feature of macromolecular drug delivery carriers because biologics such as proteins or nucleic acids are too big for passive diffusion through plasma membrane and rely on receptor-mediated endocytosis for internalization[1–3]. As a result, preferential drug delivery to desired cells can also be achieved by modifying delivery formulations with targeting ligands that recognize receptors expressed on the cells of interest [4]. In an effort to develop targeted drug delivery therapeutics for different diseases, a plethora of research has been carried out by many research groups to identify targeting ligands for a diverse array of target biomolecules or cell types [1,2].

A significant challenge in development of targeted drug delivery carriers for cancer applications is the paucity of truly unique receptors for the target cells. Several tumor-targeting strategies utilize ligands for growth factor receptors (e.g. epidermal growth factor receptor (EGFR) and human epidermal growth factor receptor 2 (HER2)), folate/transferrin receptors, or RGD-binding integrins [5–8]. Since these receptors are over-, but not exclusively, expressed on cancer cells, unintended binding could occur on non-cancer cells [7,9,10]. Further complicating the design consideration, a dilemma exists where tumor heterogeneity and/or receptor shedding compromise targeting efficiency of very tumor-specific ligands whereas utilization of ligands recognizing more ubiquitously expressed receptors may incur greater off-target side effects [11–13]. The latter may also be exacerbated by increased avidity when presented on drug carriers in a multivalent fashion. Thus, careful selection of ligands is paramount to successful design of effective targeted drug delivery systems [1,4].

Inspired from development of stimuli-responsive prodrugs such as those activated upon encounter of enzymes, reactive oxygen species, or acidic/reductive environment, the same design principle has been employed by several research groups to improve selectivity of targeting ligands. As an example, Zhu et al. has reported development of mannose-modified nanoparticles for targeting tumor-promoting, tumor-associated macrophages (TAMs) where selectivity over liver-resident Kupffer cells and splenic macrophages, also expressing mannose receptors, was enhanced by masking the nanoparticles with poly(ethylene glycol) (PEG) that can be cleaved off in the acidic tumor microenvironment [14]. Alternatively, Liu et al. utilized a legumain-specific substrate (peptide sequence alanine-alanine-asparagine or AAN) to mask cell-penetrating property of TAT peptide, the activity of which was restored upon encounter with cancer cells and

TAMs overexpressing catalytically active, plasma membrane-exposed legumain [15]. Although target selectivity is promoted in these stimuli-activated targeting systems, one potential drawback lies in their nature of one-time activation which may allow for off-target binding once the “de-masked” ligand-decorated carriers transport back into systemic circulation.

One potential strategy to obtain reversibly-activated targeting ligands is to develop pH-sensitive peptides that bind to their target based on their ionization state. With regard to biological applications in cancer, we hypothesized that acidic tumor microenvironment-selective targeting peptides could be engineered by replacing their critical binding residues with histidine (imidazole pKa ~ 6) and/or 3,5-diiodotyrosine (phenolic pKa ~ 6.5 [16]). Specifically, if the targeting peptides contain basic residues (lysine/arginine) whose cationic charges are involved in electrostatic interaction with negatively charged residues on their receptors, their corresponding substitution(s) with histidine could confer tumor microenvironment (low pH)-selective protonation of the substituted amino acids and, hence, restoration of target binding activity only in such microenvironment (Figure 5.1A). Similarly, if the targeting peptides contain tyrosine residues whose hydroxyl groups are required for engagement with its receptor (e.g. through hydrogen bonding), their corresponding substitution(s) with 3,5-diiodotyrosine could confer an analogous pH-responsive binding behavior (Figure 5.1B).

As a proof of feasibility, we investigate, in this study, the effect of histidine and 3,5-diiodotyrosine substitution(s) in an M2 macrophage-targeting peptide (M2pep) on pH-dependent binding activity [17]. M2pep peptide has been previously shown to bind to M2 macrophages and M2-like TAMs where the latter are also known to preferentially localize in the low pH, hypoxic region of tumor [17–20]. In addition, the peptide contains a known lysine essential for target binding as well as multiple tyrosine residues allowing for systematic substitution(s) and investigation [18]. Specific to M2pep, we found that appropriate substitutions of tyrosine with 3,5-diiodotyrosine resulted in desirable low pH-selective binding activity of the engineered M2pep to target M2 macrophages. Since M2-like TAMs are a known target for cancer immunotherapy owing to their tumor-promoting roles (e.g. stimulation of cancer cell proliferation, immunosuppression, as well as promotion of angiogenesis and metastasis) as opposed to M1-like TAMs which possess tumoricidal functions [21], the low pH-responsive M2pep reported here could be of translational significance in development of M2-like TAM-

targeted drug delivery systems. Further complementing M2-to-M1 selectivity of the original M2pep, a second layer of selectivity is encoded into the new peptide based on low pH activation.

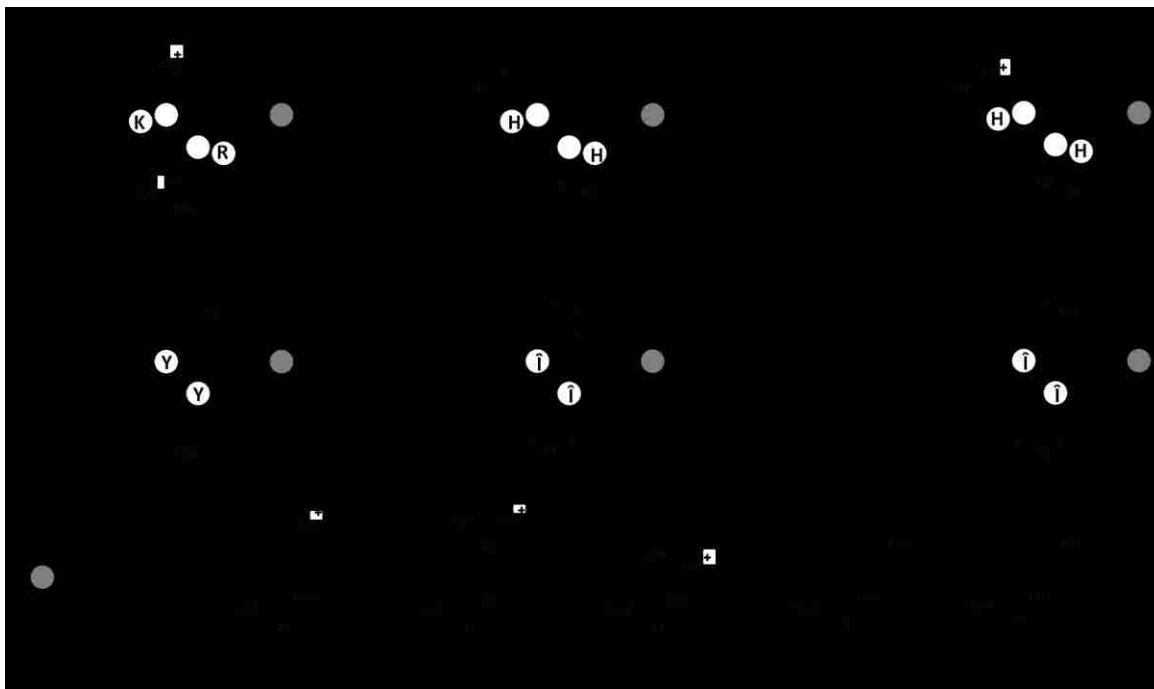


Figure 5.1 Theoretical illustration of tumor microenvironment (low pH)-responsive targeting peptide engineering via (A) histidine and (B) 3,5-diiodotyrosine substitution(s).

5.2 Results and discussion

5.2.1 Peptide synthesis

A series of peptides investigated in this study was successfully synthesized, purified, and identity-confirmed via matrix-assisted laser desorption/ionization time-of-flight mass spectrometry (MALDI-ToF MS) (Table 5.1). 3,5-Diiodotyrosine (\hat{I}) was readily incorporated into the peptides using standard automatic peptide synthesis with no observable side reaction on the unprotected hydroxyl group of the amino acid. An initial attempt to acetylate the N-terminus of Y- \hat{I} - \hat{I} peptide with acetic anhydride resulted in over-acetylation at the hydroxyl groups of 3,5-diiodotyrosine. This issue was solved by coupling the last amino acid with Ac-Tyr(tbu)-OH.

Table 5.1 Amino acid sequences and molecular weights of M2 macrophage-targeting peptides

Peptide	Amino acid sequence	Calculated Mw (Da)	Measured Mw (Da)
M2pepBiotin	YEQDPWGVKWWYGGGSKK (K-Biotin)	2,524.86	2,524.21
AcM2pep(RY)Biotin	Ac-YEQDPWGVRYWYGGGSkkk (K-Biotin)	2,700.06	2,699.45
M2pep(H9)Biotin	YEQDPWGVHWWYGGGSkkk (K-Biotin)	2,662.00	2,661.95
Î-W-Y	ÎEQDPWGVRYWYGGGSkkk (K-Biotin)	2,932.85	2,931.71
Y-Î-Y	YEQDPWGVRIWYGGGSkkk (K-Biotin)	2,909.81	2,909.33
Y-W-Î	YEQDPWGVRIWYGGGSkkk (K-Biotin)	2,932.85	2,933.13
Î-W-Î	ÎEQDPWGVRIWYGGGSkkk (K-Biotin)	3,184.65	3,184.41
Y-Î-Î	YEQDPWGVRIWIWYGGGSkkk (K-Biotin)	3,161.61	3,161.65
Ac-Y-Î-Î	Ac-YEQDPWGVRIWIWYGGGSkkk (K-Biotin)	3,203.61	3,204.08

Ac- denotes N-terminal acetylation.

Î denotes 3,5-diiodotyrosine.

Previously reported affinity-enhanced modifications are in blue.

M2pep peptides with R9Y10 and R9W10 modifications have comparable affinity to M2 macrophages [18].

pH-responsive modifications investigated in this study are in red.

5.2.2 pH-dependent binding activity of M2pep and AcM2pep(RY) at pH 6 and 7.4

The original M2 macrophage-binding peptide (M2pepBiotin) and its affinity-enhanced analog AcM2pep(RY)Biotin were first evaluated for their pH-dependent binding activities on M1 and M2 macrophages at pH 7.4 (physiological pH) and 6 (pathologically hypoxic pH). M1 macrophages were used as a control to evaluate selectivity of these peptides. In general, both M2pepBiotin and AcM2pep(RY)Biotin bind to M2 macrophages with good selectivity over M1 macrophages and with higher affinity at pH 7.4 than at pH 6, where AcM2pep(RY)Biotin shows a more drastic pH-dependent effect at 50 and 100 μ M (Figure 5.2). The observed trend in pH-dependent binding to M2 macrophages is opposite to the ideal tumor microenvironment-targeting characteristic which favors high binding at more acidic pH. These results motivated our effort to engineer new M2pep analogs that reverse the pH-dependent binding characteristic to favor high affinity binding to M2 macrophages at low pH.

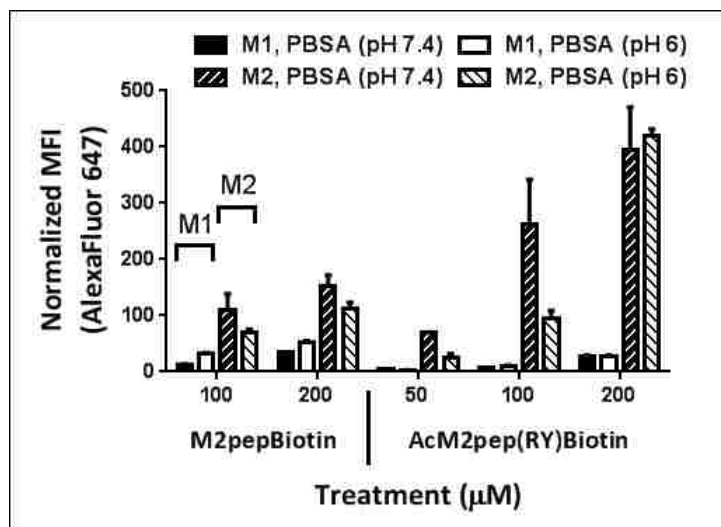


Figure 5.2 Binding M2pepBiotin and AcM2pep(RY)Biotin with M1 and M2 macrophages at pH 7.4 and 6.

5.2.3 The effect of K9H substitution on pH-dependent binding activity

Histidine is a natural amino acid with an imidazole side chain that possesses a pKa value around 6 and is variably ionized at physiological (7.4) versus endo/lysosomal (5-6) pH. Its modification is widely used in protein engineering to confer physiologically relevant, pH-dependent functionality to proteins/antibodies [22,23]. In regard to peptide development, neonatal Fc receptor (FcRn)-binding peptides have been reported with endowed pH-dependent binding activity through the presence of histidine in the sequence [24]. We therefore investigated if a lysine to histidine substitution at the 9th position of M2pepBiotin (K9H) might enable low pH-selective binding activity of the peptide. The lysine at this position is known to influence binding activity of the peptide since its substitution with arginine has been previously shown to improve affinity of the peptide [18]. We hypothesize that pH-dependent, neutral-to-positive ionization of histidine at this position may result in a pH-dependent binding behavior. Indeed, a reverse trend in binding activity of M2pep(H9)Biotin on M2 macrophages was observed where the peptide binds more strongly at pH 6 than at pH 7.4 (Figure 5.3). Nonetheless, the difference in binding activities at these pH values is relatively marginal, and the overall binding affinity of the peptide is reduced compared to the original M2pepBiotin. The reduction in binding affinity associated with the K9H modification may be due to the lower extent of protonation of histidine relative to that of lysine in this pH range or due to less favorable conformational fit of the peptide

to its receptor owing to the presence of a bulky imidazole group. While it is possible to investigate the effect of K9 substitution with 2,3-diaminopropionic acid (Dap) which is more structurally similar to lysine and possesses lower pKa on its amino side chain (6.3-7.49 depending on the surrounding environment [25]), we decided to keep the affinity-enhanced K9R modification and looked into modifications at other amino acid positions utilizing other non-natural amino acids.

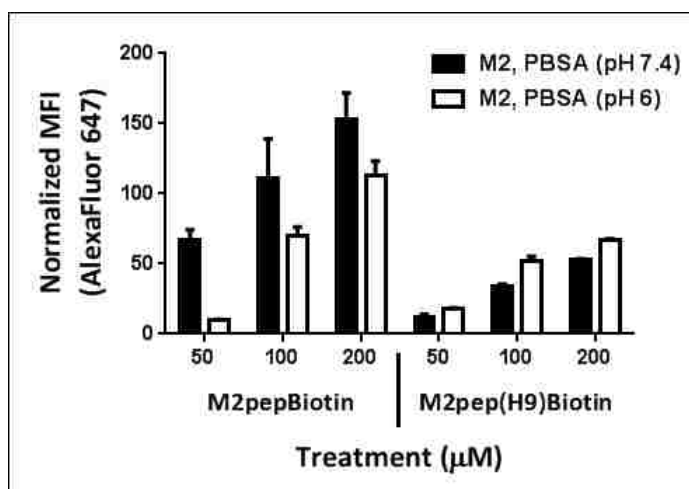


Figure 5.3 Binding of M2pepBiotin and M2pep(H9)Biotin with M2 macrophages at pH 7.4 and 6.

5.2.4 3,5-Diiodotyrosine substitutions impart pH-dependent binding to M2pep

3,5-Diiodotyrosine was chosen for investigation next since its phenolate group possesses desirable pKa around 6.5, and its Fmoc-protected amino acid is commercially available, allowing for incorporation into M2pep peptides via standard Fmoc/tbu solid phase peptide synthesis. The original M2pepBiotin contains 2 tyrosines at the 1st and 12th position whereas AcM2pep(RY)Biotin contains an additional tyrosine at the 10th position giving 3 possible sites for modification. M2pep(R9) analogs with single 3,5-diiodotyrosine mutation at each tyrosine position (Î-W-Y, Y-Î-Y, and Y-W-Î) were synthesized and evaluated for pH-dependent binding activity on M2 macrophages. At 20 μM peptide treatment, all mono-substituted analogs show higher binding activity to M2 macrophages at pH 6 than at pH 7.4 with the Y-W-Î analog (Y12Î

substitution) having the highest low-pH selectivity (Figure 5.4A). Interestingly, all mono-substituted analogs also exhibit enhanced binding activity relative to AcM2pep(RY)Biotin.

Given the encouraging result of the mono-substituted analogs, we next studied the effect of dual 3,5-diiodotyrosine substitutions on binding affinity and pH selectivity of M2pep(R9). The most pH-selective modification (Y12Î) was preserved whereas another 3,5-diiodotyrosine substitution was added at either the 1st (Î-W-Î) or 10th (Y-Î-Î) position. Both di-substituted analogs show further enhancement in binding activity over the mono-substituted ones while also retaining good low pH selectivity (Figure 5.4B). Toxicity of these peptides were observed at higher concentrations preventing us from accurately constructing the binding curves to determine $K_{D,7.4}/K_{D,6}$ for quantitative comparison of pH selectivity of each analog (data not shown). Of note, the di-substituted analogs are also more toxic than the mono-substituted ones at higher concentrations and, hence, the tri-substituted analog was not further investigated. Nonetheless, by systematically mutating different tyrosine in M2pep(R9) with 3,5-diiodotyrosine, we were able to engineer the low pH-selective binding property into the M2pep(R9) peptide and obtain Y-Î-Î as the lead analog which possesses both enhanced M2 macrophage-binding affinity and low pH binding selectivity with the potential to improve serum stability as investigated in the next section. While substituted tyrosines with tunable pKa values have been previously used to study tyrosine-dependent activity of biological enzymes (e.g. oxidase activity of engineered myoglobin [26,27]) as well as employed in tuning the range of pH sensitivity of membrane-disrupting peptides (e.g. diiodotyrosine-substituted GALA[28] and tetrafluorotyrosine-substituted magainin 2 [29]), their utility in engineering pH-responsive targeting ligands has, to our knowledge, not been reported to date. As demonstrated here, both histidine and 3,5-diiodotyrosine provide complementary options in optimization of physiologically relevant, pH-dependent functionality of peptides where the former controls a neutral-to-positive switch, and the latter controls a negative-to-neutral switch. In addition, this concept should also be applicable to other non-natural amino acids (e.g. Dap and tetrafluorotyrosine) whose side chain pKa values lie in the physiologically relevant pH, further expanding the optimization toolbox in regard to both affinity and pH-sensitivity engineering.

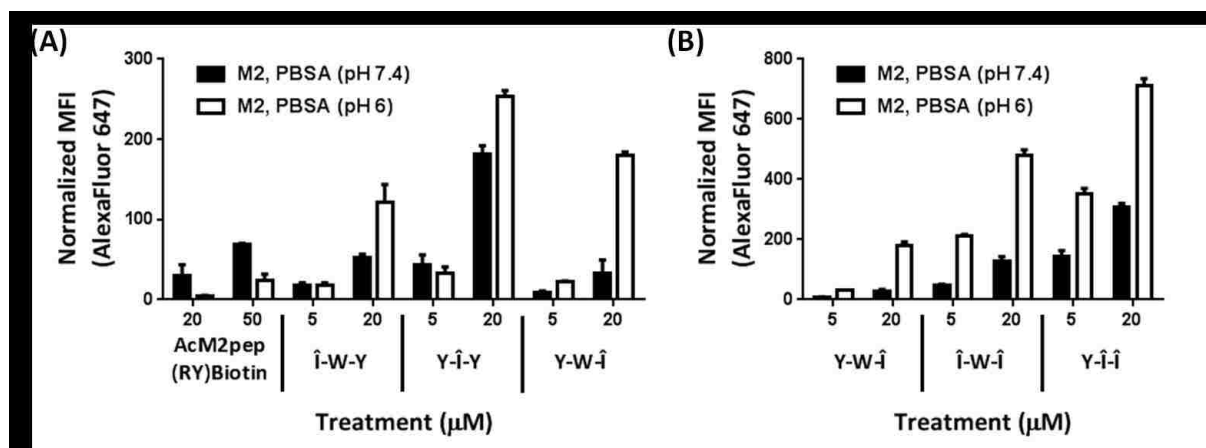


Figure 5.4 Binding of (A) mono-substituted and (B) di-substituted M2pep(R9) analogs with M2 macrophages at pH 7.4 and 6.

5.2.5 Acetylated $Y\text{-}\hat{I}\text{-}\hat{I}$ peptide exhibits improved serum stability compared to $AcM2pep(RY)Biotin$

N-terminal amines are known to have lower pKa relative to the epsilon amines of lysine side chains and may contribute to pH-dependent functionality of peptides/proteins at the physiologically relevant pH [30,31]. To investigate if a free N-terminal amine has an effect on pH-dependent binding activity of M2pep, we synthesized and compared binding activity of $Y\text{-}\hat{I}\text{-}\hat{I}$ and $Ac\text{-}Y\text{-}\hat{I}\text{-}\hat{I}$. No noticeable difference in binding activity of these peptides on M1 and M2 macrophages was observed at either pH (Figure 5.5A) implying that the N-terminal amine is not involved in the observed pH-dependent binding effect. Binding studies of the peptides were also performed on M1 macrophages to evaluate M2-to-M1 selectivity. For both peptides, an increase in binding activity on M1 macrophages is observed at pH 6, but the extent of binding remains substantially lower compared to that on M2 macrophages. In regard to tumor physiology, hypoxic region of tumor is known to more readily harbor TAMs of M2-like phenotype [19,20]. Hence, some increase in binding activity of $Y\text{-}\hat{I}\text{-}\hat{I}$ and $Ac\text{-}Y\text{-}\hat{I}\text{-}\hat{I}$ on M1 macrophages at low pH is expected to minimally compromise their M2-to-M1 selectivity in the hypoxic tumor microenvironment. This development exemplifies how tumor physiological/biological context may be rationally utilized to guide the design and evaluation of targeting peptides.

Since N-terminal acetylation does not have an effect on the binding activity of $Y\text{-}\hat{I}\text{-}\hat{I}$, we next evaluated the serum stability of $Ac\text{-}Y\text{-}\hat{I}\text{-}\hat{I}$. Pleasingly, 3,5-diiodotyrosine substitutions in $Ac\text{-}$

Y- \hat{I} - \hat{I} result in the delayed degradation kinetics of the peptide in serum compared to AcM2pep(RY)Biotin (Figure 5.5B). The intact Ac-Y- \hat{I} - \hat{I} was detectable under MALDI-ToF MS after serum incubation for at least 24 h whereas AcM2pep(RY)Biotin was not. Following the serum incubation for 48 h, the degradation of Ac-Y- \hat{I} - \hat{I} was eventually observed at the $\hat{I}10/W11$ site which coincides with the degradation site (Y10/W11) observed on AcM2pep(RY)Biotin at the 24-h time point. As demonstrated here, modifications of peptides with non-natural 3,5-diiiodotyrosine at the protease-susceptible site may serve as a useful strategy to both confer pH-dependent functionality and retardation of peptide degradation kinetics in serum.

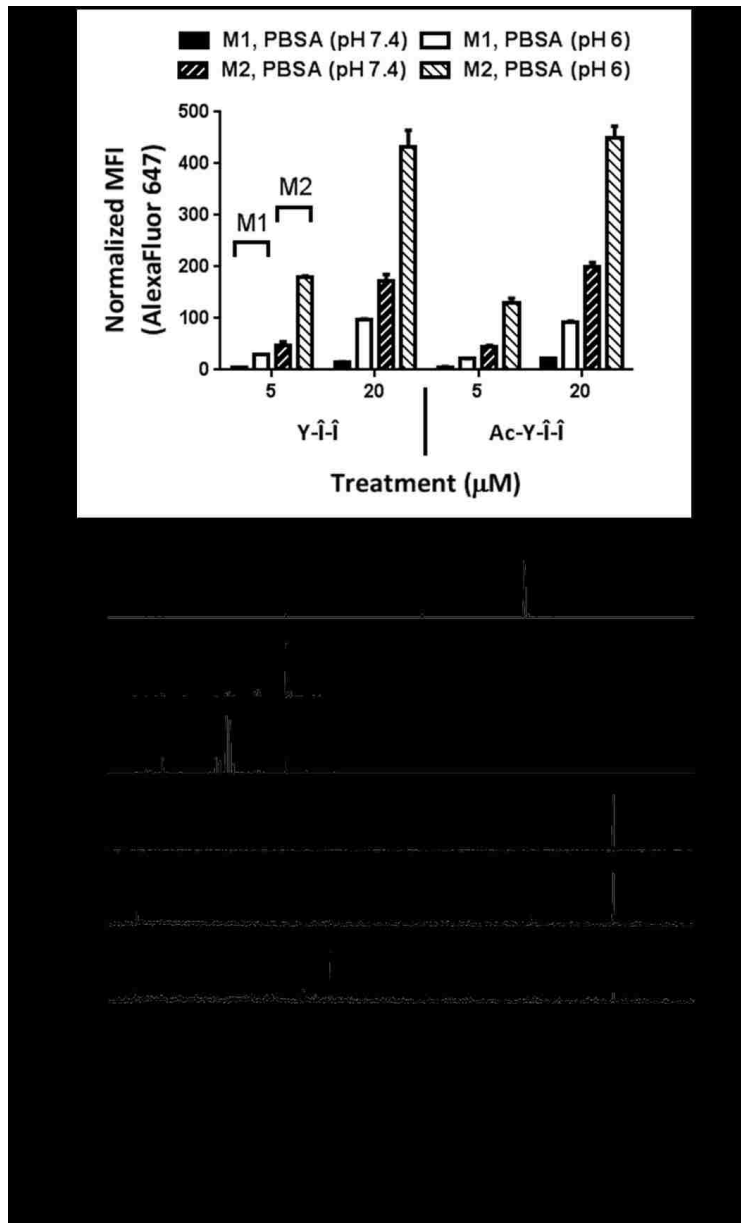


Figure 5.5 (A) Binding of Y-Î-Î and Ac- Y-Î-Î with M1 and M2 macrophages at pH 7.4 and 6. (B) Serum stability of AcM2pep(RY)Biotin and Ac-Y-Î-Î in normal mouse serum.

5.2.6 Demonstration of reversible, pH-dependent modulation of peptide binding affinity

Finally, we envision that engineering pH-dependent functionality of peptides could be a useful strategy not only in development of physiology-selective targeting peptides for *in vivo* targeting applications but also in *in vitro* experiments e.g. pull-down assays for receptor identification. For the latter application, an experiment is typically performed where a tag-labeled (e.g. biotin) targeting ligand is incubated with cell lysate containing its unknown receptor and is passed through the capture (e.g. neutravidin) beads where, ideally, only the receptor-bound ligand would be captured on the beads and subsequently eluted for analysis via sodium dodecyl sulfate polyacrylamide gel electrophoresis (SDS-PAGE) and liquid chromatography-tandem mass spectrometry (LC-MS/MS). Nonetheless, oftentimes, non-specific adsorption of non-target proteins/oligonucleotides is observed resulting in false-positive results [32]. In such case, a pH-dependent receptor elution, as an alternative to traditional bead boiling, could therefore be a complementary tool in enabling more selective elution of target receptors. To test a pH-reversible binding behavior of our engineered pH-responsive Ac-Y-Î-Î, we performed binding study of the peptide in its high binding buffer (PBSA, pH 6) on M2 macrophages followed by post-treatment incubation with PBSA at different pH (6, 7.4, and 8.5) (Figure 5.6A). In theory, post-treatment incubation in higher pH buffer should deprotonate 3,5-diiodotyrosine on Ac-Y-Î-Î ripping off its association with its target receptor. Indeed, we observed a reduction in median fluorescence intensity read-out as a function of increasing pH which indicates the pH-dependent elution of the bound peptides off the target (Figure 5.6B). In a pull-down assay, while it may be possible to selectively elute target receptor by incubation in an excess amount of untagged ligand, enhanced avidity from the multivalent effect of the ligand-bound beads sometimes require a high concentration of the untagged ligand for elution which may not be achievable due to its solubility limit. Hence, pH-dependent elution, made possible by engineering a pH-dependent binding property of targeting peptides as demonstrated here, may provide an additional strategy for this application.

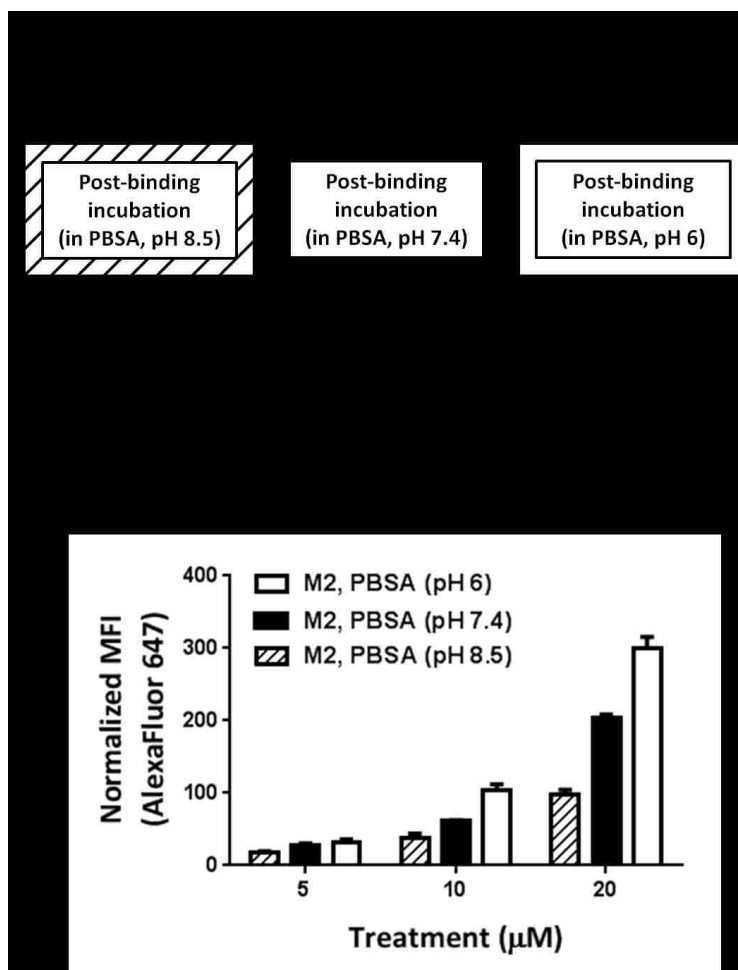


Figure 5.6 Experimental schematic (A) and result (B) of post-binding peptide elution study on M2 macrophages.

5.3 Conclusions

We report here a systematic approach in engineering pH-dependent targeting functionality of M2 macrophage-targeting peptides utilizing physiologically relevant, ionizable amino acids (histidine and 3,5-diiodotyrosine). The strategy should be widely applicable in engineering pH selectivity of other targeting peptides with potential utility in targeting low pH, hypoxic disease environments such as in cancer or inflammation as well as in improving the protocol of *in vitro* experiments such as pull-down assays.

5.4 Materials and Methods

5.4.1 Materials

Protected amino acids and 2-(6-chloro-1H-benzotriazole-1-yl)-1,1,3,3-tetramethylaminium hexafluorophosphate (HCTU) were purchased from AnaSpec (Fremont, CA) and AAPPtec (Louisville, KY). Fmoc-3,5-diiodo-Tyr-OH was purchased from Bachem (Torrance, CA). Ac-Tyr(tbu)-OH was purchased from Chem-Implex International (Wood Dale, IL). NovaPEG rink amide resin was purchased from EMD Millipore (Billerica, Massachusetts). Triisopropylsilane (TIPS), 1,3-dimethoxybenzene (DMB), N-methylmorpholine, and piperidine were purchased from Sigma-Aldrich (St. Louis, MO). The Quant*Tag Biotin quantification kit was purchased from Vector Laboratories (Burlingame, CA). Streptavidin-Alexa Fluor 647 was purchased from BioLegend (San Diego, CA). Normal mouse serum (catalog no. 10410) was purchased from Thermo Fisher Scientific (Waltham, MA).

5.4.2 Peptide synthesis

Biotinylated resin was synthesized following the previously-described protocol [18]. In brief, Fmoc-Lys(Mtt)-OH was manually coupled to NovaPEG rink amide resin using HCTU as an activator dissolved in 0.4 M N-methylmorpholine in DMF. Mtt protecting groups were removed by incubations in 2% TFA in DCM (10-15 times), and the epsilon amines were then coupled with D-biotin in the same manner. The biotinylated resin was used in the synthesis of all biotinylated peptides via a PS3 automated peptide synthesizer (Protein Technologies, Phoenix, AZ) following a standard Fmoc/tbu solid phase peptide synthesis with HCTU as an activator and piperidine as an Fmoc-deprotection agent. Fmoc-3,5-diiodo-Tyr-OH was used in the synthesis of 3,5-diiodotyrosine-containing peptide analogs. Acetylation of AcM2pep(RY)Biotin was performed on resin by incubation in acetic anhydride/TEA/DCM (0.5:0.5:5 v/v/v) for 2 h. N-terminal acetylation of Ac-Y-Î-Î was instead achieved by coupling with Ac-Tyr(tbu)-OH for the last amino acid residue. All peptides were cleaved by incubation in TFA/TIPS/DMB (92.5:2.5:5 v/v/v) for 2.5 h followed by precipitation in cold ether twice. The crude peptides were purified on an Agilent 1200 high performance liquid chromatography (HPLC) system (Agilent Technologies, Santa Clara, CA) using a Phenomenex Fusion-RP C18 semi-preparative column (Phenomenex, Torrance, CA) with water (0.1% TFA) and ACN (0.1% TFA) as mobile phases. Molecular weights of the synthesized peptides were confirmed by MALDI-ToF MS.

5.4.3 Bone marrow harvest and culture of primary macrophages

All animal handling protocols were approved by the University of Washington Institutional Animal Care and Use Committee (IACUC). Bone marrow-derived cells were harvested from female c57bl/6 mice as previously described [18]. In brief, femurs and tibia were excised from euthanized mice, nicked at each end, and flushed with RPMI 1640 medium to obtain the cells. These cells were differentiated into macrophages by culturing on Petri dishes in RPMI 1640 supplemented with 20% donor horse serum (DHS), 1% antibiotic-antimycotic (AbAm), and 20 ng/mL M-CSF. After 7 days of culture, macrophage activation was performed by replacing new media substituting M-CSF with either 25 ng/mL IFN- γ and 100 ng/mL LPS for M1 polarization or 25 ng/mL IL-4 for M2 polarization. For M1 polarization, AbAm was replaced with 1% penicillin-streptomycin (Pen-Strep). The macrophages were maintained in the activation media for 2 days before use in binding studies.

5.4.4 In vitro binding study

Stock peptide solutions (10 mg/mL in water) were quantified by the Quant*Tag Biotin quantification kit and diluted with PBS (1% albumin) (PBSA) at pH 6 or 7.4 for binding studies. Macrophages were scrapped off the Petri dishes and seeded on round-bottom 96-well plates (50,000 cells/well). The seeded macrophages were first equilibrated by washing with PBSA at the pH of interest (pH 6 or 7.4) before incubation in peptide solutions at the respective pH for 20 min on ice. Subsequently, the macrophages were washed twice in PBSA and probed for binding by incubation in streptavidin-Alexa Fluor 647 (1:1000 dilution) for 15 min on ice. After two more washes in PBSA, the macrophages were resuspended in PBS for analysis via MACSQuant Flow Cytometer (Miltenyi Biotec, San Diego, CA). Propidium iodide was added prior to running of each sample to assess for cell viability. All washing steps and incubations were performed in buffers at the desired pH under investigation (pH 6 or 7.4). Binding studies were performed with two samples per treatment, and the observed trends in binding were confirmed in at least two independent studies. For the post-binding peptide elution study, all treatment and washing steps were in PBSA at pH 6. In the study, an additional incubation in PBSA at pH 6, 7.4, or 8.5 for 20 min on ice was included following the peptide incubation step.

5.4.5 Serum stability study

The stock peptide solutions (30 μL) were diluted into normal mouse serum (300 μL). At different time points, an aliquot (40 μL) was drawn, mixed with an equal volume of ACN to precipitate serum proteins, and centrifuged at 10,000 rpm for 5 min. The supernatant solution was transferred to a clean Eppendorf tube, and residual peptides in the pellet were further extracted by sonication in 1:1 $\text{H}_2\text{O}/\text{ACN}$ (80 μL) for 10 min. The sonicated mixture was centrifuged, and the new supernatant solution was pooled with the former and dried on a SpeedVac machine. The peptide extract was resuspended by sonication for 10 min in H_2O (50 μL) followed by centrifugation. The supernatant was analyzed for peptide degradation pattern via MALDI-ToF MS.

5.5 Acknowledgments

This work was supported by NIH 1R01CA177272. Chayanon Ngambenjwong was supported by an Anandamahidol Foundation Fellowship. Julio Marco B. Pineda was supported by a Mary Gates Research Scholarship. We thank Professor Jianmin Gao (Boston College) for helpful discussions on the project.

5.6 References

- [1] T.M. Allen, Ligand-targeted therapeutics in anticancer therapy., *Nat. Rev. Cancer.* 2 (2002) 750–763. doi:10.1038/nrc903.
- [2] D. Peer, J.M. Karp, S. Hong, O.C. Farokhzad, R. Margalit, R. Langer, Nanocarriers as an emerging platform for cancer therapy, *Nat. Nanotechnol.* 2 (2007) 751–760.
- [3] L.M. Bareford, P.W. Swaan, ENDOCYTIC MECHANISMS FOR TARGETED DRUG DELIVERY, *Adv. Drug Deliv. Rev.* 59 (2007) 748–758. doi:10.1016/j.addr.2007.06.008.
- [4] M. Srinivasarao, C. V Galliford, P.S. Low, Principles in the design of ligand-targeted cancer therapeutics and imaging agents., *Nat. Rev. Drug Discov.* 14 (2015) 203–219. doi:10.1038/nrd4519.
- [5] Y.H. Bae, K. Park, Targeted drug delivery to tumors: myths, reality and possibility., *J. Control. Release.* 153 (2011) 198–205. doi:10.1016/j.jconrel.2011.06.001.
- [6] J.M. Saul, A. V Annapragada, R. V Bellamkonda, A dual-ligand approach for enhancing targeting selectivity of therapeutic nanocarriers., *J. Control. Release.* 114 (2006) 277–287. doi:10.1016/j.jconrel.2006.05.028.

- [7] C.H.J. Choi, C.A. Alabi, P. Webster, M.E. Davis, Mechanism of active targeting in solid tumors with transferrin-containing gold nanoparticles., *Proc. Natl. Acad. Sci. U. S. A.* 107 (2010) 1235–1240. doi:10.1073/pnas.0914140107.
- [8] T.G. Kapp, F. Rechenmacher, S. Neubauer, O. V Maltsev, E.A. Cavalcanti-Adam, R. Zarka, et al., A Comprehensive Evaluation of the Activity and Selectivity Profile of Ligands for RGD-binding Integrins., *Sci. Rep.* 7 (2017) 39805. doi:10.1038/srep39805.
- [9] J.M. Donaldson, C. Kari, R.C. Fragoso, U. Rodeck, J.C. Williams, Design and development of masked therapeutic antibodies to limit off-target effects: Application to anti-EGFR antibodies, *Cancer Biol. Ther.* 8 (2009) 2147–2152. <http://www.ncbi.nlm.nih.gov/pmc/articles/PMC3546534/>.
- [10] G.A. Duncan, M.A. Bevan, Computational design of nanoparticle drug delivery systems for selective targeting., *Nanoscale.* 7 (2015) 15332–15340. doi:10.1039/c5nr03691g.
- [11] J.W. Kim, J.R. Cochran, Targeting ligand-receptor interactions for development of cancer therapeutics., *Curr. Opin. Chem. Biol.* 38 (2017) 62–69. doi:10.1016/j.cbpa.2017.03.010.
- [12] J.M. Saul, A. Annapragada, J. V Natarajan, R. V Bellamkonda, Controlled targeting of liposomal doxorubicin via the folate receptor in vitro., *J. Control. Release.* 92 (2003) 49–67.
- [13] S. Muro, Challenges in design and characterization of ligand-targeted drug delivery systems., *J. Control. Release.* 164 (2012) 125–137. doi:10.1016/j.jconrel.2012.05.052.
- [14] S. Zhu, M. Niu, H. O’Mary, Z. Cui, Targeting of Tumor-Associated Macrophages Made Possible by PEG-Sheddable, Mannose-Modified Nanoparticles, *Mol. Pharm.* 10 (2013) 3525–3530. doi:10.1021/mp400216r.
- [15] Z. Liu, M. Xiong, J. Gong, Y. Zhang, N. Bai, Y. Luo, et al., Legumain protease-activated TAT-liposome cargo for targeting tumours and their microenvironment., *Nat. Commun.* 5 (2014) 4280. doi:10.1038/ncomms5280.
- [16] J.J. de Vijlder, M.T. den Hartog, Anionic iodotyrosine residues are required for iodothyronine synthesis., *Eur. J. Endocrinol.* 138 (1998) 227–231.
- [17] M. Cieslewicz, J. Tang, J.L. Yu, H. Cao, M. Zavaljevski, K. Motoyama, et al., Targeted delivery of proapoptotic peptides to tumor-associated macrophages improves survival., *Proc. Natl. Acad. Sci. U. S. A.* 110 (2013) 15919–15924. doi:10.1073/pnas.1312197110.
- [18] C. Ngambenjawong, H.H. Gustafson, J.M. Pineda, N.A. Kacherovsky, M. Cieslewicz, S.H. Pun, Serum Stability and Affinity Optimization of an M2 Macrophage-Targeting Peptide (M2pep)., *Theranostics.* 6 (2016) 1403–1414. doi:10.7150/thno.15394.
- [19] D. Laoui, E. Van Overmeire, G. Di Conza, C. Aldeni, J. Keirsse, Y. Morias, et al., Tumor hypoxia does not drive differentiation of tumor-associated macrophages but rather fine-tunes the M2-like macrophage population., *Cancer Res.* 74 (2014) 24–30. doi:10.1158/0008-5472.CAN-13-1196.

- [20] O.R. Colegio, N.-Q. Chu, A.L. Szabo, T. Chu, A.M. Rhebergen, V. Jairam, et al., Functional polarization of tumour-associated macrophages by tumour-derived lactic acid., *Nature*. 513 (2014) 559–563. doi:10.1038/nature13490.
- [21] C. Ngambenjawong, H.H. Gustafson, S.H. Pun, Progress in tumor-associated macrophage (TAM)-targeted therapeutics, *Adv. Drug Deliv. Rev.* (2017). doi:http://doi.org/10.1016/j.addr.2017.04.010.
- [22] M.L. Murtaugh, S.W. Fanning, T.M. Sharma, A.M. Terry, J.R. Horn, A combinatorial histidine scanning library approach to engineer highly pH-dependent protein switches., *Protein Sci.* 20 (2011) 1619–1631. doi:10.1002/pro.696.
- [23] C. Schroter, R. Gunther, L. Rhiel, S. Becker, L. Toleikis, A. Doerner, et al., A generic approach to engineer antibody pH-switches using combinatorial histidine scanning libraries and yeast display., *MAbs.* 7 (2015) 138–151. doi:10.4161/19420862.2014.985993.
- [24] J.T. Sockolosky, M.R. Tiffany, F.C. Szoka, Engineering neonatal Fc receptor-mediated recycling and transcytosis in recombinant proteins by short terminal peptide extensions., *Proc. Natl. Acad. Sci. U. S. A.* 109 (2012) 16095–16100. doi:10.1073/pnas.1208857109.
- [25] Y. Lan, B. Langlet-Bertin, V. Abbate, L.S. Vermeer, X. Kong, K.E. Sullivan, et al., Incorporation of 2,3-diaminopropionic acid in linear cationic amphipathic peptides produces pH sensitive vectors, *Chembiochem.* 11 (2010) 1266–1272. doi:10.1002/cbic.201000073.
- [26] Y. Yu, X. Lv, J. Li, Q. Zhou, C. Cui, P. Hosseinzadeh, et al., Defining the role of tyrosine and rational tuning of oxidase activity by genetic incorporation of unnatural tyrosine analogs., *J. Am. Chem. Soc.* 137 (2015) 4594–4597. doi:10.1021/ja5109936.
- [27] X. Liu, Y. Yu, C. Hu, W. Zhang, Y. Lu, J. Wang, Significant increase of oxidase activity through the genetic incorporation of a tyrosine-histidine cross-link in a myoglobin model of heme-copper oxidase, *Angew. Chem. Int. Ed. Engl.* 51 (2012) 4312–4316. doi:10.1002/anie.201108756.
- [28] D.H. Haas, R.M. Murphy, Design of a pH-sensitive pore-forming peptide with improved performance., *J. Pept. Res.* 63 (2004) 9–16.
- [29] F. Wang, L. Qin, P. Wong, J. Gao, Facile synthesis of tetrafluorotyrosine and its application in pH triggered membrane lysis., *Org. Lett.* 13 (2011) 236–239. doi:10.1021/ol102610q.
- [30] I.M. Pazos, I.A. Ahmed, M.I. León Berríos, F. Gai, Sensing pH via p-Cyanophenylalanine Fluorescence: Application to Determine Peptide pK(a) and Membrane-Penetration Kinetics, *Anal. Biochem.* 483 (2015) 21–26. doi:10.1016/j.ab.2015.04.026.
- [31] J.R. Sachleben, C.A. McElroy, P. Gollnick, M.P. Foster, Mechanism for pH-dependent gene regulation by amino-terminus-mediated homooligomerization of *Bacillus subtilis* anti-trp RNA-binding attenuation protein, *Proc. Natl. Acad. Sci. U. S. A.* 107 (2010)

15385–15390. doi:10.1073/pnas.1004981107.

- [32] T.N. Nguyen, J.A. Goodrich, Protein-protein interaction assays: eliminating false positive interactions, *Nat. Methods*. 3 (2006) 135–139. doi:10.1038/nmeth0206-135.

Chapter 6

MULTIVALENT POLYMERS DISPLAYING M2 MACROPHAGE-TARGETING PEPTIDES IMPROVE TARGET BINDING AVIDITY AND SERUM STABILITY

Chayanon Ngambenjawong and Suzie H. Pun

Abstract

M2 macrophages represent one of the major immune cell populations in tumor microenvironment and play significant roles in accelerating tumor progression, making them an important target for cancer therapy. Our lab has previously developed a series of M2 macrophage-targeting peptides (M2pep, AcM2pep(RY), and DFBP-cyclized M2pep(RY) (listed in the order of increasing affinity)) for active targeting of immunomodulating agents to M2 macrophages. In this study, we report synthesis and evaluation of multivalent peptide-grafted polymers based on water-soluble, biocompatible poly(*N*-(2-hydroxypropyl) methacrylamide) (polyHPMA) displaying these targeting peptides. In PBS (1% albumin), M2pep/AcM2pep(RY)-polymers, but not DFBP-cyclized M2pep(RY)-polymer, showed enhanced binding avidity to M2 macrophages over their free peptides, whereas AcM2pep(RY)/DFBP-cyclized M2pep(RY)-polymers showed some cytotoxicity to M2 macrophages. All peptide-grafted polymers are more serum-resistant than their corresponding free peptides, showing less decline in binding activity over the course of serum incubation. Interestingly, although DFBP-cyclized M2pep(RY)-polymer did not show improve binding activity over its free peptide in PBS (1% albumin), the avidity enhancement was observed in the presence of serum. Our studies present DFBP-cyclized M2pep(RY)-grafted poly(HPMA) as an improved M2 macrophage-targeting platform suitable for further incorporation of therapeutic cargos for anti-cancer M2 macrophage-targeted immunotherapy.⁶

⁶ Manuscript in preparation for submission

6.1 Introduction

Following the FDA approvals of chemotherapy drug-loaded nanoparticle formulations (e.g. liposomal doxorubicin (Doxil®) and nanoparticle albumin-bound paclitaxel (Abraxane®)) and, more recently, antibody-drug conjugates (e.g. brentuximab vedotin (ADCETRIS®) and trastuzumab emtansine (KADCYLA®)), nanomedicine has unarguably become a significant arm of research and development for cancer therapeutics in both pre-clinical and clinical stages [1–3]. Attractive features of the nanomedicine include enhanced solubility and drug loading of therapeutic drugs, prolonged systemic circulation, improved tumor accumulation via the enhanced permeability and retention (EPR) effect, and mitigation of systemic side effects. Over the years, the repertoire of nanomaterials for development of cancer nanomedicine has substantially expanded beyond traditional lipid-based formulations to encompass metallic/inorganic nanoparticles, carbon nanotubes/nanodiamonds, as well as natural/synthetic biomacromolecules [3,4].

Polymer is one of the most versatile classes of biomaterials for drug delivery applications in cancer therapy. A variety of drugs may be chemically conjugated onto polymers (polymer-drug conjugates) or may be non-covalently encapsulated in polymeric micelles/polymersomes [5,6]. Targeting ligands may be decorated onto the polymers in a multivalent fashion to enhance binding avidity and endocytosis into the target cells of interest [5,7]. Biological therapeutics such as peptide, proteins, and nucleic acids also benefit from modifications/encapsulation with polymers to enhance their stability and pharmacokinetics [8,9]. A diverse array of monomers and controlled polymerization techniques (e.g. atom transfer radical polymerization (ATRP) and reversible addition-fragmentation chain-transfer (RAFT) polymerization) enable scientists to precisely tune physicochemical properties of their polymeric carriers to improve drug's safety profile, reduce the rate of systemic clearance, favor accumulation/penetration into tumor, and in several cases, confer smart functionalities such as controlled drug release or environmental responsiveness [10,11].

Over the past decades, our understanding of tumor microenvironment (TME) and its signaling niche in governing cancer progression has been greatly accelerated. Diverse roles of different immune cell populations, either promoting or suppressing tumor development, have been extensively investigated [12]. Tumor-associated macrophages (TAMs), in particular, have been recognized for their roles in supporting cancer cell proliferation and migration, suppressing

anti-tumor immune responses, as well as stimulating angiogenesis to sustain tumor growth [13]. These TAMs preferentially display a gene expression profile characteristic of an anti-inflammatory M2 phenotype although a small population of TAMs is known to exhibit M1-like phenotype and possesses tumoricidal functions [14]. A significant attention has therefore been drawn towards development of anti-cancer immunomodulating agents targeting M2-TAMs [15,16].

Our lab has previously identified and optimized M2 macrophage-targeting peptides (M2pep) that can selectively bind to M2 macrophages and M2-TAMs over M1 cells and other leukocyte populations [17–19]. We further synthesized divalent and tetravalent M2pep using lysine-based peptidic scaffolds and showed that only the divalent M2pep enhances binding avidity to M2 macrophages while retaining selectivity over M1 macrophages [20]. Interestingly, both divalent and tetravalent M2pep were found to be toxic at higher concentrations with preferential cytotoxicity to M2 macrophages. Inspired by the pioneering works from the Kopeček lab on drug-free macromolecular therapeutics where multivalent ligand-decorated polymer initiates receptor crosslinking leading to subsequent cellular events (e.g. apoptosis) [21], we are interested in exploring the inherent M2 macrophage-cytotoxic effect of multivalent M2pep displayed onto polymers. In this study, we report the synthesis of multivalent M2pep-grafted polymers based on water-soluble, biocompatible poly(*N*-(2-hydroxypropyl) methacrylamide) (polyHPMA) backbone as well as evaluation on their macrophage-binding activity, toxicity, and serum stability.

6.2 Experimental section

6.2.1 Materials

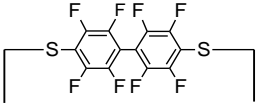
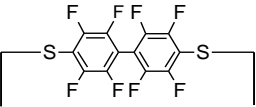
Protected amino acids and 2-(6-chloro-1H-benzotriazole-1-yl)-1,1,3,3-tetramethylammonium hexafluorophosphate (HCTU) were purchased from AAPPTec (Louisville, KY) and AnaSpec (Fremont, CA). Decafluorobiphenyl (DFBP), EZ-Link™ Amine-PEG3-Biotin, and normal mouse serum (Catalog no. 10410) were purchased from Thermo Fisher Scientific (Waltham, MA). 4-Pentynoic acid, 4-cyano-4-(phenylcarbonothioylthio)pentanoic acid *N*-succinimidyl ester (NHS-CTP), piperidine, 4-methylmorpholine, triisopropylsilane (TIPS), 1,2-ethanedithiol (EDT), 1,3-dimethoxybenzene (DMB), tris(2-carboxyethyl)phosphine hydrochloride (TCEP), copper(II) sulfate pentahydrate (CuSO₄·5H₂O), sodium ascorbate, and

tris(3-hydroxypropyltriazolylmethyl)amine (THPTA) were purchased from Sigma-Aldrich (St. Louis, MO). AcM2pep(RY)-SH peptide was purchased from GL Biochem (Shanghai, China). *N*-(2-hydroxypropyl) methacrylamide (HPMA) and *N*-(3-aminopropyl) methacrylamide hydrochloride (APMA·HCl) were purchased from Polysciences (Warrington, PA). VA-044 initiator was purchased from Wako Chemicals (Richmond, VA). 3-Maleimidopropionic acid *N*-hydroxysuccinimide ester (NHS-maleimide) was purchased from TCI America (Portland, OR). The Quant*Tag Biotin quantification kit was purchased from Vector Laboratories (Burlingame, CA). Streptavidin-FITC was purchased from BioLegend (San Diego, CA). Imidazole-1-sulfonyl azide hydrochloride was synthesized following the previously reported protocol [19].

6.2.2 Synthesis of peptides

Biotinylated peptides as well as peptides for grafting to polymers (Table 6.1) were synthesized on a PS3 automatic peptide synthesizer following the standard Fmoc/tbu solid phase peptide synthesis with HCTU as a coupling agent and piperidine as an Fmoc-deprotection agent. Biotinylated and alkyne-functionalized resins were synthesized as follows. Fmoc-Lys(Mtt)-OH (4 eq.) was manually coupled to NovaPEG rink amide using HCTU (3.9 eq.) in 0.4 N 4-methylmorpholine in DMF for 3 h. The acid-labile Mtt was deprotected on resin by incubations in 2% TFA in DCM (10-15 times) until the yellow-colored solution of Mtt-containing TFA solution disappeared. Finally, the epsilon-amine on the resin was manually coupled with D-biotin and 4-pentynoic acid to obtain biotinylated and alkyne-functionalized resins respectively. *N*-terminal acetylation was performed on resin by incubation in acetic anhydride/TEA/DCM (0.5:0.5:5 v/v/v) for 2 h. On-resin cyclization with DFBP followed the previously reported protocol utilizing Fmoc-Cys(Mmt)-OH and Fmoc-Cys(Stbu)-OH for sequential deprotection [19]. The peptides were cleaved by incubation in TFA/TIPS/DMB/EDT (90:2.5:5:2.5 v/v/v/v) cleavage cocktail for 2.5 h before precipitation in cold ether twice. EDT was included in the cleavage cocktail only when the cleaved peptides contain free thiols. The precipitated peptides were purified to more than 95% purity using Phenomenex Fusion-RP C18 semi-preparative column on the Agilent 1200 high performance liquid chromatography (HPLC) system with H₂O (0.1% TFA) and ACN (0.1% TFA) as mobile phases. Successful syntheses of the peptides were confirmed by measuring their molecular weights using matrix-assisted laser desorption/ionization time-of-flight mass spectrometry (MALDI-ToF MS).

Table 6.1 Amino acid sequences and molecular weights of the synthesized peptides

Peptide	Amino acid sequence	Calculated Mw (Da)	Measured Mw (Da)
Biotinylated peptides			
M2pep	YEQDPWGVKWWYGGGSKK(K-Biotin)	2,524.86	2,524.21
AcM2pep(RY)	Ac-YEQDPWGVRYWYGGGSKkk(K-Biotin)	2,700.06	2,699.45
			
DFBP-cyclized M2pep(RY)	CGYEQDPWGVRYWYGCkkk(K-Biotin)	3,014.28	3,014.58
Peptides for grafting			
M2pep-SH	YEQDPWGVKWWYGGGSKkkC	2,401.71	2,402.28
AcM2pep(RY)-SH	Ac-YEQDPWGVRYWYGGGSKkkc	2,448.72	2,449.18
			
DFBP-cyclized M2pep(RY)-alkyne	CGYEQDPWGVRYWYGCkkk(K-4-pentynoic acid)	2,868.08	2,869.09

Small letters denote D-amino acids.

6.2.3 Synthesis of peptide-grafted polymer

6.2.3.1 Synthesis of Biotin-functionalized RAFT chain transfer agent (Biotin-CTA)

The synthesis of Biotin-CTA was adapted from the previously reported protocol [22]. In a 25-mL round bottom flask, NHS-CTP (85 mg, 1 eq.) was dissolved in 3 mL of DCM. Amine-PEG3-Biotin (50 mg, 0.529 eq.) was separately dissolved in 1 mL of DCM together with DIEA (78.7 μ L, 2 eq.) and added to the reaction flask in 3 portions with a 10-min interval between each addition. The reaction solution was stirred under N₂ blanket for 2 d after which the crude product was concentrated and purified via silica column chromatography using EtAc/Hexane as an elution solvent system (5-15% EtAc gradient). Next, the product was further purified on the Agilent 1200 HPLC system using Phenomenex Fusion-RP C18 semi-preparative column eluted with 1:1 H₂O/ACN. Successful synthesis of Biotin-CTA was confirmed by electrospray ionization mass spectrometry (ESI-MS).

6.2.3.2 Synthesis of Biotin-poly(HPMA-*st*-APMA)

Biotin-poly(HPMA-*st*-APMA) was synthesized by RAFT polymerization in 9:1 acetate buffer (pH 5.1)/ethanol using the molar feed ratio of 390:10:1:0.5 HPMA/APMA/Biotin-CTA/VA-044. All reagents were dissolved in acetate buffer and added to a 5-mL, pear-shaped reaction flask with an exception for Biotin-CTA which was first dissolved in ethanol.

Appropriate amount of acetate buffer and ethanol were added to achieve the monomer concentration of 1M. The reaction flask was sealed with a septum and purged with N₂ for 15 min after which the flask was wrapped with Parafilm and placed on an oil bath at 44 °C for 24 h. The polymerization reaction solution was then precipitated in cold acetone twice and dried under vacuum. End-capping of the polymer was performed by dissolving the polymer in acetate buffer and reacted with VA-044 (40 eq. assuming 100% conversion of the monomers in the prior polymerization reaction) at 44 °C for 4 h. The end-capped polymer was dialyzed against water for 2 days and lyophilized. Molecular weight and polydispersity index (PDI) of the polymer were characterized by gel permeation chromatography (GPC) equipped with Shodex SB-804 HQ size exclusion chromatography (SEC) column, eluted with 150 mM acetate buffer (pH 4.4) at 0.5 mL/min flow rate, and detected with miniDAWN TREOS static light scattering and Optilab rEX refractive index detectors (Wyatt Technology, Santa Barbara, CA).

6.2.3.3 Functionalization of Biotin-poly(HPMA-*st*-APMA)

6.2.3.3.1 Maleimide functionalization (Biotin-poly(HPMA-*st*-(Mal-APMA)))

Biotin-poly(HPMA-*st*-APMA) (100 mg, 1 eq.) and NHS-maleimide (13.9 mg, 3 eq. APMA assuming 2.5% APMA content in the polymer) were dissolved in 2 mL of DMF and transferred to a 5-mL reaction flask. DIEA (274 µL, 9 eq.) was added, and the reaction was stirred under N₂ blanket at room temperature for 24 h followed with precipitation in cold ether twice. The polymer was dried under vacuum and used directly for peptide grafting without further purification.

6.2.3.3.2 Azide functionalization (Biotin-poly(HPMA-*st*-(Azi-APMA)))

Biotin-poly(HPMA-*st*-APMA) (50 mg, 1 eq.) and imidazole-1-sulfonyl azide hydrochloride (5.49 mg, 3 eq. APMA assuming 2.5% APMA content in the polymer) were dissolved in 1 mL of DMSO and transferred to a 5-mL reaction flask. CuSO₄·5H₂O (0.0274 mg, 0.01 eq., first dissolved in H₂O) and DIEA (137 µL, 9 eq.) were added to the reaction and stirred at room temperature for 24 h. The reaction solution was then dialyzed against water for 2 days and lyophilized.

6.2.3.4 Peptide grafting

6.2.3.4.1 Grafting via thiol-maleimide conjugation

M2pep-SH/AcM2pep(RY)-SH (about 8 mg, 2 eq. Mal-APMA) was dissolved in 1:1 PBS (pH 6.5, 1 mM EDTA)/ACN (0.5 mM peptide concentration) and transferred to a 25-mL reaction flask. TCEP (0.0488 mg, 0.1 eq. Mal-APMA) was added to the flask, and the reaction solution was purged with N₂ for 5 min. Biotin-poly(HPMA-*st*-(Mal-APMA)) (10 mg, 1 eq. Mal-APMA assuming 2.5% Mal-APMA content in the polymer) was dissolved in the same solvent system and added to the flask. N₂ Purging was continued for 10 min after which the reaction flask was wrapped with Parafilm, and the reaction was left to proceed at room temperature for 24 h. Subsequently, the reaction solution was extensively dialyzed against water for 3 d using a dialysis bag of 10 kDa molecular weight cut-off. The dialyzed solution was filtered through a 0.45- μ m syringe filter and lyophilized.

6.2.3.4.2 Grafting via copper(I)-catalyzed alkyne-azide cycloaddition (CuAAC)

DFBP-cyclized M2pep(RY)-alkyne (9.98 mg, 2 eq. Azi-APMA) and Biotin-poly(HPMA-*st*-(Azi-APMA)) (10 mg, 1 eq. Azi-APMA assuming 2.5% Azi-APMA content in the polymer) were dissolved in 1:1 water/DMF (1 mM peptide concentration). Next, a pre-complexed solution of CuSO₄·5H₂O (2.17 mg, 5 eq. Azi-APMA) and THPTA (3.78 mg, 5 eq. Azi-APMA) was added to the flask. Next, the reaction was purged under Ar for 10 min, followed by addition of sodium ascorbate (1.72 mg, 5 eq. Azi-APMA). The reaction was purged under Ar for 5 more min and then stirred in an oil bath at 37 °C for 3 h. The peptide-grafted polymer was purified by extensive dialysis against water for 3 d using a dialysis bag of 10 kDa molecular weight cut-off. The dialyzed solution was filtered through a 0.45- μ m syringe filter and lyophilized.

6.2.3.5 Determination of peptide valency on peptide-grafted polymers

Serial dilutions of biotinylated peptide stock solutions (M2pep, AcM2pep(RY), and DFBP-cyclized M2pep(RY)) were made, quantified for concentration using the Quant*Tag Biotin quantification kit, and correlated to their respective absorbance at 280 nm to construct peptide standard curves. The 280 nm peptide standard curves were used to quantify the concentrations of their corresponding peptides in each peptide-grafted polymer stock solution (10 mg/mL in H₂O) based on absorbance at 280 nm. The concentration of the polymer was

quantified with the Quant*Tag Biotin quantification kit, and the peptide valency on polymer was calculated by dividing the peptide concentration by the polymer concentration.

6.2.4 Bone marrow harvest and culture of primary macrophages

The animal handling protocol was approved by the University of Washington Institutional Animal Care and Use Committee (IACUC). Bone marrow-derived cells were harvested from femurs and tibia of female c57bl/6 mice as previously described [17]. The cells were cultured on Petri dishes in RPMI 1640 medium supplemented with 20% donor horse serum, 1% antibiotic-antimycotic (AbAm), and 20 ng/mL M-CSF. Macrophage polarization was performed after 7 d of culture by substituting the culture medium with the corresponding activation media where M-CSF was replaced with 25 ng/mL IFN- γ and 100 ng/mL LPS for M1 polarization or with 25 ng/mL IL-4 for M2 polarization. AbAm was substituted with 1% penicillin-streptomycin (Pen-Strep) in the M1 polarization medium. The macrophages were maintained in the activation medium for 2 d before being scraped off the Petri dishes for binding studies.

6.2.5 In vitro binding study

The stock solutions of peptide and peptide-grafted polymers were prepared at 10 mg/mL concentration in water and quantified by the Quant*Tag Biotin quantification kit. These solutions were diluted in PBS (1% albumin) (PBSA) to obtain the desired concentrations for binding studies. Macrophages were seeded on a round bottom 96-well plate (50,000 cells/well) and incubated with the peptide/peptide-grafted polymer solutions for 20 min on ice. Subsequently, the cells were washed twice in PBSA and incubated with streptavidin-FITC (1:500 dilution) for 15 min on ice. After two washes in PBSA, the cells were resuspended in 120 μ L PBS for analysis via MACSQuant Flow Cytometer (Miltenyi Biotec, San Diego, CA). Propidium iodide was added to each sample prior to analysis to exclude dead cells. Data analysis was performed on FlowJo Analysis Software (Tree Star, Ashland, OR). Median fluorescent intensity (MFI) of each sample was normalized to the MFI of the streptavidin-FITC control sample (no peptide) and was an average value of triplicate samples in the same experiment. Percentage cell viability was calculated by normalizing PI population of the treated samples to that of the streptavidin-FITC control sample.

6.2.6 *In vitro* binding study post serum incubation

The peptide and peptide-grafted polymer stock solutions were diluted in normal mouse serum as detailed in Table S6.1. At each time point, an aliquot from the serum was taken and diluted with PBS to obtain a solution of 18% v/v serum in PBS. The aliquots were heated on a water bath at 80 °C for 30 min to inactivate serum proteins and kept in a -20 °C freezer for binding studies. The binding studies followed the same procedures described in the previous section.

6.3 Results and Discussion

6.3.1 Design and Synthesis of peptide-grafted polymers

Multivalent, tagged peptide-displayed polymers were synthesized by RAFT polymerization of *N*-(2-hydroxypropyl) methacrylamide (HPMA) and *N*-(3-aminopropyl) methacrylamide (APMA) using a biotinylated chain transfer agent (Biotin-CTA) followed by peptide grafting. The base polymer, Biotin-poly(HPMA-*st*-APMA) contained exactly one biotin per polymer chain to enable accurate comparison in binding activity between the peptide-grafted polymers and biotinylated free peptides. In addition, the same base polymer was used in the synthesis of all peptide-grafted polymers so that overall degree of polymerization was consistent between polymers.

The overall synthesis schematic of the peptide-grafted polymers is shown in Scheme 6.1. Biotin-CTA was first synthesized via NHS chemistry and confirmed by ESI-MS (Calculated: 679.9 Da, Measured $[M + H]^+$: 680.7 Da). RAFT polymerization of HPMA and APMA proceeded in a controlled manner giving the polymer with an estimated molecular weight of 80 kDa and PDI 1.08 based on GPC analysis. The amine groups on Biotin-poly(HPMA-*st*-APMA) were converted to either maleimide or azide for subsequent grafting with macrophage targeting peptides. Three peptides were selected for grafting: M2pep-SH, AcM2pep(RY)-SH and DFBP-cyclized M2pep(RY)-alkyne. Of note, an initial attempt to synthesize DFBP-cyclized M2pep(RY)-SH was not successful, so the C-terminal cysteine was replaced with Lys(4-pentynoic acid). Facile conversion of amine to other functional groups, e.g. maleimide and azide, increases flexibility in the choice of peptide grafting chemistry. In this case, both thiol-maleimide and CuAAC conjugation strategies showed comparable peptide grafting efficiency with peptide valency in the range from 4.5 to 6.5 (Table 6.2). For comparison, biotinylated

M2pep peptide analogues were synthesized with sequences and molecular weights shown in Table 6.1.



Scheme 6.1 Synthesis schematic of (A) Biotin-CTA and (B) peptide-grafted polymers.

Table 6.2 A panel of peptide-grafted polymers and calculated peptide valency

Peptide-grafted biotinylated polymer (BP)	Base polymer	Grafted peptide	Valency
M2pep-BP	Biotin-poly(HPMA- <i>st</i> -(Mal-APMA))	M2pep-SH	4.5
AcM2pep(RY)-BP	Biotin-poly(HPMA- <i>st</i> -(Mal-APMA))	AcM2pep(RY)-SH	6.4
DFBP-cyclized M2pep(RY)-BP	Biotin-Poly(HPMA- <i>st</i> -(Azi-APMA))	DFBP-cyclicM2pep(RY)-alkyne	4.7

6.3.2 *In vitro* binding study

We have previously demonstrated that the M2pep binds preferentially to bone marrow-derived macrophage polarized with interleukin (IL)-4 to an anti-inflammatory, M2 phenotype compared to the macrophage polarized with interferon (IFN)- γ and lipopolysaccharide (LPS). Therefore, binding studies were performed by incubating biotinylated peptides or peptide-grafted polymers with bone marrow-derived, polarized M1 and M2 macrophages and probing for binding activity with streptavidin-FITC. M1 macrophages were used as a control to evaluate selectivity of the peptide and peptide-grafted polymers. A series of M2 macrophage-binding peptides with varying affinity to M2 macrophages (M2pep ($K_{D,M2} \sim 223 \mu\text{M}$), AcM2pep(RY) ($K_{D,M2} \sim 46.8 \mu\text{M}$), and DFBP-cyclized M2pep(RY) ($K_{D,M2} \sim 2.03 \mu\text{M}$) [19]) was investigated in comparison to their corresponding peptide-grafted polymer analogs. Consistent with their high micromolar $K_{D,M2}$, binding activities of M2pep and AcM2pep(RY) on M1 and M2 macrophages are weak at 1 and 5 μM (Figure 6.1A). In regard to both molar equivalence (comparing 1 μM peptide treatment to 1 μM peptide-grafted polymer treatment) and peptide molar equivalence (comparing 5 μM peptide treatment to 1 μM peptide-grafted polymer treatment), multivalent display of these peptides onto the HPMA polymer significantly improves their binding avidity on M2 macrophages while retaining selectivity over M1 macrophages. On the other hand, DFBP-cyclized M2pep(RY), the highest affinity free peptide analog, showed diminished binding activity when presented on the polymer platform. Although it is unclear why DFBP-cyclized M2pep(RY)-polymer did not show the enhanced binding avidity, one possibility could be that DFBP-cyclized M2pep(RY) peptides, being more hydrophobic from the additional octafluoro-diphenyl moiety in the cyclization region, are more preferentially buried into the polymer coil away from the aqueous environment and, hence, are unable to efficiently engage with target cells.

Interestingly, whereas our previously synthesized peptidic scaffold-based tetravalent M2pep loses M2-to-M1 binding selectivity and is very toxic to macrophages with less than 50%

cell viability at 5 μM treatment [20], the M2pep-polymers developed here (valency $\sim 4.5\text{-}6.5$) retain good M2-to-M1 binding selectivity and are less toxic (Figure 6.1B). Since these constructs have similar valency, the difference in binding selectivity and toxicity could be due to peptide spacing and/or backbone rigidity where the former is more rigid with closely-spaced M2pep, and the latter is more flexible with higher degree of freedom of the displayed M2pep. While the rigid peptidic scaffold-based tetravalent M2pep mediates more potent M2-selective toxicity, it is poorly water-soluble and hence may not be suitable for *in vivo* applications. On the other hand, although the M2pep-polymers are less toxic, they retain M2-to-M1 binding selectivity, are more water-soluble (empirical observation), and allow for flexibility in further conjugation with potent cytotoxic cargos, where the M2pep-polymers themselves also have some complementary cytotoxic activity selective to M2 macrophages/TAMs. In fact, the low toxicity of M2pep-polymers is also more suitable for delivery of therapeutic drugs which aim to modulate M2-TAMs without killing them (e.g. M2-to-M1 repolarization).

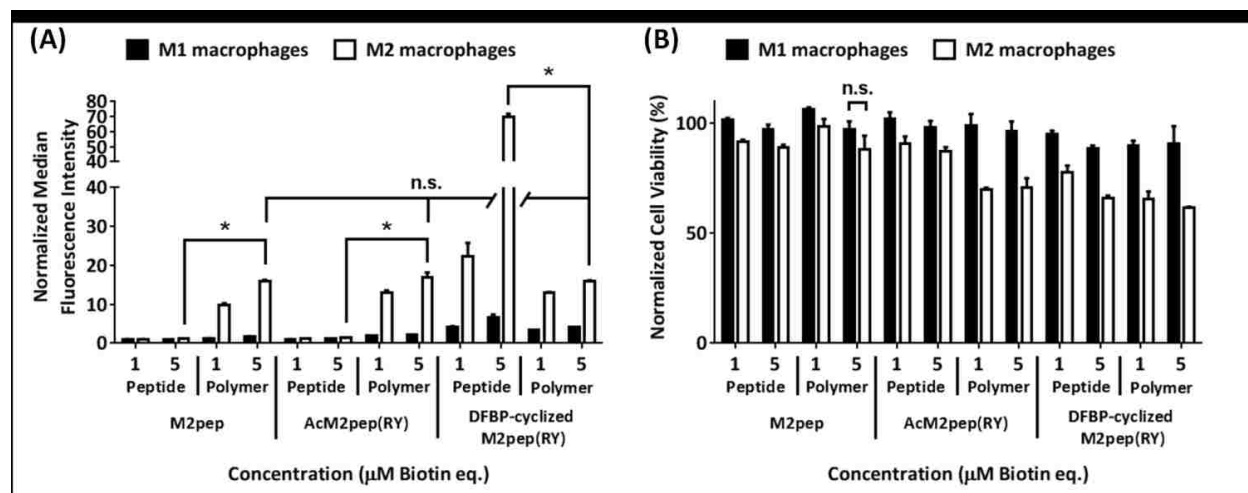


Figure 6.1 (A) Binding study of M2 macrophage-targeting peptides and peptide-grafted polymers on M1 and M2 macrophages. * denotes statistical significance ($P < 0.05$) based on Student's unpaired t-tests, and n.s. denotes non-statistical significance based on one-way ANOVA with Tukey's post-hoc tests. For clarity, only statistical analyses of 5 μM treatments are shown. (B) Their corresponding cell viability. Unless labeled, statistical significance ($P < 0.05$) was observed on the relative cell viability between M1 and M2 macrophages of the same treatment.

6.3.3 *In vitro* binding study post serum incubation

We previously reported peptide macrocyclization as a strategy to improve serum stability of M2pep [18,19]. In this study, we evaluate how binding activities of different peptide-grafted polymers are affected by serum incubation, which will be indicative of their serum stability. Biotinylated peptides and peptide-grafted polymers were incubated in normal mouse serum, and aliquots were taken at various time points, diluted in PBS, and heat-inactivated for use in binding study on M2 macrophages. Notably, all peptide-grafted polymers retained their binding activities even after incubation in serum for 24 h unlike their free peptide analogs which lost more than half of the initial binding activities during the same period of serum incubation (Figure 6.2A). Linear M2pep and AcM2pep(RY) have been previously shown to be rapidly degraded within 24 h [18]. By displaying these peptides onto HPMA polymer, their serum stability is significantly enhanced. Unlike polymeric micelles/polymersomes which can encapsulate peptides away from serum proteases, peptides on the peptide-polymer conjugates are expected to be relatively more exposed to serum environment. Hence, improvement in serum stability of peptide-polymer conjugates, such as the ones demonstrated here, is a relatively less-appreciated advantage of peptide-polymer conjugates as opposed to their well-recognized ability to mediate multivalent interaction and prolong *in vivo* circulation time. Interestingly, although the initial binding study of all peptide-grafted polymers, performed in PBSA, shows no statistical difference in the extent of binding activity among these analogs, their binding activities are significantly altered in the presence of serum with DFBP-cyclized M2pep(RY)-polymer having the highest binding activity (Figure 6.2A).

In addition, binding activity of DFBP-cyclized M2pep(RY) on M2 macrophages is significantly diminished in the presence of serum whereas the binding activity of its peptide-grafted polymer analog (DFBP-cyclized M2pep(RY)-polymer) is less affected at 1 μM and actually enhanced at 5 μM (Figure 6.2B). Since binding study in the presence of serum is more relevant to the *in vivo* environment, we propose DFBP-cyclized M2pep(RY)-polymer as the improved M2 macrophage-targeting platform suitable for further development into anti-cancer TAM-targeted drug-polymer conjugates. As demonstrated in our current study, binding behaviors of targeting peptides or peptide-grafted polymers in a common buffer (PBSA) and in serum-containing buffer could be very different and highlight the importance of *in vitro* evaluation in physiologically relevant media. Adding on to the well-recognized benefit of

prolonged *in vivo* circulation time, the accompanying improvement in serum stability of peptides on polymeric nanoparticles also represents a valuable advantage in development of therapeutic peptide-polymer conjugates.

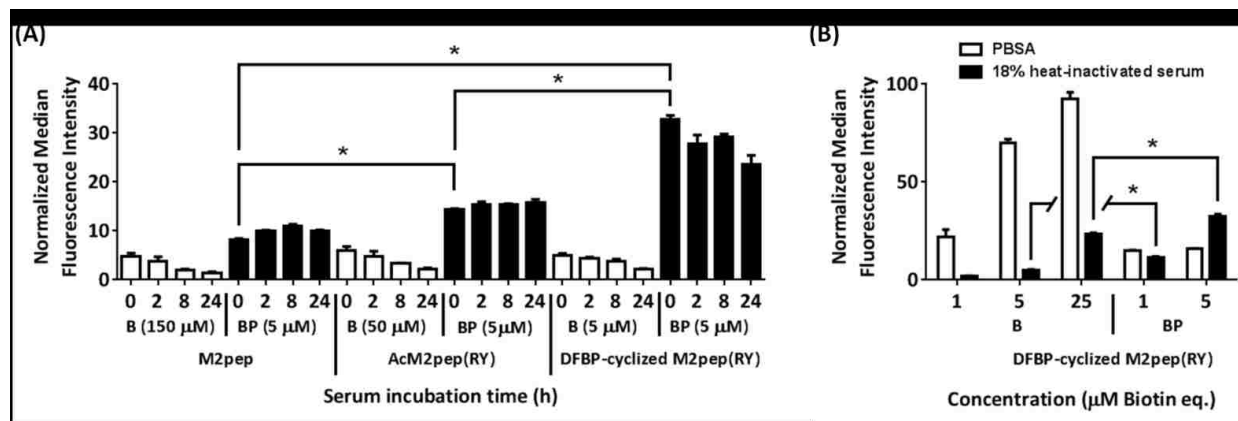


Figure 6.2 (A) Binding study of M2 macrophage-targeting peptides and peptide-grafted polymers on M2 macrophages post serum incubation. Concentrations are labeled as biotin equivalence. Binding data of the polymer analogs are shaded in black for clarity. * denotes statistical significance ($P < 0.05$) based on Student's unpaired t-tests. (B) Binding study of DFBP-cyclized M2pep(RY)-peptide/polymer in PBSA and 10% heat-inactivated serum (in PBS) on M2 macrophages. Statistical analysis comparing treatments of equimolar peptide equivalence was performed by Student's unpaired t-tests where * denotes statistical significance ($P < 0.05$).

6.4 Conclusions

In this study, we report development of multivalent HEMA-based polymer bearing multiple M2 macrophage-targeting peptides. Enhanced binding avidity and stability in the presence of serum were observed for all peptide-grafted polymers highlighting the advantages of peptide-grafted polymer as a targeted drug carrier for nanomedicine applications. AcM2pep(RY)/DFBP-cyclized M2pep(RY)-polymers possess some inherent cytotoxicity to M2 macrophages selectively over M1 macrophages which could complement the activity of their conjugated cytotoxic drugs for M2-TAM depletion application. Our investigation here suggests DFBP-cyclized M2pep(RY)-grafted polymer as a potential platform for future development of TAM-targeted therapeutics.

6.5 Acknowledgments

This work was supported by NIH 1R01CA177272. Chayanon Ngambenjawang was supported by an Anandamahidol Foundation Fellowship.

6.6 References

- [1] A. Wicki, D. Witzigmann, V. Balasubramanian, J. Huwyler, Nanomedicine in cancer therapy: challenges, opportunities, and clinical applications., *J. Control. Release.* 200 (2015) 138–157. doi:10.1016/j.jconrel.2014.12.030.
- [2] C.M. Dawidczyk, C. Kim, J.H. Park, L.M. Russell, K.H. Lee, M.G. Pomper, et al., State-of-the-art in design rules for drug delivery platforms: lessons learned from FDA-approved nanomedicines., *J. Control. Release.* 187 (2014) 133–144. doi:10.1016/j.jconrel.2014.05.036.
- [3] J. Shi, P.W. Kantoff, R. Wooster, O.C. Farokhzad, Cancer nanomedicine: progress, challenges and opportunities., *Nat. Rev. Cancer.* 17 (2017) 20–37. doi:10.1038/nrc.2016.108.
- [4] T. Sun, Y.S. Zhang, B. Pang, D.C. Hyun, M. Yang, Y. Xia, Engineered Nanoparticles for Drug Delivery in Cancer Therapy, *Angew. Chemie Int. Ed.* 53 (2014) 12320–12364. doi:10.1002/anie.201403036.
- [5] R. Duncan, Polymer conjugates as anticancer nanomedicines., *Nat. Rev. Cancer.* 6 (2006) 688–701. doi:10.1038/nrc1958.
- [6] R.H. Prabhu, V.B. Patravale, M.D. Joshi, Polymeric nanoparticles for targeted treatment in oncology: current insights, *Int. J. Nanomedicine.* 10 (2015) 1001–1018. doi:10.2147/IJN.S56932.
- [7] Y. Zhong, F. Meng, C. Deng, Z. Zhong, Ligand-directed active tumor-targeting polymeric nanoparticles for cancer chemotherapy., *Biomacromolecules.* 15 (2014) 1955–1969. doi:10.1021/bm5003009.
- [8] E.M. Pelegri-O’Day, E.-W. Lin, H.D. Maynard, Therapeutic protein-polymer conjugates: advancing beyond PEGylation., *J. Am. Chem. Soc.* 136 (2014) 14323–14332. doi:10.1021/ja504390x.
- [9] D.W. Pack, A.S. Hoffman, S. Pun, P.S. Stayton, Design and development of polymers for gene delivery., *Nat. Rev. Drug Discov.* 4 (2005) 581–593. doi:10.1038/nrd1775.
- [10] C.E. Wang, P.S. Stayton, S.H. Pun, A.J. Convertine, Polymer nanostructures synthesized by controlled living polymerization for tumor-targeted drug delivery., *J. Control. Release.* 219 (2015) 345–354. doi:10.1016/j.jconrel.2015.08.054.
- [11] N. Larson, H. Ghandehari, Polymeric conjugates for drug delivery., *Chem. Mater.* 24 (2012) 840–853. doi:10.1021/cm2031569.

- [12] D.F. Quail, J.A. Joyce, Microenvironmental regulation of tumor progression and metastasis., *Nat. Med.* 19 (2013) 1423–1437. doi:10.1038/nm.3394.
- [13] R. Noy, J.W. Pollard, Tumor-associated macrophages: from mechanisms to therapy, *Immunity*. 41 (2014) 49–61. doi:10.1016/j.immuni.2014.06.010.
- [14] A. Schmieder, J. Michel, K. Schonhaar, S. Goerdt, K. Schledzewski, Differentiation and gene expression profile of tumor-associated macrophages., *Semin. Cancer Biol.* 22 (2012) 289–297. doi:10.1016/j.semcancer.2012.02.002.
- [15] C. Ngambenjawong, H.H. Gustafson, S.H. Pun, Progress in tumor-associated macrophage (TAM)-targeted therapeutics, *Adv. Drug Deliv. Rev.* (2017). doi:http://doi.org/10.1016/j.addr.2017.04.010.
- [16] A. Mantovani, F. Marchesi, A. Malesci, L. Laghi, P. Allavena, Tumour-associated macrophages as treatment targets in oncology., *Nat. Rev. Clin. Oncol.* (2017). doi:10.1038/nrclinonc.2016.217.
- [17] M. Cieslewicz, J. Tang, J.L. Yu, H. Cao, M. Zavaljevski, K. Motoyama, et al., Targeted delivery of proapoptotic peptides to tumor-associated macrophages improves survival., *Proc. Natl. Acad. Sci. U. S. A.* 110 (2013) 15919–15924. doi:10.1073/pnas.1312197110.
- [18] C. Ngambenjawong, H.H. Gustafson, J.M. Pineda, N.A. Kacherovsky, M. Cieslewicz, S.H. Pun, Serum Stability and Affinity Optimization of an M2 Macrophage-Targeting Peptide (M2pep)., *Theranostics*. 6 (2016) 1403–1414. doi:10.7150/thno.15394.
- [19] C. Ngambenjawong, J.M.B. Pineda, S.H. Pun, Engineering an Affinity-Enhanced Peptide through Optimization of Cyclization Chemistry., *Bioconjug. Chem.* 27 (2016) 2854–2862. doi:10.1021/acs.bioconjchem.6b00502.
- [20] C. Ngambenjawong, M. Cieslewicz, J.G. Schellinger, S.H. Pun, Synthesis and evaluation of multivalent M2pep peptides for targeting alternatively activated M2 macrophages, *J. Control. Release*. 224 (2016) 103–111. doi:http://dx.doi.org/10.1016/j.jconrel.2015.12.057.
- [21] T.-W. Chu, J. Kopecek, Drug-free macromolecular therapeutics - a new paradigm in polymeric nanomedicines, *Biomater. Sci.* 3 (2015) 908–922. doi:10.1039/C4BM00442F.
- [22] M.C. Palanca-Wessels, A.J. Convertine, R. Cutler-Strom, G.C. Booth, F. Lee, G.Y. Berguig, et al., Anti-CD22 antibody targeting of pH-responsive micelles enhances small interfering RNA delivery and gene silencing in lymphoma cells., *Mol. Ther.* 19 (2011) 1529–1537. doi:10.1038/mt.2011.104.

6.7 Supplementary information

Table S6.1 Dilution schematic for binding study post serum incubation

Peptide/peptide-grafted polymer	Stock concentration (μM)	Dilution for serum incubation (Stock volume + serum volume) (μL)	Concentration in serum (μM)	Dilution for binding study (Volume of serum aliquot + PBS volume) (μL)	Final concentration for binding study (μM)
M2pep-B	240	32 + 288	24	73 + 277	5
AcM2pep(RY)-B	240	32 + 288	24	73 + 277	5
DFBP-cyclized M2pep(RY)-B	240	32 + 288	24	73 + 277	5
M2pep-BP	7400	35 + 315	740	71 + 279	150
AcM2pep(RY)-BP	2500	35 + 315	250	70 + 280	50
DFBP-cyclized M2pep(RY)-BP	250	35 + 315	25	70 + 280	5

Chapter 7

**SUMMARY OF MAJOR FINDINGS AND
RECOMMENDATION FOR FUTURE DIRECTIONS****Abstract**

This chapter provides a summary of major findings in regard to development and optimization of M2pep-based ligands for targeting murine M2 macrophages/TAMs. Preliminary evaluation of the developed M2pep/M2pep-polymer analogs on peripheral blood mononuclear cell (PBMC)-derived human macrophages is presented. Future directions are proposed in regard to (1) development of M2pep-based drug delivery systems with loaded immunomodulating agents for validation in murine models and (2) strategies to improve M2pep-based ligands for targeting human TAMs, ideally with M2-subtype selectivity.

7.1 Major findings

Tumor-associated macrophages (TAMs) have emerged as an important target for cancer immunotherapy (Chapter 1, [1]). The majority of TAMs displays tumor-promoting, M2-like phenotype with opposite functions to the less abundant tumor-killing, M1-like population. Our lab has been interested in tailoring a targeted drug delivery system selective to M2-TAMs for precise immunomodulation of this tumor-promoting population. M2 macrophage-binding peptide (M2pep) has been previously identified and verified to bind selectively to murine M2 macrophages and M2-TAMs, where its fusion to pro-apoptotic KLA peptide (M2pep-KLA) mediates some extent of M2-TAM eradication in CT26 tumor-bearing mice [2]. However, M2pep-KLA constructs show compromised activity in regard to M2-to-M1 selectivity (Chapter 2, [3]). To circumvent the problem, we direct our research efforts into investigation of alternative therapeutic cargos as well as into improving affinity and serum stability of the targeting peptide where the two latter aspects are the focus of this thesis. Amino acid sequence optimization of M2pep results in identification two affinity-enhanced modifications (K9R and W10Y) whereas cyclization of the peptide confers serum stability (Disulfide-cyclized M2pep(RY)) (Chapter 3, [4]). Further optimization of M2pep cyclization chemistry results in identification of the lead analog (DFBP-cyclized M2pep(RY)) with the apparent K_D of 2.03 μM for murine M2 macrophages (about 100-fold improvement in affinity over the original M2pep) (Chapter 4, [5]). Physiopathology-guided optimization of M2pep capitalizing on acidic tumor microenvironment as well as preferential intratumoral localization of M2-TAMs in the more acidic, hypoxic region leads to rational development of a low pH-selective M2pep analog (Ac-Y-Î-Î) which binds to target M2 macrophages more strongly as a function of decreasing pH (Chapter 5). Finally, multivalent polymer displaying M2pep peptides were synthesized and evaluated for binding avidity and serum stability. Grafting M2pep peptides onto poly(*N*-(2-hydroxypropyl) methacrylamide) improves stability and M2 macrophage-binding avidity in the presence of serum with superior performance over free M2pep peptides (Chapter 6). The strategies, investigated herein for M2pep optimization, establish a systematic guideline broadly applicable for rational development of other targeting peptides especially the ones whose receptor identities are not known.

7.2 Future directions

7.2.1 Investigation on strategies to modulate M2-TAMs utilizing different immunomodulating agents delivered via the developed M2pep-based M2-TAM-targeted delivery platform

M2pep has been optimized with enhanced affinity for M2 macrophages/TAMs with *in vivo* TAM-targeting capability demonstrated in CT26 colon cancer and 4T1 breast cancer models (Chapter 3, [4]). Different TAM-modulating agents have been reported several of which could be more effectively delivered in active targeting formulations (Chapter 1, [1]). For example, traditional chemotherapy drugs with reported cytotoxic effect on TAMs (e.g. doxorubicin and trabectedin) could benefit from reduced systemic toxicity in the targeted formulations either as direct prodrugs, targeted polymer-drug conjugates, or targeted polymeric micelles. Alternatively, M2pep-based carriers could be used to “load” TAMs with chemotherapy drugs for sustained release to nearby cancer cells analogous to the recently reported phenomena on TAM-mediated therapeutic effect of antibody-drug conjugates [6]. Opposite to TAM-killing, targeted delivery of immunomodulating agents (e.g. stimulator of interferon genes (STING) agonists DMXAA (mouse) and 2'3'-cGAMP (mouse and human)) may enhance their activity on M2-to-M1 repolarization of TAMs to further prime tumor immunomicroenvironment for anti-tumor responses [7,8]. Finally, incorporation of M2pep into nanocarriers tailored for active delivery of siRNA, mRNA, or plasmid DNA may allow for interruption of key pathways (e.g. STAT3, PI3k, and Akt) that promote tumor-promoting functions of TAMs or allow for autocrine production of cytokines (e.g. IL-12, IL-21, and IFN- γ) to restore their tumoricidal properties [1,9,10]. Although M2pep has been optimized as a murine M2-TAM-targeting agent, customized tailoring of M2pep-based drug carriers will be needed for different therapeutic cargos of interest in order to draw out their maximal efficacy while minimizing off-target side effects.

7.2.2 Towards human translation

M2pep was previously evaluated to have negligible binding to human macrophages [2]. In this section, we report a preliminary observation on the enhanced binding activity of M2pep-grafted polymers on human macrophages and provide recommendations for future optimization of M2pep-based targeting of human TAMs.

7.2.2.1 Preliminary binding studies of M2pep analogs on human macrophages

M2pep-grafted polymers developed in Chapter 6 together with their free peptide analogs (Table 7.1) were used to test their binding activity on human peripheral blood mononuclear cell (PBMC)-derived, polarized M1 and M2 macrophages. Free M2pep peptides bind weakly to both M1 and M2 macrophages whereas their peptide-grafted polymer analogs show enhanced binding avidity (Figure 7.1). Interestingly, binding activity of M2pep-BP is higher than the other AcM2pep(RY)-BP and DFBP-cyclized M2pep(RY)-BP implying that the RY modification that improves M2pep's affinity for murine M2 macrophages may not be beneficial for binding to human macrophages. Even though DFBP cyclization drastically improves binding affinity of M2pep(RY) to murine M2 macrophages, such enhancement was not observed for human macrophages. In addition, poor M2-to-M1 binding selectivity was observed for all these peptides and peptide-grafted polymers.

Table 7.1 A panel of peptides and peptide-grafted polymers and calculated peptide valency

Biotinylated peptide (B)/ Peptide-grafted biotinylated polymer (BP)	Base polymer	Grafted peptide	Valency
M2pep-B	N/A	N/A	1
AcM2pep(RY)-B	N/A	N/A	1
DFBP-cyclized M2pep(RY)-B	N/A	N/A	1
M2pep-BP	Biotin-poly(HPMA- <i>st</i> -(Mal-APMA))	M2pep-SH	4.5
AcM2pep(RY)-BP	Biotin-poly(HPMA- <i>st</i> -(Mal-APMA))	AcM2pep(RY)-SH	6.4
DFBP-cyclized M2pep(RY)-BP	Biotin-Poly(HPMA- <i>st</i> -(Azi-APMA))	DFBP-cyclicM2pep(RY)-alkyne	4.7

N/A = not applicable

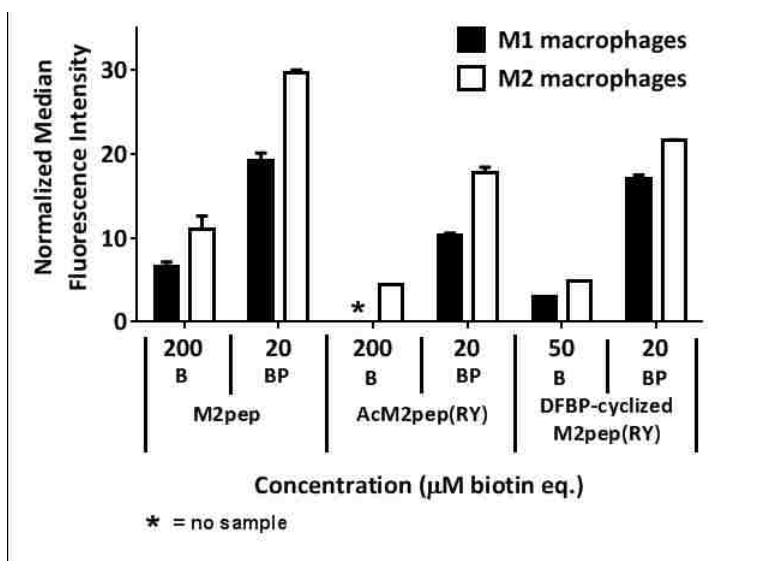


Figure 7.1 Binding study of M2 macrophage-targeting peptides and peptide-grafted polymers on human M1 and M2 macrophages.

A new panel of M2pep-grafted polymers was synthesized to evaluate the effect of single mutation (K9R or W10Y) on their binding activity on human macrophages (Table 7.2). Even though AcM2pep(RY)-BP has lower binding activity compared to M2pep-BP (Figure 7.1), M2pep(R9)-BP with only a single K9R modification in the grafted peptide shows higher binding activity than M2pep-BP (Figure 7.2). Nonetheless, all these peptide-grafted polymers show poor M2-to-M1 and M2-to-M0 binding selectivity. Of note, additional studies performed using human macrophages from diverse donors are needed to confirm the observed trend. While these preliminary studies suggest M2pep-grafted polymers as a potential platform for pan-macrophage-targeting, additional studies are also needed to evaluate their selectivity against other cell populations e.g. other leukocytes.

Table 7.2 A panel of peptide-grafted polymers and calculated peptide valency

Biotinylated polymer (BP)	Base polymer	Grafted peptide	Valency
M2pep-BP	Biotin-poly(HPMA- <i>st</i> -(Mal-APMA))	M2pep-SH	4.5
M2pep(R9)-BP	Biotin-poly(HPMA- <i>st</i> -(Mal-APMA))	M2pep(R9)-SH	5.4
M2pep(Y10)-BP	Biotin-Poly(HPMA- <i>st</i> -(Mal-APMA))	M2pep(Y10)-SH	5.8

N/A = not applicable

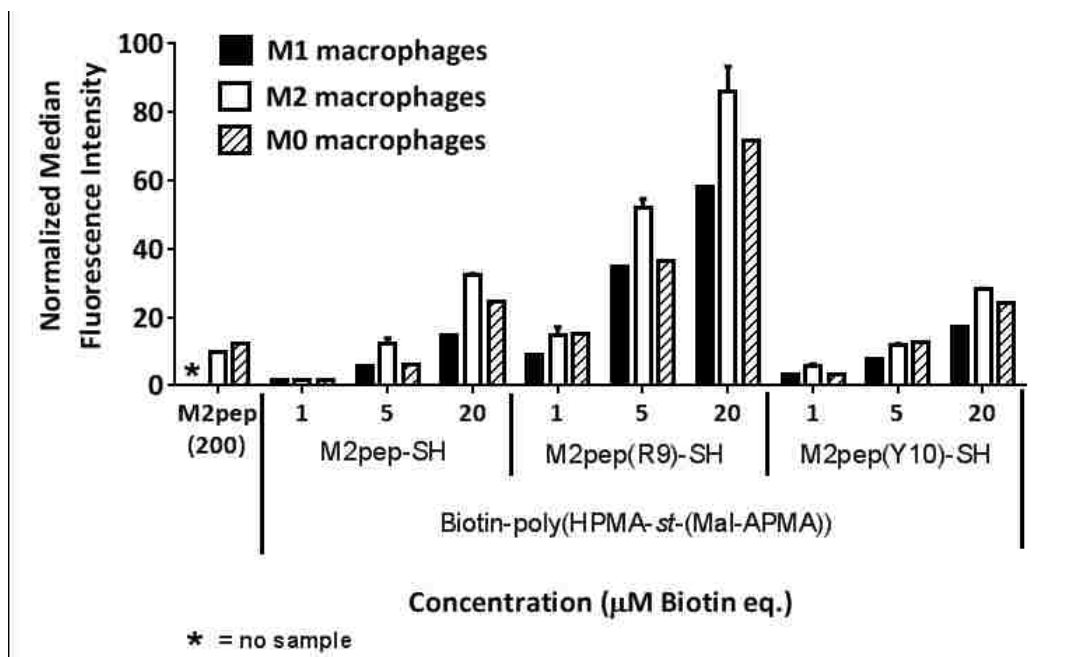


Figure 7.2 Binding study of peptide-grafted polymers on human M0, M1, and M2 macrophages.

7.2.2.2 Proposed strategies to improve affinity/selectivity of M2pep towards human M2 macrophages/TAMs

7.2.2.2.1 Extended library screening

Even though binding activity of M2pep on human macrophages could be enhanced on multivalent polymers, it is still desirable to optimize the affinity of the free peptide for applications such as M2pep-drug conjugates or molecular imaging. One possible strategy is to engineer an extended peptide phage display library for panning on human macrophages where the display sequences include a random extended region in tandem with the M2pep(R9) sequence. Alternatively, a one-bead-one-compound (OBOC) screening technology may be employed to construct the extend M2pep(R9) library for panning [11]. In addition, both approaches are also adaptable for construction of cyclic peptide library to preserve the previously observed serum stability of cyclic M2pep. Although it is premature to assume, it may also be possible that the extended M2pep(R9) would improve both affinity and selectivity if the extended peptide navigates onto the subtype-distinct region (e.g. surface glycosylated surface), if exists, of the receptor. Future studies on receptor identification and glycosylation patterns of the receptor on macrophages/TAMs of different subtypes will shed light on feasibility of the

proposed strategy as well as aiding in better design of the next generation M2pep for human macrophage/TAM-targeting.

7.2.2.2.2 Tumor microenvironment-responsive M2pep for human TAM-targeting

Proof-of principle development of low pH-selective M2pep utilizing 3,5-diiodotyrosine has been reported in Chapter 5 the concept of which may be applicable for targeting hypoxic TAMs over resident macrophages in humans. Although some basal binding activity observed at pH 7.4 for Ac-Y-ÎÎ may be acceptable for murine applications where the peptide binds selectively to M2 over M1 macrophages, this residual activity may not be ideal for human TAM-targeting where M2pep-polymer binds more indiscriminately to macrophages of different subtypes. To increase stringency for low pH-selective binding (targeting hypoxic TAMs over resident macrophages), the substituted tyrosine with lower phenolate pKa than 3,5-diiodotyrosine (e.g. tetrafluorotyrosine) may be investigated. We envision that binding activity of the new analog at physiological pH will be almost completely suppressed whereas partially compromised binding activity in the acidic tumor will be compensated via multivalent display of the peptide onto polymer. Future optimization on the suitable low pH-selective M2pep analogs as well as the multivalent presentation on polymer will be needed to derive a targeted carrier selective to human TAMs over resident macrophages.

7.2.2.2.3 Selectivity enhancement via heterobivalent display of multiple targeting peptides

Although it is assumed that M2pep receptor is expressed to a different extent on murine M2, M1, and M0 macrophages resulting in the observed M2-selectivity of M2pep, this differential expression of M2pep receptor may not be the case for human macrophages as seen in the preliminary binding study of M2pep-polymers (Figure 7.2). Nonetheless, the utility of M2pep as a pan-human macrophage-binding peptide might be enhanced for macrophage subtype-selectivity by co-presenting M2pep with other ligands (e.g. mannose, folate, or transferrin) that are known to bind with good M2-to-M1 selectivity but may possess less M2-selectivity relative to some other cell populations. By compromising some extent of M2-to-non macrophage selectivity and optimizing the ratiometric display of different targeting peptides, we may be able to derive a targeted platform with useful selectivity to M2 macrophages against other cell populations based on the overall difference in the combined receptor density [12,13].

Alternatively, it may also be possible to promote TAM-to-resident macrophage selectivity by co-displaying M2pep with tumor microenvironment-responsive peptides (e.g. pH low insertion peptide (pHLIP)) [14]. Nevertheless, as mentioned earlier, evaluation on selectivity of M2pep-polymers to human macrophages relative to other cell populations has yet to be studied and verified in PBMC-derived macrophages from multiple donors before moving forward with further optimization.

7.2.2.2.4 Optimization of polymeric backbone for display of M2pep

All M2pep-grafted polymers synthesized and evaluated in this thesis are based on poly(HPMA) with a fixed molecular weight (80 kDa) and valency (4-6) in order to evaluate the multivalent effect of different M2pep analogs. However, the optimal polymer molecular weight and peptide valency have not been determined and are likely to be different between mouse and human macrophages due to their differing size and receptor density. While it may be more desirable to lower the molecular weight of the backbone to slightly below 50 kDa to allow for eventual clearance via kidneys, poor solubility of M2pep necessitates high ratio of HPMA per peptide to keep the multivalent peptide-polymer water-soluble. This problem might be alleviated by investigation into more hydrophilic monomers e.g. zwitterionic carboxybetaine methacrylamide or sugar-based monomers. Multivalent display of M2pep onto self-assembled polymeric micelles could be an alternative strategy which is also more amenable for loading of a variety of drugs not restricted by availability of functional groups for conjugation. Nonetheless, a challenge exists on how to appropriately choose the animal models, ideally possessing a robust population of human macrophages, for evaluation of these systems ensuring their relevance for clinical translation.

7.3 References

- [1] C. Ngambenjawong, H.H. Gustafson, S.H. Pun, Progress in tumor-associated macrophage (TAM)-targeted therapeutics, *Adv. Drug Deliv. Rev.* (2017). doi:<http://doi.org/10.1016/j.addr.2017.04.010>.
- [2] M. Cieslewicz, J. Tang, J.L. Yu, H. Cao, M. Zavaljevski, K. Motoyama, et al., Targeted delivery of proapoptotic peptides to tumor-associated macrophages improves survival., *Proc. Natl. Acad. Sci. U. S. A.* 110 (2013) 15919–15924. doi:10.1073/pnas.1312197110.
- [3] C. Ngambenjawong, M. Cieslewicz, J.G. Schellinger, S.H. Pun, Synthesis and evaluation

- of multivalent M2pep peptides for targeting alternatively activated M2 macrophages, *J. Control. Release.* 224 (2016) 103–111. doi:<http://dx.doi.org/10.1016/j.jconrel.2015.12.057>.
- [4] C. Ngambenjawong, H.H. Gustafson, J.M. Pineda, N.A. Kacherovsky, M. Cieslewicz, S.H. Pun, Serum Stability and Affinity Optimization of an M2 Macrophage-Targeting Peptide (M2pep)., *Theranostics.* 6 (2016) 1403–1414. doi:10.7150/thno.15394.
- [5] C. Ngambenjawong, J.M.B. Pineda, S.H. Pun, Engineering an Affinity-Enhanced Peptide through Optimization of Cyclization Chemistry., *Bioconjug. Chem.* 27 (2016) 2854–2862. doi:10.1021/acs.bioconjchem.6b00502.
- [6] F. Li, M. Ulrich, M. Jonas, I.J. Stone, G. Linares, X. Zhang, et al., Tumor associated macrophages can contribute to antitumor activity through FcγR-mediated processing of antibody-drug conjugates., *Mol. Cancer Ther.* (2017). doi:10.1158/1535-7163.MCT-17-0019.
- [7] C.M. Downey, M. Aghaei, R.A. Schwendener, F.R. Jirik, DMXAA causes tumor site-specific vascular disruption in murine non-small cell lung cancer, and like the endogenous non-canonical cyclic dinucleotide STING agonist, 2'3'-cGAMP, induces M2 macrophage repolarization., *PLoS One.* 9 (2014) e99988. doi:10.1371/journal.pone.0099988.
- [8] L. Corrales, L.H. Glickman, S.M. McWhirter, D.B. Kanne, K.E. Sivick, G.E. Katibah, et al., Direct activation of STING in the tumor microenvironment leads to potent and systemic tumor regression and immunity, *Cell Rep.* 11 (2015) 1018–1030. doi:10.1016/j.celrep.2015.04.031.
- [9] Z.-G.T. Xiao-Lin Yu, Bi-Tao Wu, Ting-Ting Ma, YanXiao-Lin Yu, Bi-Tao Wu, Ting-Ting Ma, Yan Lin, Feng Cheng, Hai-Yu Xiong, Chang-Li Xie, Cui-Ying Liu, Qin Wang, Zi-Wei Li, Zhi-Guang Tu Lin, Feng Cheng, Hai-Yu Xiong, Chang-Li Xie, Cui-Ying Liu, Qin Wang, Zi-Wei Li, Overexpression of IL-12 reverses the phenotype and function of M2 macrophages to M1 macrophages, *Int J Clin Exp Pathol.* 9 (2016) 8963–8972.
- [10] M. Xu, M. Liu, X. Du, S. Li, H. Li, X. Li, et al., Intratumoral Delivery of IL-21 Overcomes Anti-Her2/Neu Resistance through Shifting Tumor-Associated Macrophages from M2 to M1 Phenotype., *J. Immunol.* 194 (2015) 4997–5006. doi:10.4049/jimmunol.1402603.
- [11] T. Liu, Z. Qian, Q. Xiao, D. Pei, High-throughput screening of one-bead-one-compound libraries: identification of cyclic peptidyl inhibitors against calcineurin/NFAT interaction., *ACS Comb. Sci.* 13 (2011) 537–546. doi:10.1021/co200101w.
- [12] L. Xu, J.S. Josan, J. Vagner, M.R. Caplan, V.J. Hruby, E.A. Mash, et al., Heterobivalent ligands target cell-surface receptor combinations in vivo., *Proc. Natl. Acad. Sci. U. S. A.* 109 (2012) 21295–21300. doi:10.1073/pnas.1211762109.
- [13] J.M. Saul, A. V Annapragada, R. V Bellamkonda, A dual-ligand approach for enhancing targeting selectivity of therapeutic nanocarriers., *J. Control. Release.* 114 (2006) 277–287. doi:10.1016/j.jconrel.2006.05.028.

- [14] D. Weerakkody, A. Moshnikova, M.S. Thakur, V. Moshnikova, J. Daniels, D.M. Engelman, et al., Family of pH (low) insertion peptides for tumor targeting., Proc. Natl. Acad. Sci. U. S. A. 110 (2013) 5834–5839. doi:10.1073/pnas.1303708110.